Bronze Metallurgy in Iron Age Central Europe:
A Metallurgical Study of Early Iron Age Bronzes from Stična, Slovenia

by

Elizabeth Myers Cooney

B.A. Chemistry and Greek & Roman Studies (2003)
Illinois Wesleyan University

SUBMITTED TO THE DEPARTMENT OF MATERIALS SCIENCE
AND ENGINEERING IN PARTIAL FULFILLMENT OF THE
REQUIREMENTS FOR THE DEGREE OF

MASTER OF SCIENCE IN MATERIALS SCIENCE AND ENGINEERING
AT THE
MASSACHUSETTS INSTITUTE OF TECHNOLOGY

JUNE 2007

Signature of Author……
Department of Materials Science and Engineering
February 2, 2007

Certified by……
Heather Lechtman
Professor of Archaeology and Ancient Technology
Thesis Supervisor

Accepted by……...
Samuel M. Allen
POSCO Professor of Physical Metallurgy
Chair, Departmental Committee on Graduate Students

Bronze Metallurgy in Iron Age Central Europe:
A Metallurgical Study of Early Iron Age Bronzes from Stična, Slovenia

by

Elizabeth Myers Cooney

Submitted to the Department of Materials Science and Engineering on
February 2, 2007 in Partial Fulfillment of the Requirements for the
Degree of Master of Science in Materials Science and Engineering

ABSTRACT

The Early Iron Age (750-450 BCE) marks a time in the European Alpine Region in which cultural ideologies surrounding bronze objects and bronze production were changing. Iron was becoming the preferred material from which to make many utilitarian objects such as weapons and agricultural tools; this change can be clearly seen in the different treatments of bronze object deposits from the Late Bronze Age to the Early Iron Age. The Early Iron Age hillfort settlement of Stična in what is now southeastern Slovenia was one of the first incipient commercial centers to take advantage of the new importance placed on iron, conducting trade with Italy, Greece, the Balkans, and northern Europe. This metallurgical study of bronze funerary objects from Stična identifies construction techniques, use patterns, and bronze metallurgical technologies from the ancient region of Lower Carniola. This information is then used to explore the cultural importance of bronze at Early Iron Age Stična and to compare the bronze work of Lower Carniola with that of other regions in central Europe and Italy from this time of great change in Iron Age Europe.

Thesis Supervisor: Heather Lechtman
Title: Professor of Archaeology and Ancient Technology

Table of Contents

Acknowledgements 5

Chapter 1: **Introduction** 6

Chapter 2: **Background**
2.1: The Early Iron Age in Slovenia 8
2.2: The Early Iron Age at Stična 8
2.3: Bronze in the Early Iron Age 10

Chapter 3: Provenance and Reliability of Study Materials
3.1: Mecklenburg Excavations at Stična 14
3.2: Reliability of Materials from Stična 15

Chapter 4: Methods
4.1: Metallurgical studies 18
4.1.1: Compositional analyses 18
4.1.2: Metallographic analyses 20
4.2: Artifact sampling selection 21
4.3: Documentation and sampling procedures 22

Chapter 5: Data 27
5.1: Bronze rings 28
5.1.1: Segmented leg ring (MIT 5339) 30
5.1.2: Segmented leg ring (MIT 5336) 56
5.1.3: Segmented upper arm ring (MIT 5341) 63
5.1.4: Segmented arm ring/bracelet (MIT 5334) 73
5.1.5: Segmented child's arm ring/bracelet (MIT 5335) 78
5.1.6: Zoned arm ring/bracelet (MIT 5344) 85
5.1.7: Zoned arm ring/bracelet (MIT 5346) 95
5.1.8: Zoned arm ring/bracelet (MIT 5340) 103
5.1.9: Hollow arm ring/bracelet (MIT 5366) 114
5.1.10: Flat arm ring/bracelet (MIT 5365) 135
5.1.11: Flat finger ring (MIT 5353) 146
5.1.12: Segmented foot ring (5342) 156
5.1.13: Hollow foot rings (not sampled) 169

5.2: Fibulae 173
5.2.1: Serpentine fibula (MIT 5330) 174
5.2.2: Serpentine fibula with disc (MIT 5352) 184
5.2.3: Navicular fibula (MIT 5348) 202
5.2.4: Knobbed fibula (MIT 5331) 215
5.2.5: Fibula spring (MIT 5332) 219
5.2.6: Additional fibula types not sampled 224

5.3: Belt Attachments 228
5.3.1: Rivets (MIT 5343) 229
5.3.2: Belt Attachment (MIT 5368) 241
5.3.3: Hook (MIT 5345) 256
5.3.4: Segmented ring belt attachment (5350) 263
5.3.5: Additional belt attachment types not sampled 271

5.4: Miscellaneous Objects 280
5.4.1: Tweezers (MIT 5329) 281
5.4.2: Tweezers (MIT 5333) 286
5.4.3: Earring (5367) 290
5.4.4: Earring wire (MIT 5337 and MIT 5351) 299
5.4.5: Spirals (MIT 5338) 319
5.4.6: Buttons (MIT 5349) 327
5.4.7: Lump 337
5.4.8: Additional miscellaneous objects not sampled 341

Chapter 6: Results and Discussion
6.1: General tin and lead composition trends 347
6.2: Rings 348
6.3: Fibulae 350
6.4: Belt attachments 352
6.5: Miscellaneous objects 353
6.6: Alloy composition as a function of processing 354
6.7: Copper ore and smelting practices 356
6.8: Bronzes from Stična compared to bronzes from other EIA Eastern Alpine Region sites 357

Chapter 7: Conclusions and Future Work
7.1: General Conclusions 371
7.2: Future Work 373

References 374

Appendix 377
A.1: Original ICP-ES bulk compositional analysis data
A.2: Original INAA bulk compositional analysis data

Acknowledgements

I would like to thank those who put a significant amount of time and effort into this thesis. Without their guidance and support, none of this would have been possible.

Professor Heather Lechtman (DMSE) from MIT.

The Peabody Museum of Archaeology and Ethnology at Harvard University for permission to study and sample objects from the Mecklenburg Collection and for permission to publish both my photographs of objects and archived photographs from the Mecklenburg Collection.

The staff of the Peabody Museum, especially Dr. Patricia Capone, Mr. Scott Fulton, Ms. T. Rose Holdcraft, Dr. Genevieve Fisher, Ms. Susan Haskell, Ms. Patricia Kervick, Ms. Julie Brown, and other staff and numerous student assistants for their help in studying and sampling the Mecklenburg materials.

The Center for Materials Research in Archaeology and Ethnology at MIT for providing funding for the analyses and publication permissions.

Thanks to those who helped with analysis: Prof. Dorothy Hosler (DMSE), Dr. Elizabeth Hendrix (formerly DMSE) and Dr. Nilanjan Chatterjee (EAPS) from MIT.

Thanks to those who helped with background on the Early Iron Age in Central Europe: Dr. Curtis Runnels (Boston University) and Dr. Peter Wells (University of Minnesota).

And warm thanks to my friends and family: Jennifer Meanwell, Mary Kremer Myers, Mary Jane Myers, Barbara Myers, Dennis and Becky Cooney, and, most importantly, my husband Kevin.

Chapter 1: Introduction

The Early Iron Age (750-450 BCE) marks a time in the European Eastern Alpine region in which cultural ideologies surrounding bronze objects and bronze production were changing. Iron was becoming the preferred material from which to make many utilitarian objects such as weapons and agricultural tools; this change can be seen clearly in the different treatments of bronze object deposits from the Late Bronze Age to the Early Iron Age (Giumlia-Mair 2005).

Metallurgical studies on objects with firm contexts from different regions are key to understanding not only bronze technologies in the EIA but also to understanding interactions amongst regional groups in the Eastern Alpine region during this extremely important time of social change (Giumlia-Mair 2000; Trampuž Orel 1999).

The purpose of the metallurgical study of bronze funerary objects from the site at Stična, reported here, is to identify construction techniques, use patterns, and bronze metallurgical technologies from the ancient region of Lower Carniola. The study combines composition analyses of various bronze objects with metallographic analyses to serve as a reference metallurgical study for the area. This study also publishes the first metallographic data on bronze objects from the EIA in Slovenia. This information can be used to compare the bronze metallurgy of Lower Carniola with that of other regions in Central Europe and Italy from this time of great change in Iron Age Europe.

Eastern Alpine region bronze metallurgy in the EIA is different from earlier bronze technologies. Synthesizing previously published data from several technical studies on bronze objects from Eastern Alpine sites in northern Italy and the site of S. Lucia di Tolmino/Most na Soči in northwest Slovenia, Giumlia-Mair shows that Eastern Alpine EIA bronze metallurgy is more technically advanced than Bronze Age metallurgy was (Giumlia-Mair 2005; Giumlia-Mair 2000).

Giumlia-Mair's study of the EIA bronze objects from the site of S. Lucia di Tolmino/Most na Soči in northwest Slovenia is a systematic study of the construction techniques used for different bronze object classes (Giumlia-Mair 1995; Giumlia-Mair 1998). The provenience of her sample is the systematic excavation of the necropolis at Most na Soči. S. Lucia di Tolmino/Most na Soči is the type site for the Slovenian Iron

Age culture group known as Sv. Lucija, which had close ties to the Este culture in northern Italy (Hencken 1978; Mason 1996).

Giumlia-Mair uses chemical composition analyses of the artifacts to show that the Early Iron Age people living at Most na Soči had a developed metallurgy in which different tin bronze alloys were intentionally used or alloyed with lead for different classes of objects. However, Giumlia-Mair does not publish metallographic data on any of the objects analyzed in her studies.

Other archaeometallurgical research carried out on Slovenian bronze artifacts has been almost exclusively on Bronze Age artifacts from hoards or isolated finds (Trampuž Orel 1999; Trampuž Orel 1995; Trampuž Orel *et al* 1991). Very little metallography has been undertaken; most of the analyses are for chemical composition

The Early Iron Age (EIA) hillfort settlement of Stična (approximately 625-425 BCE) in ancient Lower Carniola, now southeastern Slovenia (Figure 2.1), was one of the first incipient commercial centers to take advantage of the new importance placed on iron, conducting trade with Italy, Greece, the Balkans, and northern Europe (Wells 1984; Greis 2006). In exchange for iron, extralocal goods such as salt, glass, amber, tin, and fine ceramics were imported to Stična. Despite this new focus on iron, bronze continued to be important, and hundreds of bronze objects ranging from decorative rings and fibulae to vessels, armor, and horse gear were made, collected, worn, and buried in the 140 tumuli surrounding the settlement (Giumlia-Mair 2005; Wells 1981; Wells 1984).

The bronze funerary objects from Stična examined in this study come from the Mecklenburg Collection of the Peabody Museum of Archaeology and Ethnology at Harvard University. Scientifically excavated in the early twentieth century, these objects have a firm context on which this metallurgical study rests. This allows for correlations to be made between the composition and processing of bronze objects and the graves from which they come, providing associations between bronze objects, grave type, age (where applicable), and associated artifact assemblages.

Chapter 2: Background

2.1: The Early Iron Age in Slovenia

The beginning of the Early Iron Age (EIA), approximately 750-450 BCE, marks a period in Europe's Eastern Alpine region in which societies were changing significantly from their Bronze Age predecessors. During the eighth and seventh centuries BCE, large hillfort communities and commercial centers were developing throughout the Eastern Alpine region (Wells 1981, 1984). These commercial sites were centered around the production and trade of a particular good. For example, the type site of Hallstatt in Austria existed solely because of the trade in salt. EIA Slovenia was divided into seven distinct culture groups, and the richest, most densely populated of these groups was in Lower Carniola in central-southeastern Slovenia (Hencken 1978). The site of Stična in Lower Carniola was the largest of the hillfort settlements and one of the first commercial centers to develop during the EIA in the Eastern Alpine region (Wells 1981). A map showing EIA Slovenia, including geographical areas, topography, and sites mentioned frequently in the text, is shown in Figure 2.1.

Slovenia is in the eastern part of the Alpine network. Its landscape spans from the high Alps in the northwest of the country to the Dinaric range in the south and the southwest to the Pannonian Plain in the east. The Sava and Drava rivers and their river valleys provide communication routes and fertile agricultural fields. The country is highly forested with pasture lands in the river valleys. The site of Stična is located in the foothills of the Alps approximately 30 km southeast of modern Ljubljana (Wells 1981).

2.2: The Early Iron Age at Stična

Remains of the hillfort settlement and cemetery at Stična are still visible. The settlement is on a low, flat-topped hill overlooking the surrounding plain. The settlement, measuring about 400 x 800 m, is enclosed by earth and stone walls and is further subdivided by a long, interior wall running east-west along its center and by a small "corral" along its western edge (Greis 2006). Approximately 140 extant burial mounds

(tumuli) are located to the south and southeast of the settlement (Figure 2.2). These tumuli are still visible despite modern agricultural activity in the area (Figure 2.3) (Wells 1981, 1984). A typical tumulus at Stična was approximately 40 m in diameter and was rimmed by a low stone wall. Tumuli usually contain an average of seventeen graves rich in grave goods such as amber, bronze, ceramics, glass, and iron. Tumuli had a life span of about a century over which graves and layers of earth were actively being added to the mound (Greis 2006).

These tumulus burials, a ubiquitous feature at Iron Age sites in the Eastern Alpine region, started appearing at the beginning of the EIA. Prior to the EIA, burials in the Eastern Alpine region were primarily flat, cremation graves with few associated grave goods. The switch in burial practice to tumuli laden with grave goods at the beginning of the EIA marks other changes in the region as well. Iron, which had been in limited use during the Late Bronze Age, became more commonly used, and it allowed for an intensified production of new and better tools (such as axes, chisels, and hammers) and weapons (such as swords, spearheads and arrowheads). As iron became more important across the region, trade grew with and amongst iron-ore producing sites (Collis 1997; Phillips 1980).

Stična became a commercial center during this time because of its high level of iron production. The area around Stična is rich in high grade iron ores such as hematite and limonite that occur in rich surface sedimentary deposits (Wells 1984). Large deposits of iron slag have been found on the surface of the hillfort settlement. Unfortunately, due to a lack of excavation at the settlement, no iron workshops have yet been investigated (Wells 1984). The iron produced at Stična led to trade with Italy, Greece, the Balkans, and northern Europe (Wells 1984; Greis 2006). In exchange for iron, extralocal goods such as salt, glass, amber, tin, wine, olive oil and fine ceramics were imported to Stična. Though iron was the largest export from Slovenia, other exports to foreign locales such as northern Italy may have included slaves, cattle, hides, resin, pitch, wax, honey, and cheese (Wells 1980, 1984).

2.3: Bronze in the Early Iron Age

Bronze remained important in the EIA even as iron production and use intensified. However, the role of bronze in society appears to have changed drastically at this time. During the Bronze Age in the Eastern Alpine region, tin bronze was used for utilitarian objects, weapons, and jewelry. With the intensification of iron production, the use of bronze became limited primarily to mostly small, decorative items (Giumlia-Mair 2005). Bronze is almost never found as a grave good in Bronze Age burials, but it is a common grave good in EIA tumuli. In the Bronze Age bronze objects were deposited in ritualistic hoards, primarily in streams and bogs, instead of being removed from general circulation through burial as grave goods (Collis 1997; Phillips 1980).

In addition to the changed role of bronze in society, bronze technology also changed from the Bronze Age to the EIA. Composition analysis studies of bronzes from Bronze Age and other EIA Eastern Alpine region sites demonstrate that leaded bronzes, which were not known in the Bronze Age, came into use in the EIA in some areas of the Eastern Alpine region (Trampuž Orel 1999, 1995; Trampuž Orel *et al* 1991; Giumlia-Mair 2003, 2005). The tin content of tin bronzes also increased, which is probably attributable to an increased trade in tin, a resource which is not found in central Europe at all and must be imported (Giumlia-Mair 2003, 2005).

Overall, the EIA marked a high point for Lower Carniola, which faded into obscurity in the Late Iron Age as the Etruscans in Italy and Archaic cultures in Greece began to expand their areas of influence (Wells 1984).

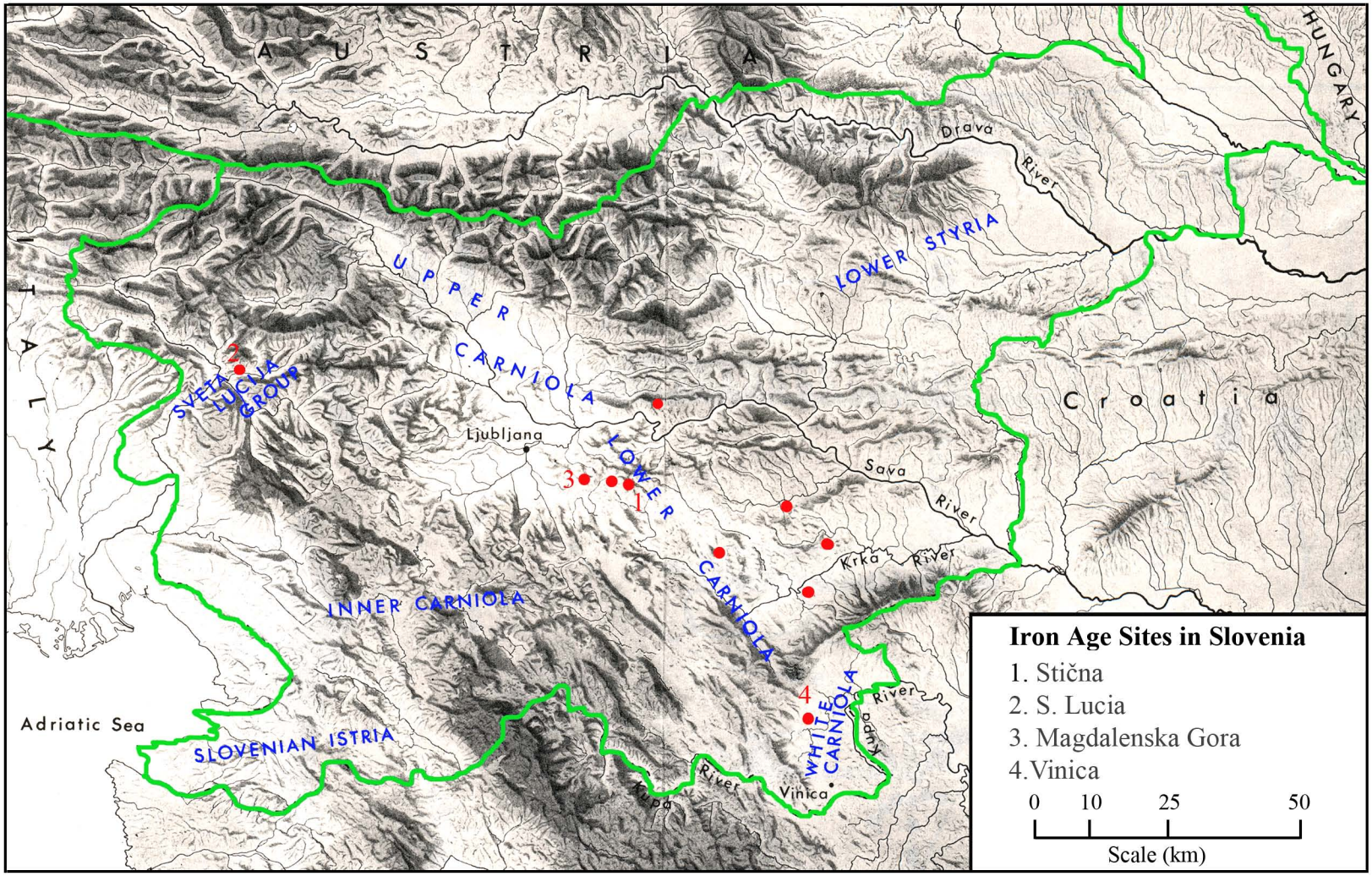

Figure 2.1: Iron Age sites and geographic areas in Slovenia. The four sites mentioned most often in the text are numbered. (Map after Hencken 1978).

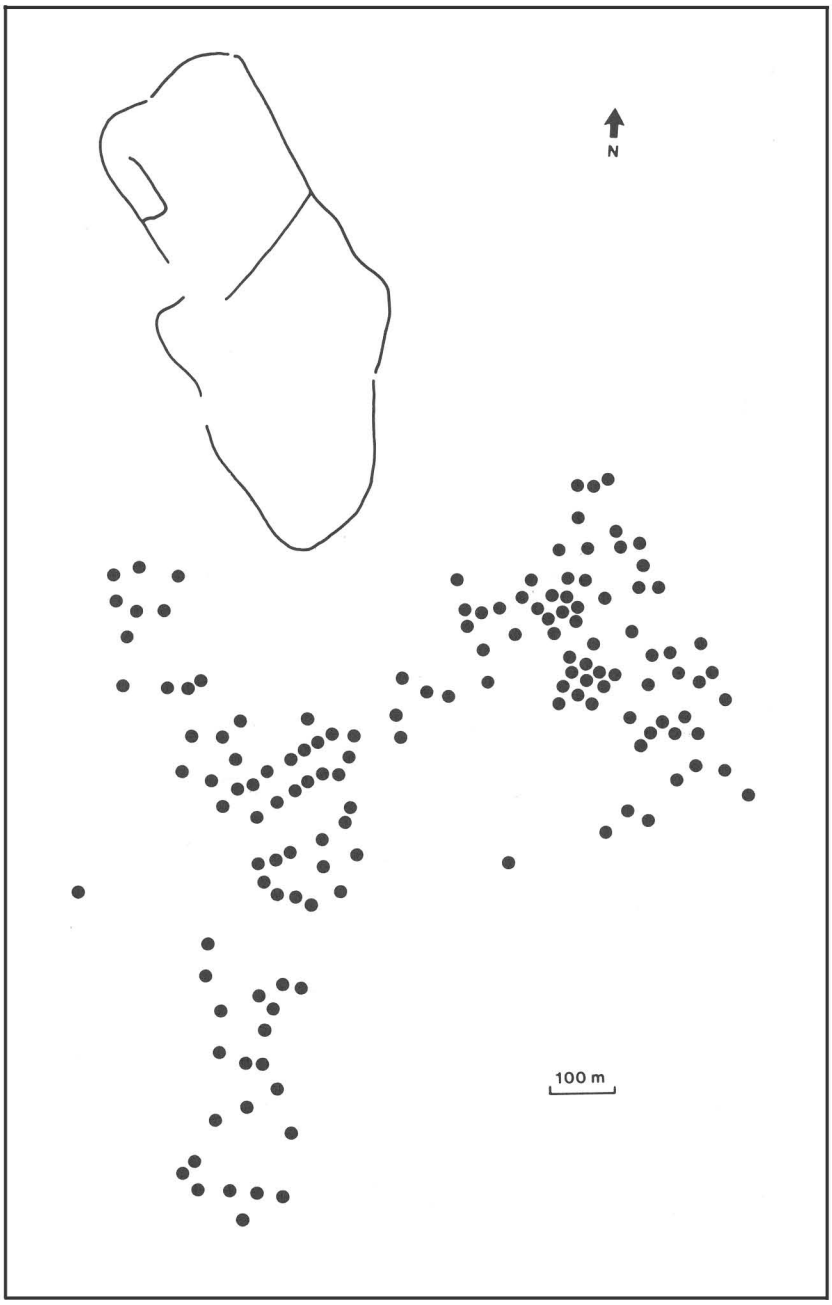

Figure 2.2: Site plan of Stična, Slovenia, showing the walls of the hillfort excavated by Gabrovec and the location of burial mounds still visible today that surround it. (Wells 1984:92).

Figure 2.3: Stična as it was between 1905-1914 when excavated by Mecklenburg. This photograph, taken by Mecklenburg, shows one surviving tumulus at Stična. It can be seen in the photograph that Stična is located in a hilly, open area and that the land was being used agriculturally at the time of excavation.

Chapter 3: Provenance and Reliability of Study Materials

3.1: Mecklenburg Excavations at Stična

The Mecklenburg collection at Harvard's Peabody Museum consists of thousands of objects excavated by the Duchess of Mecklenburg in Slovenia and Austria from 1905 to 1914 (Greis 2006). The Duchess excavated 186 graves and over a thousand objects from Stična alone. The objects in this collection from Stična are published in a comprehensive catalogue by Wells (1981). His publication includes a brief description of each grave assemblage and drawings of many of the objects.

Stična is the largest, most important, and best studied Early Iron Age site in Lower Carniola. While more recent excavations have outlined the perimeter walls of the hillfort settlement at Stična, the majority of the excavations at the site have been of tumuli and graves. The Mecklenburg excavations at Stična unearthed material solely from graves. This focus on grave assemblages was typical among antiquarians and archaeologists excavating at the turn of the century as it enable excavation of a large amount of high quality material quickly (Sklenár 1983; Greis 2006).

Recent excavations at Stična (from 1946 to 1964) have been scientific in accordance with modern archaeological standards (Gabrovec 1974). The Mecklenburg excavations at Stična were less so, although they were considered careful, scientific excavations in their day (Greis 2006). Documentation from the Mecklenburg excavations is scarce. There are no maps showing where the excavated tumuli are located at Stična. Of the eleven tumuli excavated, only one has any drawing showing how graves were related to one another in a horizontal fashion (Wells 1981), and no schematics were made showing how graves were related to one another vertically.

This lack of horizontal or vertical association between graves has much to do with the excavation techniques used at Stična. Mecklenburg cut vertically into the tumuli, cutting back vertical blocks of earth (Figure 3). This form of excavation provides little or no information on horizontal relationships between graves. Few drawings, photographs, and descriptions of graves or objects exist. The fact that some do exist is testament to the

Duchess of Mecklenburg's commitment to documentation of her excavations, which was rare in her day (Greis 2006).

The funerary nature of this material has both advantages and disadvantages. Depending on how the objects are counted, the Mecklenburg Collection contains over 200 individual bronze objects. Because so much bronze exists in graves at Stična, there is a large amount of well preserved bronze objects available for study. However, the corpus of bronzes lacks breadth; the majority of the bronzes are small, decorative items. Because only grave goods have been excavated, bronzes used and kept in workshops, domestic settings, agricultural settings, and other contexts are unavailable for study.

The largest disadvantage of the excavations at Stična is that they do not control for time. An individual tumulus was used over the course of about a century (Greis 2006). Due to the poor record-keeping associated with the Mecklenburg excavations, the vertical and horizontal associations between graves were not recorded, so inferences about the age of a grave cannot be made on the basis of stratigraphic evidence. At best, the age of all materials from Stična must be estimated at the approximate age of the site, between 625-425 BCE (Greis 2006).

3.2: Reliability of Materials from Stična

Of the eleven tumuli represented in the Mecklenburg excavations at Stična, Tumulus IV has by far the best surviving records (Wells 1981). The excavation notes for Tumulus IV record, in most cases, grave orientation, grave dimensions, including length, width, and depth, and association of large stones with graves, including large stone covering slabs and circular and stacked stone arrangements within graves. Evidence for cremations and inhumations is also recorded; almost no graves have any surviving bone, so evidence for cremation vs. inhumation usually is in the form of layers of burnt earth. The types and amounts of grave goods, and, in some cases, the arrangement of various grave goods with respect to one another are also recorded. Some of the notes label certain graves as belonging to a child, though it is unclear what criteria were used to distinguish between the graves of children and adults.

As the Mecklenburg collection changed hands several times before being accessioned by the Peabody Museum in the late 1930s, some of the grave assemblages in Tumulus IV went missing or were mixed together. Wells (1981) reports both the grave assemblages recorded in the excavation notes and the excavation assemblages as they existed when obtained by the Peabody.

The combination of grave goods present in Tumulus IV is similar to that of the other tumuli excavated by Mecklenburg at Stična (Wells 1981). In addition, the excellent records of the excavation of Tumulus IV show that the combination of grave goods, the grave structures, and burial rites associated with this tumulus are similar to tumuli at Stična that were excavated using more modern techniques (Gabrovec 1974; Mason 1996; Wells 1981). This similarity allows with some caution for conclusions based on the study of materials from Tumulus IV to be applied to materials from Stična as a whole.

Because of the excellent excavation records kept for Tumulus IV, the bronze objects examined in this study are restricted to those from Tumulus IV.

Figure 3: This photograph taken of the St. Vid tumulus at Stična shows the vertical, step-wise excavation technique used by Mecklenburg at the site. The tumulus was cut back in pieces vertically, revealing little if anything about the horizontal relationships between graves.

Chapter 4: Methods

4.1: Metallurgical Analyses

No metallurgical analysis of an object is complete unless both the composition and the microstructure of the metal are determined. Both the material composition of the object and its processing, which is determined by microstructural analysis, result from conscious engineering choices. Thus, both compositional and metallographic analyses must be carried out.

4.1.1: Compositional Analyses

The composition of a material has a direct impact on both the ways a material can be used and the ways in which it can be manipulated during processing. The composition of a metal or an alloy bears directly on the physical properties the alloy exhibits. One of the most important aims of metallurgical study is to determine the relationships between alloy composition, physical properties, and deliberate engineering choices made by those who produced the metal object.

Prior to the sampling and compositional analysis of the Stična materials, it was assumed that they were made from tin bronze. Previous studies of Early Iron Age bronze objects from the Eastern Alpine region showed that metal smiths purposefully chose different copper-tin alloys ranging from 0-14 weight percent tin for different classes of objects with different intended uses. As copper and tin form a solid solution when copper is alloyed with tin in concentrations up to 15.8 weight percent, only one single phase will be present in objects made of copper alloyed with 0-14 weight percent tin (Figure 4.1). It is impossible to make even a rough estimate of alloy composition from the microstructure of a single-phase material. Because the evidence of alloy choice in the Stična materials was expected to fall within such a small range of tin compositions, bulk compositional analyses were integral to this study of Eastern Alpine region metallurgical technologies.

It was also assumed prior to the start of the study that at least some of the tin bronzes from Stična were leaded bronzes. Previous studies of Early Iron Age bronze objects from the Eastern Alpine region showed that metal smiths added lead to their tin bronzes in concentrations ranging from 0.5 – 14.5 weight percent lead (Giumlia-Mair

1995). Because lead and copper are almost entirely immiscible and because lead has a much lower freezing point than tin bronze (Figure 4.2), the lead in these alloys solidifies from the melt to fill the interdendritic spaces created by the primary alloy, and it is not homogenously distributed throughout a casting. If a leaded tin bronze is further worked after casting, lead globules form along the grain boundaries (Davis 2001). While this phenomenon increases the fluidity and castability of tin bronze (Gettens 1969), it also makes bulk compositional analysis necessary for an accurate determination of the lead concentrations in leaded tin bronze alloys. Bulk compositional analyses are the standard complement to metallographic analyses in metallurgical studies.

The preferred method of bulk compositional analysis is through instrumental neutron activation analysis (INAA) and/or through inductively coupled plasma techniques (either inductively coupled mass spectrometry, ICP-MS, or inductively coupled plasma emission spectrometry, ICP-ES). At MIT archaeological metals are conventionally analyzed by INAA followed by ICP. By contrast, an electron microbeam probe is able to conduct point analyses only.

Bulk chemical analyses are able to determine the major, minor, and trace elements present in a metal sample. Because trace amounts of elements can markedly alter the physical properties of a metal, it is important to determine those trace elements using a method that is able to determine them with high accuracy. Bulk analyses are designed to determine even the smallest amounts of trace elements, whereas an electron microbeam probe is almost never used for trace element determinations because of its lack of sensitivity for most elements at the ppm or ppb range.

In the case of almost all ancient metal artifacts made of alloys (such as tin bronze), because of the solidification dynamics of the material, as it freezes from the molten state the alloying element (tin in the case of tin bronze) will not be uniformly distributed throughout the solid metal. This phenomenon is known as segregation, and its effects can lead to a dramatic range of compositional inhomogeneities throughout a solid metal. Thus, the only reliable way to determine the overall composition of a metal alloy in an artifact is through bulk chemical analysis. Because the electron microbeam probe can only be used for point-by-point determinations, while it provides an excellent record

of alloy segregation, it is not a reliable method for determining the overall composition of an alloying element(s) in a metal.

Bulk compositional analyses should be carried out in a two-stage process. The standard bulk compositional analysis strategy used at CMRAE is to have archaeological metal compositional samples analyzed first by INAA and second by ICP-ES. The minimum weight requirement of a sample for bulk analysis is 100 mg. This two-stage process is highly preferable because there are certain elements that each of these methods is unable to detect reliably. When used in conjunction with one another, these methods are able to detect almost every element present in a metal sample. As INAA analysis does not destroy the solid analytical sample, the same 100 mg sample is used for both INAA and ICP-ES.

Often, INAA and ICP-ES will report slightly different values for the same element in a sample. Both methods can underreport element compositions, especially for elements like tin, which in the case of ICP-ES can be hard to digest into a solution for analysis. Although the results from both techniques are reported here, the higher value has been weighed more heavily in the final object analysis to compensate for any underreporting.

If a sample is too mineralized (corroded) to yield enough metal for a bulk analysis, the electron microbeam probe can be used as an imperfect proxy to yield at least some information about the major element composition of an object.

4.1.2: Metallographic Analyses

Metallographic analysis reveals an object's microstructure, which holds clues as to the engineering and manufacturing processes behind an object and an object's intended and actual use patterns, among other things.

A metal's microstructure directly impacts many of its properties, including hardness, elasticity, and strength. When an object is designed, the maker decides how best to develop the properties desired by manipulating the microstructure of the metal or alloy used to fashion the object. By examining an object's microstructure, one can discern the intended engineering. The engineering and design of an object are key to understanding its intended use.

Similarly, by examining an object's microstructure, one can determine what kind of processes went into making that object. Certain types of microstructures can come about only as a result of specific processes having been used such as casting, working, and annealing. The existence of these specific structures informs an observer that a certain process took place. Certain patterns of use will also affect the microstructure, and these microstructural features can often be detected.

4.2: Artifact Sampling Selection

The corpus of bronze artifacts excavated at Stična and available for sampling from the Peabody's Mecklenburg collection was confined to those from Tumulus IV as discussed previously in the Materials chapter. This restriction limited the number of reliable graves from which objects were available for study to 50 (Wells 1981). Thirty-four (68%) of these 50 graves contained bronze objects.

The 29 objects sampled in this study come from 21 of the 34 bronze-containing graves in Tumulus IV. Thus, 61 % of the reliable bronze-containing graves in Tumulus IV are represented in this study. Of the reliable Stična graves excavated by Mecklenburg, including those in Tumulus IV, 105 graves contain bronze objects. Twenty percent of the reliable bronze-containing graves from Stična as a whole are represented in this study.

From the possible pool of objects, selection of those available for sampling was limited by the Peabody Museum to broken objects not of a quality fit for museum display and to objects of which there were several other examples in the collection.

As metallographic analyses are time consuming, there was a time restriction on how many objects could be sampled for metallographic analysis. Metallographic analyses were further restricted to objects from which a representative sample still metallic enough for analysis could be taken and to objects from graves without any recorded evidence of burning or crematory fires. Bulk compositional analysis sampling was restricted to objects large and metallic enough to yield at least a 100 mg sample.

Given all these restrictions, it was not possible to sample objects from every grave and from every object type. The Peabody Museum approved the sampling of 31 objects chosen as the most representative group from the available pool. These 31 objects were grouped into four distinct object types: rings, fibulae, belt attachments, and

miscellaneous. Upon sampling, two objects proved to have too little metal remaining for analysis, leaving the final sample count at 29 objects. Fifteen of these objects were slated for both bulk compositional and metallographic analysis, five for metallographic analysis with compositional analysis on the electron microbeam probe, and nine for bulk compositional analysis alone.

Wells (1981) counts 74 bronze objects in reliable graves in Tumulus IV. Using Wells' count, 39% of bronze objects from Tumulus IV are represented in this study. Wells (1981) counts 271 bronze objects from reliable graves excavated by Mecklenburg at Stična. Again using Wells' count, 11% of the total bronze objects at Stična are represented in this study. Additional statistical breakdowns by object type are found in the Data section.

Many objects which were not available for sampling were also studied and photographed. These objects are discussed with their appropriate object type in the Data section.

4.3: Documentation and Sampling Procedures for All Objects

All objects from which samples were removed were examined at the Peabody Museum of Archaeology and Ethnology at Harvard University in the Spring of 2006. Before samples were removed, all objects were examined by the naked eye and with a low power stereoscopic microscope. All objects were drawn to scale and measurements were recorded. Photographs were taken using a Nikon Coolpix 5900 digital camera and were processed into black and white high-resolution images with Adobe Photoshop CS.

Several objects which were not sampled were also photographed. These objects either represent intact objects identical or similar to sampled objects, or they represent classes of objects that were not able to be sampled for this study.

Thirty-one objects were sampled: 16 for both metallographic and bulk compositional analyses, 9 for bulk compositional analysis only, and 6 for metallographic analyses with compositional analyses on the electron microbeam probe. These objects were sampled in the Conservation Laboratory at the Peabody Museum under the supervision of Peabody conservators Scott Fulton and T. Rose Holdcraft. All objects were sampled using a jeweler's saw and wooden block with the exception of MIT 5347, a

metal lump, which was drilled using a clean steel drill bit. The saw and block were cleaned and the saw blade was changed for each object to insure that no contamination of the samples took place. Only two objects proved upon sampling to have too little metal to analyze: Peabody 40-77-40/13498, a bridle knob, and Peabody 40-77-40/13306, a hollow hook. All samples for bulk compositional analyses were weighed using a digital analytical scale to insure that they weighed at least 100 mg. The locations on each object from which samples were taken were recorded on the object drawings.

The samples were taken to MIT to prepare them for analysis. The twenty five samples taken for bulk compositional analyses were cleaned using a combination of mechanical cleaning and chemical cleaning with warm, 15% strength formic acid to remove as much corrosion product as possible from the intact metal. These cleaned samples were sent to ACTLABS for INAA and ICP-ES analysis. Compositions were subsequently reported in weight percentages.

The metallographic samples were either cold mounted with Buehler epoxy or were hot mounted with mounting compounds from Mark V. The orientation in which each sample was mounted was recorded on the object drawings. Once mounted, each sample was prepared using standard metallographic procedures. The mounted samples were ground flat using a series of wet silicon carbide papers with progressively smaller grit sizes (240, 320, 400, 600). The mounted samples were then polished to a mirror finish using six micron diamond paste followed by one micron diamond paste. The samples were subsequently polished with 0.3 micron α-alumina and, when necessary, 0.05 micron γ-alumina suspensions. Buehler polishing wheels and supplies were used.

Observations of the as-polished samples were made using a Leitz metallographic microscope. Photomicrographs of the as-polished samples were taken using a Leica metallographic microscope equipped with a DC300 digital camera and IM50 image processing software. All further manipulations were done in Photoshop CS.

The as polished samples were etched to reveal their microstructures. A discussion of the etchant(s) used for each sample follows in the Data chapter. Observations of the etched samples were made using a Leitz metallographic microscope. Photomicrographs of the etched samples were taken using a Leica metallographic microscope equipped with

a DC300 digital camera and IM50 image processing software. All further manipulations were done in Photoshop CS.

The Electron Microanalysis Facility in the Department of Earth, Atmospheric, and Planetary Sciences at MIT was used for all electron microbeam probe work under the direction of Dr. Nilanjan Chatterjee.

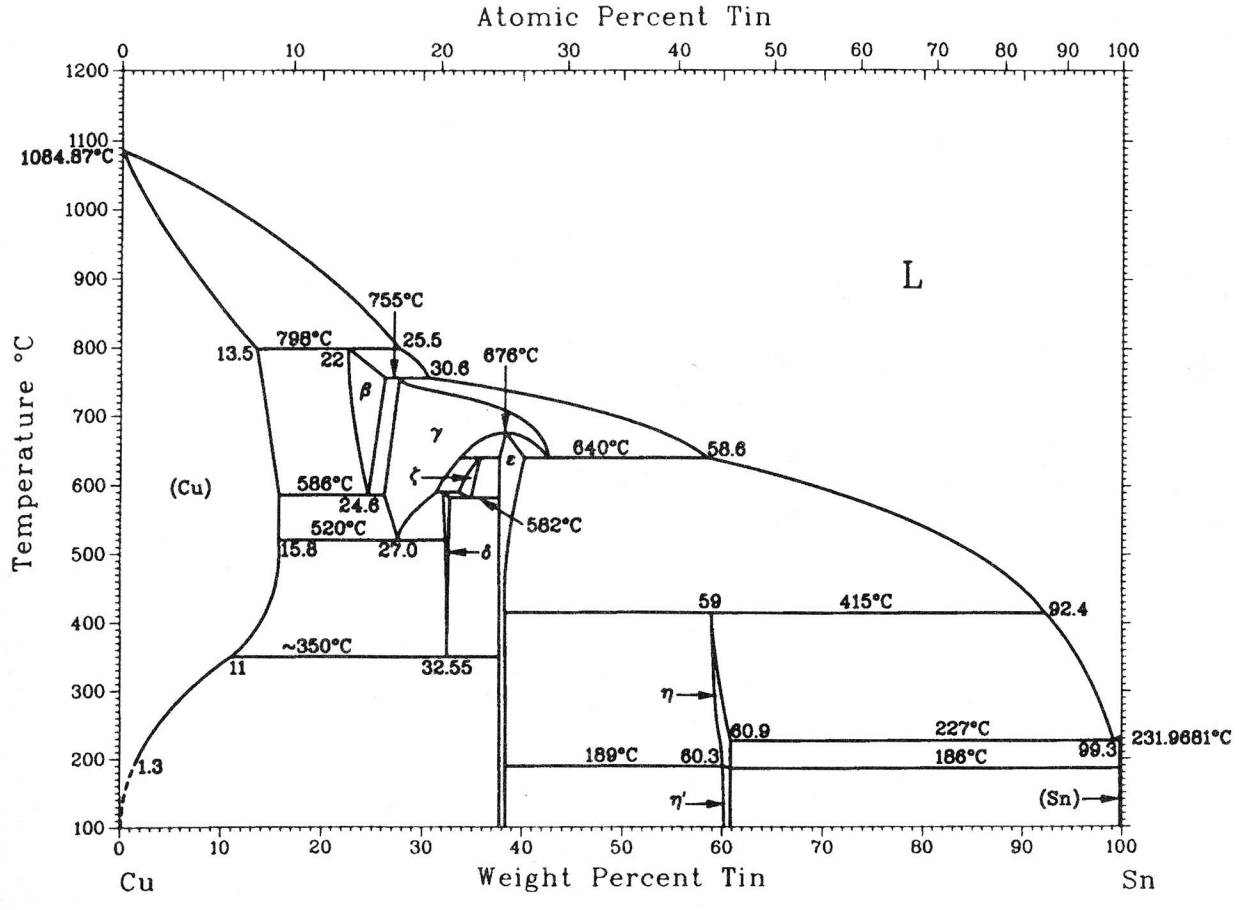

Figure 4.1: Copper-tin (Cu-Sn) binary phase diagram. (Davis 2001:377).

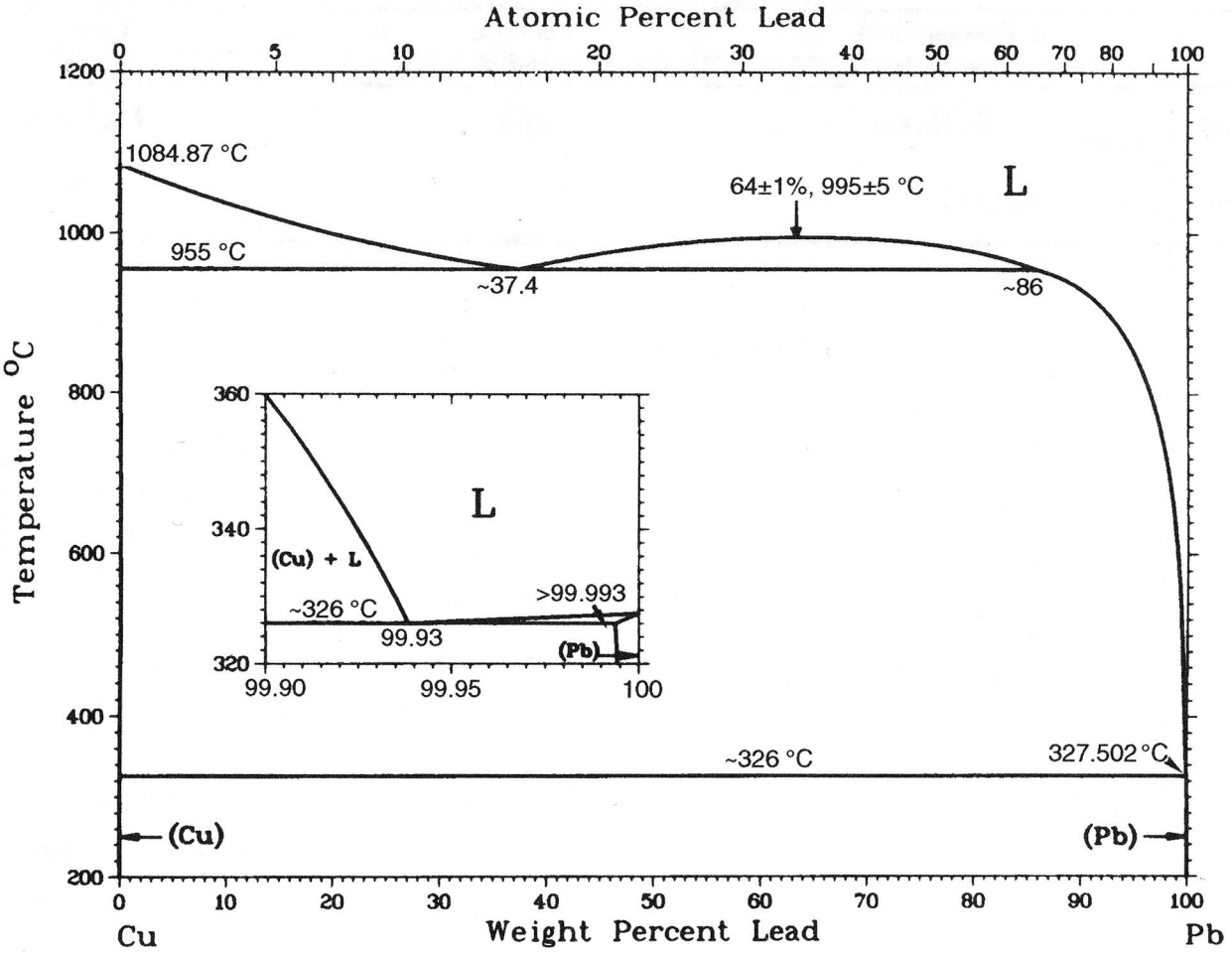

Figure 4.2: Copper-lead (Cu-Pb) binary phase diagram. (Davis 2001: 374).

Chapter 5: Data

Chapter 5 contains data on the 29 objects sampled and on additional objects not sampled for this study. Chapter 5 is divided into four sections according to the four object classes into which bronze items were placed for this study: rings (Section 5.1), fibulae (Section 5.2), belt plates and attachments (Section 5.3), and miscellaneous objects (Section 5.4).

The main categories are divided further into subsections, each of which contains data for an individual sampled object. The background and provenance, initial observations, sampling data, composition data, and metallographic data (where applicable) for each object are presented and discussed in each subdivided section. Photographs, drawings, diagrams with key object features and measurements, diagrams of locations from which samples were removed, photomicrographs, and other key figures are located at the end of each subsection.

5.1: Bronze Rings

Bronze rings (bracelets, arm rings, leg rings, foot rings, etc.) are the most common class of bronze objects found at Stična; there are 171 objects classified as "rings" from Stična. There are over 40 objects of various sizes and forms classified as "bronze rings" in Tumulus IV. The most common type of bronze ring is known as a "segmented" ring. This type of ring is patterned with repeating raised segments separated from one another by semi-annular grooves (Figure 5.1).

Twelve bronze rings were sampled: two leg rings (Sections 5.1.1 and 5.1.2), one upper arm ring (Section 5.1.3), seven arm rings or bracelets with various forms of decoration (Sections 5.1.4, 5.1.5, 5.1.6, 5.1.7, 5.1.8, 5.1.9, and 5.1.10), one finger ring (Section 5.1.11), and one foot ring (Section 5.1.12). Six of these rings are segmented rings, and two others incorporate zones of segmentation in their design. Additional rings which were not able to be sampled are discussed in Section 5.1.13.

Six rings were sampled for both bulk composition and metallographic analysis, three for bulk composition analysis only, and three for metallographic analysis in conjunction with composition analysis on the electron microbeam probe.

In the following descriptions the term "outside surface" refers to the ring surface which is away from the body and visible when worn. The term "inside surface" refers to the ring surface which is against the body when worn. The "thickness" of a ring refers to the distance between the outside and inside surfaces of the ring, i.e. how far above the body the outside surface of the ring is raised when worn. The "width" of a ring refers to how wide the ring would have appeared when worn, i.e. the distance between the two outside edges of a ring when the outside surface is viewed straight on.

Segmented rings have a few additional descriptive terms that need definition. These terms are illustrated in Figure 5.1. A segmented decoration pattern is found on the outside surface of a ring and consists of a repeated pattern of raised surfaces (segments) separated from one another by troughs (grooves). Here the term "groove width" refers to the distance from one groove to another. "Segment length" refers to the distance from the end of one groove to the beginning of the subsequent groove. The term "segment width" refers to the same dimension as the ring's width, i.e. the distance between the two sides of a ring or segment.

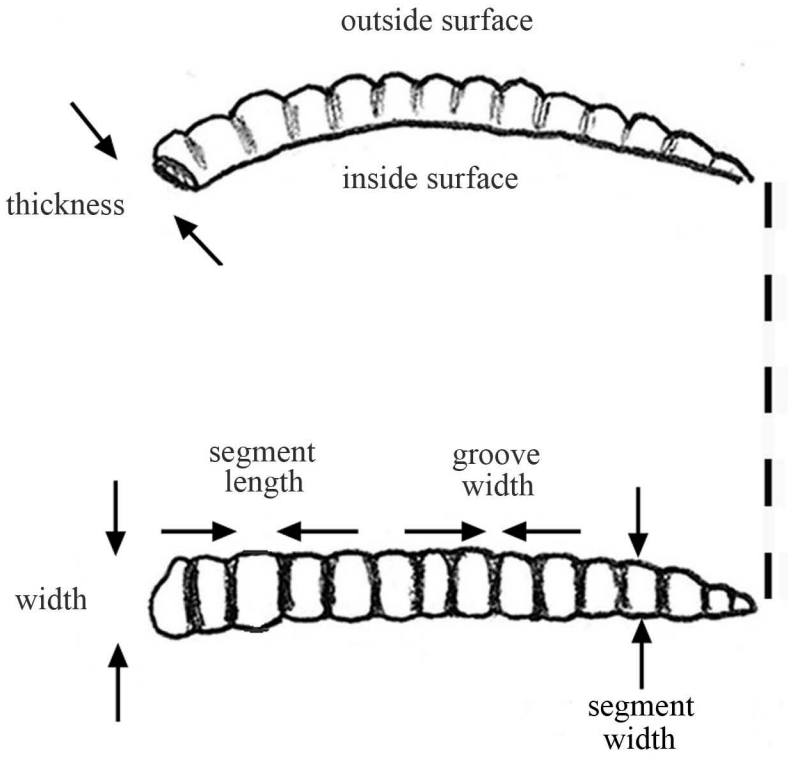

Figure 5.1: Descriptive terms used for rings and segmented rings.

5.1.1: Segmented leg ring (MIT 5339/Peabody 40-77-40/14267)

5.1.1a: Provenance and Background

MIT 5339, identified by Wells (1981) as a fragmented thin, segmented bronze ring (Figures 5.1.1.i and 5.1.1.ii), came from Grave 2 of Tumulus IV. Grave 2 was covered by a stone slab 0.85 m in diameter. The grave was 2.8 m long, 0.85 m wide, and 0.6 m deep. It contained some remains of a skeleton oriented east-west.

MIT 5339 and an identical segmented ring were found around the surviving leg bones. Other grave goods included transparent blue glass beads, a bronze serpentine fibula (MIT 5330, discussed in Section 5.2.1), a coarse ware urn, and a spindle whorl.

A similar intact, segmented leg ring with tapered, overlapping ends comes from Grave 12 (Figure 5.1.1.iii).

5.1.1b: Initial Examination and Observations

The segmented leg ring was photographed (Figures 5.1.1.i and 5.1.1.ii), drawn to scale, and measured (Figures 5.1.1.iv and v).

The ring is solid and circular in shape with a diameter of 10.02 cm. It is almost completely intact, but a fragment 42.3 mm long has broken off one of its ends. One original, intact end remains on the ring while the other original, intact end is part of the fragment. The ring weighs 48.7 g and the broken fragment weighs 2.7 g.

The ring is semi-closed and originally had two tapered, overlapping ends. The ring has a lenticular cross section. The cross section changes size across the ring; at its thickest point the cross section is 6.7 mm wide x 6.0 mm thick. The two tapered ends have differing thicknesses; the end on the main ring is 3.3 mm wide x 3.3 mm thick while the intact tapered end on the fragment is 2.4 wide x 1.9 mm thick (Figure 5.1.1.v).

The ring is segmented. When the ring is viewed flying flat (Figure 5.1.1.i), the segments appear convex in profile. When the exterior surface is viewed straight on (Figure 5.1.1.ii, the segments appear to be rectangles with slightly bulging sides and rounded extremities.

The segments vary in size across the ring and diminish in width and length as the ring tapers down to its ends. The largest segment is 6.0 mm wide x 3.8 long at a point

where the ring is 5.8 mm thick. The segment at the intact tapered end of the ring is 3.3 mm wide x 2.4 mm long (Figure 5.1.1.v).

While the segment width and length change along the length of the ring, the groove width --the distance between segments-- remains fairly constant at 1.5 mm. Each groove proceeds along the entire outside surface of the ring, the inside surface is ungrooved and smooth. The grooves have a rounded, concave, semi-annular shape

The ring's inside surface is slightly faceted along the longitudinal axis. Instead of being a completely smooth curved surface, at least three facets are present at very small angles to one another.

The ring is structurally robust. The surface is intact and is covered with various shades of friable green corrosion product. In a few areas there are textile pseudomorphs present in the external corrosion product. These pseudomorphs wrap around the circumference of the ring and appear to have been caused by fine crinkles in the fabric next to which the ring was buried. Under magnification, impressions of the fabric's weave and individual threads can be seen in the pseudomorphs (Figure 5.1.1.iv).

5.1.1c: Sampling

Two samples were removed from MIT 5339 as transverse sections (Figure 5.1.1.vi). Sample MIT 5339a was removed for bulk composition analysis and MIT 5339b was removed for metallographic analysis. The bracelet is highly metallic, and the metal is light gold in color.

5.1.1d: Compositional Analysis

Bulk composition analysis shows that the ring is mostly copper with a main alloying element of tin at a concentration of 13.7 weight percent. The segmented leg ring is a high tin bronze. Other major and minor elements include Ni (2.04 %), Pb (0.372%), Sb (0.163%), As (0.101%), Fe (0.18%), and Co (0.023%). Bulk composition analysis data are shown in Table 5.1.1 and in the Appendix.

Table 5.1.1: Bulk Composition Analysis Data for MIT 5339

	Sn	Pb	Sb	As	Ni	Co	Ag	Fe
ICP-ES	13.7	0.372	0.163	0.101	2.04	0.022	n.a.	0.038
INAA	11.2	n.a.	0.126	0.085	2.06	0.0232	0.071	0.18

(values in weight %) n.a. = not analyzed n.d. = not determined

5.1.1e: Metallographic Analysis

MIT 5339b was mounted as a transverse section (Figure 5.1.1.vii). The polished section reveals that the ring's circumference is distinctly faceted. Microstructural features of interest include a large cavity in the center of the sample. This cavity may be part of a larger, center line shrinkage cavity produced during a casting operation. A large declivity filled with corrosion is also present at the edge of the sample. Two distinct types of small inclusions are present in high densities in the sample. One type is light blue-green in color, and the other is light gray in color. The inclusions are homogenously distributed throughout the sample, and they do not exhibit any apparent alignment.

The sample was etched for two seconds with potassium dichromate followed by two seconds with aqueous ferric chloride to reveal a microstructure characterized by equiaxed grains with annealing twins (Figure 5.1.1.viii). There are a few deformation lines along the edges near the ring's surface (Figure 5.1.1.ix). The blue-green inclusions did not etch, indicating that they are not Cu-Sn eutectoid.

The transverse section was ground down and repolished three additional times in an attempt to determine how the grooves were made. No new information was revealed about the ring or the groove in this way; the transverse cross section remained roughly the same shape and size as it was viewed at different points along the segment. The final transverse cross section after the fourth grinding and polishing operation is shown in Figure 5.1.1.x, and the etched microstructure at that point is shown in Figure 5.1.1.xi. Both the as-polished and etched microstructures are the same as those seen in Figures 5.1.1.vii-5.1.1.ix.

After the transverse cross section had been examined, the sample was turned ninety degrees and was mounted along its longitudinal axis.

The longitudinal section as-polished clearly shows the ring's segments and grooves in relation to one another (Figure 5.1.1.xii). The cut edge on the sample's apparent right is adjacent to the transverse cross section shown in Figure 5.1.1.x, and the corrosion along this cut edge corresponds to the same declivity seen along the apparent left of the transverse cross section shown in Figure 5.1.1.x.

The outline of the segments and grooves is maintained in external corrosion product of the longitudinal section. The longitudinal section shows that the ring fragment is highly corroded internally, especially close to the ring's surfaces. This high level of corrosion makes it impossible to see the microstructure of the metal at the very surface of the grooves and segments, although the microstructure of the metal beneath the grooves and segments can be seen in a few areas.

While the green-blue and gray inclusions showed no apparent alignment in the transverse cross section, in the longitudinal cross section they are elongated and regularly aligned. In the bulk of the metal these inclusions are aligned parallel to the ring's longitudinal axis (Figure 5.1.1.xiii). Near the grooves and segments, however, the inclusions are oriented at an angle to the longitudinal axis and parallel to the walls of the grooves and segments (Figure 5.1.1.iv). The alignments of the inclusions in the bulk metal indicate that the ring must have been heavily worked when shaped. The alignment of the inclusions roughly parallel to the walls of the grooves and segments indicates that the metal beneath the grooves was compressed during their fabrication, causing the metal to deform on either side of the tool used to shape the groove.

The sample was etched for two seconds with potassium dichromate and for two seconds with aqueous ferric chloride to reveal a microstructure characterized by equiaxed grains with annealing twins. Areas close to the ring's outside surface directly beneath a groove (Figure 5.1.1.xv) and directly beneath a segment (Figure 5.1.1.xvi) show no deformation lines. There are a few deformation lines scattered throughout the bulk of the sample and near the ring's inside surface (Figure 5.1.1.xvii).

The sample was ground down to further expose the ring's longitudinal cross section (Figure 5.1.1.xviii). The microstructural features after the second grinding operation are the same as in the longitudinal cross section discussed above. There is also a crack propagating through the center of the ring perpendicular to the longitudinal axis.

This crack passes through the segment second to the sample's apparent right in Figure 5.1.1.xviii.

The longitudinal sample after the second grinding operation was examined with the electron microbeam probe so that the composition of the blue-green and gray inclusions could be determined (Figure 5.1.5.ixx). The gray inclusions were determined to be copper sulfide inclusions, and the blue-green inclusions were shown to have a composition of 51.9 weight percent copper, 37.4 weight percent tin, and 12.9 weight percent nickel.

The longitudinal sample was etched for two seconds with potassium dichromate and for two seconds with aqueous ferric chloride to reveal a microstructure characterized by equiaxed grains with annealing twins. As in the first longitudinal section, few to no deformation lines are present beneath the segments and grooves at the sample's outside surface, and there is a low density of deformation lines close to the inside surface of the ring. There is a high density of deformation lines to the apparent left of the crack running through the center of the sample (Figure 5.1.1.xx.) This high density of deformation lines is present nowhere else in the sample and is most likely caused by stress placed on the metal at this point due to the presence of the crack.

5.1.1f: Discussion

The ring is a high tin bronze with a tin concentration of almost 14 weight percent. There is only 0.372 weight percent lead present in the sample, indicating that lead was not purposefully added to the alloy to produce a leaded bronze. There is also an unusually high amount of nickel present in the alloy, around two weight percent. This nickel likely comes from the copper's parent ore. While the ring's high tin content would have made it relatively hard, it also would have made the metal slightly brittle.

Both the transverse and longitudinal cross sections of the ring show large areas of internal corrosion throughout the ring. The shape of these zones suggests that they correspond to macro-shrinkage cavities, indicating that the stock metal from which the ring was made was likely cast. Other than these large areas of internal corrosion, the ring has a low density of internal porosities.

The transverse cross section shows that the ring surface exhibits five distinct facets. The facets are not equal in length, and the angles at which they meet one another vary. They come together to give the ring an overall lenticular cross section. The ring's microstructure, discussed below, indicates that these facets were made as the metal was worked to provide a roughly round cross section.

Both the transverse and longitudinal cross sections have two distinct inclusion types. The first inclusion type is blue-green in color. Analysis on the electron microbeam probe shows that these inclusions are a copper-tin-nickel mix. The second inclusion type is gray in color. Analysis on the electron microbeam probe shows that these inclusions are copper sulfides.

While these two inclusion types are homogenously distributed and not aligned in any way when viewed in transverse cross section, when viewed in longitudinal cross section they are elongated and have a specific orientation. In the bulk of the ring and close to the ring's inside surface these elongated inclusions are oriented parallel to the ring's longitudinal axis. This indicates that the stock metal was hammered to lengthen it and to shape it into a ring. The inclusions close to the ring's outside surface directly beneath the segments and grooves are oriented at an angle to the ring's longitudinal axis that matches the angle at which the walls of the grooves rise and fall in relationship to the longitudinal axis.

The inclusions' elongation and specific orientation indicate that the outside surface of the ring was heavily worked perpendicular to the ring's longitudinal axis. The angles at which the inclusions beneath the segments and grooves are oriented indicate that the grooves and segments were compressed into the metal with a tool similar to a chasing tool; the grooves and segments were not cast nor were they engraved into the metal. This most likely happened after the metal was bent into a circle to create a semi-closed ring with overlapping ends as the decoration was not deformed by hammering after it was created.

When etched, the ring's microstructure is characterized by equiaxed grains with annealing twins. This microstructure indicates that the ring was subject to several cycles of working and annealing during its manufacture. Most of the metal, including the areas beneath the segments and grooves, exhibit few to no deformation lines, indicating that

these areas were not worked after the ring's final anneal. There is a low density of deformation lines close to the ring's inside surface, and a high density of deformation lines adjacent to a crack that runs through the center of the ring. These deformation lines are most likely caused by use wear.

5.1.1g: Conclusions

- The ring is a high tin bronze with a tin concentration of almost 14 weight percent. The low lead concentration indicates that lead was not purposefully added to the alloy to produce a leaded bronze. There is an unusually high amount of nickel present in the alloy, around two weight percent, which likely comes from the copper's parent ore.
- While the ring's high tin content would have made it relatively hard, it also would have made the metal slightly brittle.
- The stock metal from which the ring is made was cast. The ring was subject to several cycles of working and annealing during its manufacture.
- The stock metal was worked in such a way that its cross section has five distinct facets, giving it an overall lenticular cross section.
- The grooves and segments were worked into the metal by compressing it through use of a tool similar to a chasing tool. This most likely occurred after the metal had been bent into a circle to create a semi-closed ring with overlapping ends.
- The ring was left in an annealed condition, and the few deformation lines present in the microstructure were most likely caused by use wear.

Figure 5.1.1.i: Segmented leg ring. (MIT 5339/Peabody 40-77-40/13267). Photograph by E. Cooney.

Figure 5.1.1.ii: Segmented leg ring. (MIT 5339/Peabody 40-77-40/13267). Segmented sampled for analysis. Photograph by E. Cooney.

Figure 5.1.1.iii: Segmented leg ring (Peabody 40-77-40/13317). This leg ring is similar to MIT 5339. The overlapping tapered ends of this intact semi-closed ring can be seen. Photograph by E. Cooney.

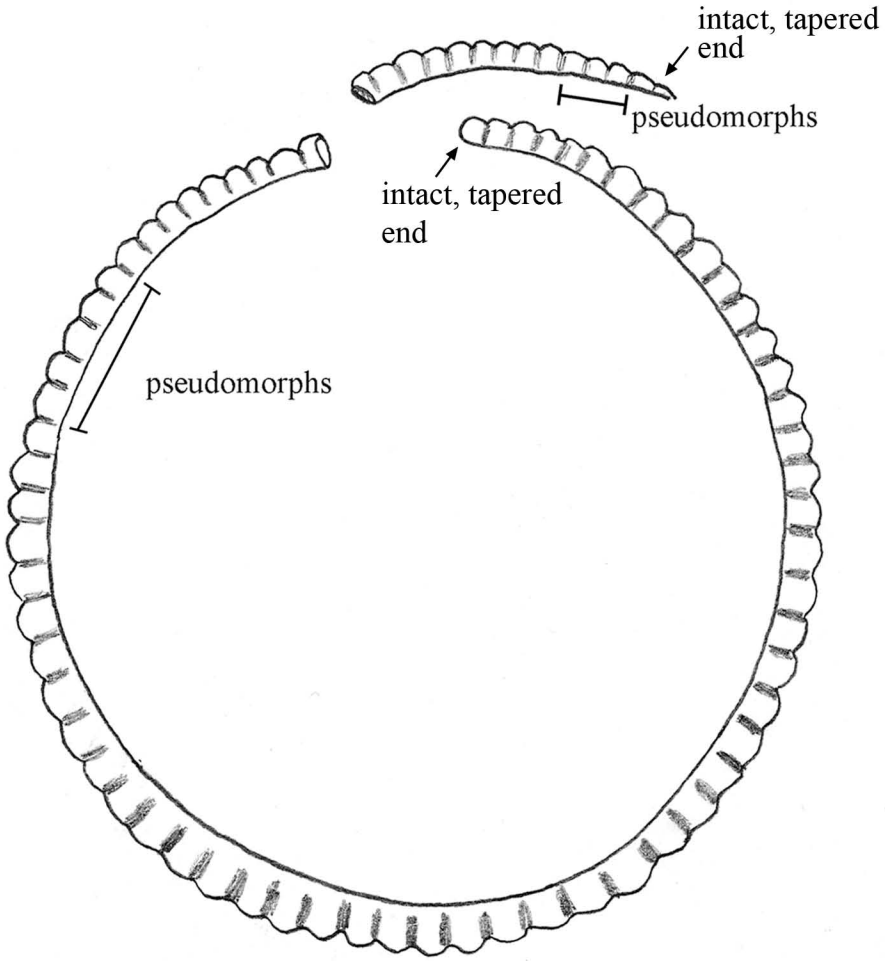

Figure 5.1.1.iv: Segmented leg ring (MIT 5339). Key object features.

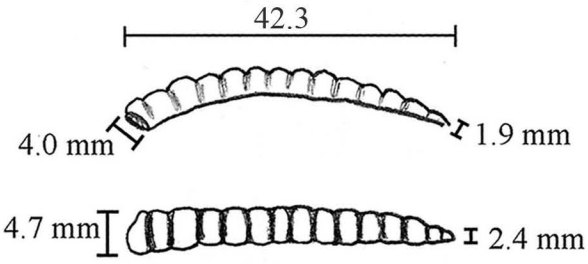

mass of ring: 48.7 g
mass of fragment: 2.7 g

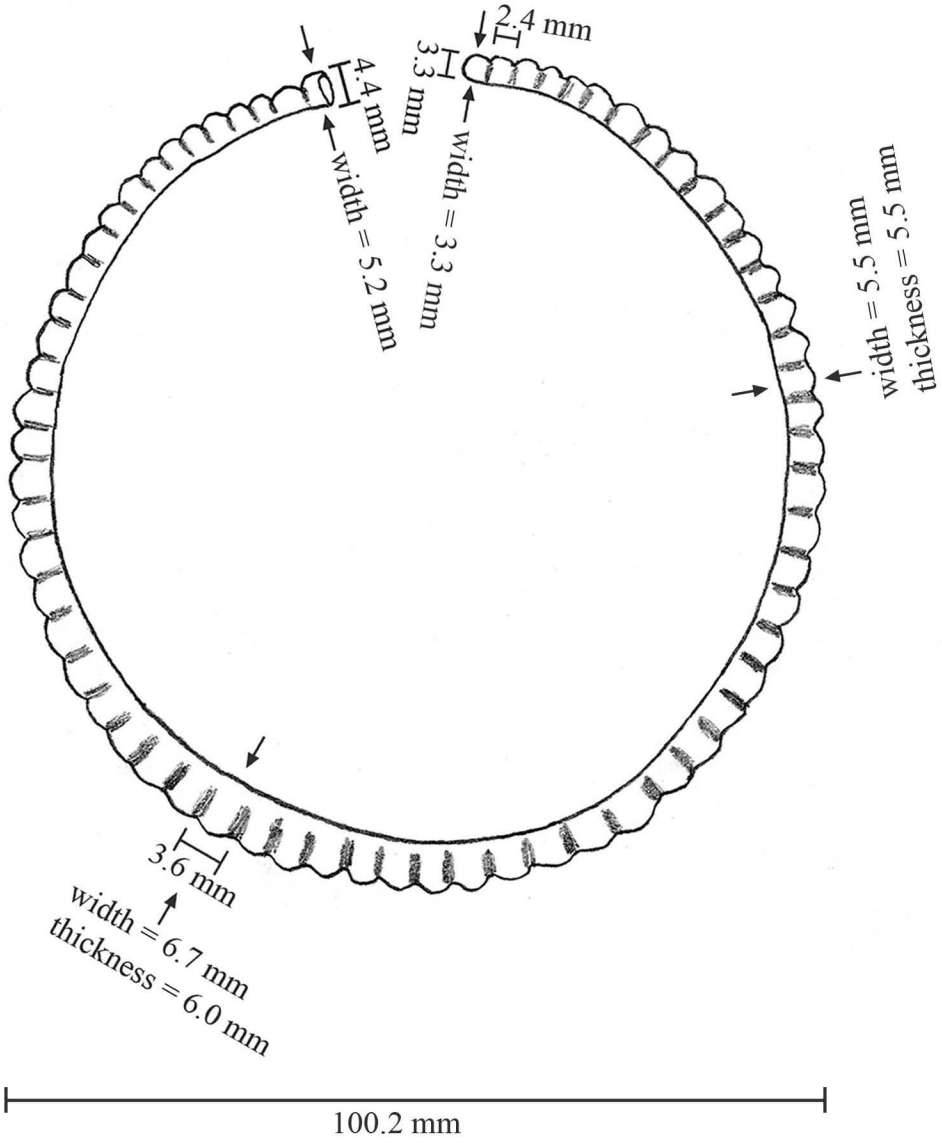

Figure 5.1.1.v: Segmented leg ring (MIT 5339). Drawing and measurements.

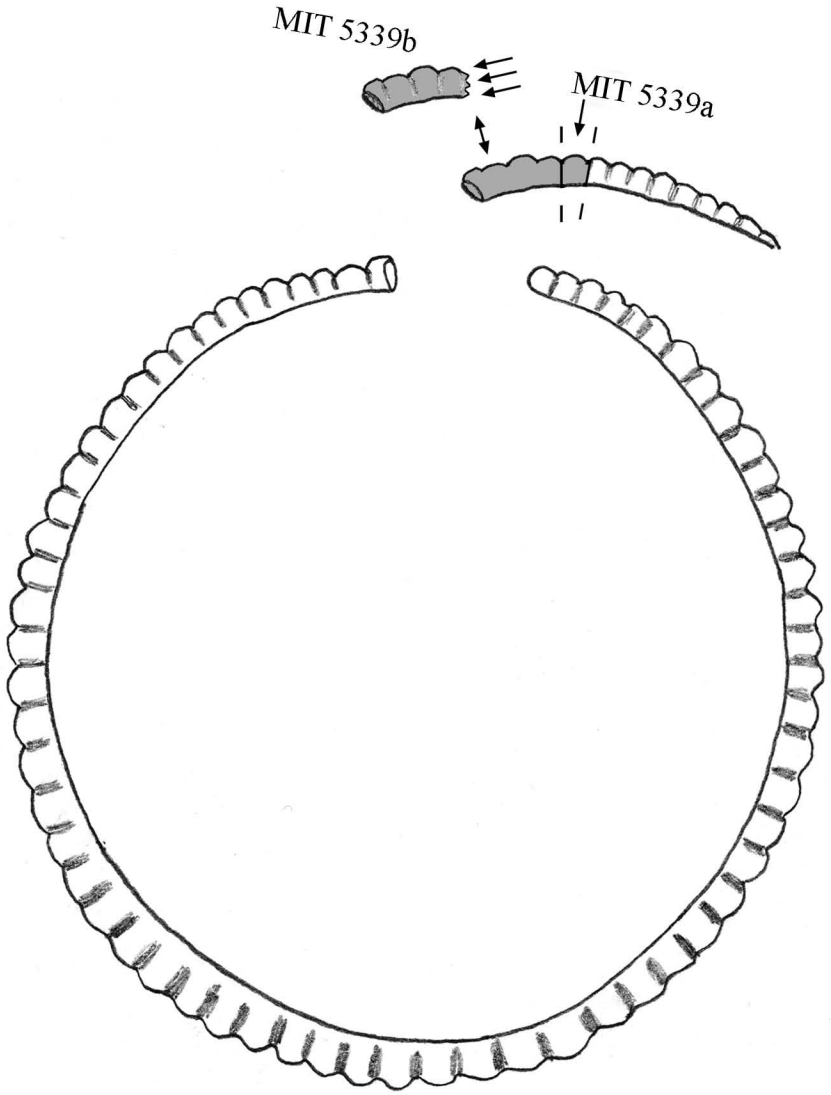

Figure 5.1.1.vi: Segmented leg ring (MIT 5339). Samples removed for analysis. MIT 5339a was removed with transverse cuts for bulk compositional analysis. MIT 5339b was removed with a transverse cut for metallographic analysis and was mounted transversely as noted.

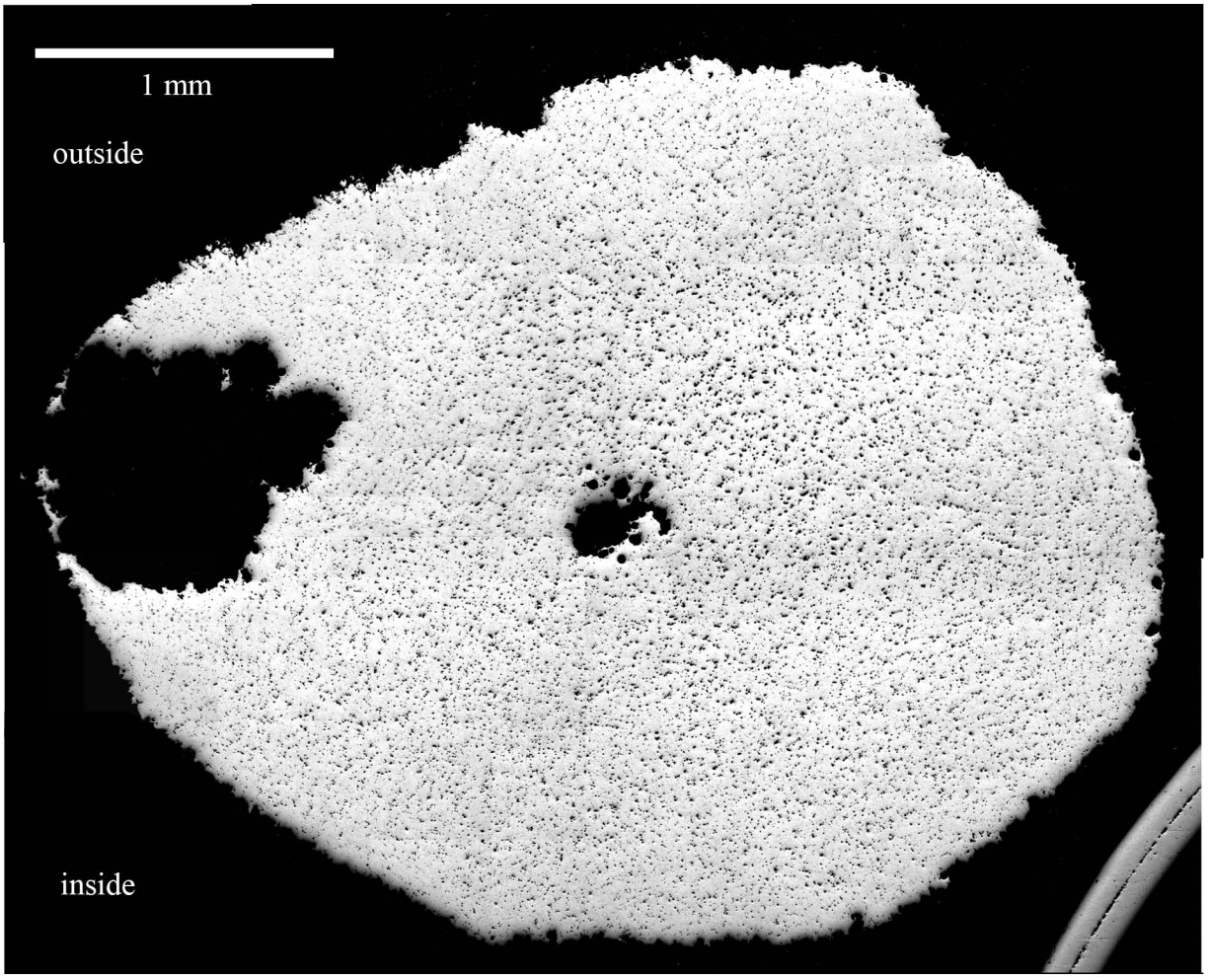

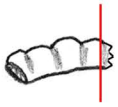
point through which cross section is taken

Figure 5.1.1.vii: Segmented leg ring (MIT 5339/Peabody 40-77-40/13267). Transverse cross section, as polished. Microstructural features of interest include a large shrinkage cavity in the sample's center and a declivity filled with corrosion product on the ring's apparent left side. Other features include a high density of porosities and two types of inclusions. The first type consists of green-blue inclusions that do not appear to be Cu-Sn eutectoid. The second type is a light gray copper sulfide inclusion. (MIT Images 5339b-7-21).

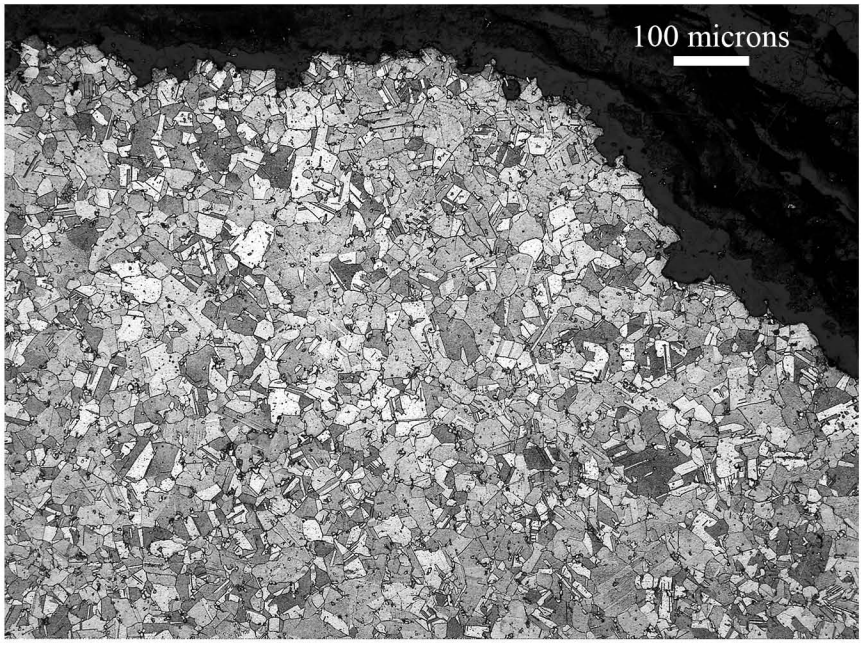

Figure 5.1.1.viii: Segmented leg ring (MIT 5339/Peabody 40-77-40/13267). Transverse cross section. Etch: 2 sec potassium dichromate and 2 sec aqueous ferric chloride. x100. Microstructural features of interest include the equiaxed grains with annealing twins present along the outside edges of the ring at a point where two of the ring's facets meet. (MIT Image 5339b-29.)

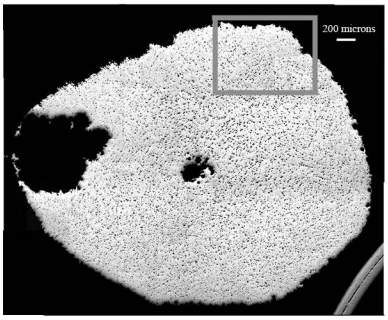

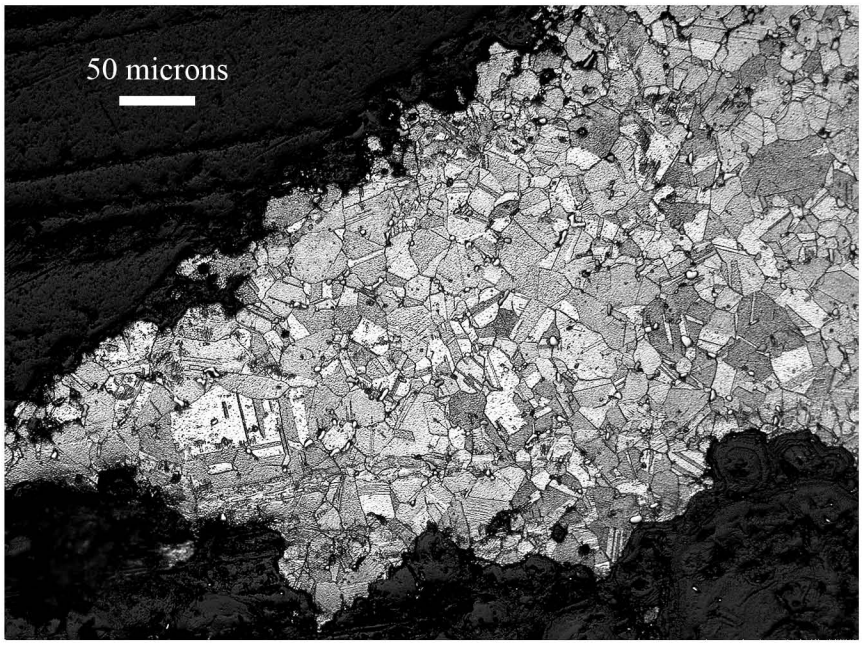

Figure 5.1.1.ix: Segmented leg ring (MIT 5339/Peabody 40-77-40/13267). Transverse cross section. Etch: 2 sec potassium dichromate and 2 sec aqueous ferric chloride. x200. Microstructural features of interest include the equiaxed grains with annealing twins present along the outside edges of the ring at the declivity. A few deformation lines are also present (MIT Image 5339b-30)

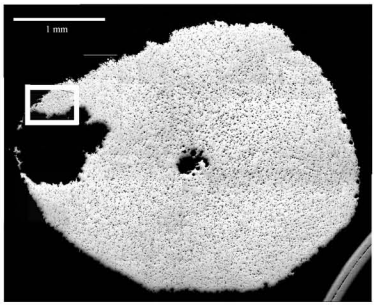

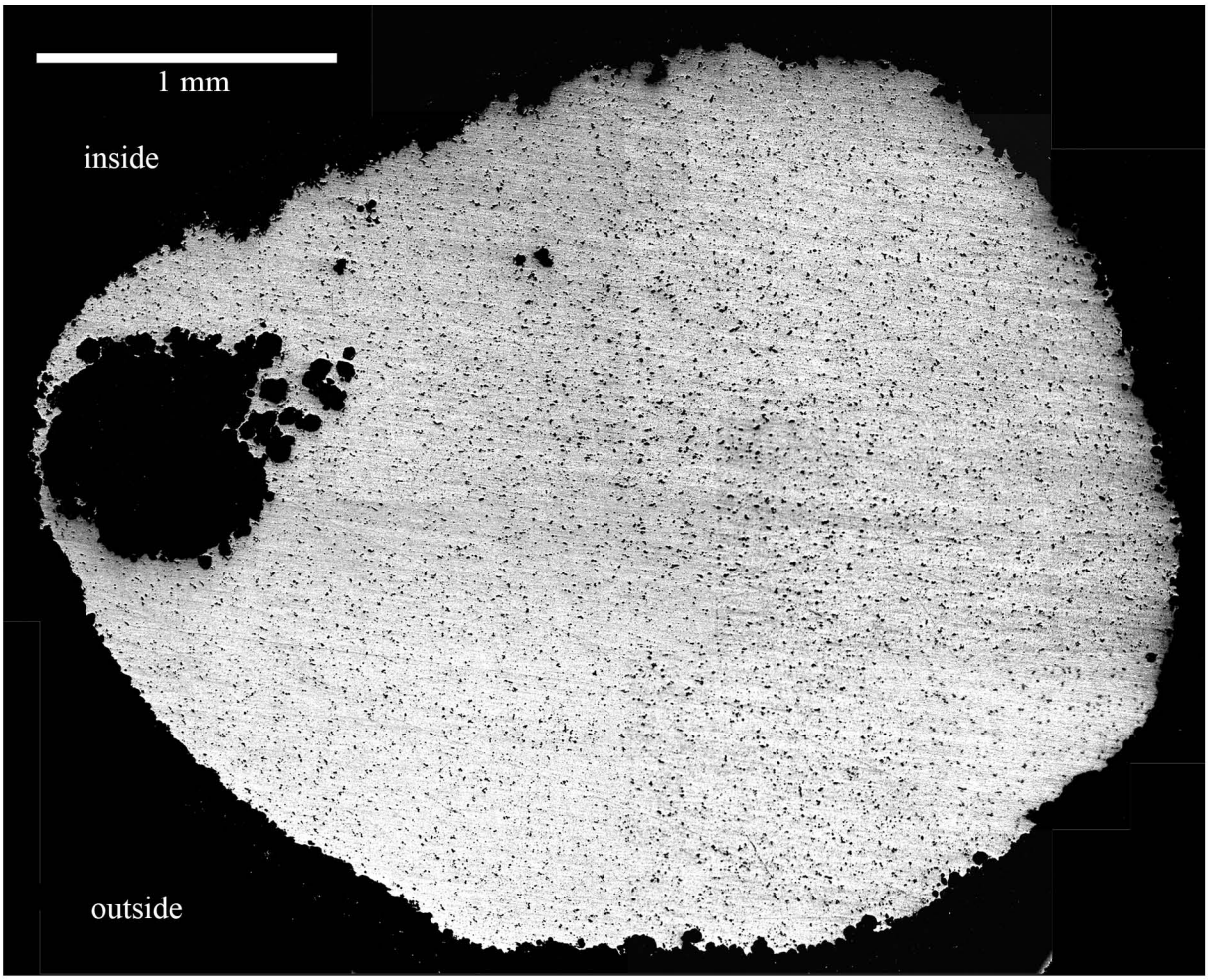

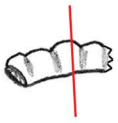

point through which cross section is taken

Figure 5.1.1.x: Segmented leg ring (MIT 5339/Peabody 40-77-40/13267). Transverse cross section, as polished. Microstructural features of interest include a declivity filled with corrosion product on the ring's apparent left side. Other features include a low density of porosities and two types of inclusions. The first type consists of green-blue inclusions that do not appear to be Cu-Sn eutectoid. The second type is light gray copper sulfide inclusions. The large, central pore is not present in this location (MIT Images 5339b-52-66).

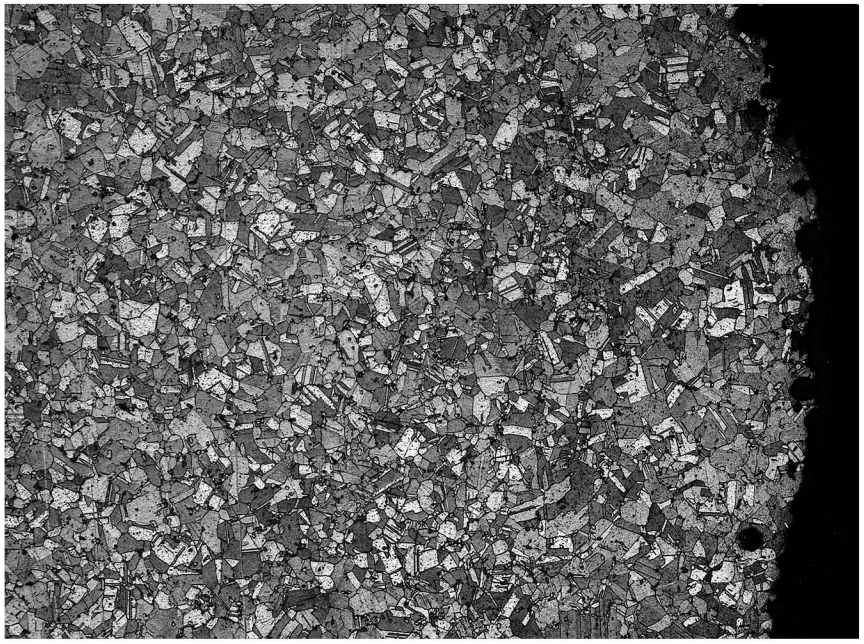

Figure 5.1.1.xi: Segmented leg ring (MIT 5339/Peabody 40-77-40/13267). Transverse cross section after 4th grinding operation. Etch: 2 sec potassium dichromate and 2 sec aqueous ferric chloride. x100. Microstructural features of interest include equiaxed grains with annealing twins along the outside edge of the ring. (MIT Image 5339b-68).

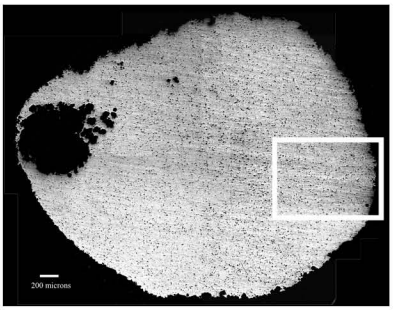

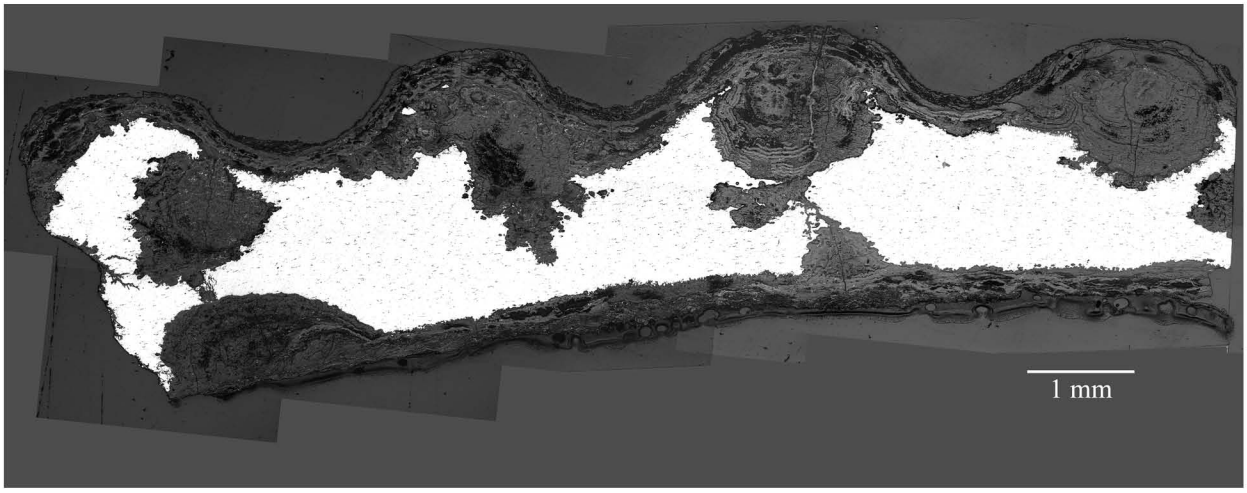

Figure 5.1.1.xii: Segmented leg ring (MIT 5339/Peabody 40-77-40/13267). Longitudinal cross section, as polished. The undulating outline of the segments and grooves can be seen in the longitudinal section's external corrosion product. The longitudinal section shows that the ring fragment is highly corroded internally, especially along the outer surfaces of the ring. This high level of corrosion makes it impossible to see the microstructure at the very surface of the grooves and segments. The green-blue inclusions and gray copper sulfide inclusions are elongated and regularly aligned. In the sample's bulk metal they are oriented parallel to the ring's longitudinal axis and near the ring's surface they are oriented parallel to the walls of the segments and grooves. (MIT Images 5339b-74-87).

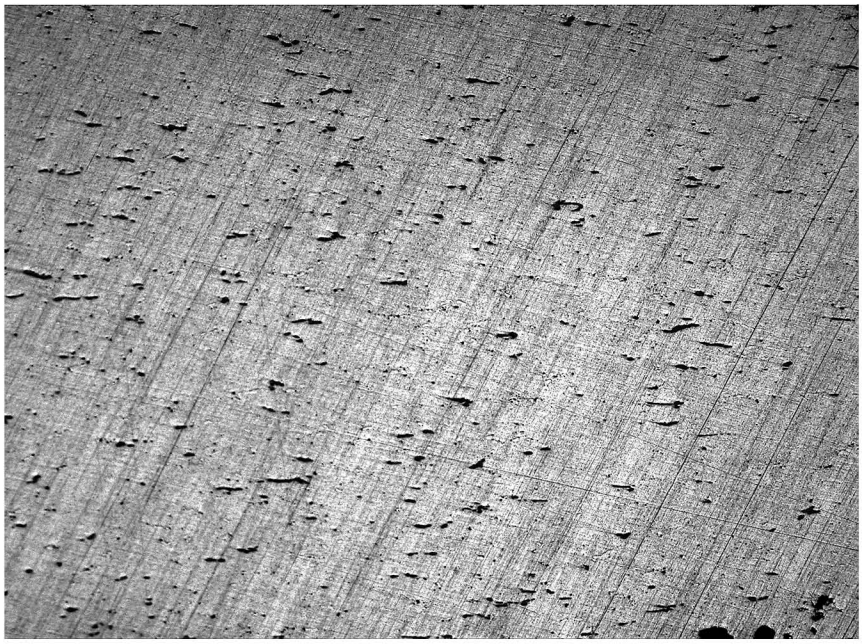

Figure 5.1.1.xiii: Segmented leg ring (MIT 5339/Peabody 40-77-40/13267). Longitudinal cross section, as polished. x100. The blue-green inclusions and gray copper sulfide inclusions in the bulk metal of the sample are elongated and oriented parallel to the ring's longitudinal axis. The scratches in the photomicrograph are an artifact of the polishing process.
(MIT Image 5339b-88).

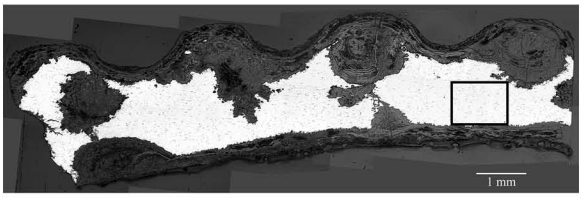

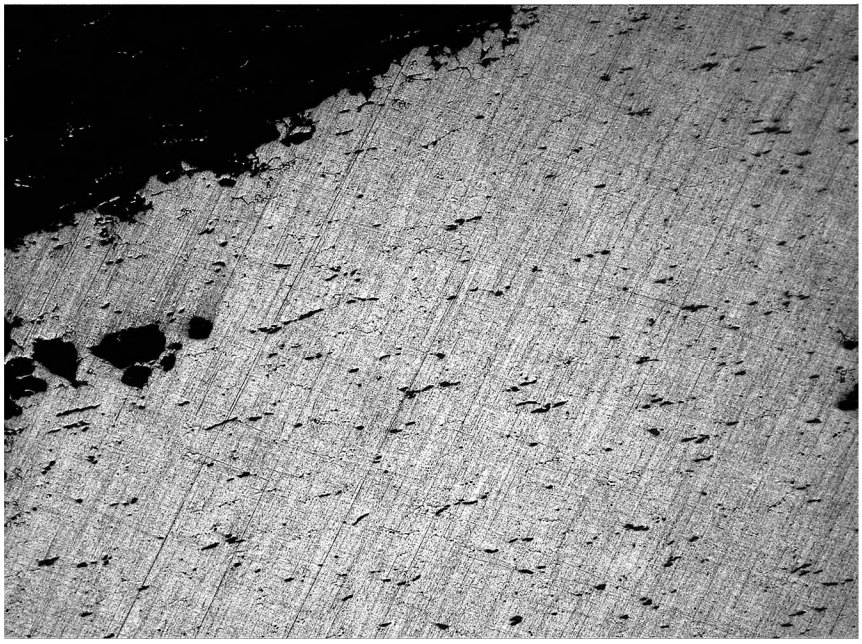

Figure 5.1.1.xiv: Segmented leg ring (MIT 5339/Peabody 40-77-40/13267). Longitudinal cross section, as polished. x100. The blue-green inclusions and gray copper sulfide inclusions close to the ring's surface are aligned at an angle to the longitudinal axis and parallel to the walls of the groove at this location. The scratches in the photomicrograph are an artifact of the polishing process. (MIT Image 5339b-89).

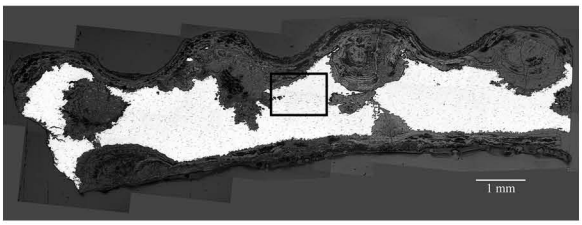

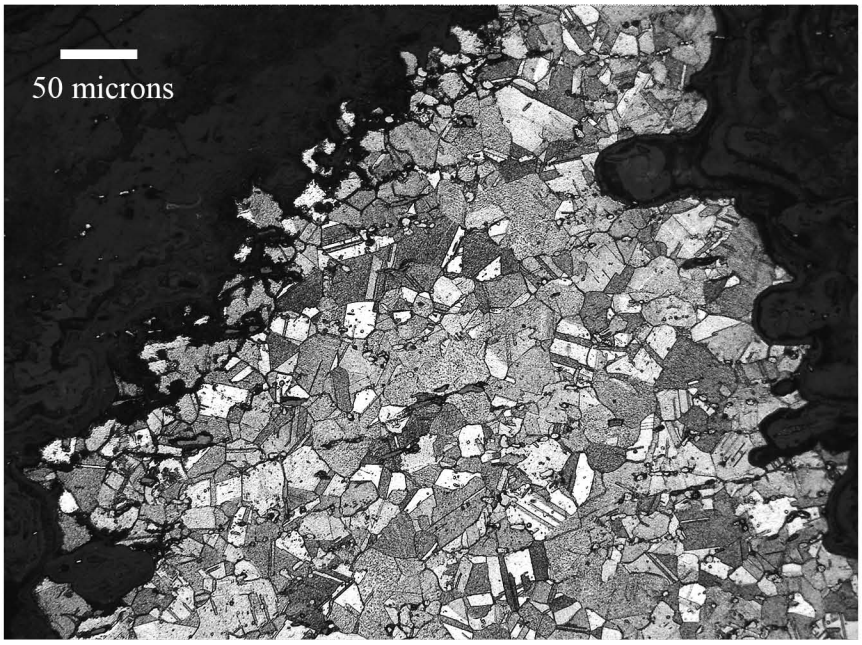

Figure 5.1.1.xv: Segmented leg ring (MIT 5339/Peabody 40-77-40/13267). Longitudinal cross section. Etch: 2 sec potassium dichromate and 2 sec ferric chloride. x200. Microstructural features of interest include equiaxed grains with annealing twins free from deformation lines in an area directly beneath a groove. (MIT Image 5339b-95).

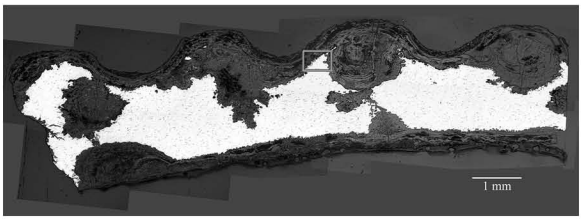

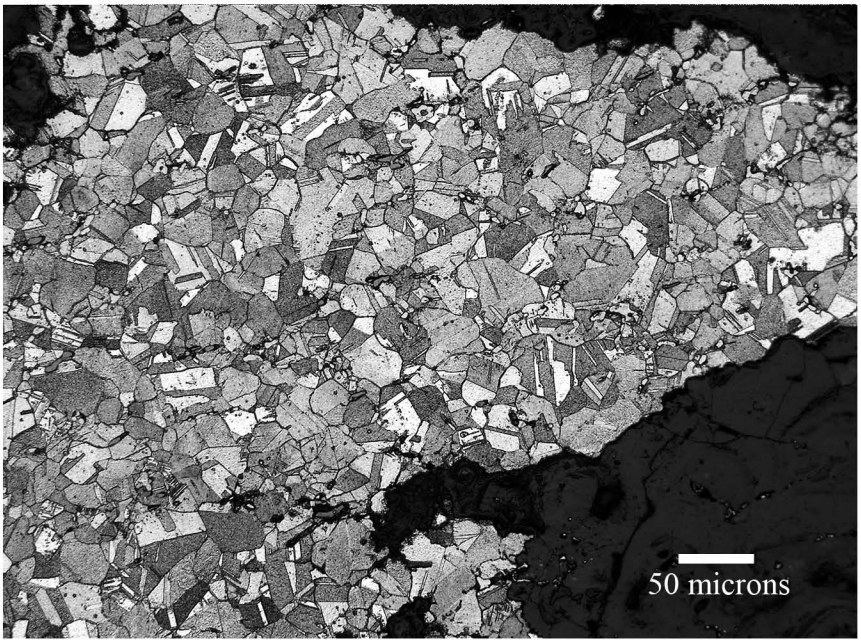

Figure 5.1.1.xvi: Segmented leg ring (MIT 5339/Peabody 40-77-40/13267). Longitudinal cross section. Etch: 2 sec potassium dichromate and 2 sec ferric chloride. x200. Microstructural features of interest include equiaxed grains with annealing twins free from deformation lines in an area directly beneath a segment. (MIT Image 5339b-99.)

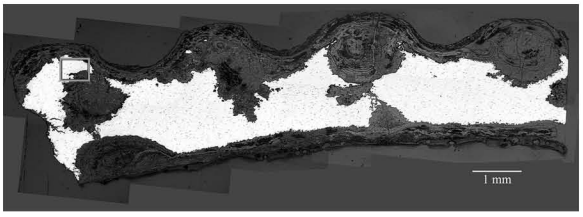

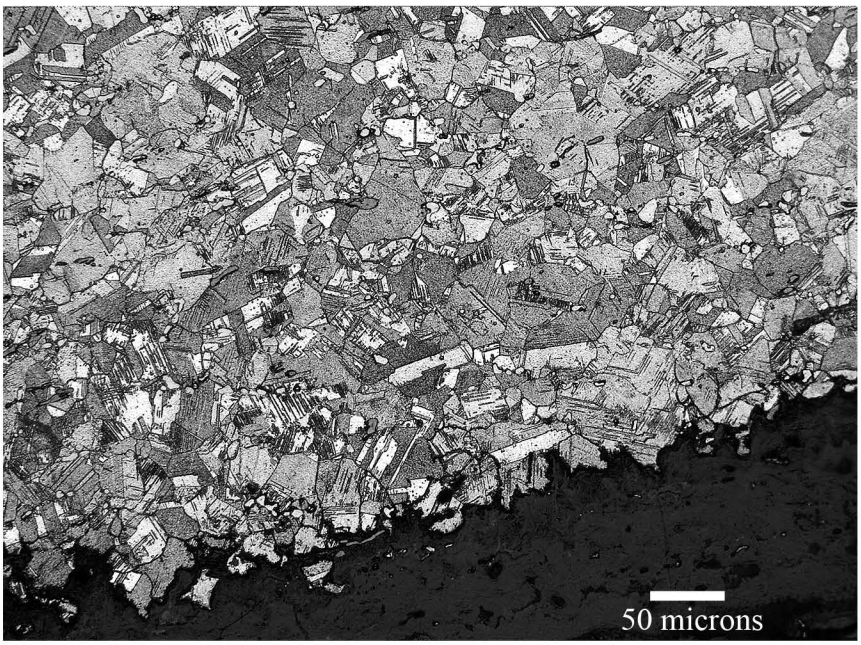

Figure 5.1.1.xvii: Segmented leg ring (MIT 5339/Peabody 40-77-40/13267). Longitudinal cross section. Etch: 2 sec potassium dichromate and 2 sec ferric chloride. x200. Microstructural features of interest include equiaxed grains with annealing twins and deformation lines in the bulk of the sample and close to the inside surface of the ring. (MIT Image 5339b-96).

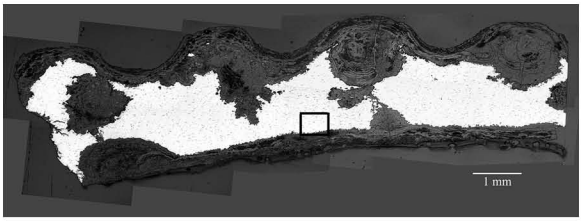

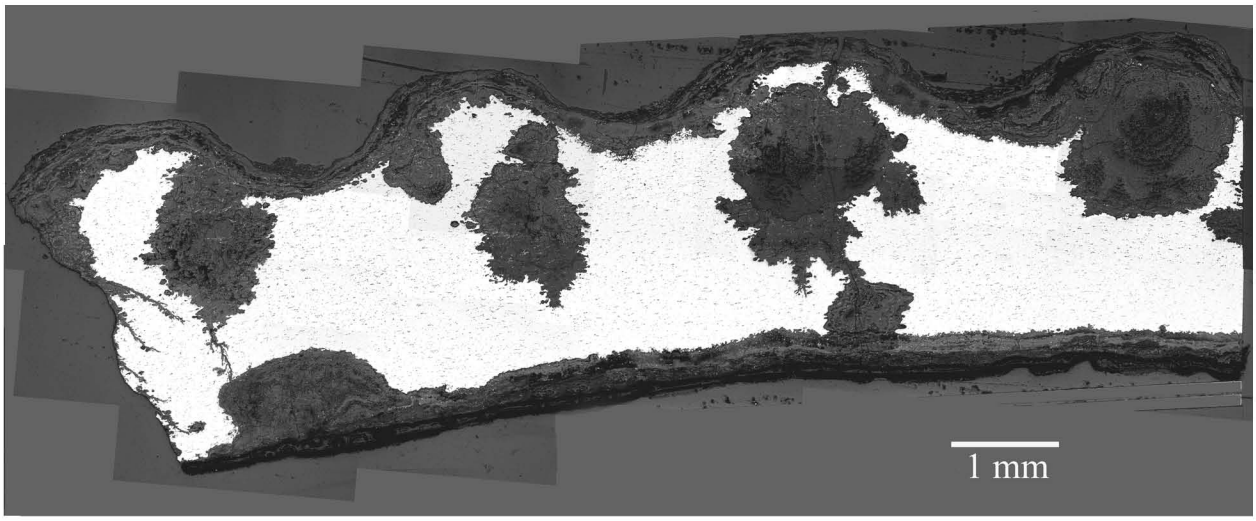

Figure 5.1.1.xviii: Segmented leg ring (MIT 5339/Peabody 40-77-40/13267). Longitudinal cross section after second grinding operation, as polished. The outline of the segments can be seen in the longitudinal section's external corrosion product. The longitudinal section shows that the ring fragment is highly corroded internally, especially along the outer surfaces of the ring. The green-blue inclusions and gray copper sulfide inclusions are elongated and regularly aligned parallel to the ring's longitudinal axis. A crack propogates through the segment second to the apparent right of the sample into the ring's center. (MIT Images 5339b-101-120.)

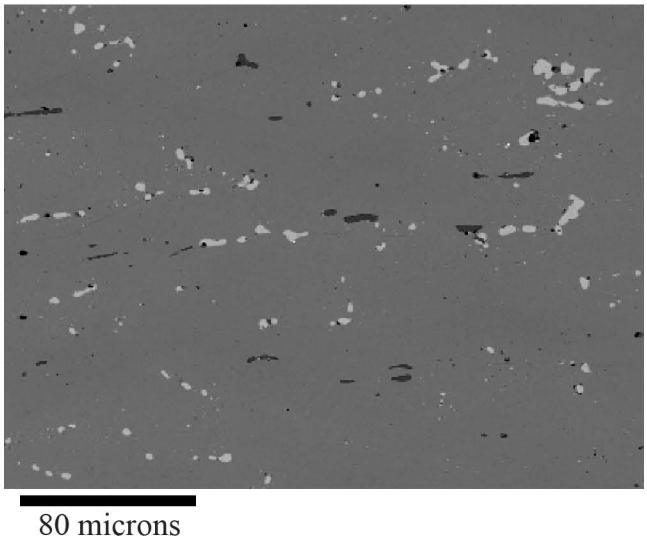

Figure 5.1.1.ixx: Segmented leg ring (MIT 5339/Peabody 40-77-40/13267). Backscattered electron image of the longitudinal section after 2nd grinding showing the elongated inclusions oriented parallel to the longitudinal axis. The dark appearing inclusions correspond to the gray copper-sulfide inclusions discussed previously. The light appearing inclusions correspond to the green-blue inclusions discussed earlier. The electron microbeam probe gives the composition of these light appearing inclusions as 51.9 weight percent copper, 37.4 weight percent tin, and 12.9 weight percent nickel.

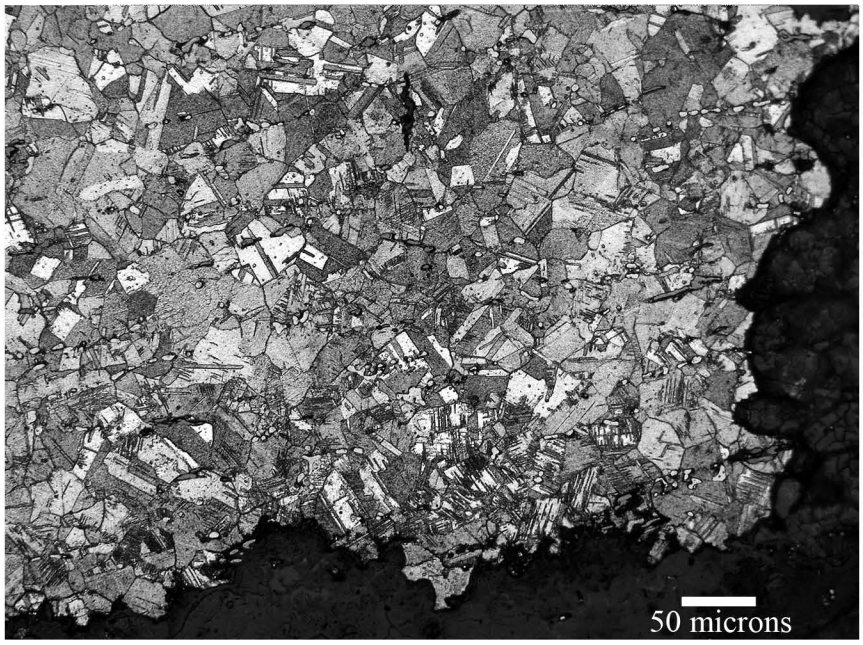

Figure 5.1.1.xx: Segmented leg ring (MIT 5339/Peabody 40-77-40/13267). Longitudinal cross section. Etch: 2 sec potassium dichromate and 2 sec aqueous ferric chloride. x200. Microstructural features include a high density of deformation lines directly to the left of the crack propogating through the ring. (MIT Image 5339b-124).

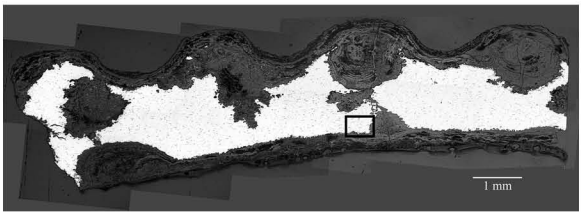

5.1.2: Segmented Leg Ring (MIT 5336/Peabody 40-77-40/13402)

5.1.2a: Provenance

MIT 5336 (Figure 5.1.2.i) consists of six fragments from at least two separate segmented rings. Both these rings both come from Grave 26 and are identified by Wells (1981) as thin, segmented bronze rings. The Peabody Museum further identifies them as segmented leg rings. These rings were associated with a small burned area and sherds of a large, reddish-brown vessel. The excavation notes suggest that this grave may have been disturbed in antiquity.

5.1.2b: Initial Examination and Observations

The fragments of the segmented leg rings were photographed (Figure 5.1.2.i). The fragment chosen for sampling was photographed individually (Figure 5.1.2.ii). The largest fragment and the fragment chosen for sampling were drawn to scale and measured (Figures 5.1.2.iii and iv).

The rings are broken into six pieces, and four of the fragments have intact, tapered ends, indicating that the fragments originally came from solid semi-closed rings with overlapping, tapered ends. The ring fragments are completely covered by friable light green corrosion product. Together the six fragments weigh 66.8 grams.

The largest fragment has an intact, tapered end and maintains enough of the original ring to show that the ring was roughly circular with a diameter of 9.94 cm. The cross section is lenticular and is 4.2 mm wide x 3.7 mm thick at the tapered end and 5.4 mm wide x 5.5 mm thick at the fractured end. Textile pseudomorphs in the shape of loose threads can be seen on the inside surface of the rings' largest fragment.

The fragment chosen for sampling (Figure 5.1.2.ii) weighs 3.3 g and has a plano-convex cross section 5.5 mm wide x 5.0 mm thick. Textile pseudomorphs in the shape of threads are present along its inside surface.

Although the segmented pattern has been worn away or completely obscured in many areas on the fragments, it is clear that the rings were originally segmented along their entire length. Only a few areas have a surface intact enough for the segments and grooves to be measured and observed. The best preserved area is on the largest fragment

where the segments and grooves are shaped and spaced uniformly. The segments are 5.5 mm wide x 2.5 mm long at a point where the ring is 5.4 mm thick. Each groove proceeds along the entire outside surface of the ring, the inside surface is ungrooved and smooth. The grooves have a rounded, concave, semi-annular shape and are approximately 0.7 mm wide. Because of the extent of the corrosion, the width of the segments and grooves at the tapered ends cannot be compared accurately with those at the middle of the rings.

The fragment chosen for sampling had a freshly cut end revealing a highly metallic interior (Figure 5.1.2.ii). This fragment was sampled by Murray in 1985 as part of a Harvard, Department of Anthropology class laboratory assignment; the text of his report is on file with the Peabody Museum.

5.1.2c: Sampling

Sample MIT 5336 was removed from the ring fragment as a transverse section (Figure 5.1.2.v) for bulk composition analysis. This sample was removed adjacent to the previous cut made by Murray. The fragment had a light gold metallic core surrounded by a fairly thick layer of dark gray, friable corrosion at its edges.

5.1.2d: Composition Analysis

Bulk composition analysis determined that the segmented ring is a mostly copper-tin-lead alloy with the main alloying elements of tin at a concentration of 4.68 weight percent and lead at a concentration of 1.88 weight percent. The alloy is a leaded, low tin bronze. Other major and minor elements include Sb (0.791%), Ni (0.757%), Ag (0.433%), and As (0.376%). Bulk composition analysis data are given in Table 5.1.2 and in the Appendix.

Table 5.1.2: Bulk Composition Analysis Data for MIT 5336

	Sn	**Pb**	**Sb**	**As**	**Ni**	**Co**	**Ag**	**Fe**
ICP-ES	4.68	1.88	0.788	0.399	0.675	0.014	n.a.	0.008
INAA	2.65	n.a.	0.791	0.376	0.757	0.0178	0.433	n.d.

(values in weight %) n.a. = not analyzed n.d. = not determined

5.2.1e: Conclusions

- The segmented leg ring is a leaded, low tin bronze with a tin concentration of 4.68 weight percent and a lead concentration of 1.88 weight percent.
- MIT 5336 has a much lower tin concentration and a slightly higher lead concentration than MIT 5339, the segmented leg ring discussed in Section 5.1.1.

Figure 5.1.2.i: Segmented leg rings. (MIT 5336/Peabody 40-77-40/13402). Photograph by E. Cooney.

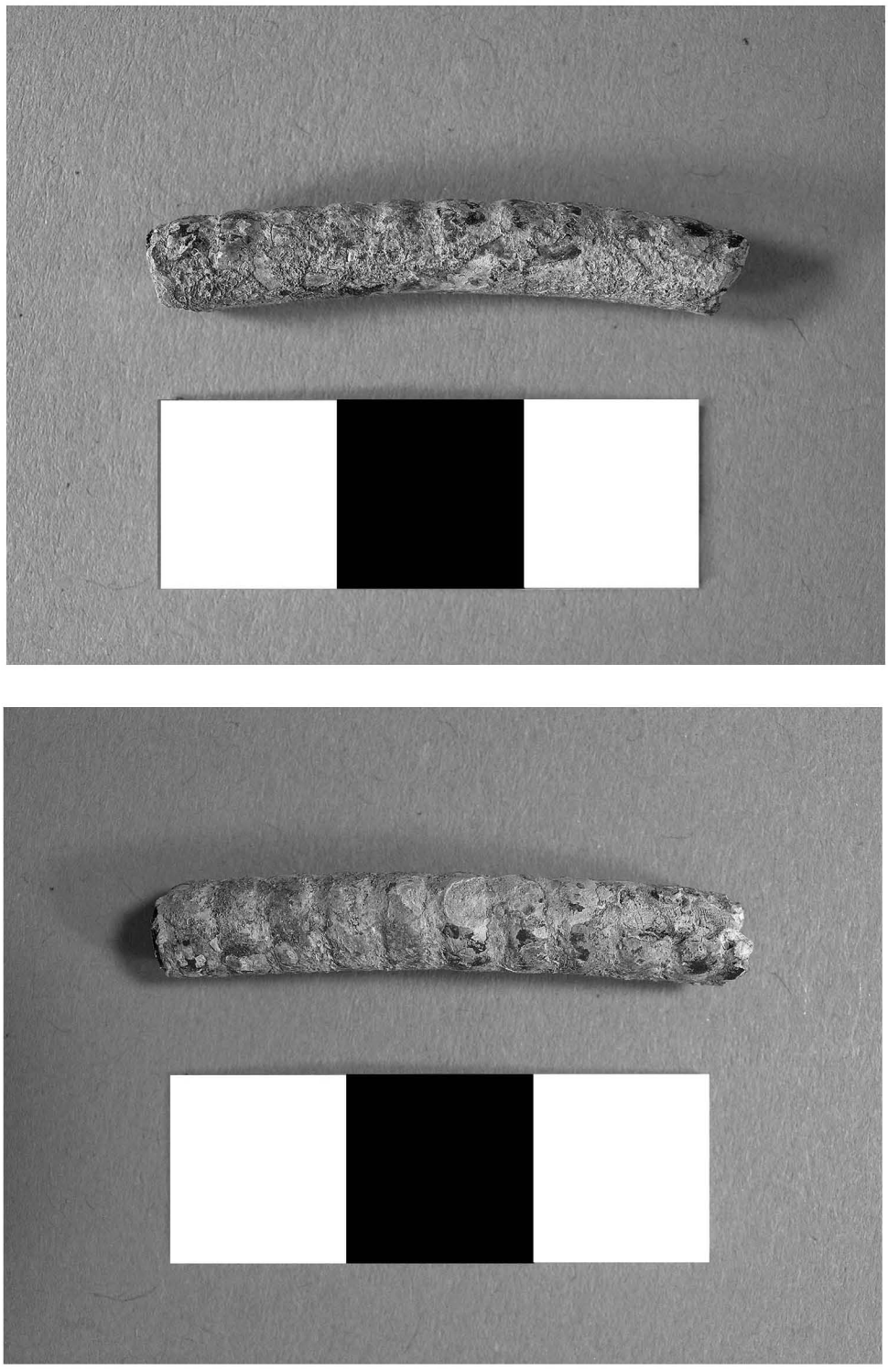

Figure 5.1.2.ii: Segmented leg rings, segment chosen for sampling. (MIT 5336/Peabody 40-77-40/13402). Photographs by E. Cooney.

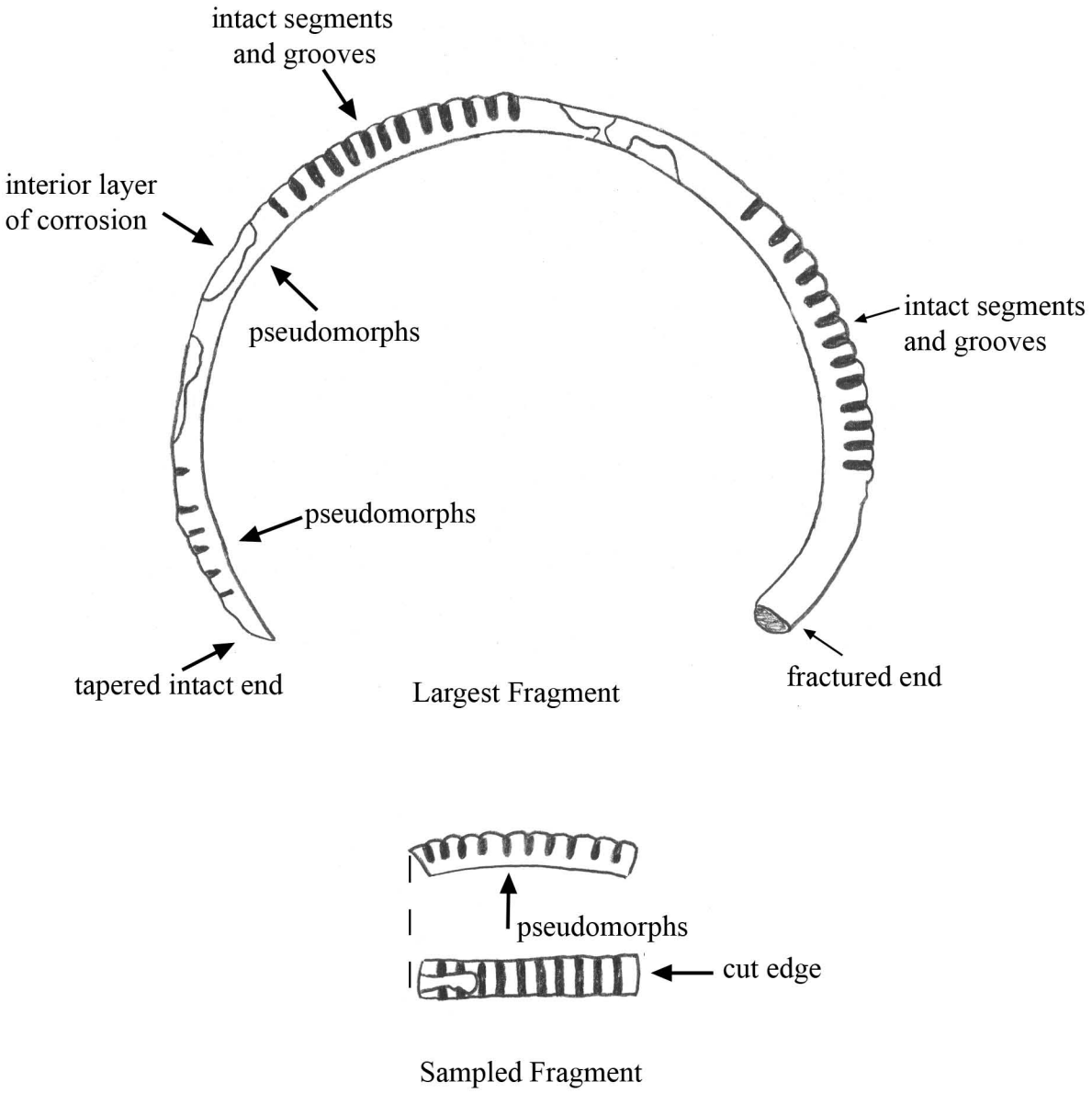

Figure 5.1.2.iii: Segmented leg ring (MIT 5336). Key object features.

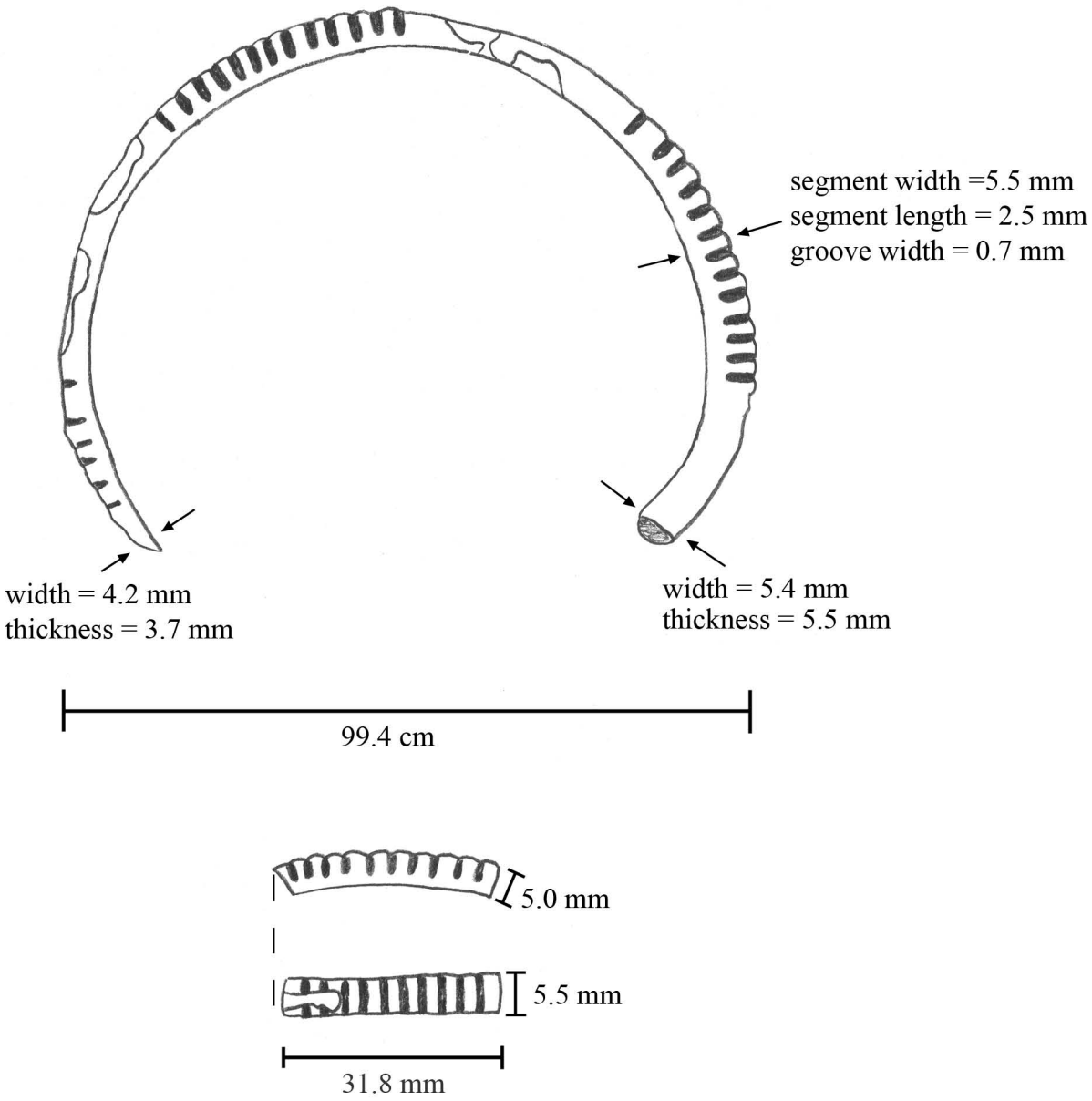

Figure 5.1.2.iv: Segmented leg ring (MIT 5336). Drawing and measurements.

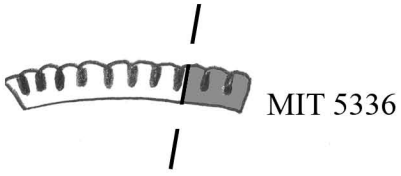

Figure 5.1.2.v: Segmented leg ring (MIT 5336). Sample MIT 5336 was removed for bulk compositional analysis.

5.1.3: Segmented upper arm ring (MIT 5341/Peabody 40-77-40/13426)

5.1.3a: Provenance and Background

MIT 5341 (Figure 5.1.3.i) is a fragmented upper arm ring from Grave 28 (Wells 1981). The excavation notes indicate that Grave 28 was a cremation grave.

Associated grave goods include a second, similar segmented upper arm ring and a segmented arm ring/bracelet.

Although from a cremation grave, MIT 5341 was analyzed for metallographic analysis because it is the only fragmented upper arm ring in Tumulus IV.

5.1.3b: Initial Examination and Observations

The upper arm ring was photographed (Figures 5.1.3.i and 5.1.3.ii), drawn to scale, measured, and observed (Figures 5.1.3.iii and 5.1.3.iv).

The segmented upper arm has been broken into three fragments. It does not appear that any additional pieces are missing from the ring. The ring was originally roughly circular in shape with a diameter of 120.8 mm. It is solid and has a lenticular cross section that varies in area across the ring. Fragments B and C maintain intact ends comprised of segments decorated by incised lines running perpendicular to the ring's longitudinal axis. These intact ends do not appear to have overlapped, indicating that the upper arm ring was an open ring. The third fragment has a cut edge, indicating that it was previously sampled. No record of this bracelet having been sampled previously could be found in the Peabody's archives.

The bracelet is structurally robust. Fragment A weighs 27.5 g. It is 64.4 mm long, 9.0 mm wide, and 7.8 mm thick.

Fragment B weighs 49.6 g. At its broken end, Fragment B has a width of 8.9 mm and a thickness of 7.4 mm. Its intact end is 7.5 mm wide and 7.1 mm thick.

Fragment C weighs 41.9 g. Its broken end is 8.9 mm wide and 7.8 mm thick. Its intact end is 7.4 mm wide and 6.3 mm thick. The segment comprising the intact end measures 7.2 mm in length.

The segments are all evenly spaced and smooth. They range in segment length from 6.1 to 7.2 mm. Each groove proceeds along the entire outside surface of the ring;

the inside surface is ungrooved and smooth. The grooves have a rounded, concave, semi-annular shape and a consistent width of 1.5 mm across the ring.

The ring is covered with a thin layer of dark and light green, friable corrosion product. In a few areas earthy accretions still adhere to the outside surface.

5.1.3c: Sampling

Fragment A was sampled twice with transverse cuts (Figure 5.1.3.v). Sample MIT 5341a was removed for bulk composition analysis. Sample MIT 5341b was removed for metallographic analysis and was mounted transversely as noted. The ring was highly metallic, and the metal was light gold in color.

5.1.3d: Bulk Composition Analysis

Bulk composition analysis shows that the upper arm ring is made from a leaded, low tin bronze with tin present at a concentration of 4.97 weight percent and lead present at a concentration of 3.04 weight percent. Additional minor and trace elements include Sb (0.469%), As (0.373%), Ni (0.284%), Ag (0.254%), Fe (0.23%), and Co (0.03%). Bulk composition analysis data are given in Table 5.1.3 and in the Appendix.

Table 5.1.3: Bulk Composition Analysis Data for MIT 5341 (Upper Arm Ring)

	Sn	**Pb**	**Sb**	**As**	**Ni**	**Co**	**Ag**	**Fe**
ICP-ES	4.97	3.04	0.416	0.35	0.293	0.02	n.a.	<0.005
INAA	4.36	n.a.	0.469	0.373	0.284	0.0309	0.254	0.23

(values in weight %) n.a. = not analyzed n.d. = not determined

5.1.3e: Metallographic Analysis

Sample 5341b was mounted transversely. In the polished section, microstructural features of interest include large porosities homogenously distributed throughout the sample and equiaxed grains outlined by internal corrosion product around the edges of the sample (Figure 5.1.3.vi). A few blue-green inclusions are also present distributed homogenously throughout the sample. The porosities indicate that the metal comprising the bracelet was cast, but as they do not outline dendrites, the metal must have been worked after casting.

The sample was etched for three seconds with alcoholic ferric chloride and for three seconds with ferric nitrate to reveal a microstructure characterized by equiaxed grains with annealing twins (Figure 5.1.3.vii). This final anneal may have occurred as a result of the heat of the cremation fire; it is impossible to determine whether the ring was purposefully left in an annealed state.

5.1.3f: Discussion

The upper arm ring is a low tin, leaded bronze. The metal comprising the ring was cast to shape and then worked. It is not clear if the segments were cast in place or if they were engraved into the metal. Because the ring is an open ring, it is likely that the ring was first cast as an ingot of stock material before being worked into its final, circular, open ring shape. The low concentration of tin would have made the ring relatively soft and malleable. This malleability would have made it easier to work such a thick, weighty piece of metal into its final, circular shape. Because of its weight and relative softness, the ring was likely for decorative, ritual use only.

5.1.3e: Conclusions

- The upper arm ring is a low tin, leaded bronze with tin present at a concentration of 4.97 weight percent and lead present at a concentration of 3.04 weight percent.
- The ring was most likely cast as an ingot and was subsequently worked into a circular ring shape.
- The low tin concentration would have made the ring relatively malleable. Because of its weight and relative softness, the ring was likely for decorative, ritual use only.

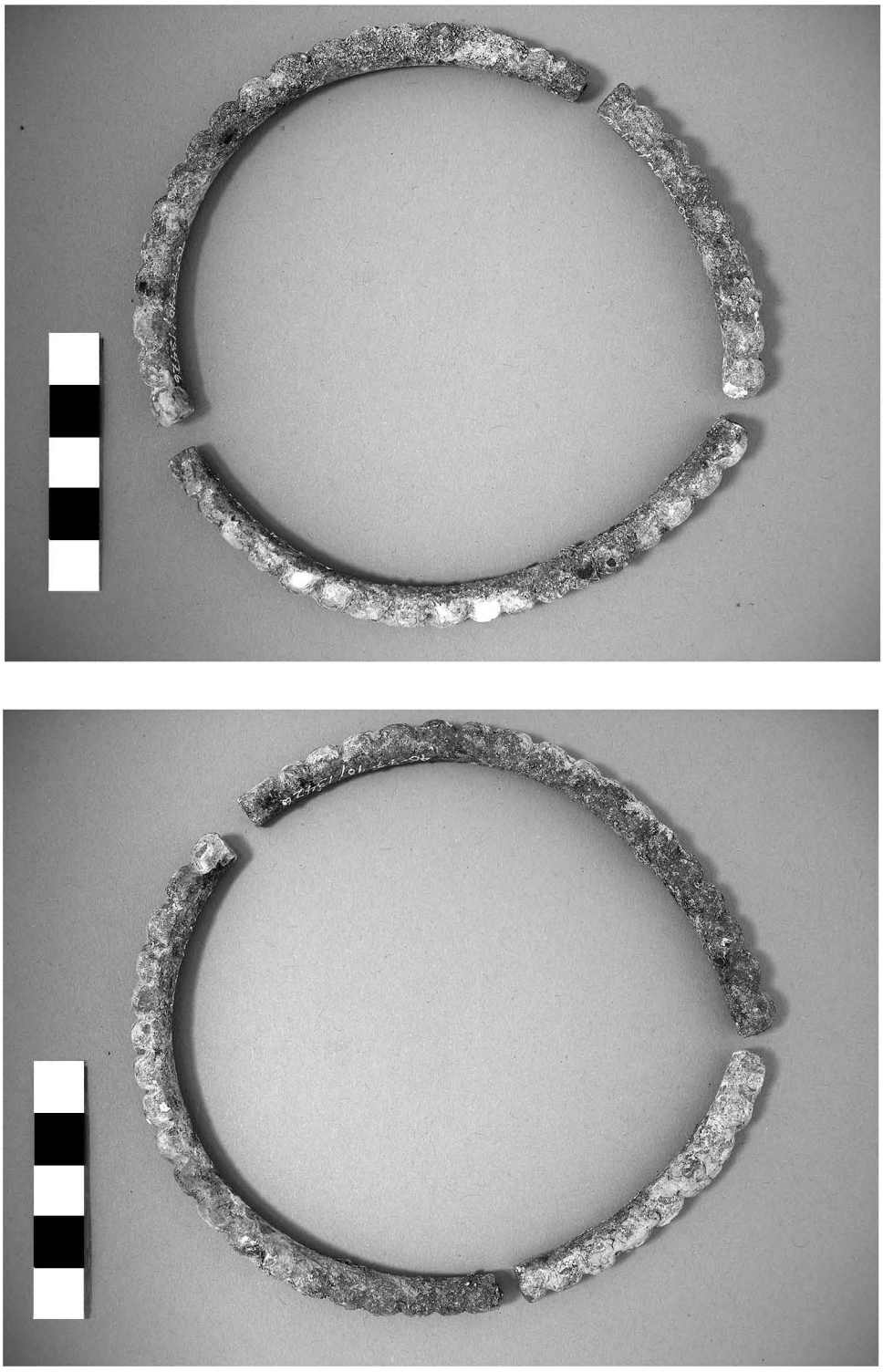

Figure 5.1.3.i: Segmented upper arm ring. (MIT 5341/Peabody 40-77-40/13426). Photograph by E. Cooney.

FIgure 5.1.3.ii: Segmented upper arm ring. (MIT 5341/Peabody 40-77-40/13426). Fragment chosen for sampling. Photograph by E. Cooney.

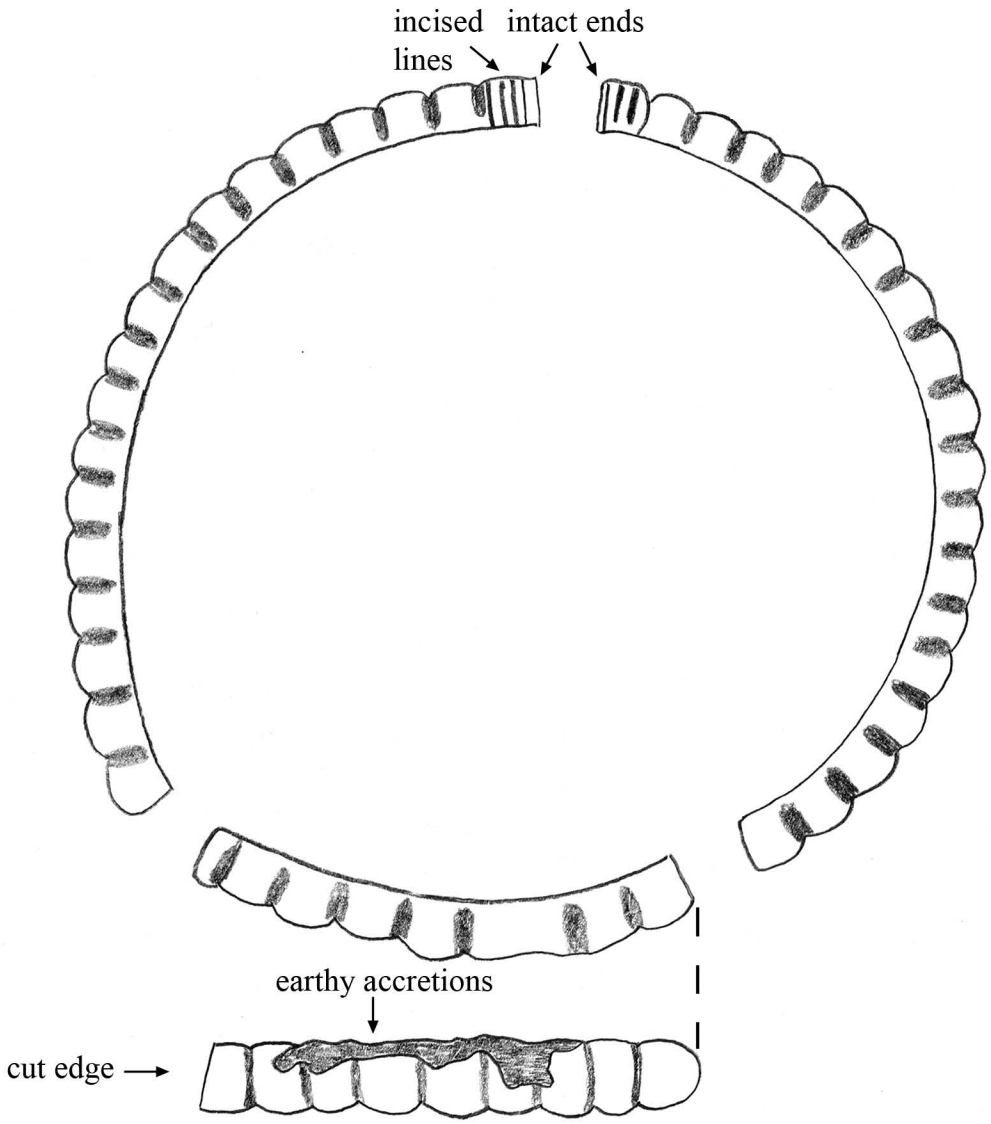

Figure 5.1.3.iii: Segmented upper arm ring (MIT 5341). Key object features.

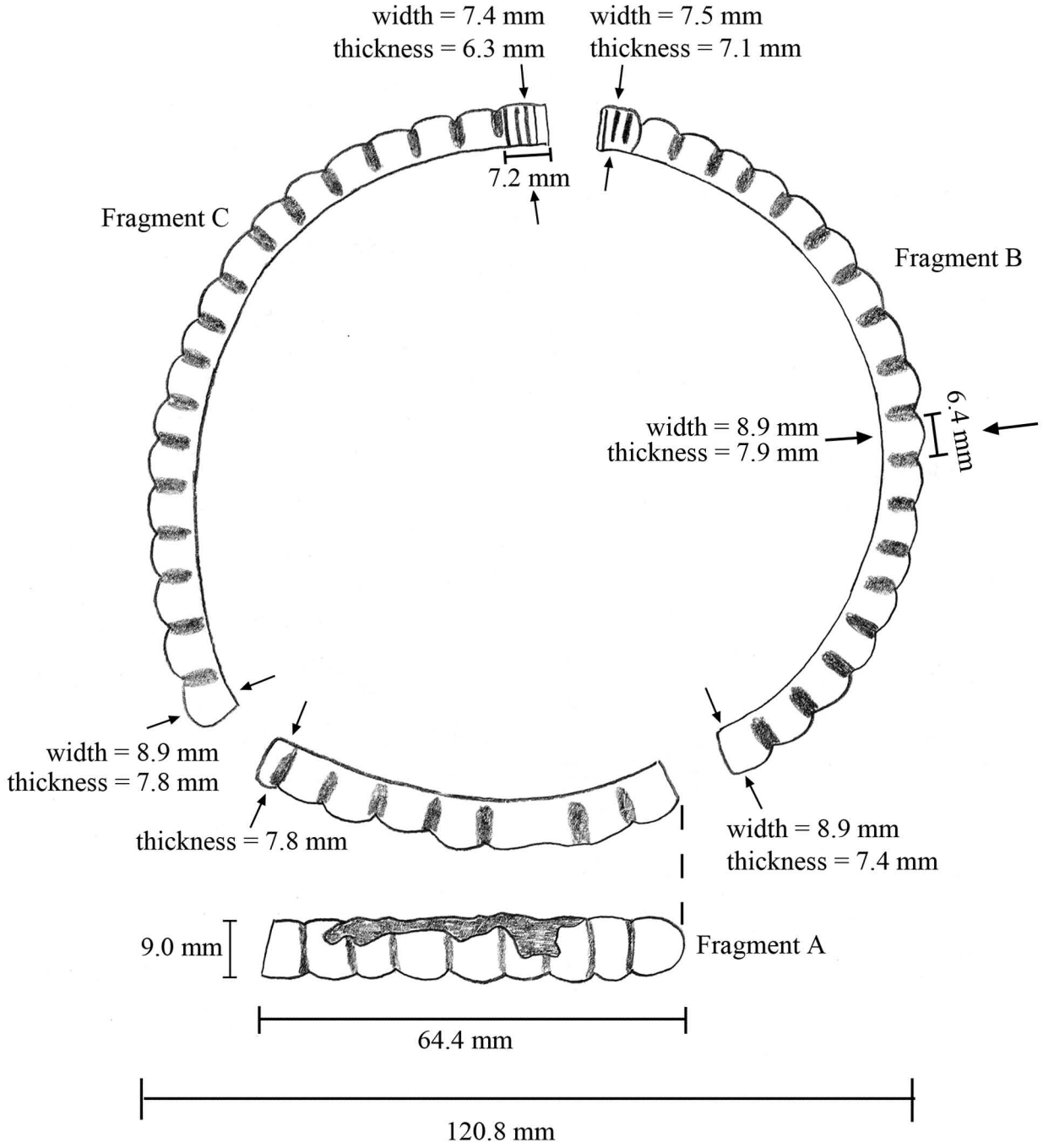

Fragment A = 27.5 g
Fragment B = 49.6 g
Fragment C = 41.9 g

Figure 5.1.3.iv: Segmented upper arm ring (MIT 5341). Drawing and measurements.

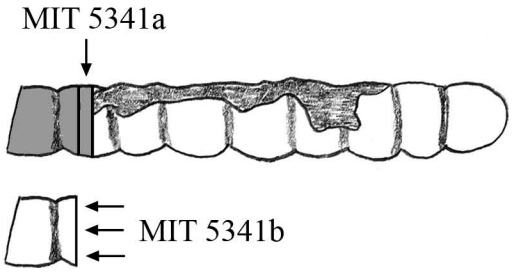

5.1.3.v: Samples removed from segmented upper arm ring. MIT 5341a was removed for bulk compositional analysis. MIT 5341b was removed for metallographic analysis and was mounted transversely as noted.

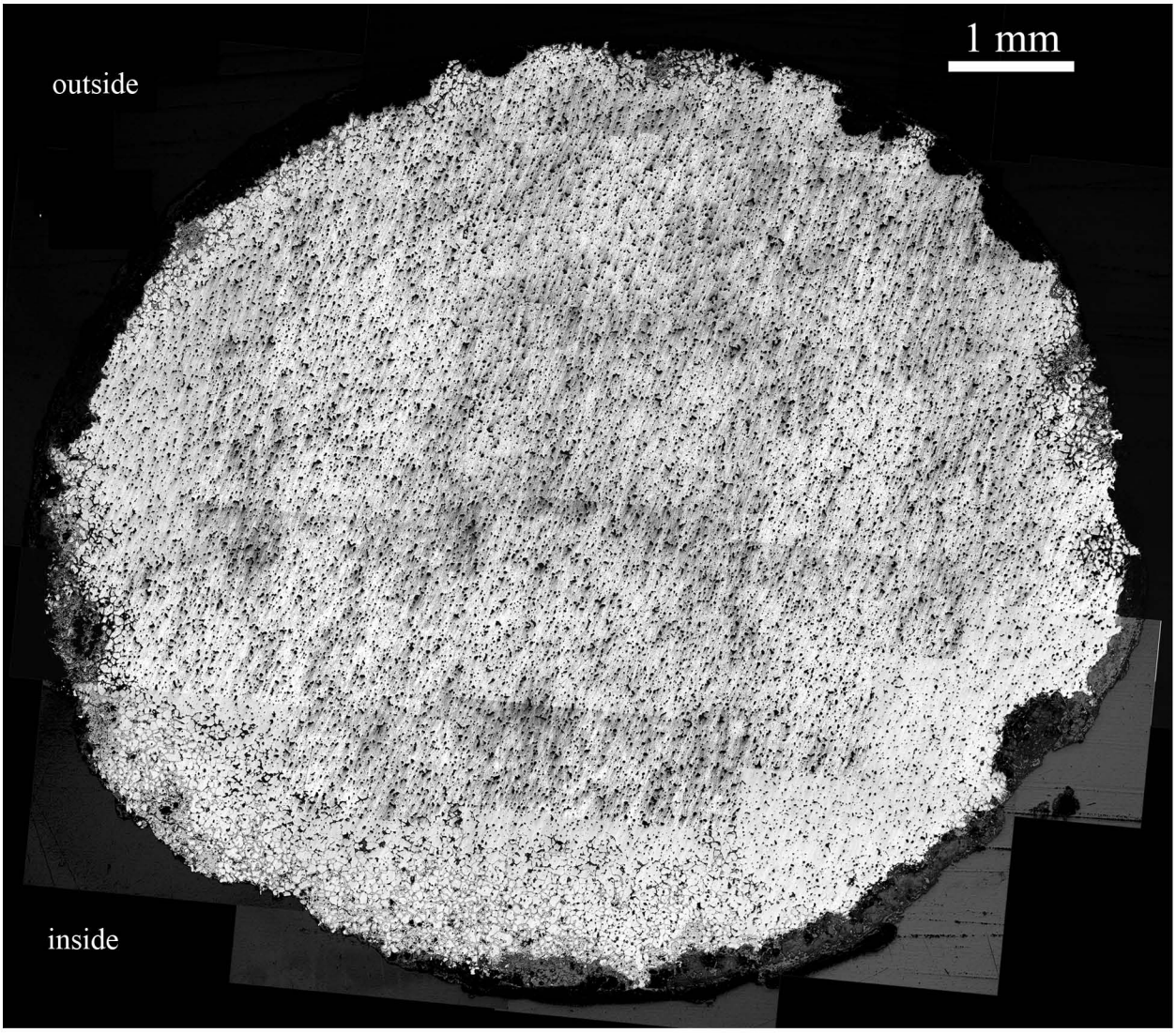

Figure 5.1.3.vi: Segmented upper arm ring (MIT 5341/Peabody 40-77-40/13426). Transverse cross section, as polished. The smeared appearance of the photomicrograph is an artifact of the polishing process. Microstructural features of interest include porosities/dark material homogenously distributed throughout the sample and the equiaxed grains outlined by internal corrosion product around the edges of the sample. (MIT Images 5341b-08-39.)

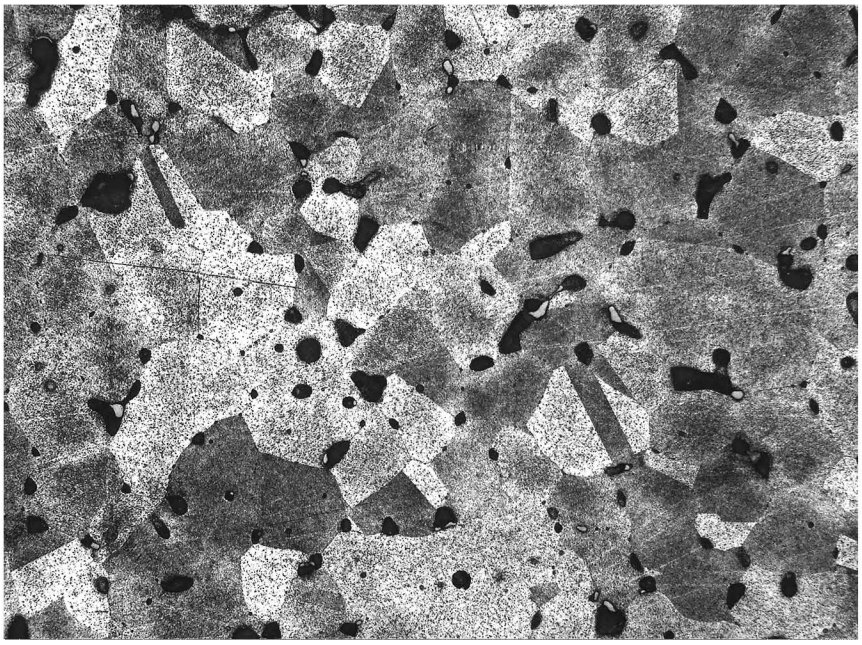

Figure 5.1.3.vii: Segmented upper arm ring (MIT 5339/Peabody 40-77-40/13426). Transverse cross section. Etch: 3 sec alcoholic ferric chloride and 3 sec ferric nitrate. x200. Microstructural features of interest include equiaxed grains with annealing twins, homogenously distributed porosities filled with lead, and a low density of light green inclusions. (MIT Image 5341b-45.)

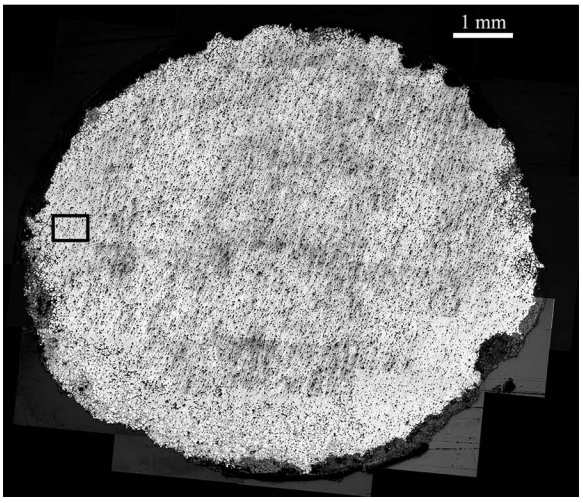

5.1.4: Segmented Arm Ring/Bracelet (MIT 5334/Peabody 40-77-40/13370)

5.1.4a: Provenance

MIT 5334 (Figure 5.1.4.i) consists of four fragments from two different thin, segmented arm rings/bracelets. These rings were found in Grave 20 beneath two stones and were associated with a layer of burned earth. Also found in Grave 20 were sherds from a brownish-gray vessel with some graphite coating and fifteen amber beads (Wells 1981).

5.1.4b: Initial Examination and Observations

Because the four fragments were easily identifiable as belonging to two specific rings, only the two fragments from a single bracelet were chosen for examination and sampling. These were photographed (Figure 5.1.4.i), drawn to scale, and measured (Figures 5.1.4.ii and 5.1.4.iii).

The ring is broken into two fragments. It is solid and circular with a diameter of 5.92 cm. The ring is a semi-closed ring with overlapping, tapered ends; each of the two fragments contains one of the original, tapered ends. The cross section is plano-convex. At its tapered end the cross section of the smaller fragment measures 1.4 mm wide x 1.1 mm thick, and at its fractured end the cross section measures 5.4 mm wide x 3.7 mm thick. At its tapered end the larger fragment's cross section measures 3.3 mm wide x 2.7 mm thick and at its fractured end its cross section measures 4.9 mm wide x 3.8 mm thick. The smaller fragment weighs 5.6 g and the larger fragment weighs 10.5 g.

The ring is solid and structurally robust. The surface, however, once covered entirely with corrosion product, has been cleaned mechanically. The cleaned areas show tiny scratches perpendicular to the longitudinal axis of the ring, most likely the marks of a cleaning tool. Only three segments and grooves remain on the bracelet. These segments and grooves are located at the very tip of the larger fragment's tapered end. They are too small and corroded to observe and measure the relative sizes of segment to groove. Each groove proceeds along the entire outside surface of the ring, and the inside surface is ungrooved and smooth.

The larger fragment has a freshly cut end revealing a highly metallic interior (Figure 5.1.4.ii). This fragment was sampled by Murray (1985) as part of a Harvard, Department of Anthropology class laboratory assignment; the text of his report is on file with the Peabody Museum.

5.1.4c: Sampling

Sample MIT 5334 was removed as a transverse section for bulk composition analysis (Figure 5.1.4.iii). This sample was removed adjacent to the sample removed by Murray. The ring was noticeably hard to cut, highly metallic, and light, whitish gold in color.

5.1.4d: Composition Analysis

Bulk composition analysis determined that the ring is a copper-tin alloy with tin present at a concentration of 14.5 weight percent. The ring is a high tin bronze. Other minor elements include Pb (0.38%), Sb (0.158%), Ni (0.158%), and As (0.165%). Silver, iron, and cobalt are present in trace amounts. Bulk composition analysis data are shown in Table 5.1.4 and in the Appendix.

Table 5.1.4: Bulk Composition Analysis for MIT 5334

	Sn	**Pb**	**Sb**	**As**	**Ni**	**Co**	**Ag**	**Fe**
ICP-ES	14.5	0.38	0.158	0.165	0.158	0.013	n.a.	0.005
INAA	13.1	n.a.	0.140	0.144	0.130	0.0190	0.093	n.d.

(values in weight %) n.a. = not analyzed n.d. = not determined

5.1.4e: Conclusions

- MIT 5334, a segmented arm ring/bracelet, is a high tin bronze ring with 14.5 weight percent tin. It is only very lightly leaded; the concentration of lead is 0.38 weight percent. It is not clear if this small amount of lead was deliberately alloyed with the copper and tin.
- The concentrations of tin and lead in MIT 5334 resemble the concentrations of tin and lead in MIT 5339 (13.5 weight percent and 0.372 weight percent respectively). MIT 5334 does not have the large concentration of Ni that is present in MIT 5339 (2 weight percent), however.

Figure 5.1.4.i: Segmented arm ring/bracelet. (MIT 5334/Peabody 40-77-40/13370). Photograph by E. Cooney.

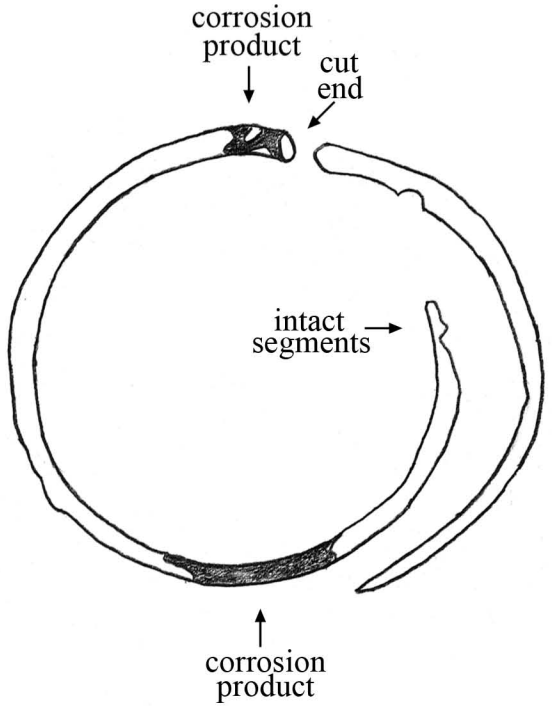

Figure 5.1.4.ii: Segmented arm ring/bracelet (MIT 5334). Key object features.

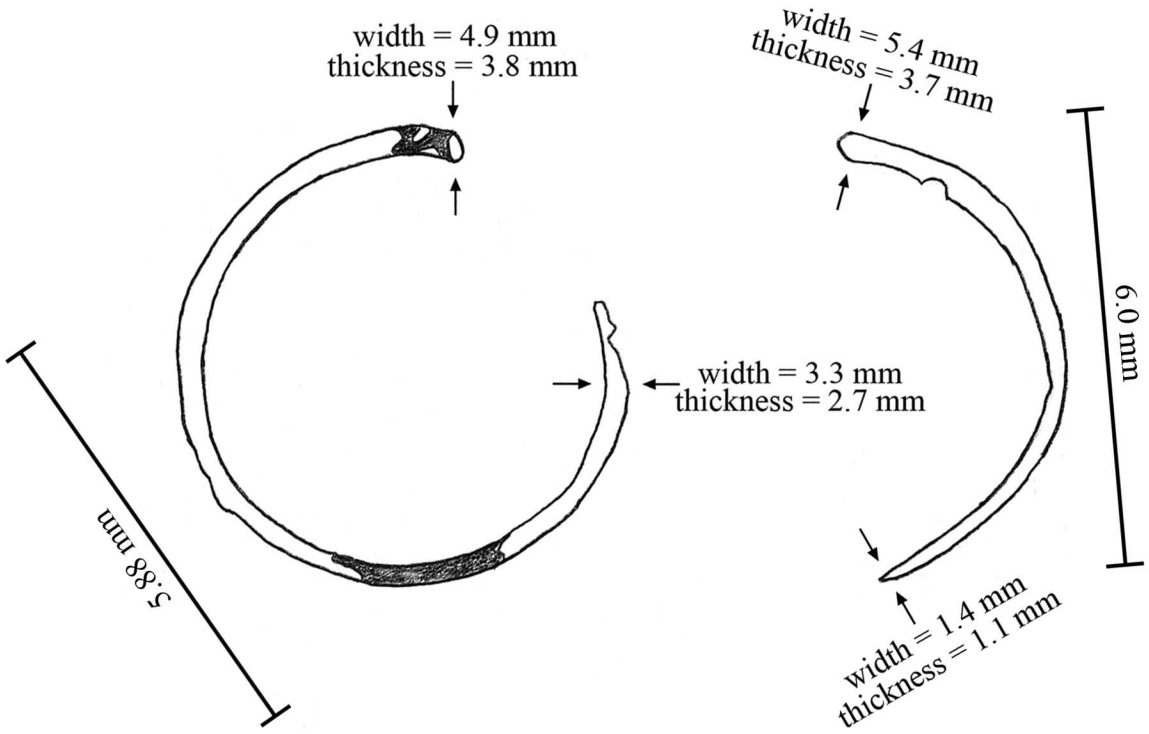

ring weight = 10.5 g
fragment weight = 5.6 g

Figure 5.1.4.iii: Segmented arm ring/bracelet (MIT 5334). Drawing and measurements.

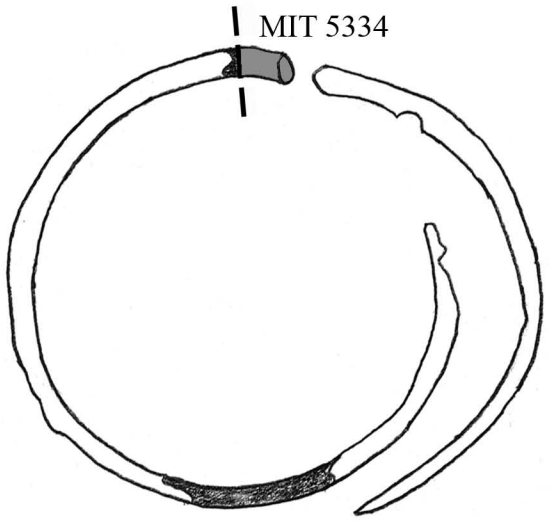

Figure 5.1.4.iv: Segmented arm ring/bracelet (MIT 5334).
Sample MIT 5334 was removed for bulk compositional analysis.

5.1.5: Segmented Child's Arm Ring (MIT 5335/Peabody 40-77-40/13373)

5.1.5a: Provenance

MIT 5335 (Figure 5.1.5.i) is a fragment of a segmented arm ring. It is from Grave 21, identified by the excavators as a child's grave (Wells 1981) The grave was 1.4 m long, 0.7 m wide, and 0.4 m deep. At the foot end were sherds of two ceramic vessels with a red slip and graphite coating, nine small bronze segmented arm rings, and twenty beads of amber and glass. MIT 5335 is one of the nine segmented bronze rings from Grave 21, four of which are intact and five of which are fragmented. Figure 5.2.5.ii shows one of the intact segmented rings. The overlapping, tapered ends can be seen clearly. The majority of these rings are fairly corroded.

Three other graves in Tumulus IV are classified as childrens' graves. It is not clear why the excavators classified these graves as childrens' graves. No skeletal remains are recorded, not all of them contained objects noticeably smaller than similar objects from adult graves, and the grave sizes are not notably smaller than the sizes recorded from adult graves.

5.1.5b: Initial Examination and Observations

MIT 5335 was photographed (Figure 5.1.5.i), drawn to scale, and measured (Figures 5.1.5.iii and iv).

The ring fragment is slightly oval in shape and is mostly intact. The width of the oval is 6.24 cm and the length of the oval is 5.92 cm. Both ends of the ring have been broken, so no original ends remain. The ring is solid, and its cross section is roughly circular. The thickest and best preserved section of the ring is 5.4 mm wide x 5.3 mm thick, and at the two broken ends the cross section is 2.7 mm wide x 2.6 mm thick and 4.6 mm wide x 4.4 mm thick. The ring weighs 11.4 g.

The ring is structurally intact except for the missing ends. Even though the original ends are missing, the decreasing cross sectional area from the center of the ring to one of the fragmented edges suggests that the ring was semi-closed with overlapping, tapered ends. The associated segmented rings that are still intact are also semi-closed with overlapping, tapered ends (Figure 5.1.5.ii).

The condition of the ring's surface is poor. The surface is entirely corroded and still has some earthy accretions clinging to it. The corrosion product is a light green and is highly friable. On the inside surface one portion of the ring parallel longitudinal striations can be seen in the earthy accretions and corrosion product. These striations are mostly likely the products post-excavation cleaning.

The original segmented decoration has been mostly destroyed and/or obscured by the extensive corrosion, and the segments and grooves are only observable on a few better preserved portions of the ring. The segments on the best preserved section of the ring are bulbous, about 5.4 mm wide x 4.0 mm long at a point where the ring is 5.3 mm thick. Each groove proceeds along the entire outside surface of the ring, and the inside surface is ungrooved and smooth. The grooves are all about 1.7 mm wide with semiannular, smooth contours. The interior surface of the ring is smooth.

5.1.5c: Sampling

Sample MIT 5335 was removed for bulk composition analysis by a transverse cut adjacent to a fractured end of the ring (Figure 5.1.5.v). Under a thick layer of green corrosion product the ring was highly metallic, and the metal was light, whitish gold in color. The ring was cut easily.

5.1.5d: Composition Analysis

Bulk composition analysis determined that the ring is a copper-tin alloy with a Sn tin concentration of 5.94 weight percent. The ring is a medium tin bronze. Other major and minor elements include Ni (1.5%), As (0.345%), Ag (0.282%), Sb (0.265%), Co (0.179%), and Pb (0.127%). Iron is present in trace amounts. Composition analysis data are given in Table 5.1.5 and in the Appendix.

Table 5.1.5: Bulk Compositional Analyses for MIT 5335

	Sn	**Pb**	**Sb**	**As**	**Ni**	**Co**	**Ag**	**Fe**
ICP-ES	5.94	0.127	0.265	0.345	1.5	0.179	n.a.	0.006
INAA	5.20	n.a.	0.224	0.249	1.55	0.173	0.282	n.d.

(values in weight %) n.a. = not analyzed n.d. = not determined

5.1.5e: Conclusions

- The child's segmented arm ring is a medium tin bronze with 5.94% weight percent tin. It is not a leaded tin bronze, and the low concentration of lead (0.127 weight %) is likely present because of its presence in the copper ore from which the ring's copper was smelted.

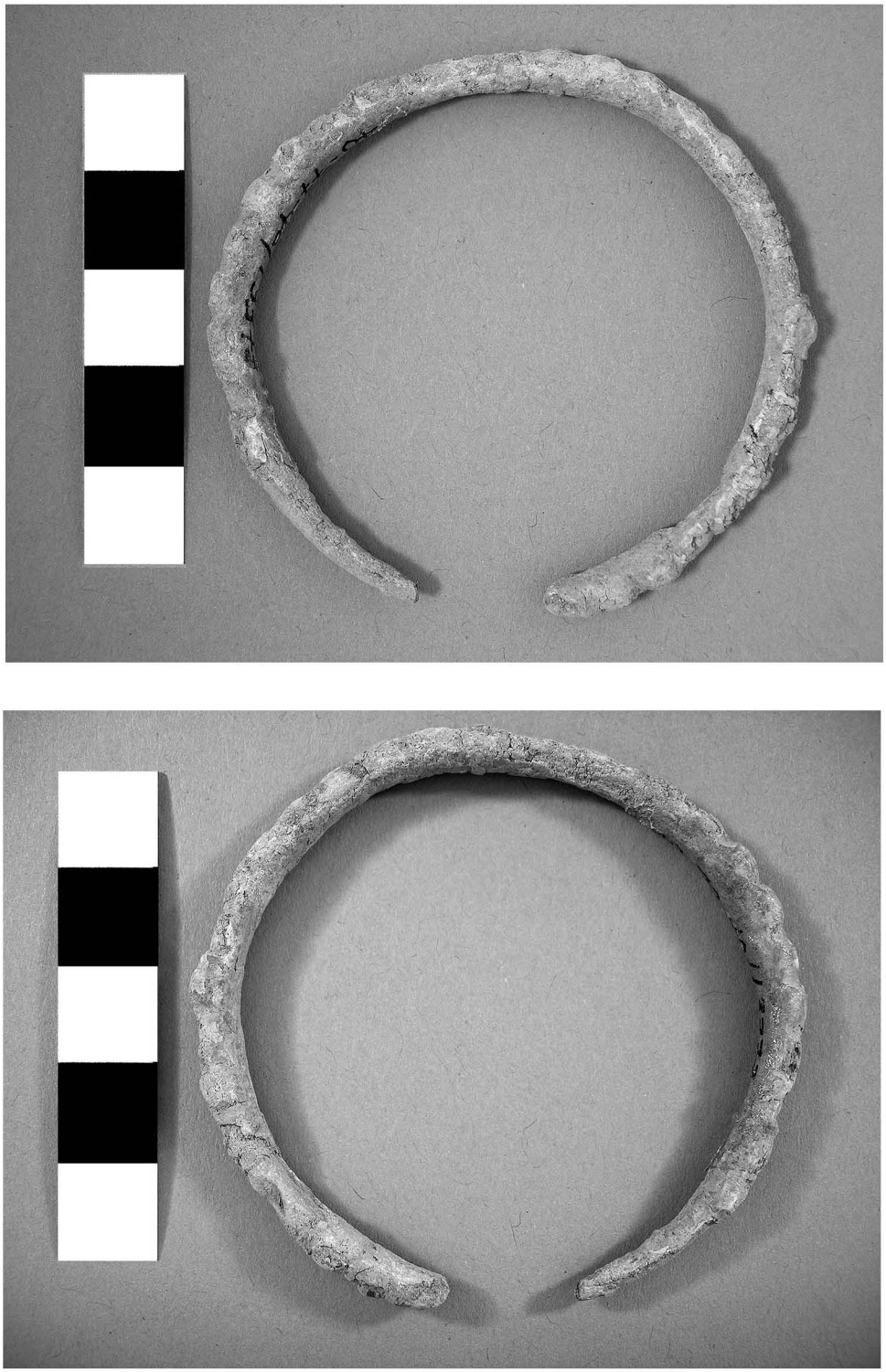

Figure 5.1.5.i: Child's segmented arm ring/bracelet. (MIT 5335/Peabody 40-77-40/13373). Photograph by E. Cooney.

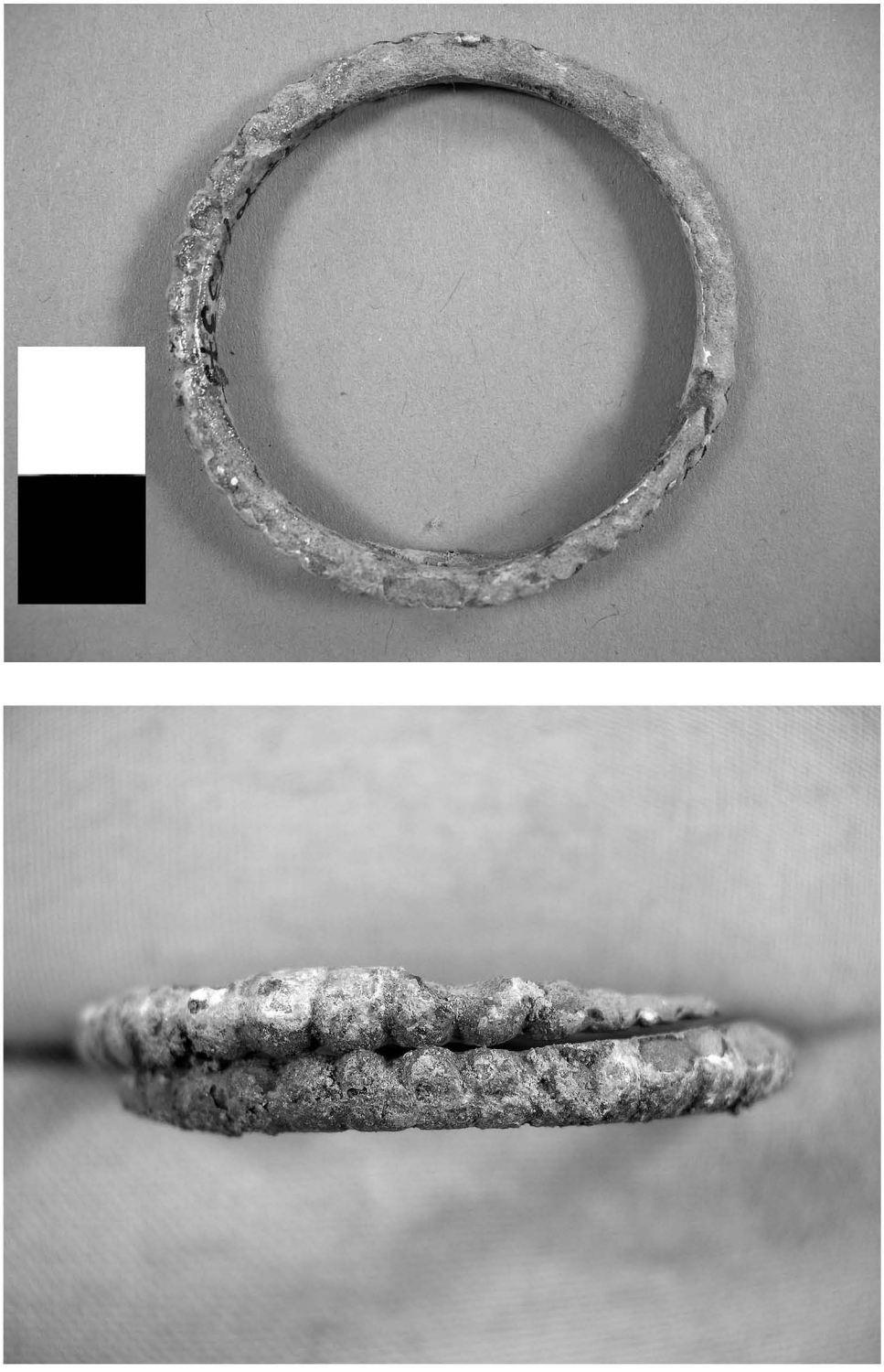

Figure 5.1.5.ii: Child's segmented arm ring/bracelet. (Peabody 40-77-40/13375). One of the intact segmented arm rings from Tumulus IV, Grave 21. The tapered, overlapping ends of the ring can be seen. Photograph by E. Cooney.

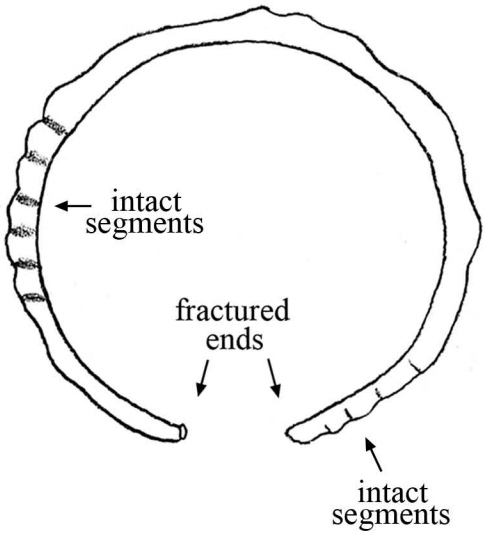

Figure 5.1.5.iii: Child's segmented arm ring/ bracelet (MIT 5335). Key object features.

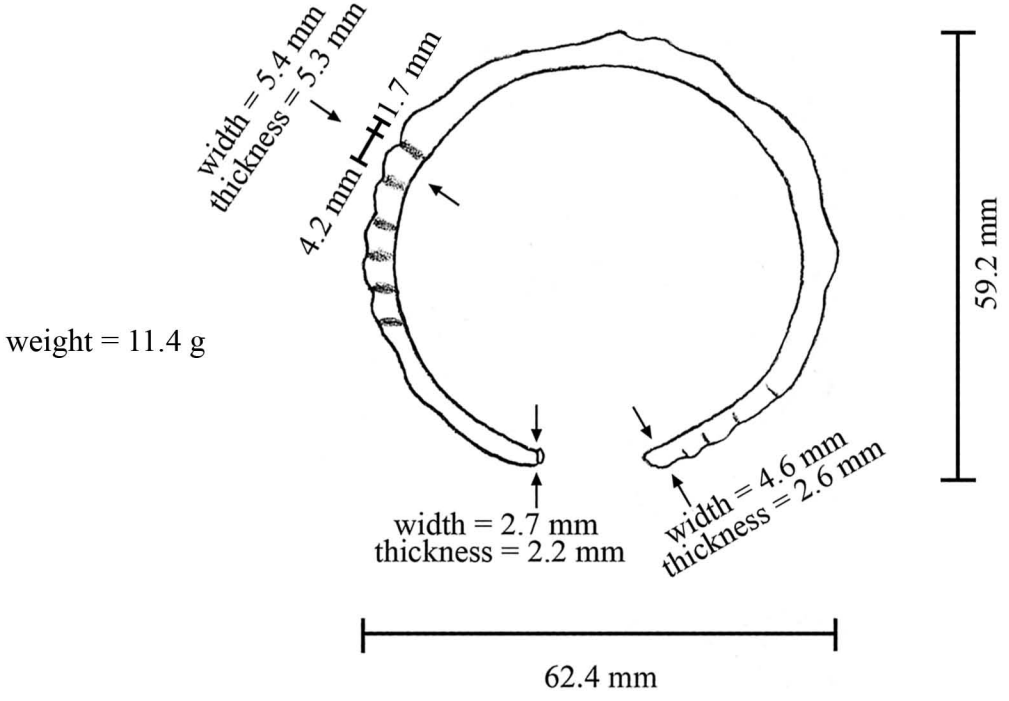

Figure 5.1.5.iv: Child's segmented arm ring/bracelet (MIT 5335). Drawing and measurements.

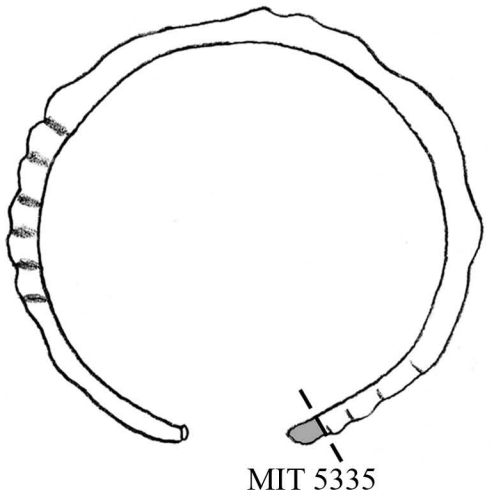

Figure 5.1.5.v: Child's segmented arm ring/ bracelet (MIT 5335). Sample MIT 5335 was removed for bulk compositional analysis.

5.1.6: Zoned arm ring/bracelet (MIT 5344/Peabody 40-77-40/13314)

5.1.6a: Provenance

MIT 5344 (Figure 5.1.6.i) is a zoned armed ring/bracelet from Grave 11 (Wells 1981). Associated grave goods included a second, similar zoned bronze arm ring/bracelet, a small knobbed bronze ring resembling a ring belt attachment, six glass beads, and a spindle whorl.

5.1.6b: Initial Examination and Observations

MIT 5344 was photographed (Figures 5.1.6.i and 5.1.6.ii), drawn to scale, and measured (Figures 5.1.6.iii and 5.1.6.iv).

The solid ring is a semi-closed ring with overlapping, tapered ends. One of these overlapping ends has been broken off from the main body of the ring. The main body of the ring is circular with a diameter of 6.87 cm. The cross section is that of a rounded trapezoid, and it varies in area across the ring. At its thickest area the cross section is 6.9 mm wide x 6.0 mm thick, and at the ring's intact, tapered end the cross section is 2.7 mm wide x 3.0 mm thick. The ring weighs 30.4 g without its fragmented end.

The fragmented end maintains its original, intact, tapered shape. The fragment is 5.88 cm long and weighs 10.5 g. The cross section at the intact tapered end is 3.7 mm wide x 3.5 mm thick and is 6.4 mm wide by 4.8 mm thick at the fractured end.

The ring is structurally robust. The surface is covered with various shades of green corrosion product. In some areas the corrosion product is quite friable and has been chipped away, obscuring the surface decoration. In other areas on the ring the corrosion product takes the form of a sturdy, smooth, dark green patina, and the decoration can be seen clearly. A few pseudomorphs resembling a loosely woven cloth are present in some areas on the interior surface of the ring.

The ring is decorated with repeating, alternating zones of segments and grooves and incised lines running perpendicular to the longitudinal axis of the ring. The segmented zones contain three segments and four grooves. The segments are 1.5 mm long and are rectangular in shape. Each groove proceeds along the entire outside surface

of the ring; the inside surface is ungrooved and smooth. The grooves have a concave, rectangular shape and are 1.5 mm wide.

5.1.6c: Sampling

The fragment end of MIT 5344 was sampled twice (Figure 5.1.6.v). Sample MIT 5344a was removed with a transverse cut from the intact, tapered end for bulk composition analysis. Sample MIT 5344b was removed for metallographic analysis and was mounted transversely as noted.

5.1.6d: Bulk Composition Analysis

Bulk composition analysis determined that the zoned arm ring/bracelet is a copper-tin-lead alloy with the main alloying elements of tin at a concentration of 11.3 weight percent and lead at a concentration of 1.87 weight percent. The ring is a leaded tin bronze. Other minor and trace elements include Sb (0.753%), As (0.501%), Ag (0.248%), Ni (0.200%), Co (0.017%), and Fe (0.028%). Bulk composition analysis data are given in Table 5.1.6 and in the Appendix.

Table 5.1.6: Bulk Composition Analysis Data for MIT 5344 (Zoned Arm Ring)

	Sn	**Pb**	**Sb**	**As**	**Ni**	**Co**	**Ag**	**Fe**
ICP-ES	11.3	1.87	0.753	0.501	<0.005	0.017	n.a.	0.028
INAA	9.32	n.a.	0.678	0.403	0.200	0.0142	0.248	n.d.

(values in weight %) n.a. = not analyzed n.d. = not determined

5.1.6e: Metallographic Analysis

Sample 5344b was mounted transversely. The as-polished sample (Figure 5.1.6.vi) shows the ring's rounded trapezoid cross section.
Microstructural features of interest include a large, center line shrinkage cavity and a high density of porosities and gray copper sulfide inclusions homogenously distributed throughout the sample. Several pools of blue-green Cu-Sn eutectoid were also observed. The center line shrinkage cavity indicates that the stock metal from which the ring was subsequently shaped was cast.

The sample was etched for twelve seconds with potassium dichromate and for four seconds with aqueous ferric chloride to reveal a microstructure characterized by equiaxed grains and annealing twins (Figure 5.1.6.vii). High densities of deformation lines are present at the ring's surface across its entire circumference (Figure 5.1.6.viii).

5.1.6f: Discussion

The ring is a leaded tin bronze with the main alloying elements of tin at a concentration of 11.3 weight percent and lead at a concentration of 1.87 weight percent.

The stock metal comprising the bracelet was originally cast to shape. The equiaxed grains and annealing twins indicate that the bracelet was subsequently subject to several cycles of working and annealing and that the bulk metal was left annealed. The high density of deformation lines at the bracelet's surface indicates that the ring was lightly worked at the surface after its final anneal and that it was left in a worked condition.

The ring was roughly cast to shape as a rod-ingot, then hammered to its final shape as a somewhat circular, semi-closed ring. The zones of lines and the grooves running perpendicular to the ring's longitudinal axis were likely incised into the metal with an engraving tool. The lines and grooves were probably incised after the bracelet had been bent to its circular shape to avoid being marred by the hammering required to bend the metal into a circle.

5.1.6g: Conclusions

- The zoned arm ring/bracelet is a leaded tin bronze with a tin composition of 11.3 weight percent and a lead composition of 1.87 weight percent.
- The stock metal comprising the ring was cast and subjected to several cycles of working and annealing to accomplish the final ring form. The ring was lightly worked at its surface after the final anneal and the surface was left in a worked condition.
- The zones of lines and grooves running perpendicular to the ring's longitudinal axis were most likely incised into the metal with an engraving tool.

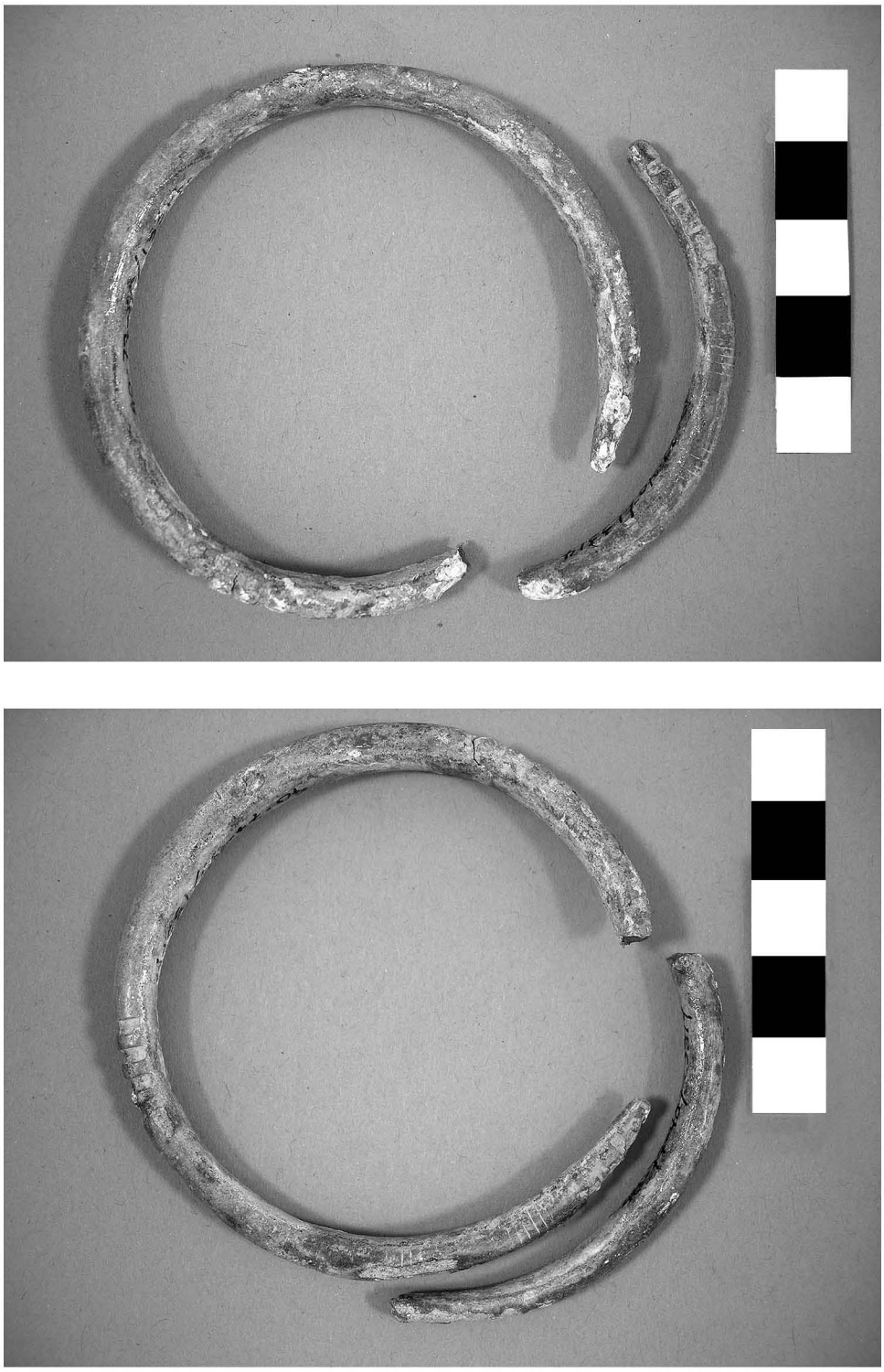

Figure 5.1.6.i: Zoned arm ring/bracelet (MIT 5344/Peabody 40-77-40/13314). Photograph by E. Cooney.

Figure 5.1.6.ii: Zoned arm ring/bracelet (MIT 5344/Peabody 40-77-40/13314). Segment chosen for sampling. Photograph by E. Cooney.

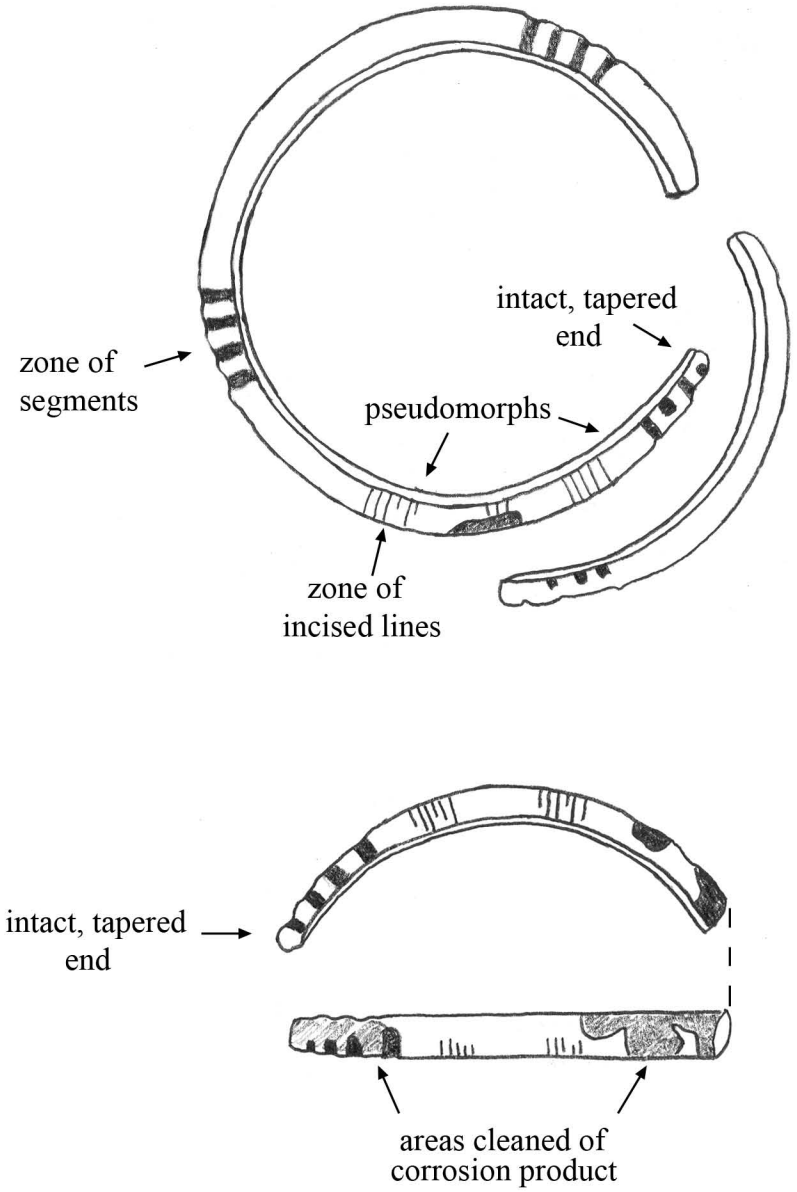

Figure 5.1.6.iii: Zoned arm ring/bracelet (MIT 5344). Key object features.

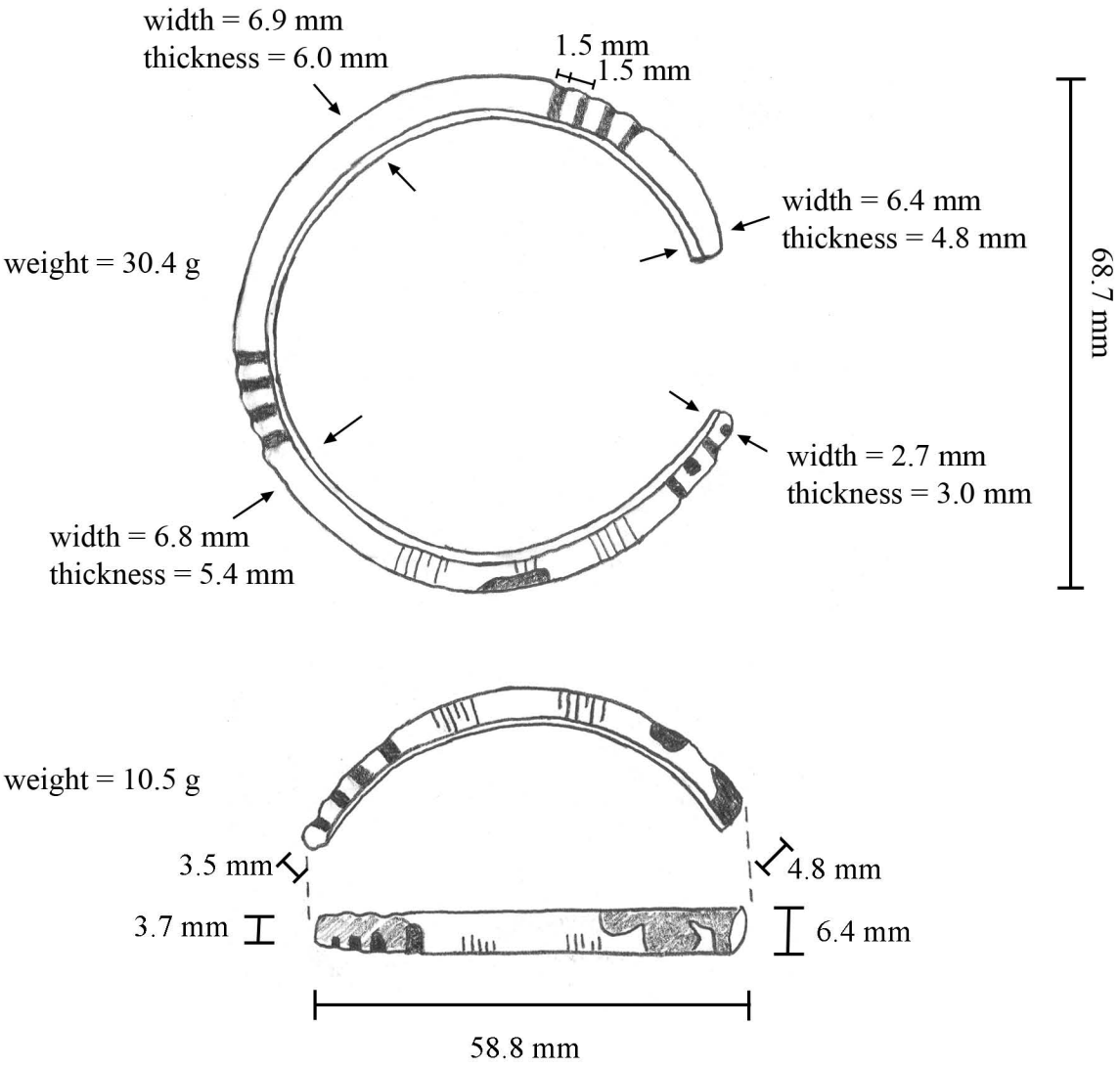

Figure 5.1.6.iv: Zoned arm ring/bracelet (MIT 5344). Drawing and measurements.

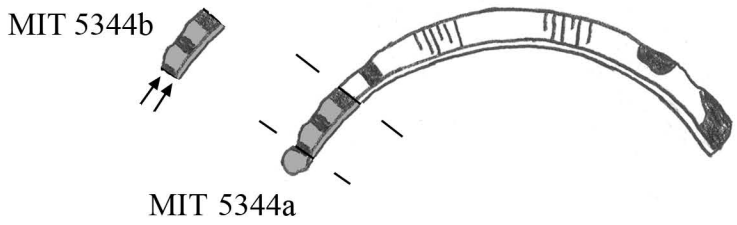

Figure 5.1.6.v: Samples removed from zoned arm ring/bracelet. Sample MIT 5344a was removed for bulk composition analysis. Sample MIT 5344b was removed for metallographic analysis and was mounted transversely as noted.

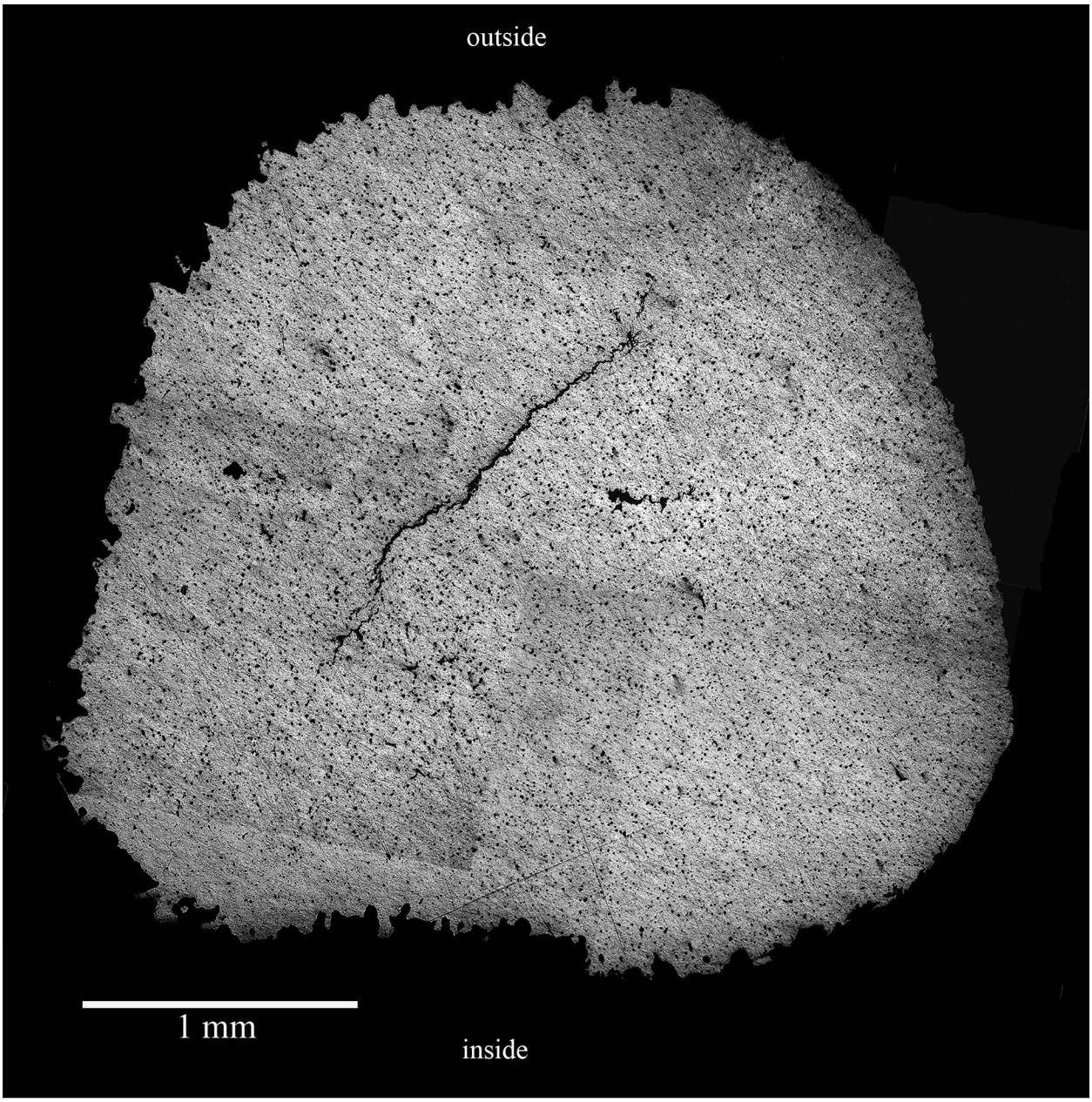

Figure 5.1.6.vi: Zoned arm ring/bracelet (MIT 5344/Peabody 40-77-40/13314). Transverse cross section, as polished. The cross section is a rounded trapezoid. Microstructural features of interest include a large, center line shrinkage cavity and a high density of porosities and gray copper sulfide inclusions homogenously distributed throughout the sample.
(MIT Image 5344b-01-08).

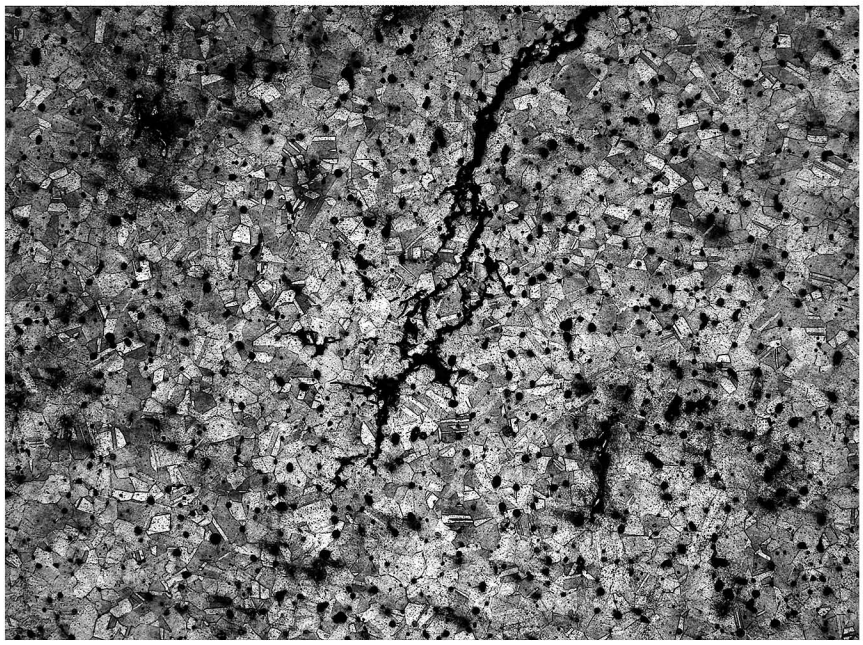

Figure 5.1.6.vii: Zoned arm ring/bracelet (MIT 5344/Peabody 40-77-40/13314). Transverse cross section. Etch: 12 sec potassium dichromate and 4 sec ferric chloride. x100. Microstructural features of interest include equiaxed grains with annealing twins surrounding the center line porosity. (MIT Image 5344b-31).

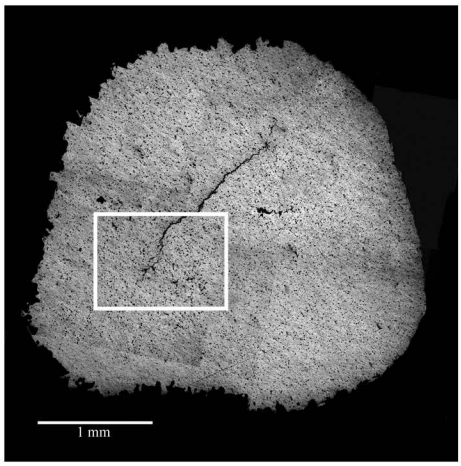

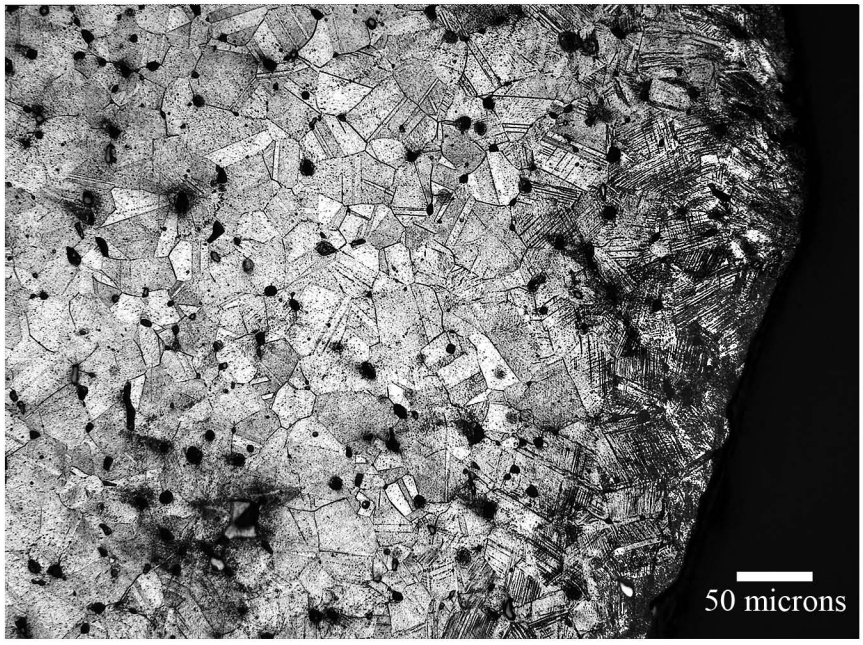

Figure 5.1.6.viii: Zoned arm ring/bracelet (MIT 5344/Peabody 40-77-40/13314). Transverse cross section. Etch: 12 sec potassium dichromate and 4 sec ferric chloride. x200. Microstructural features of interest include equiaxed grains with annealing twins and a high density of deformation lines at the very surface of the ring. (MIT Image 5344b-30).

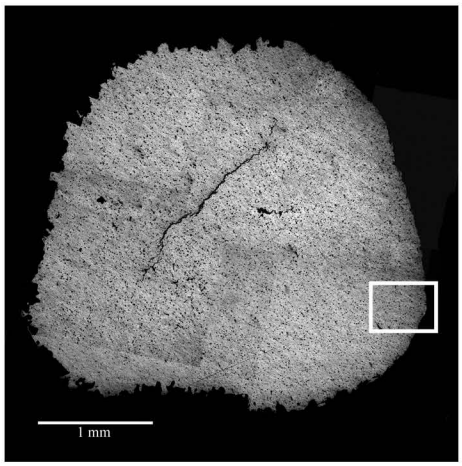

5.1.7: Zoned arm ring/bracelet (MIT 5346/Peabody 40-77-40/13505)

5.1.7a: Provenance and Background

MIT 5346 (Figure 5.1.7.i) is a fragment of a zoned arm ring/bracelet from Grave 41b described by Wells as decorated by "zones defined by ridges, containing oblique incised lines; at the surviving end is ribbing (1981: 65). This decoration makes MIT 5346 unique in Tumulus IV.

Grave 41b was found 35 centimeters below the surface of the tumulus in a layer of sod. Associated grave goods included 188 glass beads and 47 amber beads.

5.1.7b: Initial Examination and Observations

The zoned arm ring/bracelet was photographed (Figures 5.1.7.i and 5.1.7.ii), drawn to scale, measured, and observed (Figures 5.1.7.iii and 5.1.7.iv).

MIT 5436 is a single fragment from a zoned arm ring/bracelet. Its surface is highly corroded, and the corrosion almost entirely obscures the ring's decoration. The surviving decoration consists of several zones of oblique lines separated from one another by undecorated surface metal and a single zone of lines running perpendicular to the ring's longitudinal axis. Due to the extent of corrosion, it is unclear if the fragment contains an original intact end; therefore, it is unclear if the ring was open, semi-closed, or closed. It is also unclear how far the decoration once spread across the outer surface of the ring. No decoration is visible on the inside surface of the ring, but it is not clear if this is because the inside surface was not decorated or if the decoration is obscured by the extensive corrosion present on the fragment's inside surface.

The fragment is 63.7 mm long. On one end the ring is 7.5 mm wide and 7.5 mm thick, and on the other end the ring is 5.7 mm wide and 6.0 mm thick. The fragment weighs 19.8 g.

5.1.7c: Sampling

The zoned arm ring/bracelet fragment was sampled twice (Figure 5.1.7.v. Sample MIT 5346a was removed for bulk composition analysis. Sample MIT 5346b was

removed for metallographic analysis and was mounted transversely as noted. The bracelet was highly mineralized, and little metal remained intact.

5.1.7d: Bulk Composition Analysis

Bulk composition analysis data shows that the ring is a copper-tin-lead ternary alloy with a tin composition of 8.72 weight percent and a lead composition of 1.65 weight percent. The ring is a leaded tin bronze. Other major, minor, and trace elements include Sb (1.39%), As (0.793%), Ag (0.719%), Ni (0.275%), Fe (0.158%), and Co (0.01%). Bulk composition analysis data are shown below in Table 5.1.7 and in the Appendix.

Table 5.1.7: Bulk Composition Analysis Data for MIT 5346 (Zoned Arm Ring)

	Sn	**Pb**	**Sb**	**As**	**Ni**	**Co**	**Ag**	**Fe**
ICP-ES	8.72	1.65	1.39	0.793	0.275	0.01	n.a.	0.158
INAA	6.10	n.a.	1.37	0.672	0.252	0.0098	0.719	n.d.

(values in weight %) n.a. = not analyzed n.d. = not determined

5.1.7e: Metallographic Analysis

Sample MIT 5346b was mounted as a transverse section. The polished section reveals that the ring is highly mineralized (Figure 5.1.7.vi). Only a small core of metal remains intact in the center of the sample. This metallic core is highly porous, and internal corrosion product in the metal outlines equiaxed grains.

The sample was etched for three seconds with concentrated nitric acid to reveal a microstructure characterized by equiaxed grains and annealing twins (Figure 5.1.7.vii). Due to the extensive corrosion it is unclear if deformation lines are present in the sample.

5.1.7f: Discussion

The ring is a leaded tin bronze with a tin composition of 8.72 weight percent and a lead composition of 1.65 weight percent. The high density of porosities indicates that the metal comprising the ring was originally cast to shape, and the equiaxed grains and annealing twins indicate that the ring was worked and annealed at least once. The high level of mineralization inhibits further analysis of the sample.

5.1.7g: Conclusions

- The ring is a leaded tin bronze with a tin composition of 8.72 weight percent and a lead composition of 1.65 weight percent.
- The metal comprising the ring was cast to shape, and the ring was worked and annealed at least once before being left in an annealed condition.

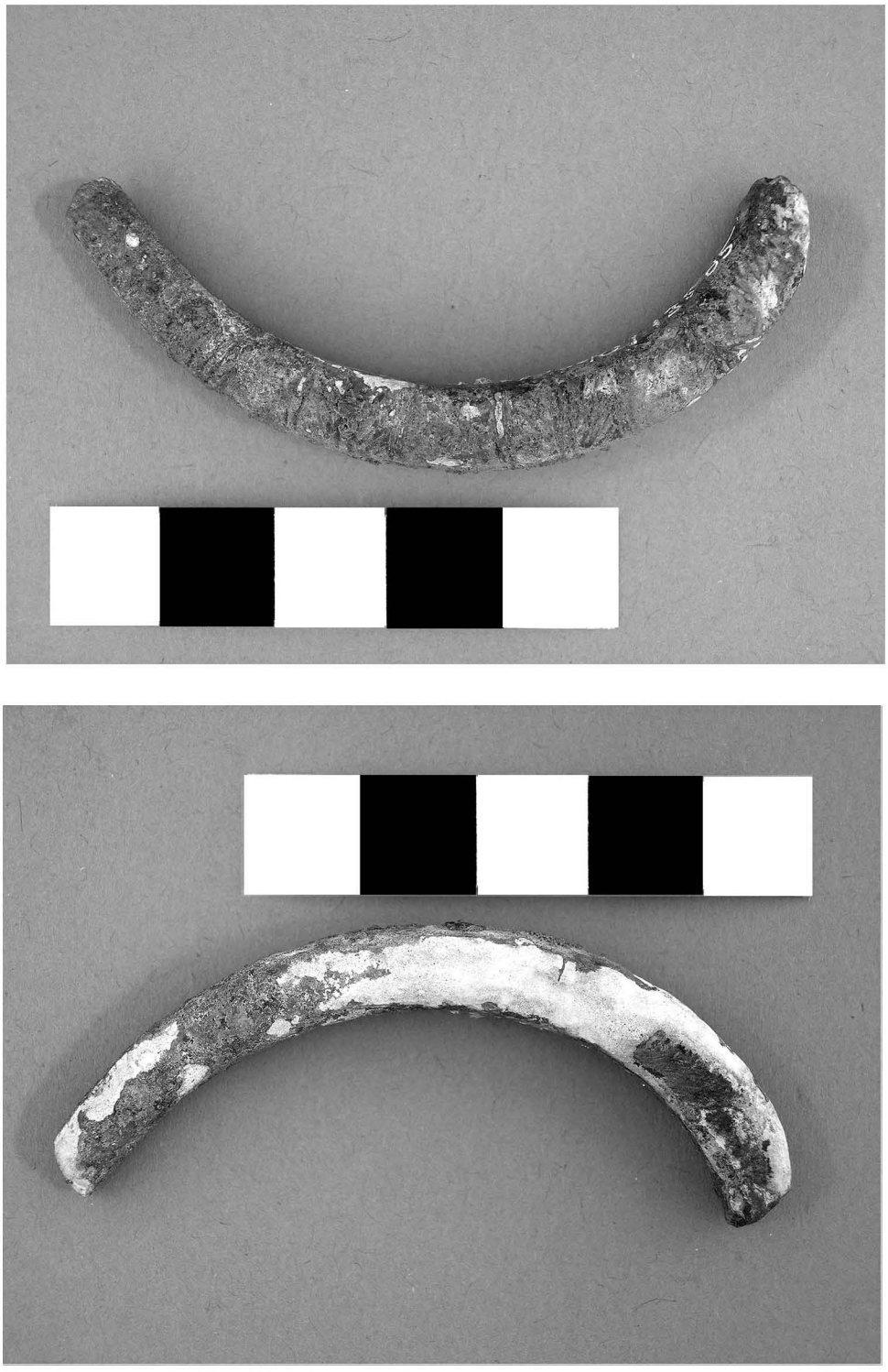

Figure 5.1.7.i: Zoned arm ring/bracelet. (MIT 5346/Peabody 40-77-40/13505). Photograph by E. Cooney.

Figure 5.1.7.ii: Zoned arm ring/bracelet. (MIT 5346/Peabody 40-77-40/13505). Photograph by E. Cooney.

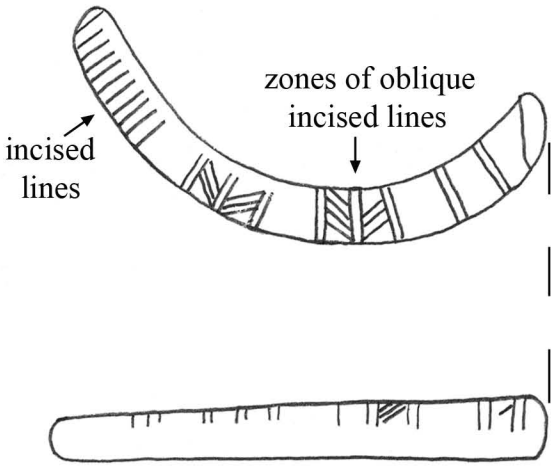

Figure 5.1.7.iii: Zoned arm ring/bracelet (MIT 5346). Key object features.

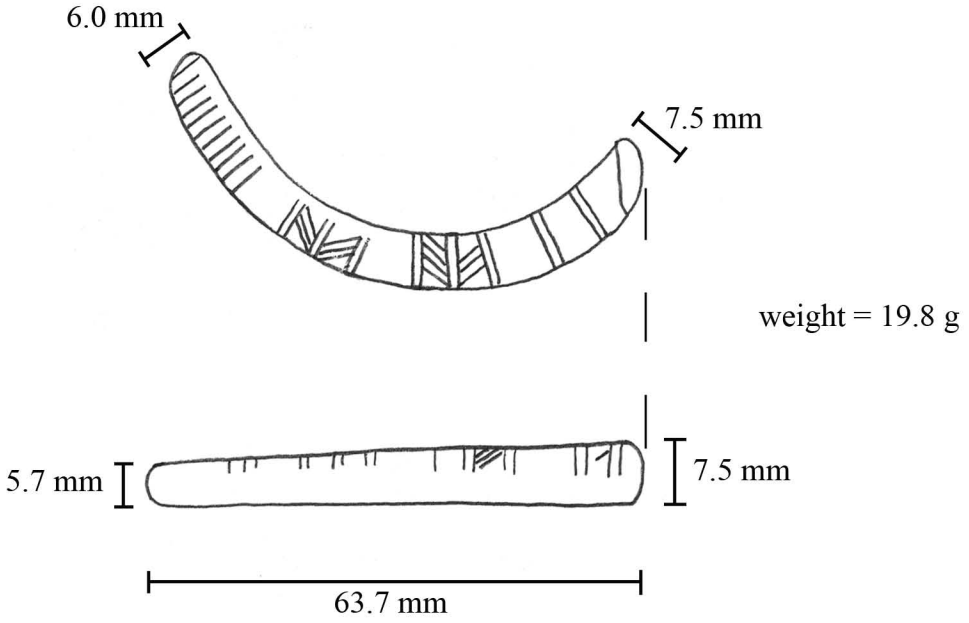

Figure 5.1.7.iv: Zoned arm ring/bracelet (MIT 5346). Drawing and measurements.

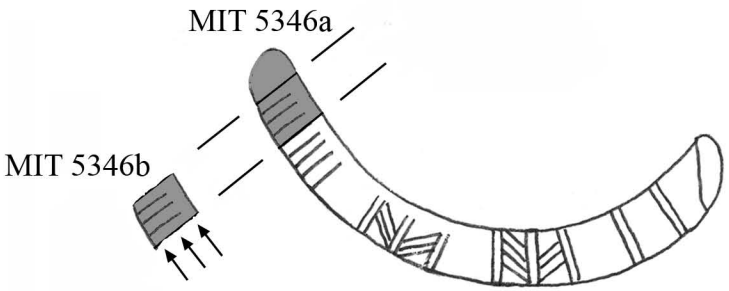

Figure 5.1.7v: Zoned arm ring/bracelet (MIT 5346). Samples MIT 5346a was removed for bulk compositional analysis. MIT 5346b was removed for metallographic analysis and was mounted as a transverse section.

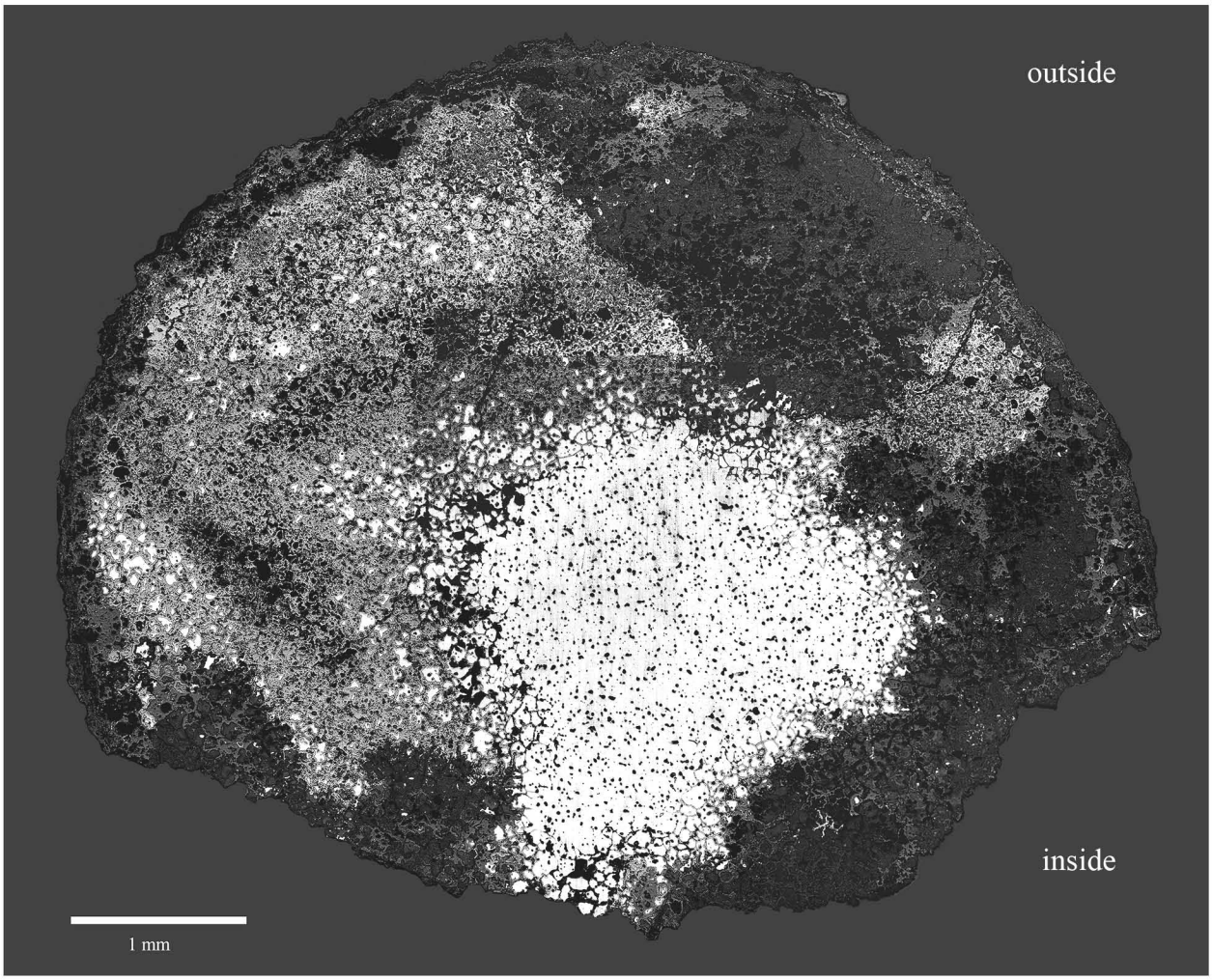

Figure 5.1.7.vi: Zoned arm ring/bracelet (MIT 5346/Peabody 40-77-40/13505). Transverse cross section, as polished. Microstructural features of interest include the extensive corrosion surrounding the remaining metallic core of the sample, a high density of porosities, and equiaxed grains in the remaining metal that are outlined by internal corrosion product.
(MIT Image 5346b-01-18.)

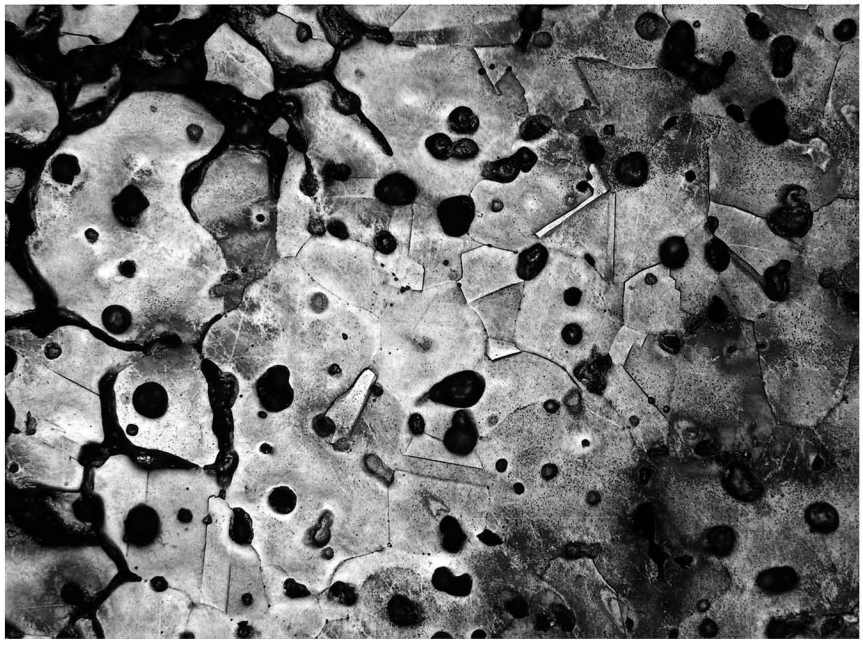

Figure 5.1.7.vii: Zoned arm ring/bracelet (MIT 5346/Peabody 40-77-40/13505). Transverse cross section. Etch: 3 sec concentrated nitric acid. x200. Microstructural features of interest include equiaxed grains and annealing twins in the still-metallic core of the sample. (MIT Image 5346b-19).

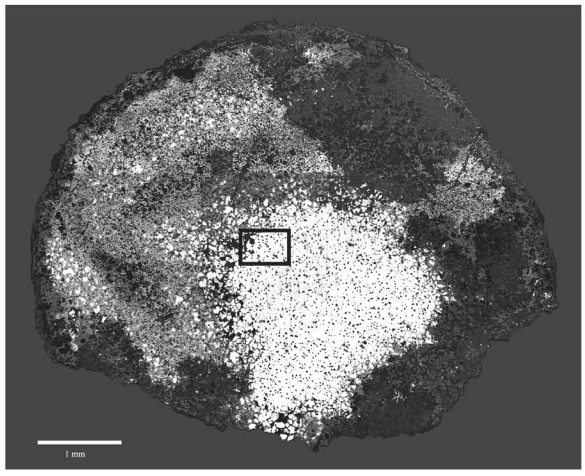

5.1.8: Zoned arm ring/bracelet (MIT 5340/Peabody 40-77-40/13393)

5.1.8a: Provenance and Background

MIT 5340 (Figures 5.1.8.i and 5.1.8.ii) is a fragmented zoned arm ring/bracelet from Grave 23 (Wells 1981). Grave 23 was oriented north-south and was 2.1 m long, 0.9 m wide, and 1.6 m below the surface of the tumulus. At the head end of the grave five stones were packed together. A second, intact, identical zoned arm ring/bracelet was found with MIT 5340; this second ring is a semi-closed ring with overlapping, tapered ends. Other associated grave goods include 89 amber beads, one glass bead, and a spindle whorl.

A zoned arm ring/bracelet similar to the two from Grave 23 is found in Grave 11 of Tumulus IV (Figure 5.1.8.iii).

5.1.8b: Initial Examination and Observations

The zoned arm ring/bracelet was photographed (Figures 5.1.8.i and 5.1.8.ii), drawn to scale, measured, and observed (Figures 5.1.8.iii and 5.1.8.iv).

The zoned arm ring is broken into three fragments. The superficial condition of the fragments is quite poor. The ring is partly covered with a thick layer of friable green corrosion product. Zones of incised lines running perpendicular to the ring's longitudinal axis can be seen in the corrosion product. The thick layer of corrosion product has been chipped away from several areas of the ring, revealing the surviving, dark, oxidized metal beneath. This remaining metal appears to be structurally robust, and the same zones of incised lines visible in the corrosion product can be seen in the surviving metal. None of the fragments contains an intact end, but the length of the fragments indicates that the ring must have been semi-closed with overlapping ends.

Fragment C is the largest fragment and contains enough of the original ring that the ring's diameter can be measured to be 53.2 mm. Fragment C has a cross section that varies in thickness from 5.6 mm wide by 6.0 mm thick to 4.6 mm wide by 4.8 mm thick. Fragment C weighs 16.2 g.

Fragment B is the smallest fragment. It is 15.8 mm long and weighs 0.6 g.

Fragment A is 40.2 mm long. It is covered with corrosion product at its two broken ends, but in its center the corrosion product has been removed to reveal the surviving metal. The surviving metal is 4.2 mm wide by 4.3 mm thick. Fragment A weighs 4.2 g. The surviving metal was light gold in color.

5.1.8c: Sampling

Fragment A was sampled twice (Figure 5.1.8.vi). Sample MIT 5340a was removed with a transverse cut for bulk composition analysis. Sample MIT 5340b was removed adjacent to MIT 5340a for metallographic analysis and was mounted transversely as noted.

5.1.8d: Bulk Composition Analysis

Bulk composition analysis determined that the zoned arm ring is primarily a copper tin alloy with the main alloying element of tin at a concentration of 12.3 weight percent The alloy is a high tin bronze. Lead is present at a concentration of 0.825 weight percent; it is unclear if the lead was purposefully added to the alloy. Other major and minor elements include Sb (0.58%), As (0.554%), Ni (0.310), Ag (0.242 %), Fe (0.23%), and Co (0.029%). Bulk composition analysis data are given in Table 5.1.8 and in the Appendix.

Table 5.1.8: Bulk Composition Analysis Data for MIT 5340 (Zoned Arm Ring)

	Sn	**Pb**	**Sb**	**As**	**Ni**	**Co**	**Ag**	**Fe**
ICP-ES	12.3	0.825	0.58	0.554	0.283	0.029	n.a.	0.012
INAA	10.3	n.a.	0.565	0.444	0.310	0.0328	0.242	0.23

(values in weight %) n.a. = not analyzed n.d. = not determined

5.1.8e: Metallographic Analysis

Sample MIT 5340b was mounted as a transverse section. The as-polished sample (Figure 5.1.8.viii) shows that over half the sample is completely mineralized. Due to the extent of mineralization, the original outline of the bracelet's transverse cross section is unclear. The cross section appears to be diamond shaped, but it is not clearly rounded or clearly faceted like the cross section of some of the other arm rings. Because the

mineralization occurs at the bracelet's outside surface, it is impossible to observe the incised lines.

At the interface between the mineralized portion of the bracelet and the surviving metal, internal corrosion product in the surviving metal outlines equiaxed grains with annealing twins and deformation lines. The surviving metal has a high density of small porosities homogenously distributed throughout the sample. A few gray copper sulfide inclusions with no apparent alignment are also distributed homogenously throughout the sample. Two pools of blue-green Cu-Sn eutectoid were observed.

The sample was etched for twenty seconds with potassium dichromate and for four seconds with ferric chloride to reveal a microstructure characterized by equiaxed grains with annealing twins. A light density of deformation lines is present along the ring's outer surface, although few deformation lines are present in the interior of the sample.

5.1.8f: Discussion

The zoned arm ring/bracelet is a high tin bronze with a tin composition of 12.3 weight percent. Lead is present in the alloy at a concentration of 0.825 weight percent. It is unclear if this amount of lead, which is less than one weight percent but greater than 0.5 weight percent, was purposefully added to the alloy. The high tin content would have made the bracelet very hard. The high tin and low lead concentrations make the MIT 5340 similar to the alloy used to make MIT 5334, the segmented arm ring discussed in Section 5.1.4.

Over half the bracelet has been completely mineralized. The remaining metal is quite porous, indicating that the metal comprising the bracelet was originally cast. The equiaxed grains and annealing twins indicate that the bracelet was subject to several cycles of working and annealing. The light density of deformation lines indicates that the ring was lightly worked after its final anneal and that it was left in a worked condition.

The ring was originally a semi-closed ring with tapered ends. It most likely was roughly cast to shape as an ingot and then hammered to its final shape as a circular, semi-closed ring. The zones of lines running perpendicular to the ring's longitudinal axis were most likely incised deeply into the metal with an engraving tool, as they can still be

observed with the naked eye in the surviving, exposed metal of the bracelet. The lines were most likely incised after the bracelet had been bent to its circular shape, or they would have been affected by the hammering required to bend the metal into a circle.

5.1.8g: Conclusions

- The zoned arm ring/bracelet is a high tin bronze with a tin composition of 12.3 weight percent. Lead is present in the alloy at a concentration of 0.825 weight percent; it is unclear if lead was purposefully added to the alloy.
- The high tin and low lead concentrations make the alloy used to make MIT 5340 similar to the alloy used to make MIT 5334, the segmented arm ring discussed in Section 5.1.4.
- The metal comprising the ring was cast, and the ring was subjected to several cycles of working and annealing. The ring was lightly worked after its final anneal and was left in a worked condition.
- The zones of lines running perpendicular to the ring's longitudinal axis were most likely incised deeply into the metal with an engraving tool.

Figure 5.1.8.i: Zoned arm ring/bracelet. (MIT 5340/Peabody 40-77-40/13393). Photograph by E. Cooney.

Figure 5.1.8.ii: Zoned arm ring/bracelet. (MIT 5340/Peabody 40-77-40/13393). Photograph by E. Cooney.

Figure 5.1.8.iii: Zoned arm ring/bracelet. (Peabody 40-77-40/13313). This arm ring from Grave 11 has zones of incised lines perpendicular to the longitudinal axis of the ring. The tapered, overlapping ends are still intact. Peabody 40-77-40/13313 is similar to MIT 5340. Photograph by E. Cooney.

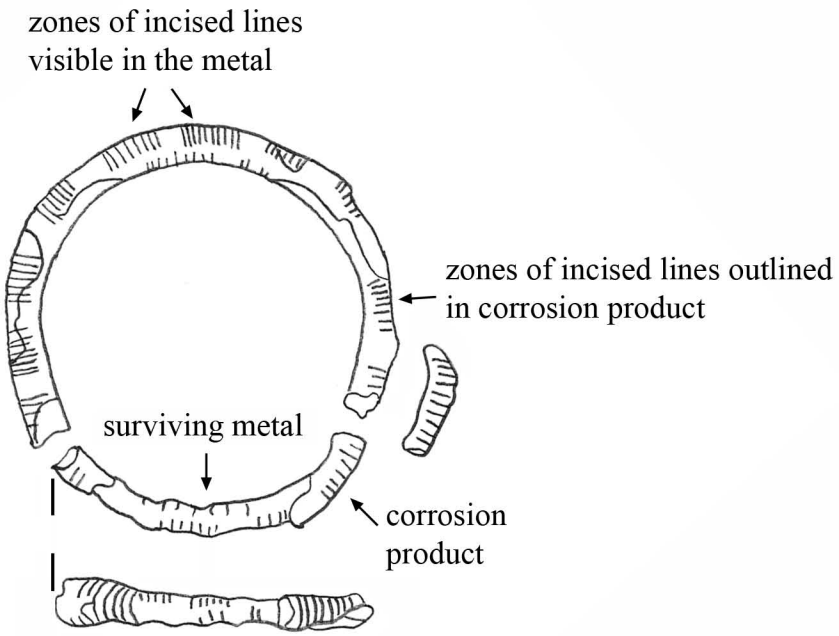

Figure 5.1.8.iv: Zoned arm ring/bracelet (MIT 5340). Key object features.

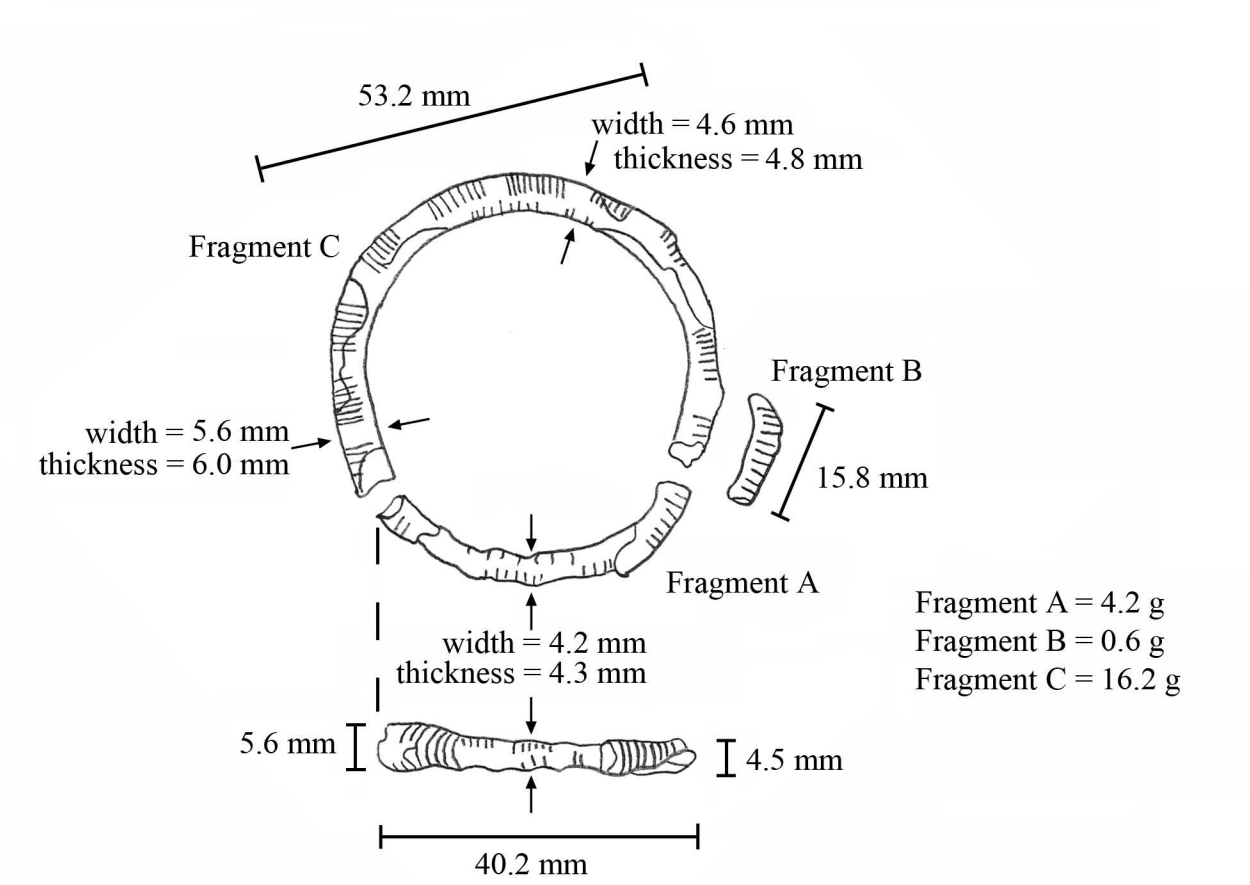

Figure 5.1.8.v: Zoned arm ring/bracelet (MIT 5340). Drawing and measurements.

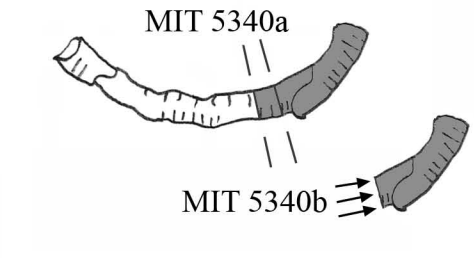

Figure 5.1.8.vi: Zoned arm ring/bracelet (MIT 5340). Sample 5340a was removed for bulk compositional analysis. Sample 5340b was removed for metallographic analysis and was mounted transversely as noted.

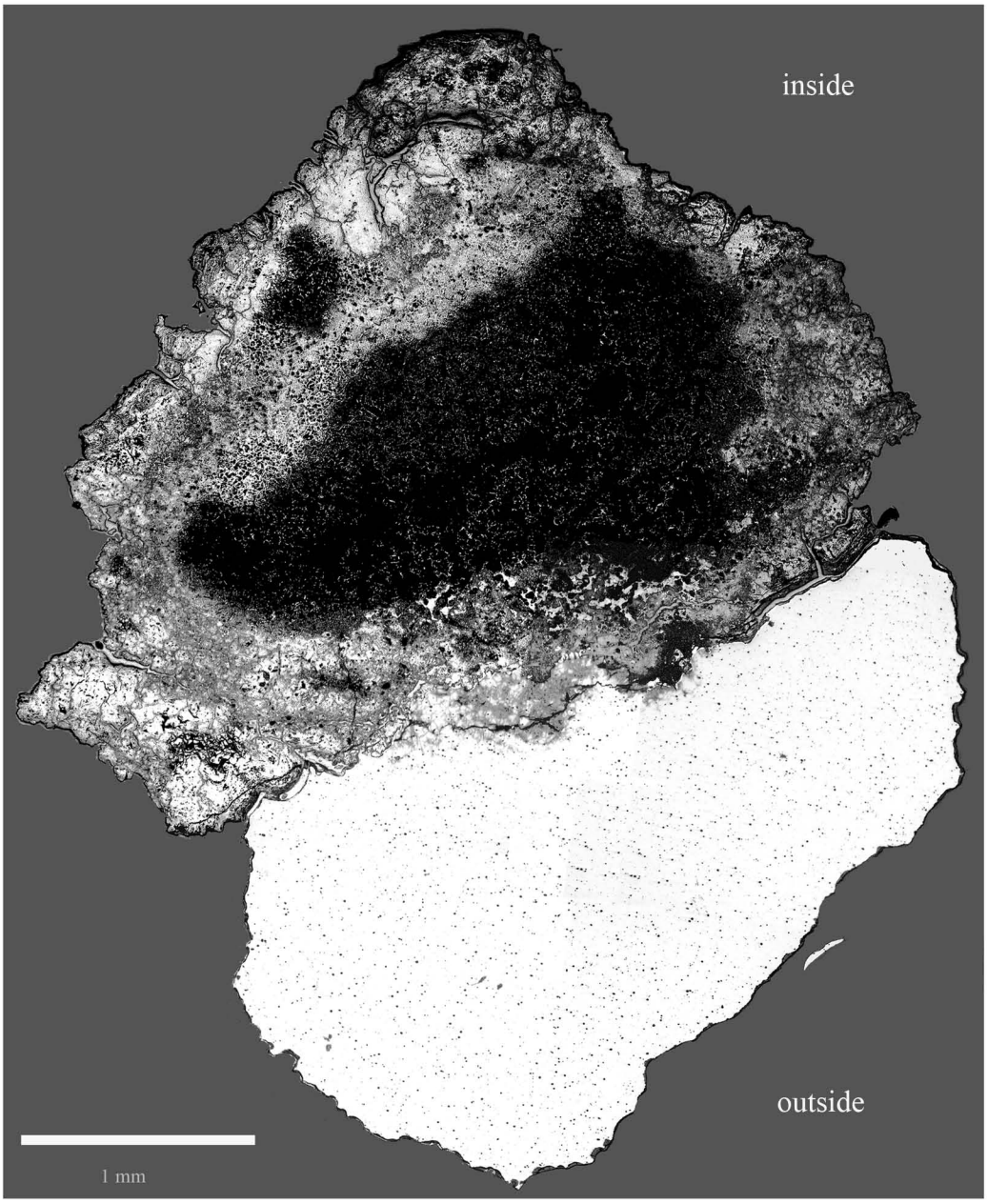

Figure 5.1.8.vii: Zoned arm ring/bracelet (MIT 5340/Peabody 40-77-40/13393). Transverse section, as polished. Over half the sample is completely mineralized. It is unclear what the original outline of the bracelet's cross section was. In the remaining metal a high density of small porosities can be seen homogenously distributed throughout the sample. A few gray copper sulfide inclusions are also homogeously distributed throughout the sample. (MIT Images 5340b-01-11).

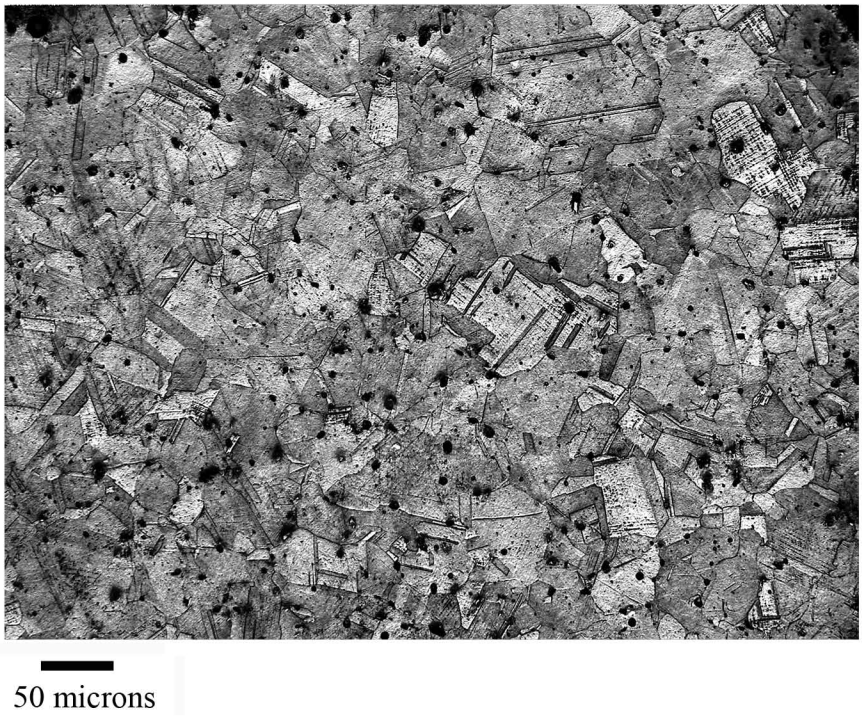

Figure 5.1.8.viii: Zoned arm ring/bracelet (MIT 5340/Peabody 40-77-40/13393). Transverse cross section. Etch: 20 sec potassium dichromate and 4 sec ferric chloride. x200. Microstructural features of interest include equiaxed grains with annealing twins and a light density of deformation lines along the bracelet's surface. (MIT Image 5340b-23).

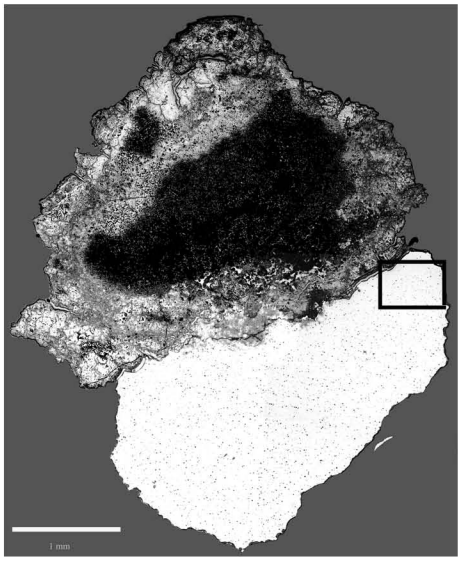

5.1.9: Hollow arm ring/bracelet (MIT 5366/Peabody 40-77-40/13482)

5.1.9a: Provenance and Background

MIT 5366 (Figures 5.1.9.i and 5.1.9.ii), identified by Wells as a hollow bronze ring (1981) came from Grave 40. Grave 40 was a cremation grave 2.1 m below the surface of the tumulus and oriented southeast-northwest. MIT 5366 is one of two fragmented hollow bronze rings in Grave 40; these rings are different sizes and have different forms of decoration.

Associated grave goods include a belt plate assemblage of which other surviving pieces include fragments of sheet bronze with and without rivets, bronze sheet with a band and hook of iron, a hollow bronze hook with rivet, a solid hook (MIT 5345, discussed in Section 5.3.3) and a small segmented bronze ring belt attachment (MIT 5350, discussed in Section 5.3.4). Other grave goods include an iron spearhead, sherds of at least four different pottery vessels, and a spindle whorl. The presence of a spindle whorl and an iron weapon raise questions as to the sex of the individual cremated in Grave 40.

MIT 5366 is one of five hollow rings (two arm rings, one finger ring, and two foot rings, discussed in Section 5.1.13) found in Tumulus IV. There are several other similarly decorated hollow arm rings from other tumuli at Stična. MIT 5366 has the same decoration pattern, zones of indented grooves that run perpendicular to the length of the ring, as MIT 5340, discussed in Section 5.1.8. Even though MIT 5366 is from a cremation grave, it was analyzed metallographically so that composition analysis could be carried out on the electron microbeam probe; it was deemed too fragile to be sampled for bulk composition analysis.

5.1.9b: Initial Examination and Observations

The hollow arm ring/bracelet was photographed (Figures 5.1.9.i and 5.1.9.ii), drawn to scale, measured, and observed (Figures 5.1.9.iii and 5.1.9.iv).

All that remains of the hollow arm ring are two fragments. The cross section of the ring is oval, and there is a seam present along the inside of the ring parallel to the ring's longitudinal axis. The ring appears to have been made from rectangular sheet bent

around until the two long edges met at the seam. The sheet is 0.9 mm thick. The original ring was most likely circular and closed, much like the hollow foot rings discussed in Section 5.1.13.

The ring is decorated with zones of four grooves that run perpendicular to the longitudinal axis of the ring. These grooves divide each zone into three raised, rounded sections. The zones of grooves are separated from one another by larger raised, rounded sections (see Figure 5.1.9.iii). At some broken edges the profile of the zoned decoration can be seen clearly in the sheet metal. Under magnification the very beginning of each groove is somewhat diamond shaped, and it appears that the grooves were cut into the bracelet with a sharp tool like an engraving tool.

The smallest fragment (Figures 5.1.9.i and 5.1.9.ii) weighs 1.1 g and is 28.3 mm long, 5.7 mm thick, and 6.5 mm wide. The larger fragment weighs 4.6 g, is 62.9 mm long, 5.7 mm thick, and 5.5 mm wide.

The ring is structurally robust away from its broken edges, which are fragile and highly mineralized. The ring is covered in mottled dark and light green corrosion product that is somewhat friable.

5.1.9c: Sampling

Two samples were removed from the hollow arm ring/bracelet with transverse cuts (Figure 5.1.9.v). Sample 5366a was removed for metallographic analysis and was mounted transversely as noted. Sample 5366b was also removed for metallographic analysis and was mounted longitudinally as noted. It was ground down until the center of the bracelet was exposed. Composition analysis was carried out with the electron microbeam probe.

5.1.9d: Metallographic and Electron Microbeam Probe Analyses

Sample 5366a was mounted as a transverse section. As polished, (Figure 5.1.9.vi), the bracelet's seam and the hollow interior of the bracelet can be seen clearly. The two ends of the sheet are bent together so there is no space between them. There is a larger amount of external corrosion product on the exterior metal of the ring than there is

on the surface of the metal in the hollow interior. This is most likely because the exterior of the ring was exposed to the elements while the interior was protected.

Other microstructural features of interest in the transverse as-polished sample include a few scattered pools of blue-green copper-tin eutectoid, a high density of porosities, and a few gray copper sulfide inclusions with no apparent alignment scattered homogenously throughout the sample.

Sample 5366b was mounted as a longitudinal section and was ground down until the center plane of the bracelet was exposed (Figure 5.1.9.vii). The external corrosion product on the outside, exterior metal shows the original outlines of the zoned decoration clearly. The photomicrograph shows that the decoration is not completely symmetrical; the grooves of different zones are not exactly identical. The rounded sections and the grooves separating them are slightly different shapes and sizes from zone to zone. It can also be seen that the surface contour of the metal along the hollow interior of the ring does not follow the peak and trough contour of the exterior, decorated surface.

Other microstructural features of interest in the longitudinal as-polished sample include a few scattered pools of blue-green copper-tin eutectoid, a high density of porosities, and a few gray copper-sulfide inclusions with no apparent alignment scattered homogenously throughout the sample. Viewed in the microscope, the internal corrosion product appears to outline some equiaxed grains (Figure 5.1.9.x).

MIT 5366b was analyzed with an electron microbeam probe to determine its composition. The composition of a series of six points across the longitudinal section whose locations are indicated in Figure 5.1.9.viii was determined, and the average value of the six is given in the table in Figure 5.1.9.viii. The average composition of the bracelet is given below in Table 5.1.9.

Table 5.1.9: Average Composition of MIT 5366

Cu	**Sn**	**Pb**	**Sb**	**As**	**Ni**	**Co**	**Ag**	**Fe**
87.90	12.13	0.501	n.d	0.186	0.104	0.007	n.d.	0.005

(all values in weight %) n.d = not detected

The ring is a copper-tin alloy with an average tin composition of 12.13 weight percent. Lead is present at an average concentration of about 0.5 weight percent. Due to

the inhomogenous presence of lead in the sample, which is discussed below, the composition of lead is probably underreported. Minor and trace elements appear in relatively low amounts.

The electron microbeam probe was also used to analyze some of the sample's microstructural features. The green-blue eutectoid pools were analyzed to verify their identification as eutectoid microconstituents. Figure 5.1.9.ix.a shows a backscattered electron image of a eutectoid pool. The electron microbeam probe determined the composition of the pool as 23.55 weight percent tin and 76 weight percent copper; this composition falls into the compositional range of a Cu-Sn eutectoid. The light gray-appearing material is the eutectoid δ phase, and the dark gray-appearing material within the δ phase is the eutectoid α phase. The porosities appear black in color, and they are partially filled with lead, which appears bright in color. The same eutectoid pool is shown in the color photomicrograph in Figure 5.1.9.ix.b where it is light green in color.

The electron microbeam probe was also used to analyze some internal corrosion product. Figure 5.1.9.xa shows a backscattered electron image of what appears in the photomicrograph (Figure 5.1.9.x.b) as a large area of internal corrosion. The backscattered electron image shows that this area of corrosion includes large pools of lead inhomogenously scattered throughout the corrosion product and also present in some porosities. The lead again appears bright in color. An EDS spectrum of the bright appearing material confirms that it is lead (Figure 5.1.9.xi). The inhomogenous distribution of lead in the bracelet is doubtless why the average lead composition as determined by the electron microbeam probe's point analysis appears to be low. The true lead composition of the bracelet is most likely higher than 0.5 weight percent.

The transverse cross section, MIT 5366a, was etched for 4 seconds with potassium dichromate and for 3 seconds with aqueous ferric chloride to reveal a microstructure characterized by equiaxed grains with annealing twins and a few pools of Cu-Sn eutectoid scattered throughout the sample (Figure 5.1.9.xii). A low density of deformation lines can also be found throughout the sample (Figure 5.1.9.xiii).

It is unclear if this microstructure formed by as a result of a deliberate annealing of the ring or if it was caused by the heat of a cremation fire. The light density of deformation lines indicates that it may have been the former and that the bracelet was

lightly worked after its final anneal. The size of the grains along the outside of the bracelet (Figure 5.1.9.xii), where the decoration is present, and along the inside of the bracelet (Figure 5.1.9.xiii) appear to be the same, indicating that the outside surface of the bracelet where the decoration is present was not much more heavily worked than the inside surface.

The longitudinal cross section, MIT 5366b, was etched for 7 seconds with potassium dichromate and for 1 second with aqueous ferric chloride. The same microstructure (Figure 5.1.9.xiv) as that revealed in the transverse section is present: equiaxed grains with annealing twins and a few pools of Cu-Sn eutectoid scattered throughout the sample. Due to the extent of corrosion at the outside surface of the bracelet, it is impossible to discern if the grains at the outside, exterior surface are smaller than grains along the bracelet's interior surface.

Figure 5.1.9.xiv shows the grains near the outside, exterior surface. There is a light density of deformation lines along the exterior surface. This same light density of deformation lines can also be seen elsewhere in the sample (Figure 5.1.9.xv), indicating that the ring was slightly worked after its final anneal.

5.1.9e: Discussion

The bracelet is comprised of thin sheet made from a tin-bronze alloy with approximately 12.13 weight percent tin. There is at least 0.5 weight percent lead also present in the alloy, although this value is probably somewhat underreported due to the inhomogenous presence of lead throughout the sample. The high amount of tin and low amount of lead made an alloy that was harder and more easily hammered into thin sheet than a lower tin bronze or more heavily leaded alloy (Giumlia-Mair 1995). As the ring was hollow and made from thin bronze sheet, the metal needed to be hard or the bracelet risked being deformed easily.

The high density of porosities indicates that the metal comprising the sheet was originally cast. The metal was then subject to several cycles of cold-working and annealing to render it into thin sheet.

The thin sheet was likely made into a hollow ring in a manner similar to that used to fashion two hollow, circular Chimú bangle bracelets described by Lechtman (1996). Such hollow rings

> can be accomplished without great difficulty by hammering the sheet into a trough of the desired U-section. The former or mold containing the former or trough must itself be convex, not flat. When the sheet is hammered down into the trough, it adopts the U-shaped contour. At the same time, as the sheet moves progressively along the convex former, it curves of itself, eventually becoming circular. Thus, the annular form and the desired cross section are achieved simultaneously. One the ring is complete, its hollow interior can be filled with a resilient material, such as wax…the top edges of the U are then bent in, toward each other, and hammered down over the solid core, until they meet to form a circumferential seam. It is an easy matter to melt the core material out (Lechtman 1996).

The decoration was most likely formed with an engraving tool after the sheet had been formed into a hollow ring but before the resilient material, most likely wax or bitumen, was melted out. An engraving tool would have cut away excess metal to leave behind a somewhat diamond shaped contour at the beginning of each groove, similar to those seen upon examination of the ring's groove decorations. A chasing tool, which would have compressed the metal, would likely have produced contours of a different shape from those evident on the exterior of the ring. Also, a chasing tool, by compressing, or working, the metal, would have affected the metal beneath the decoration in a way that is not seen in MIT 5366. An engraving tool would cut the grooves without deforming (or working) the surrounding metal.

By contrast, if a chasing tool had been used and the ring had not been annealed after the decoration was achieved, a high density of deformation lines would be present within the grains along the outside, exterior surface of the ring, particularly in the vicinity

of each groove. In addition, the porosities and inclusions in the metal would become elongated and oriented in the direction of metal flow on either side of the compressed groove. If a chasing tool had been used and the ring annealed after the decoration was formed, those heavily worked near-surface grains would have recrystallized to form smaller grains than those of the metal in the interior. Neither of these features—elongated pores and inclusions and small grains at the surface-- is present in samples MIT 5366a or MIT 5366b. In addition, the shape of the interior surface on the outside of the ring observed in the longitudinal section suggests that the metal above it was never compressed or subject to the forces of a chasing tool.

It is not clear if the metal was purposefully left in an annealed state. It would make sense if it were for two reasons: first, the heavily worked metal that resulted from shaping the bracelet would have been brittle, and second, it would have been easier to create the decoration with an engraving tool if the metal were somewhat soft than if it were hardened from hammering.

5.1.9.f: Conclusions

- The hollow arm ring/bracelet is made from a tin-bronze alloy with a tin composition of approximately 12 weight percent. It also contains at least 0.5 weight percent lead. This composition is consistent with the composition of other objects made from sheet metal at S. Lucia (Giumlia-Mair 1995).
- The high density of porosities indicates that the metal comprising the sheet was cast originally. The metal was then subject to several cycles of cold-working and annealing to render it into thin sheet.
- The thin sheet was hammered in or around a former simultaneously to create the desired hollow, oval cross section and to render the circular ring. The hollow bracelet was then filled with a resilient material, and the ends were further hammered together to form the seam.
- The grooved decoration was likely formed with engraving tools once the ring was shaped.

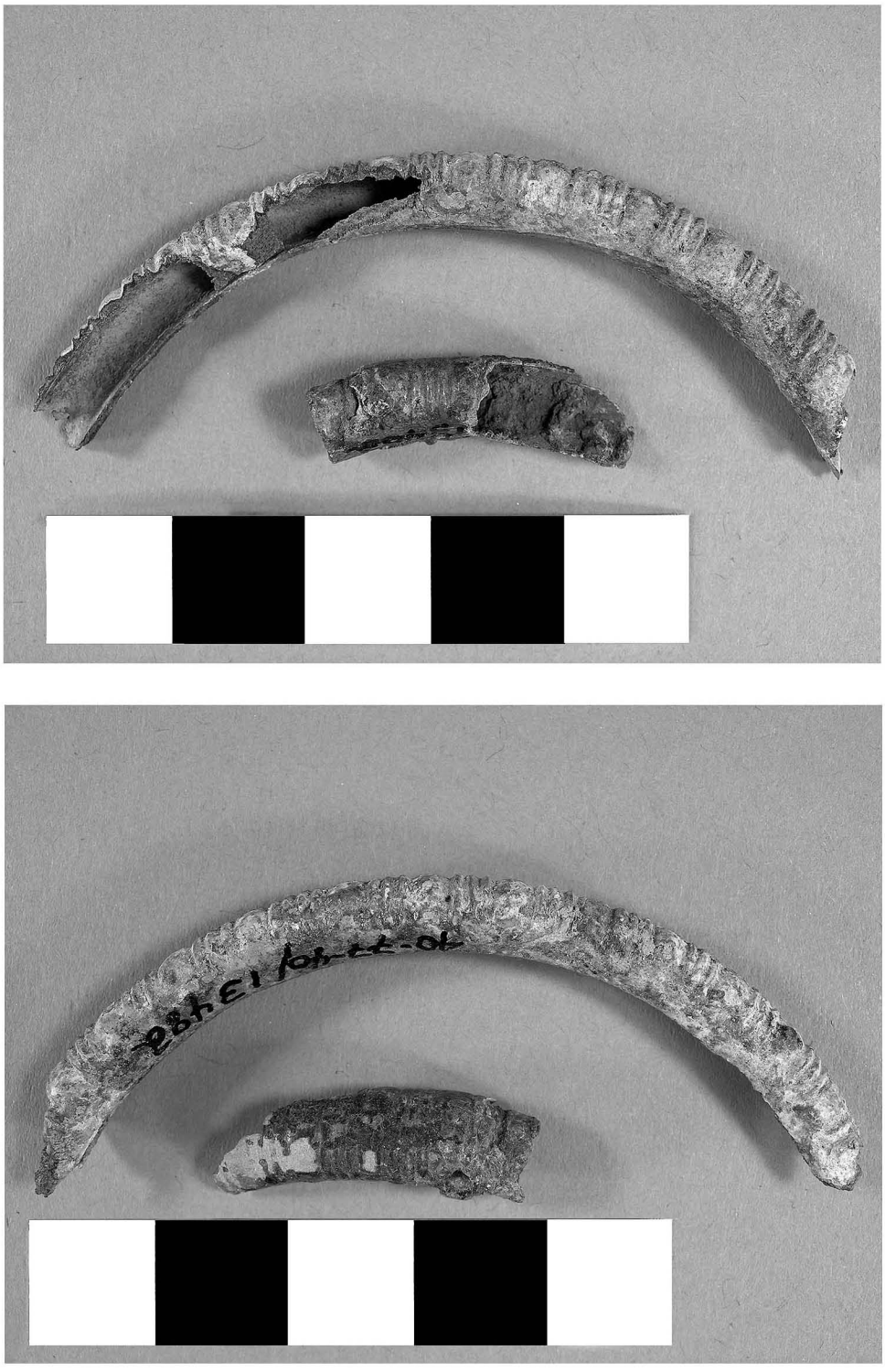

Figure 5.1.9.i: Hollow arm ring/bracelet. (MIT 5366/Peabody 40-77-40/13482). Photograph by E. Cooney.

Figure 5.1.9.ii: Hollow arm ring/bracelet. (MIT 5366/Peabody 40-77-40/13482). Photograph by E. Cooney.

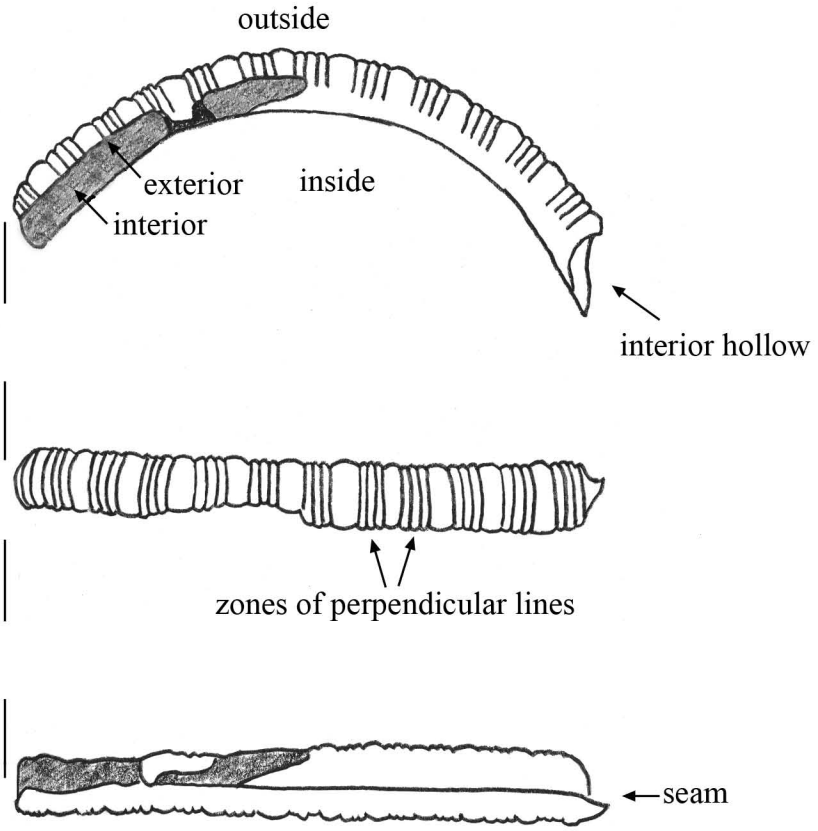

Figure 5.1.9.iii: Hollow arm ring/bracelet (MIT 5366). Key object features.

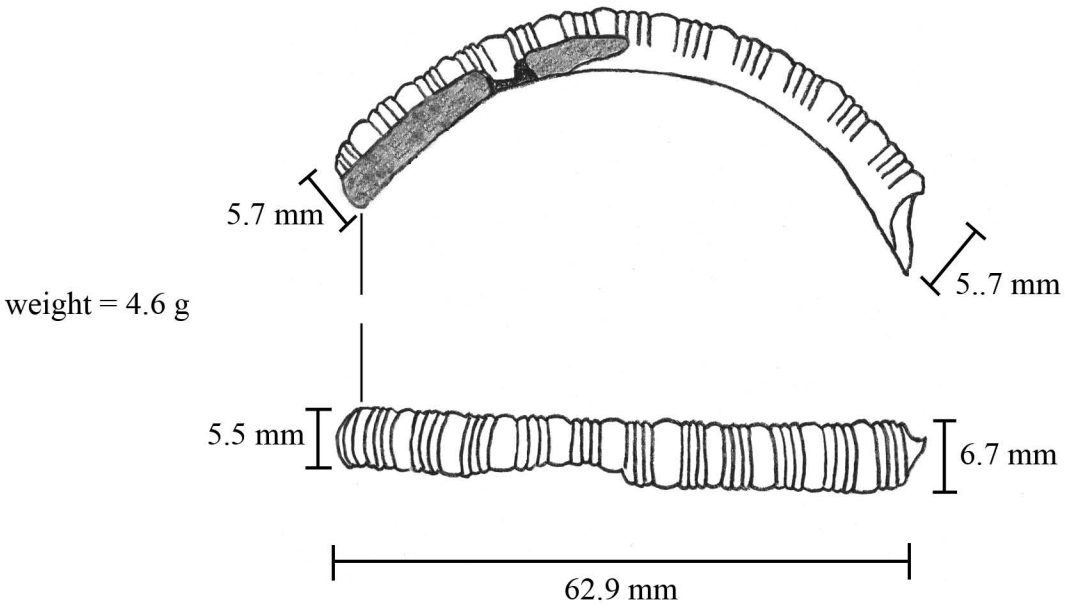

Figure 5.1.9.iv: Hollow arm ring/bracelet (MIT 5366). Drawing and measurements.

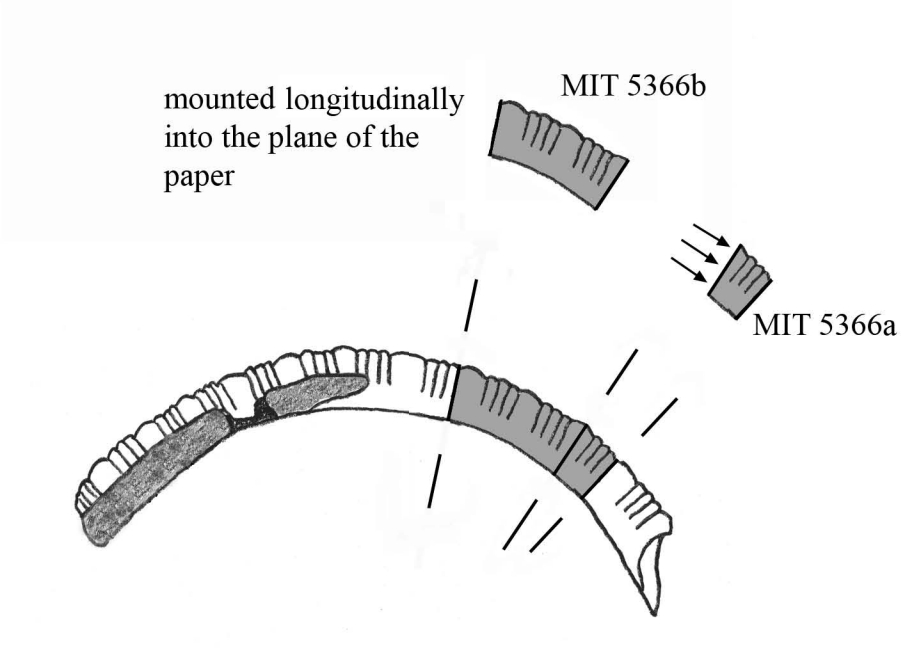

Figure 5.1.9.v: Hollow arm ring/bracelet (MIT 5366). Sample MIT 5366a was removed for metallographic analysis and was mounted transversely as noted. Sample 5366b was removed for metallographic analysis and was mounted longitudinally as noted. It was then ground down until the center of the bracelet was exposed. Composition analysis was determined on the electron microbeam probe.

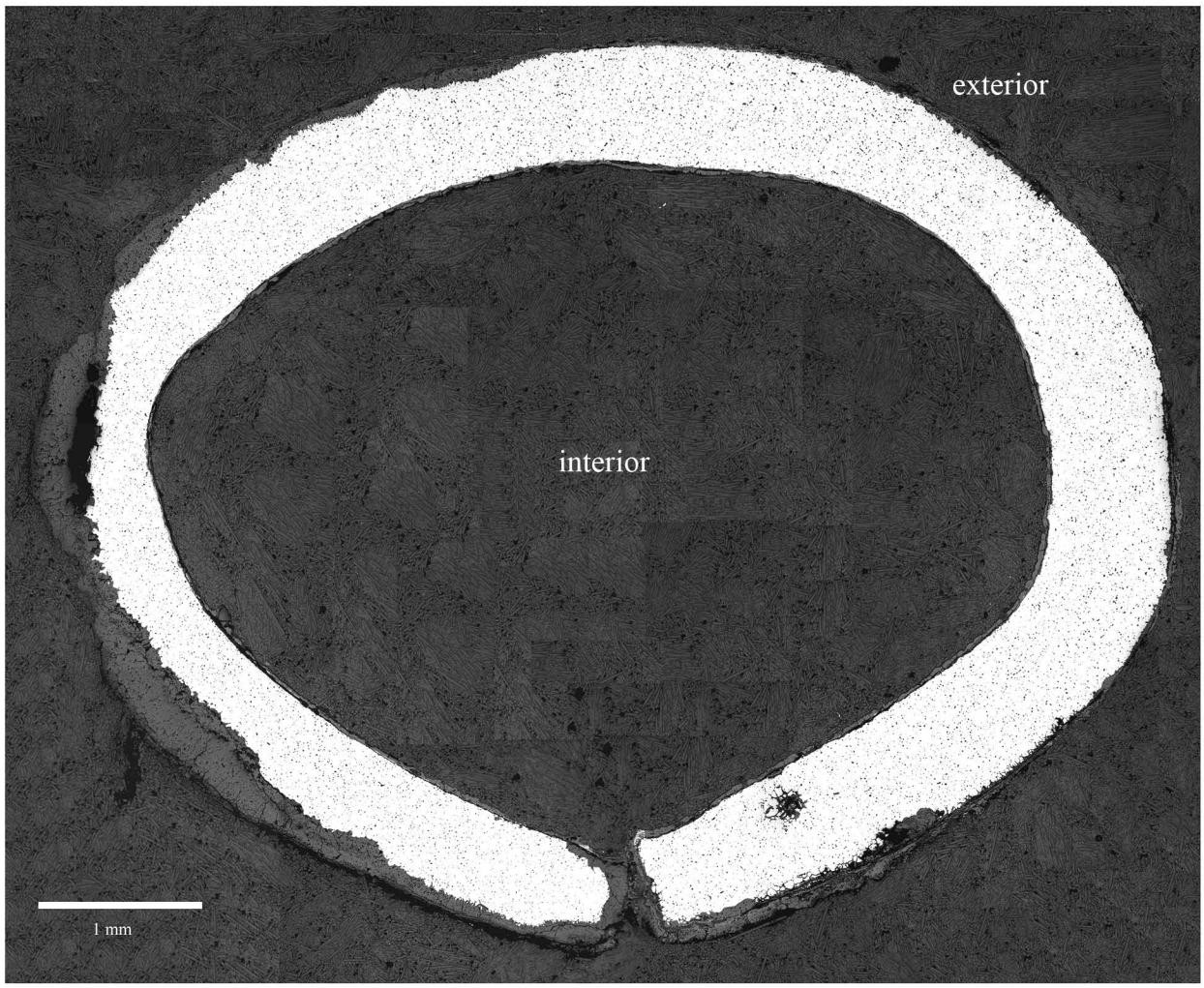

Figure 5.1.9.vi: Hollow arm ring/bracelet (MIT 5366/Peabody 40-77-40/13482). Sample MIT 5366a, transverse cross section. As polished. The photomicrograph clearly shows the bracelet's mechanical seam. The two ends of the sheet comprising the bracelet meet to create the seam. Other microstructural features of interest include a larger amount of corrosion product on the bracelet's exterior as compared to the corrosion on the bracelet's interior and a high density of porosities. (MIT Images 5366a-01-10).

Key

outside surface

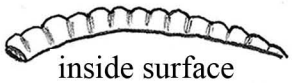

inside surface

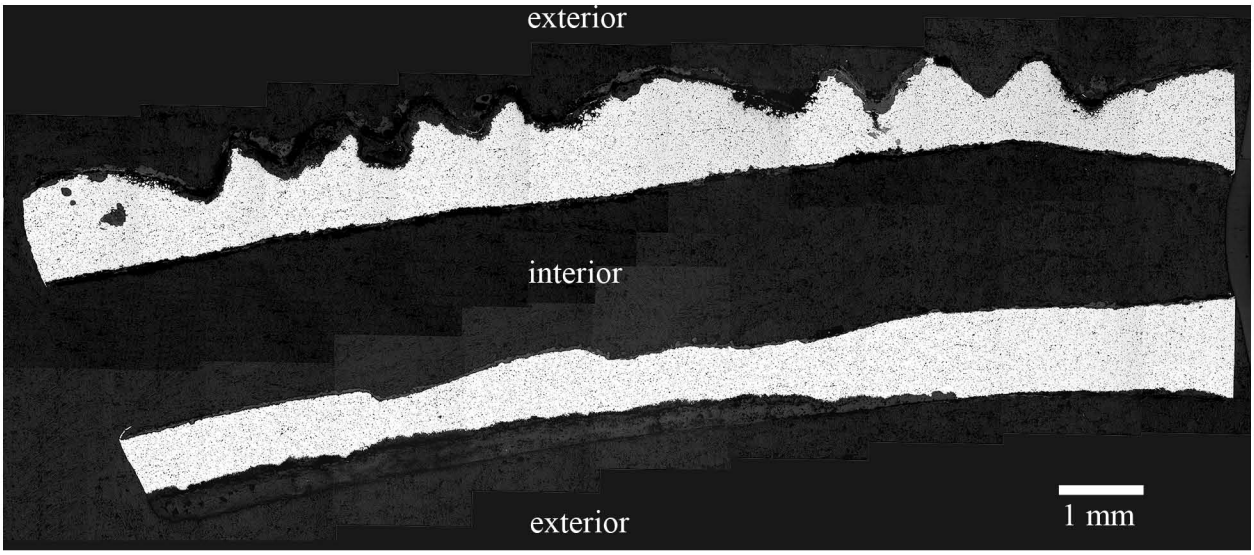

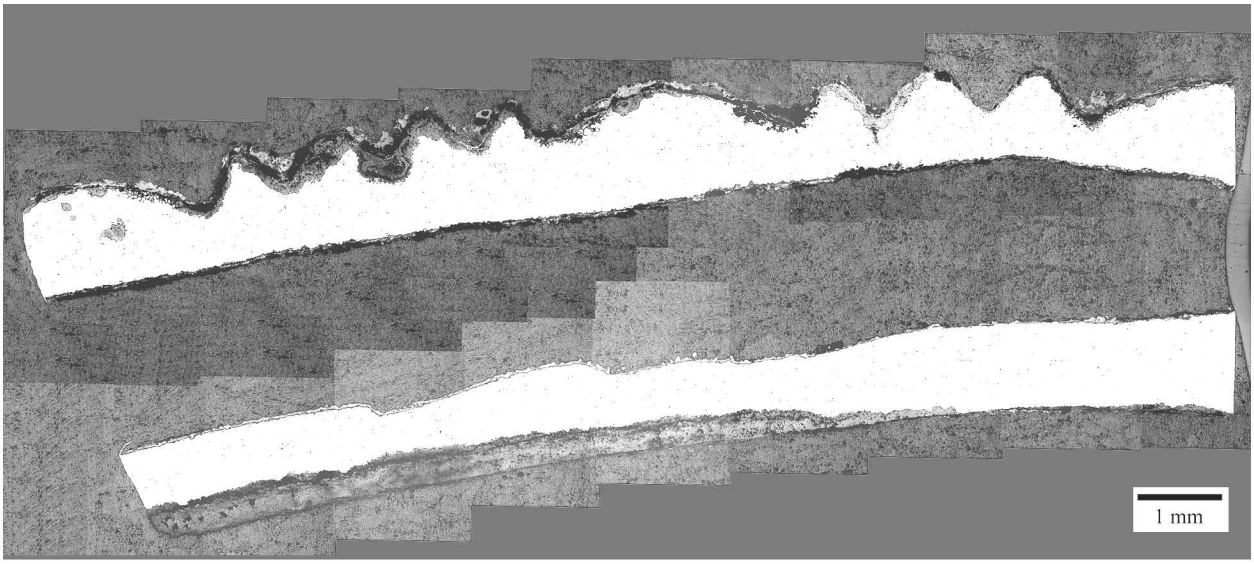

Figure 5.1.9.vii: Hollow arm ring/bracelet (MIT 5366/Peabody 40-77-40/13482). Sample MIT 5366b, longitudinal cross section. As polished. (MIT Images 5366b-33-53).
Above: Photomicrograph shows the high density of porosities homogenously distributed throughout the sample.
Below: Photomicrograph shows a larger amount of corrosion product on the bracelet's exterior as compared to the corrosion on the bracelet's interior. The original outline of the zoned decoration can be seen in the ring's external corrosion product. It is clear that the decoration is not completely symmetrical; the decoration's peaks and troughs are slightly different shapes and sizes across the ring.

Key

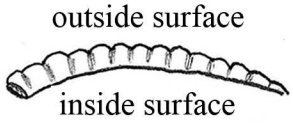

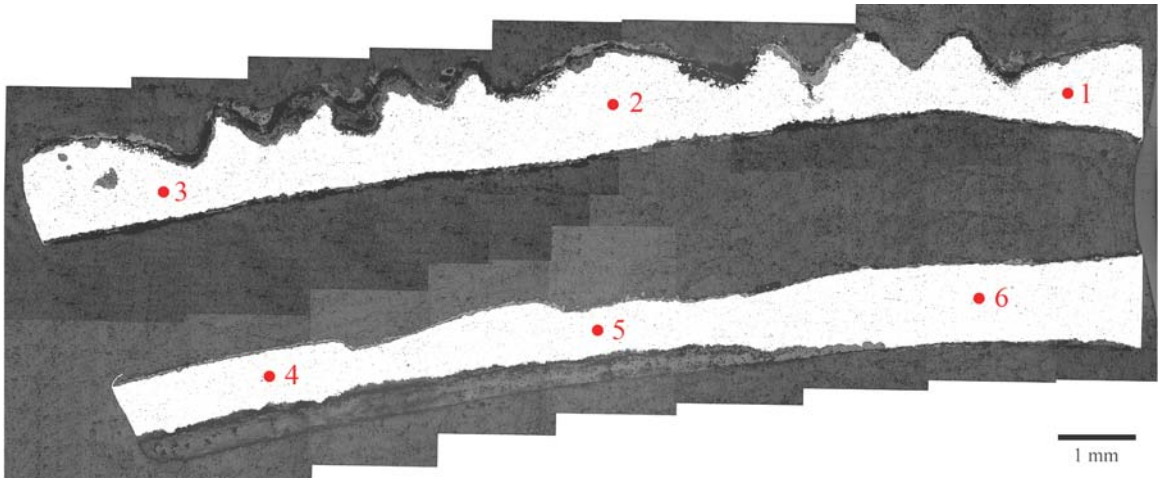

Electron Microbeam Probe Compositional Data

	Cu	Sn	Pb	Sb	As	Ni	Co	Ag	Fe
Pt 1	86.18	12.18	0.7245	n.d.	0.1438	0.1158	0.0054	n.d.	0.0278
Pt 2	89.06	12.52	0.1198	n.d.	0.2251	0.1011	0.0023	n.d.	0.0041
Pt 3	89.21	11.65	0.4626	n.d.	0.1825	0.09	0.0312	n.d.	n.d.
Pt 4	88.39	12.21	0.1275	n.d.	0.2045	0.11	0.0044	n.d.	n.d.
Pt 5	87.73	11.55	0.1356	n.d.	0.1835	0.1009	n.d.	n.d.	n.d.
Pt 6	86.81	12.65	1.4372	n.d.	0.1746	0.1082	n.d.	n.d.	n.d.
Average	87.90	12.13	0.5012	n.d.	0.1857	0.1043	0.0072	n.d.	0.0053

(all values in weight %) n.d.= not determined

Figure 5.1.9.viii: Hollow arm ring/bracelet (MIT 5366b/Peabody 40-77-40/13482).
Above: Points at which compositional data were taken by the electron microbeam probe.
Below: Electron microbeam probe compositional data from each point.

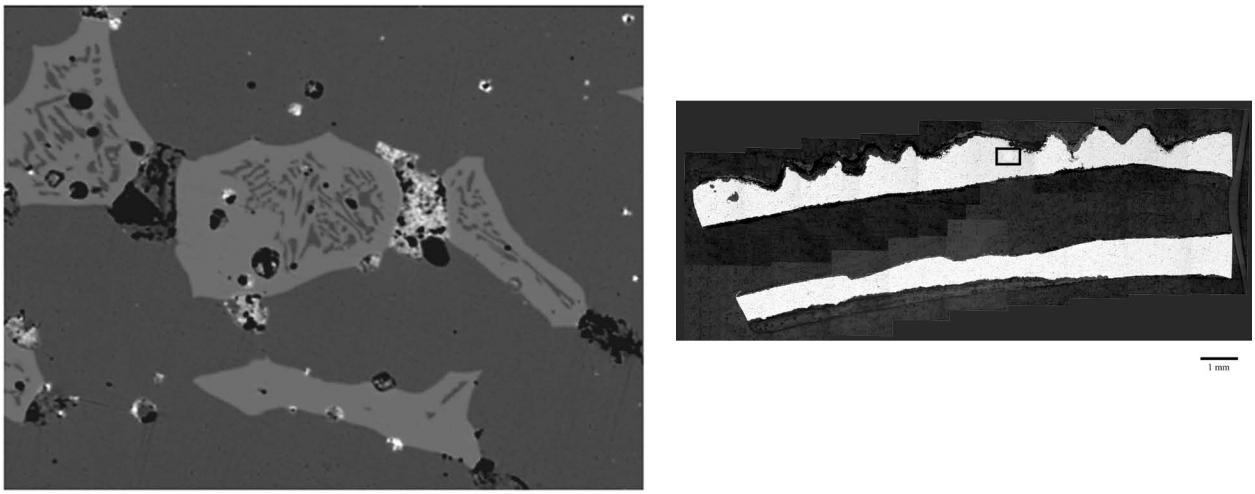

(a)

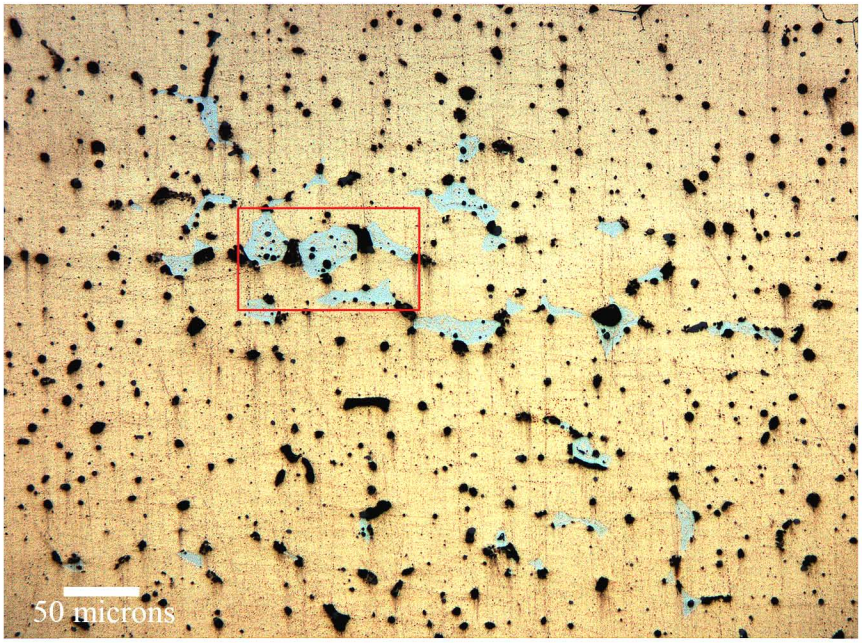

(b)

Figure 5.1.9.ix: Hollow arm ring/bracelet (MIT 5366b/40-77-40/13482).
(a) Backscattered electron image of a Cu-Sn eutectoid pool. The electron microbeam probe determined the composition of the eutectoid pool as 23.55 weight % Sn and 76 weight % Cu. The light gray- appearing material is the eutectoid's δ phase, and the dark gray appearing material is the primary α phase alloy. The porosities appear black in color, and they are partially filled with lead, which appears bright in color.
(b) Photomicrograph at x200 showing slightly elongated pools of eutectoid. The eutectoid is light green. (MIT Image 5366b-58.)

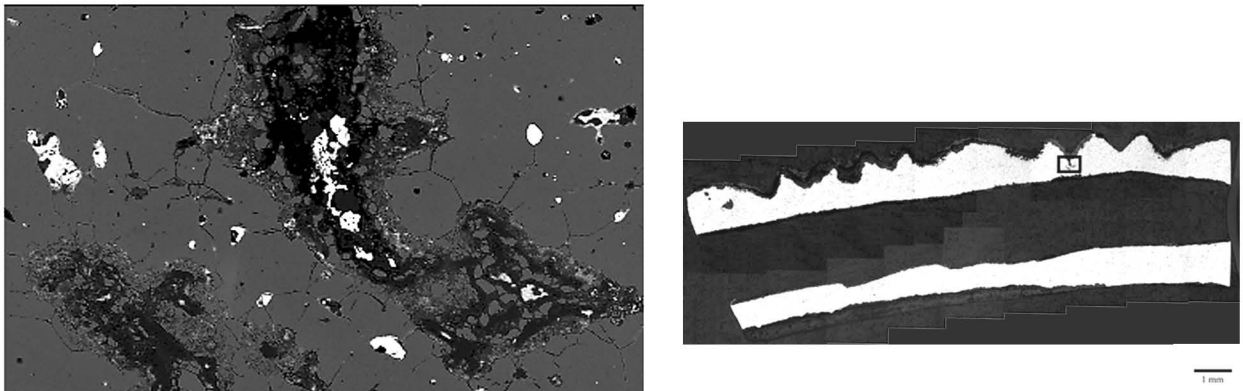

Figure 5.1.9.x: Hollow arm ring/bracelet (MIT 5366b/40-77-40/13482).
(a) Backscattered electron image showing internal corrosion product, porosities, and pools of lead. The lead appears light in color, and the pores and corrosion product appear dark.
(b) As-polished photomicrograph at x200 shows the internal corrosion product, porosities, and pools of lead, all of which appear dark in color. The internal corrosion outlines equiaxed grains.

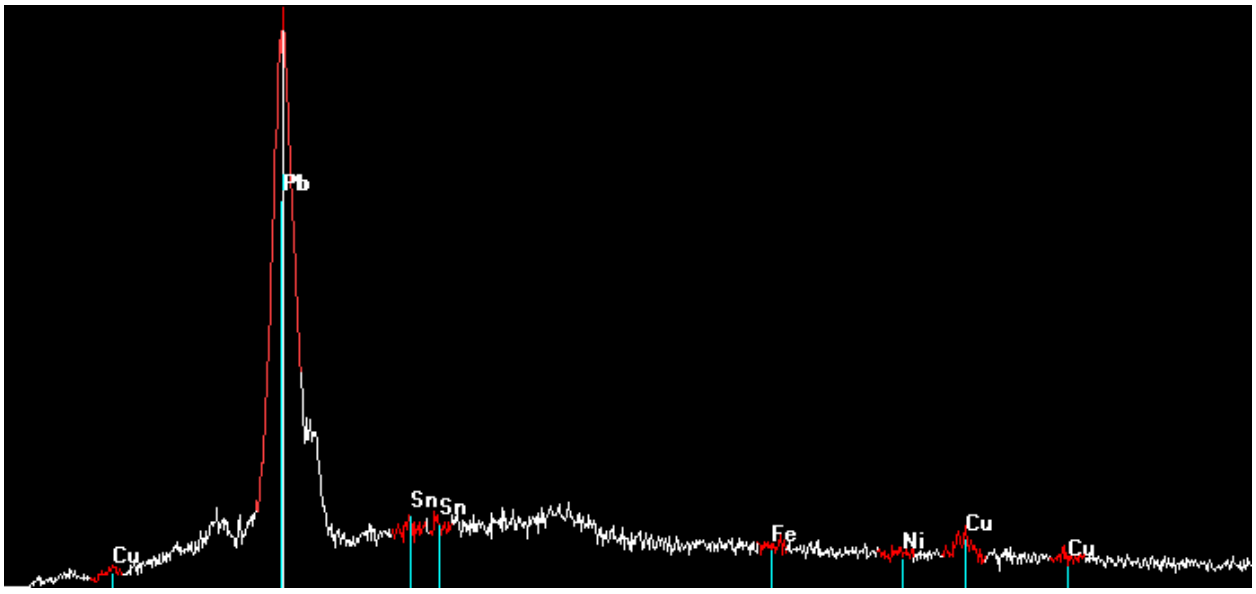

Figure 5.1.9.xi: Hollow arm ring/bracelet (MIT 5366b/Peabody 40-77-40/13482). EDS spectrum of the light-appearing material in the backscattered electron image of the hollow arm ring (see Figure 5.1.9.x). The spectrum identifies this material as lead.

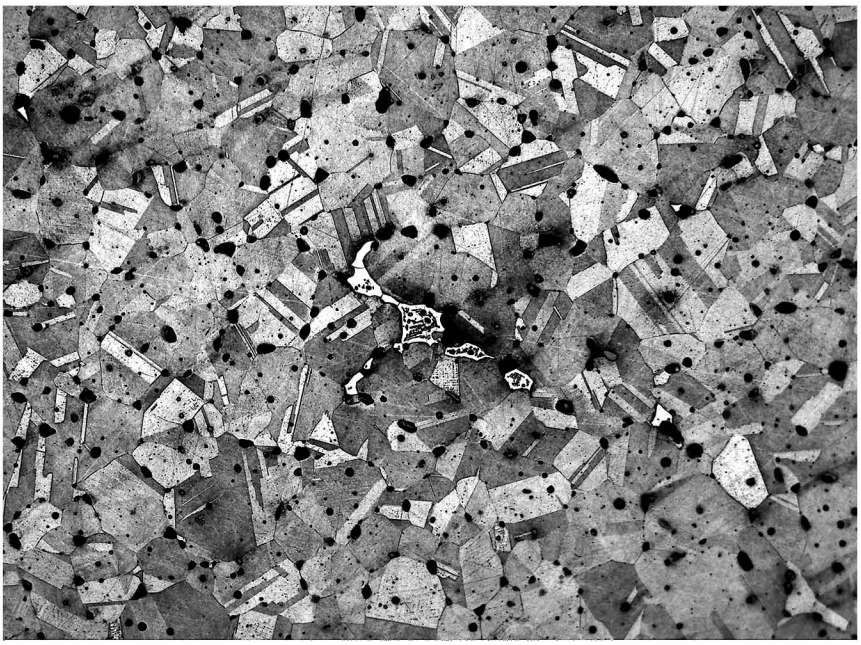

Figure 5.1.9.xii: Hollow arm ring/bracelet (MIT 5366/Peabody 40-77-40/13482). Transverse cross section. Etch: 4 sec potassium dichromate, 3 sec ferric chloride. x200. Microstructural features of interest include equiaxed grains with annealing twins and a pool of Cu-Sn eutectoid. (MIT Image 5366b-15).

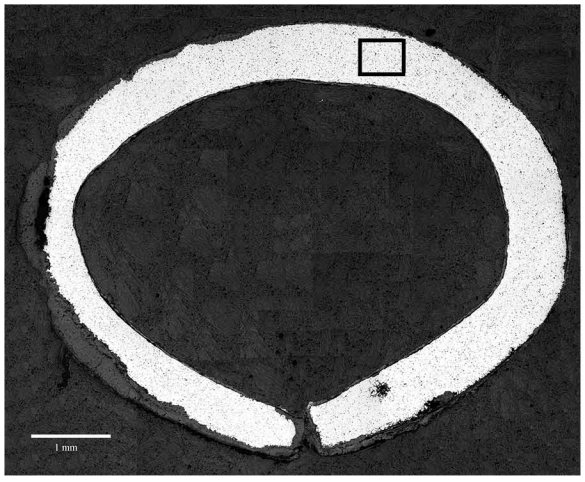

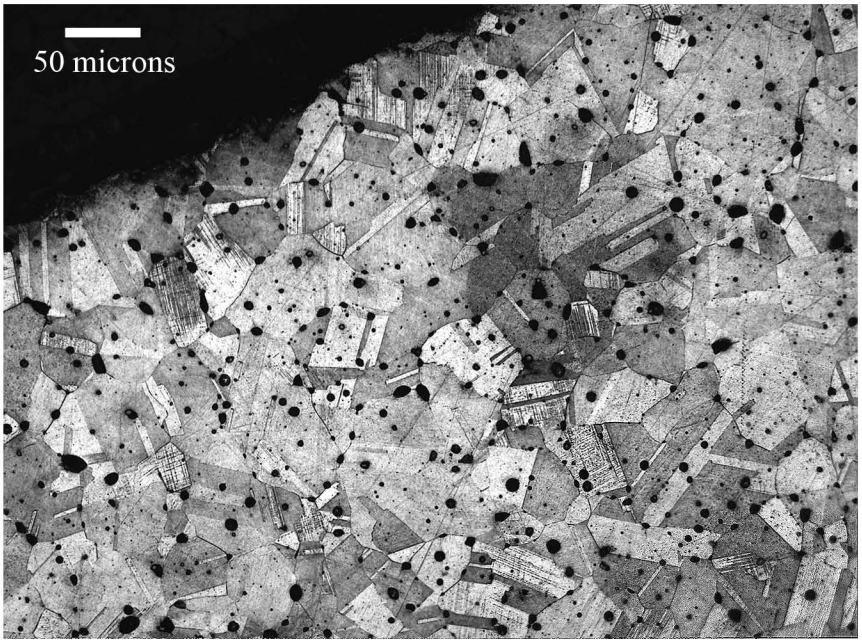

Figure 5.1.9.xiii: Hollow arm ring/bracelet (MIT 5366/Peabody 40-77-40/13482). Transverse cross section. Etch: 4 sec potassium dichromate, 3 sec ferric chloride. x200. Microstructural features of interest include equiaxed grains with annealing twins and some equiaxed grains with deformation lines near the interior of the ring, close to the seam. (MIT Image 5366b-13).

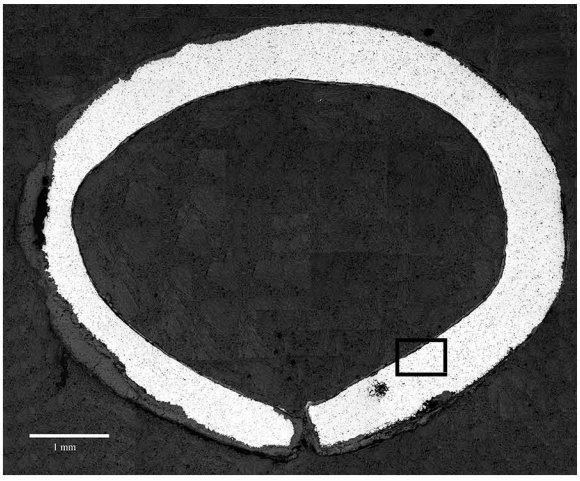

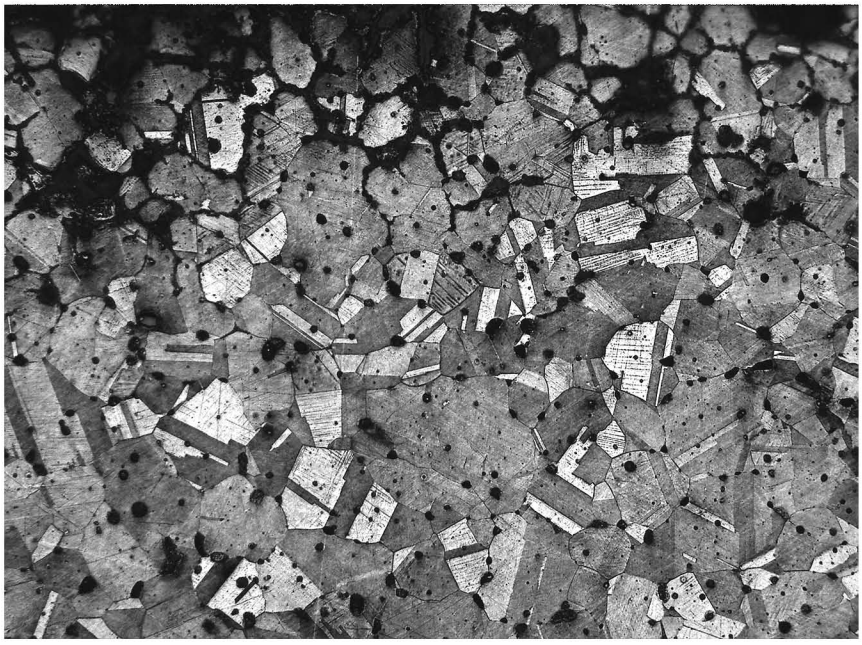

Figure 5.1.9.xiv: Hollow arm ring/bracelet (MIT 5366/Peabody 40-77-40/13482). Longitudinal cross section. Etch: 7 sec potassium dichromate and 1 sec ferric chloride. x200. Microstructural features of interest include equiaxed grains with annealing twins and some equiaxed grains with deformation lines at the outside surface of the decoration. (MIT Image 5366b-29).

Figure 5.1.9.xv: Hollow arm ring/bracelet (MIT 5366/Peabody 40-77-40/13482). Longitudinal cross section. Etch: 7 sec potassium dichromate and 1 sec ferric chloride. x200. Microstructural features of interest include equiaxed grains with annealing twins and some equiaxed grains witha few deformation lines (MIT 5366b-22).

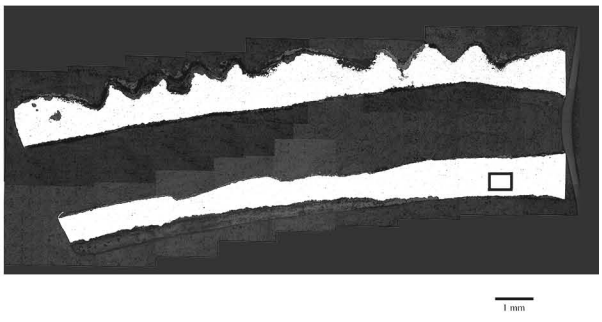

5.1.10: Flat arm ring/bracelet (MIT 5365/Peabody 40-77-40/13459)

5.1.10a: Provenance and Background

MIT 5365 (Figures 5.1.10.i and 5.1.10.ii) consists of three fragments from a flat arm ring from Grave 35 (Wells 1981). Grave 35 was 2.75 m long, 0.9 m wide, and 0.5 m deep, and it was found 1.6 m below the surface of the tumulus. Associated grave goods include a second, identical flat bronze arm ring, a bronze finger ring, fifty-seven small amber beads, an earring, and a footed gray bowl.

MIT 5365 is one of nine flat arm rings in Tumulus IV.

5.1.10b: Initial Examination and Observations

The flat arm ring/bracelet was photographed (Figures 5.1.10.i and 5.1.10.ii), drawn to scale, measured, and observed (Figures 5.1.9.iii and 5.1.9.iv).

There are three surviving fragments of the flat arm ring. These fragments are decorated by two grooves that separate the bracelet's outside surface into three distinct raised sections. The inside surface of the ring is flat and smooth. Longitudinal striations, perhaps from a polishing tool, can be seen when the inside surface is viewed under magnification. Fragment A has an intact, tapered end decorated with an incised chevron design. Fragment B is the only fragment that has an area with both original edges still present.

Fragment A is 60.1 mm long. Its intact, tapered end with the chevron design is 2.3 mm wide and 1.6 mm thick. Its fractured end is 6.9 mm wide and 1.9 mm thick. It weighs 2.6 g.

Fragment B is 50.7 mm wide. At the area that still retains its original edges, the sample is 6.6 mm wide and 1.9 mm thick. Fragment B weighs 1.9 g.

Fragment C is 30.4 mm long. Its fragmented edges are 6.9 mm and 6.2 mm wide. It is 1.7 mm thick and weighs 0.9 g.

The fragments appear to be highly mineralized at their edges. The surface is covered with a friable mottled dark and light green corrosion product. A few pseudomorphs from large, loose fibers are found on the inside surface of Fragment C.

5.1.10c: Sampling

Sample MIT 5365 was removed from Fragment B with two transverse cuts and was mounted transversely for metallographic analysis (Figure 5.1.11.iv). Composition analysis was undertaken with the electron microbeam probe.

5.1.10d: Metallographic analysis

Sample MIT 5365 was mounted as a transverse section. As polished (Figure 5.1.10.vi), the two grooves and three raised sections on the ring's outside surface and the smooth, flat inside surface can be clearly seen in the ring's external corrosion product. There is a low density of porosities and a high density of gray copper sulfide inclusions present in the sample. These inclusions are elongated and are oriented parallel to the ring's longitudinal axis, indicating that the ring was heavily worked perpendicular to the longitudinal axis. Equiaxed grains with deformation lines are outlined by the ring's internal corrosion product (Figure 5.1.10.vii).

The photomicrograph in Figure 5.1.10.viii shows the metal and corrosion product at and directly beneath one of the ring's grooves. The original contour of groove can be clearly seen in the external corrosion product. The orientation of the elongated copper sulfide inclusions does not change around or underneath the groove, indicating that the metal directly beneath the groove was not subject to working by a compressive force. The microstructure immediately beneath the groove is the same as the metal in the bulk of the ring. This indicates that the grooves were not pressed into the metal with a chasing tool, but rather that the grooves were made by cutting metal away from the ring with an engraving tool.

Sample MIT 5365 was analyzed with an electron microbeam probe to determine its composition. The compositions of a series of six points across the sample whose locations are indicated in Figure 5.1.10.ix were determined and are shown in the table in Figure 5.1.10.ix. The average composition of the bracelet is given in Table 5.1.10.

Table 5.1.10: Average Composition of MIT 5365

Cu	Sn	Pb	Sb	As	Ni	Co	Ag	Fe
89.46	10.64	0.027	n.d.	0.152	0.398	0.044	0.014	0.0415

(values in weight %) n.a. = not analyzed n.d. = not determined

The ring is a tin bronze with 10.64 weight percent tin. There is almost no lead present in the sample. Trace elements are present in small amounts.

Sample MIT 5365 was etched for three seconds with potassium dichromate and for three seconds with aqueous ferric chloride to reveal a microstructure characterized by equiaxed grains with annealing twins and a high density of deformation lines (Figure 5.1.10.x).

5.1.10e: Discussion

The ring is a tin bronze with approximately 10.6 weight percent tin. There is almost no lead present. Trace elements are present in very amounts, indicating that the copper making up the alloy may have been purified copper.

This alloy composition closely matches the alloy composition of bronze sheet metal from S. Lucia (Giumlia-Mair 1995). At S. Lucia, the majority of bronze sheet is made of an alloy containing between 9-13 weight percent tin and has less than 0.5 weight percent lead. The bronze sheet from S. Lucia also has low concentrations of trace elements, which is interpreted by Giumlia-Mair to mean that the copper comprising these alloys was purified.

The elongated gray copper sulfide inclusions show that the ring was heavily hammered perpendicular to the ring's longitudinal axis. This likely occurred when the metal was reduced to thin sheet. The undeformed orientation of the copper sulfide inclusions beneath the grooves indicates that the grooves were made with an engraving tool, not a chasing tool.

The equiaxed grains, annealing twins, and deformation lines indicate that the ring was subject to several cycles of working and annealing and that the ring was left in a worked state.

5.1.10f: Conclusions

- The ring is a tin bronze with approximately 10.6 weight percent tin. The tin bronze was not alloyed with lead. Trace elements are present in small concentrations, indicating the copper may have been purified.

- The ring's composition closely matches the composition of sheet bronze used for vessels at St. Lucia (Giumlia-Mair 1995:69)
- The metal was reduced to thin sheet through repeated cycles of working and annealing. The ring was left in a worked state.
- The grooves and raised segments were made with an engraving tool.

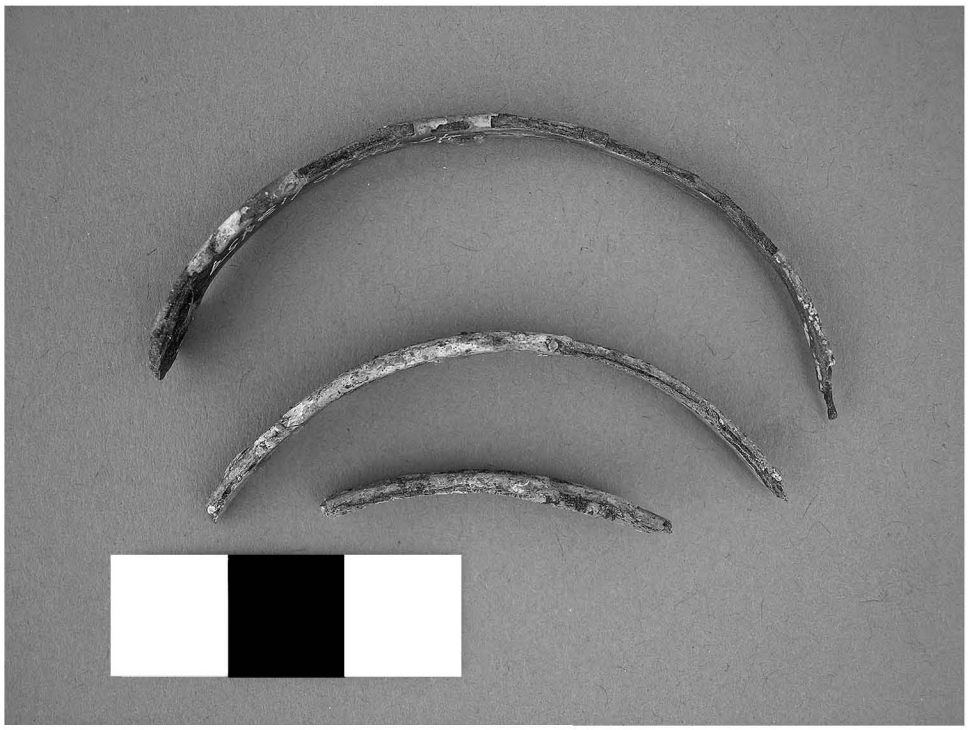

Figure 5.1.10.i: Flat arm ring/bracelet. (MIT 5365/Peabody 40-77-40/13459). Photograph by E. Cooney.

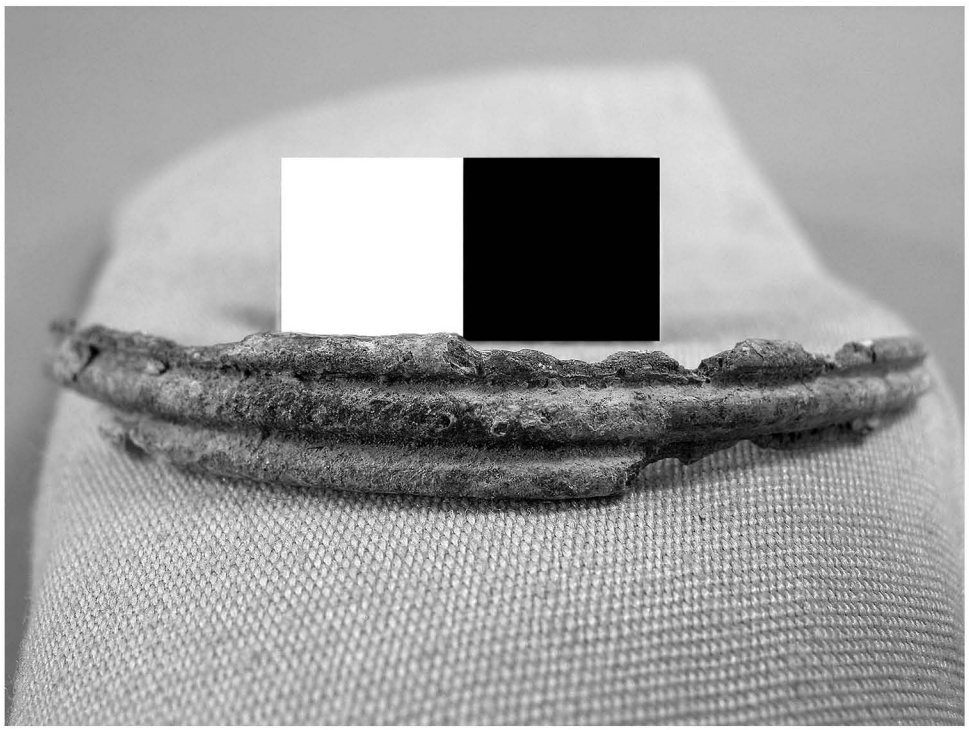

Figure 5.1.10.ii: Flat arm ring/bracelet, Fragment B. (MIT 5365/Peabody 40-77-40/13459). Photograph by E. Cooney.

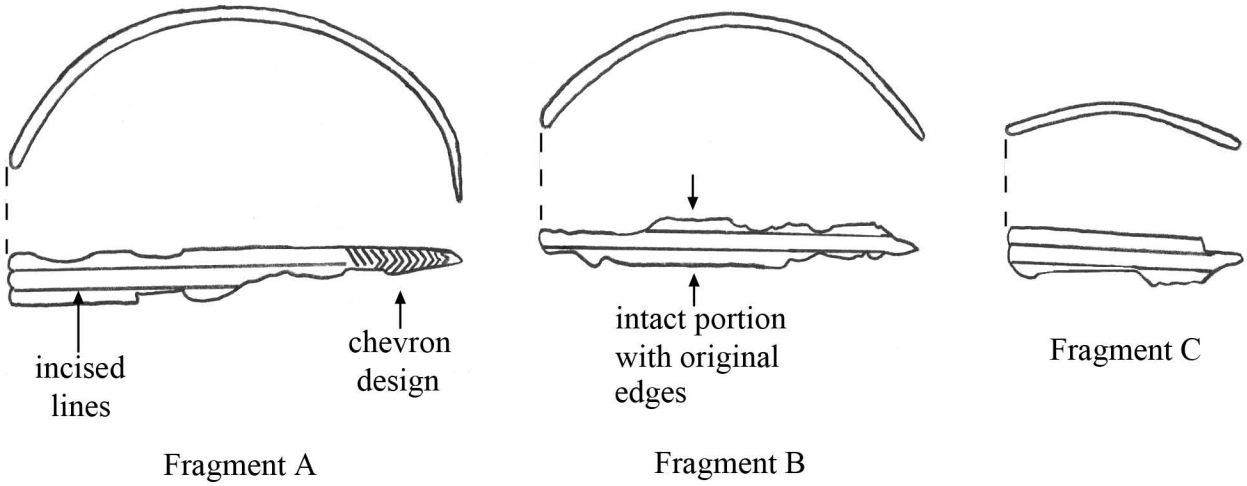

Figure 5.1.10.iii: Flat arm ring (MIT 5365). Key object features.

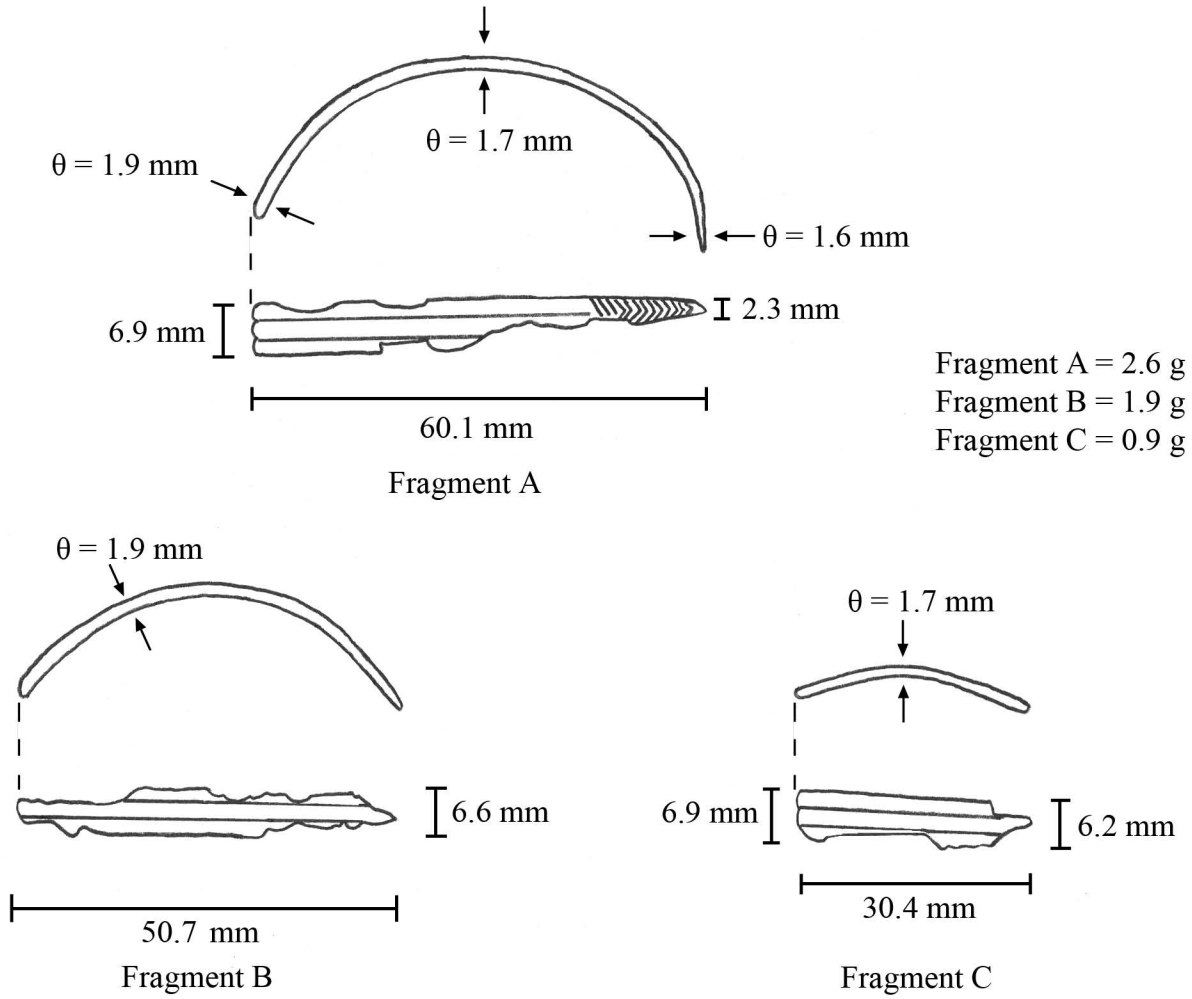

Figure 5.1.10.iv: Flat arm ring (MIT 5365). Drawing and measurements.

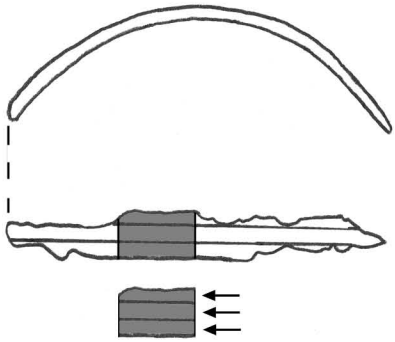

Figure 5.1.10.v: Flat arm ring (MIT 5365). Sample MIT 5365 was removed for metallographic analysis and was mounted transversely as noted. Compositional analysis was determined with the electron microbeam probe.

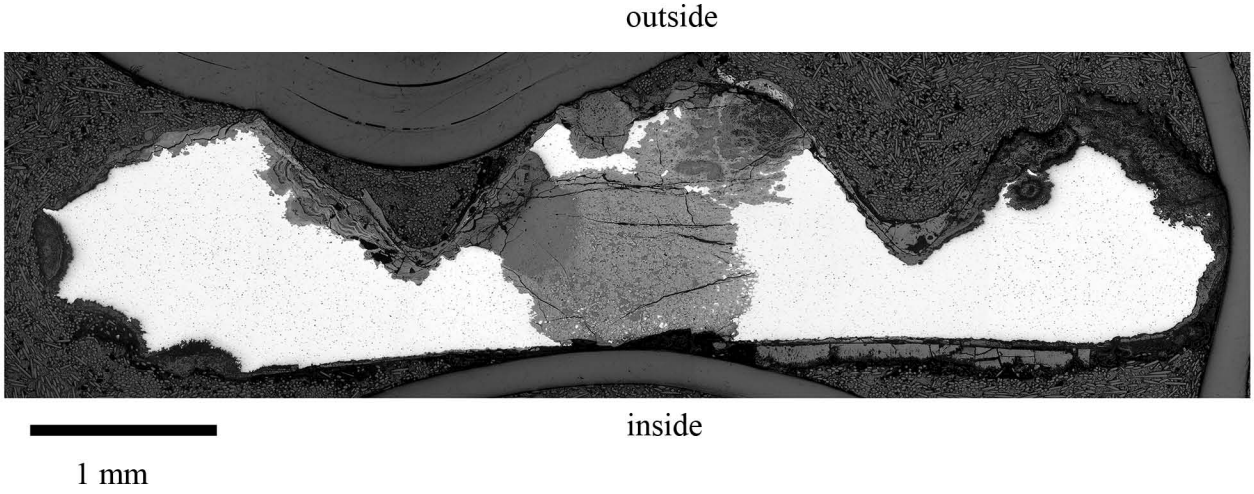

Figure 5.1.10.vi: Flat arm ring (MIT 5365/Peabody 40-77-40/13459). Transverse cross section, as polished. The flat inside surface of the ring can be seen clearly in the as polished sample. The original outline of the incised lines and raised zones can be seen in the ring's external corrosion product. Other microstructural features of interest include a high density of elongated gray copper sulfide inclusions aligned parallel to the ring's longitudinal axis, a very light density of porosities, and internal corrosion product outlining equiaxed grains with a high density of deformation lines. (MIT Images 5365-01- 06.)

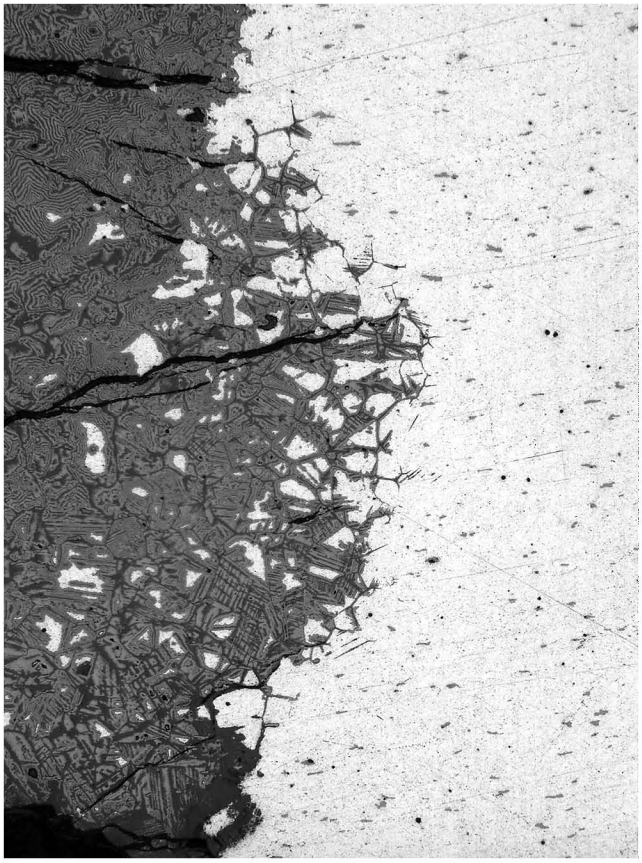

Figure 5.1.10.vii: Flat arm ring/bracelet (MIT 5365/Peabody 40-77-40/13459). Transverse section, as polished. x200. Microstructural features of interest include elongated gray copper sulfide inclusions aligned parallel to the ring's longitudinal axis and equiaxed grains with a high density of deformation lines outlined in the ring's internal corrosion product. (MIT Image 5365-10.)

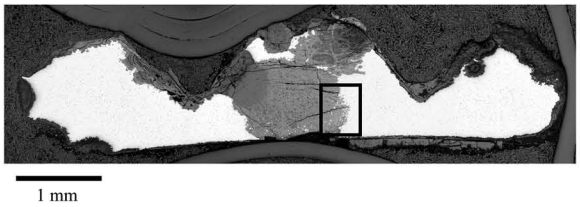

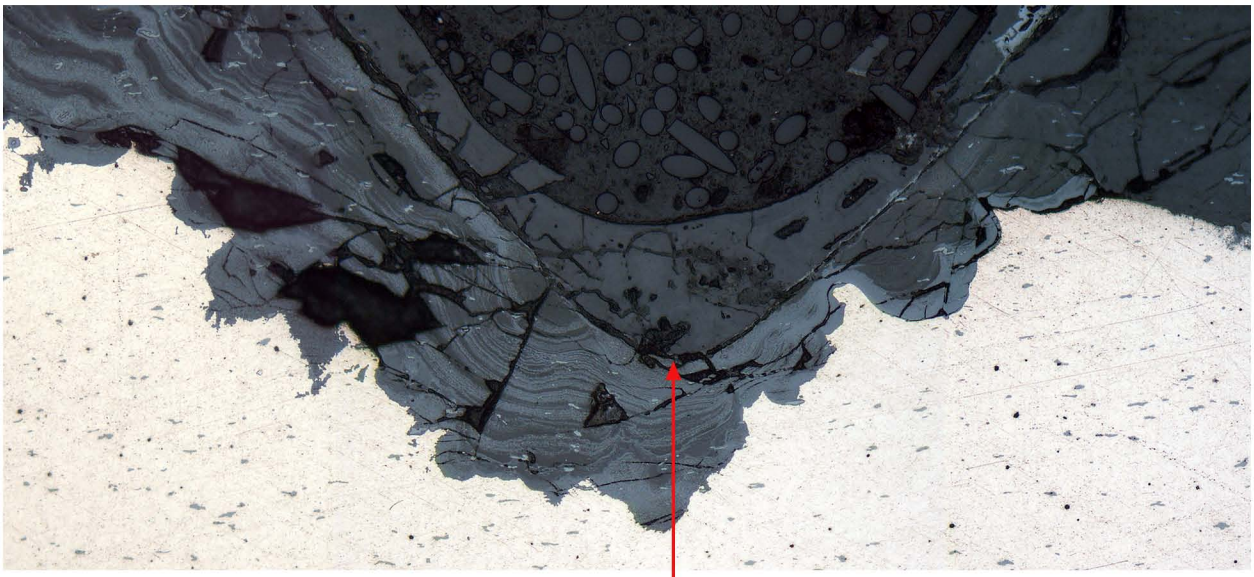

Figure 5.1.10.viii: Flat arm ring/bracelet (MIT 5365/Peabody 40-77-40/13459). Transverse section, as polished. x200. The original outline of the groove can be seen in the corrosion product. The gray copper sulfide inclusions can be seen in both the metal and the internal corrosion product. The orientation of the inclusions does not change underneath the groove as compared to the bulk of the metal. This indicates that the metal beneath the groove was not subject to any direct pressure different from the metal in the bulk of the ring. Therefore, a chasing tool could not have been used to create the ring's decoration. The decoration and grooves must have been created using an engraving tool. (MIT Images 5365-06-08).

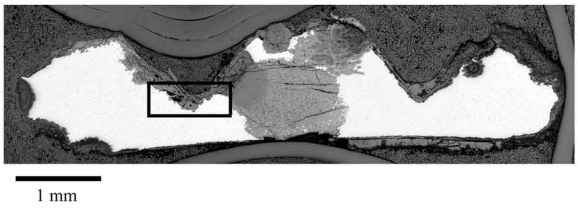

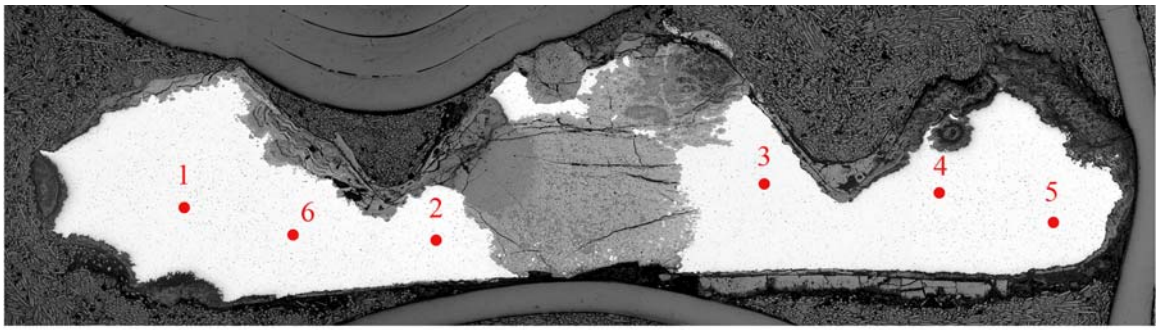

Electron Microbeam Probe Compositional Data

	Cu	Sn	Pb	Sb	As	Ni	Co	Ag	Fe
1	90.87	11.27	n.d.	n.d.	0.1739	0.5104	0.0275	0.0083	0.0142
2	89.38	10.7	n.d.	n.d.	0.0967	0.4111	n.d.	0.0313	0.0521
3	89.37	10.98	0.134	n.d.	0.16	0.3508	0.178	0.027	0.0431
4	89.95	9.39	n.d.	n.d.	0.2195	0.3362	0.0374	n.d.	0.0528
5	88.23	10.77	n.d.	n.d.	0.2169	0.3975	n.d.	0.0181	0.0365
6	88.97	10.71	0.030	n.d.	0.0452	0.381	0.0188	n.d.	0.0505
Avg.	**89.46**	**10.64**	**0.027**	**n.d.**	**0.152**	**0.398**	**0.044**	**0.014**	**0.0415**

(values in weight %) n.d. = not determined

Figure 5.1.10.ix: Flat arm ring/bracelet (MIT 5365/Peabody 40-77-40/13459).
Above: Points at which compositional data were taken by the electron microbeam probe.
Below: Electron microbeam probe compositional data from each point.

Figure 5.1.10.x: Flat arm ring/bracelet (MIT 5365/Peabody 40-77-40/13459). Transverse cross section. Etch: 3 sec potassium dichromate and 3 sec ferric chloride etch. x200. Microstructural features of interest include equiaxed grains and annealing twins with a high density of deformation lines. (MIT Image 5365-12).

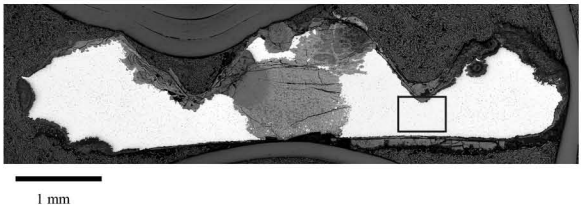

5.1.11: Flat finger ring (MIT 5353/Peabody 40-77-40/13443)

5.1.11a: Provenance and Background

MIT 5353 (Figure 5.1.11.i) is a flat ring from Grave 31 (Wells 1981). Grave 31 was described by the excavators as a child's grave. It was 2.5 m long, 0.6 m wide, and the bottom was 2.45 m below the tumulus surface. MIT 5353 was identified by the excavators as a fragment of an earring, but it is more likely a fragment from a finger ring. Associated grave goods include two blue glass beads and two small, undecorated ceramic vessels.

5.1.12b: Initial Examination and Observations

The flat finger ring was photographed (Figure 5.1.11.i) drawn to scale, measured, and observed (Figures 5.1.9.ii and 5.1.9.iii).

The ring is fragmented and has been broken almost exactly in half. Only one-half of the ring survives. The finger ring is a smaller version of MIT 5365, discussed in Section 5.1.10. The flat finger ring is decorated by two grooves that separate the bracelet's outside surface into three distinct raised sections. The inside surface of the ring is flat and smooth. There is a line or crack on the inside surface extending across the ring parallel to the longitudinal axis. This line is intersected by striations parallel to the ring's transverse axis. These striations are similar to the striations found on the inside surface of MIT 5365, and they were most likely made by a polishing tool. Also like MIT 5365, there is an intact, tapered end decorated with an incised chevron design. When the outside surface is viewed straight on, one of the edges is flat and straight while the other edge is curved (Figure 5.1.11.ii).

The ring's diameter is 20.5 mm. At the intact, tapered end with the chevron design the ring is 0.5 mm thick and 1.2 mm wide. At its fractured end the ring is 0.9 mm thick and 3.0 mm wide. The ring weighs 0.4 g (Figure 5.1.11.iii).

The ring is structurally robust and its surface is covered with a shiny, smooth dark green patina.

5.1.12c: Sampling

MIT 5353 was sampled transversely adjacent to the fractured end (Figure 5.1.11.iv). Sample MIT 5353 was mounted transversely for metallographic analysis. The ring was highly metallic, and the metal was light gold in color. Composition analysis was undertaken with the electron microbeam probe.

5.1.12d: Metallographic Analysis

Sample MIT 5353 was mounted as a transverse section. As polished (Figure 5.1.11.v), the original outline of the surface grooves and raised segments can be seen in the external corrosion product. The inside surface does not appear to be very flat or smooth. Other microstructural features of interest include a low density of small, elongated gray copper sulfide inclusions and a few homogeneously distributed pools of blue-green Cu-Sn eutectoid. There is a high density of very small porosities.

Sample MIT 5353 was analyzed with the electron microbeam probe to determine its composition. The compositions of a series of five points across the sample whose locations are indicated in Figure 5.1.11.vi were determined and are shown in the table in Figure 5.1.11.vi. The average composition of the bracelet is given below in Table 5.1.11.

Table 5.1.11: Average Composition of MIT 5353

Cu	Sn	Pb	Sb	As	Ni	Co	Ag	Fe
89.65	10.54	0.453	0.114	0.216	0.368	n.d.	0.080	0.005

(values in weight %) n.a. = not analyzed n.d. = not determined

The ring is a tin bronze with 10.54 weight percent tin. There is 0.453 weight percent lead present in the sample. The lead value may be slightly underreported, as the densely distributed small porosities probably contain some inhomogeneously distributed lead. The tin composition is almost exactly the same as the tin composition in the alloy comprising MIT 5365. Minor and trace elements appear in slightly higher amounts than they did in the sheet metal comprising MIT 5366 and 5365.

Sample MIT 5353 was etched for 10 seconds with potassium dichromate to reveal flow lines in the metal (Figure 5.1.11.vii). These areas of compositional inhomogeneity show the direction in which metal flowed when the ring was worked. The metal close to the outside surface and directly beneath a groove was compressed more heavily than the

metal close to the inside surface. The direction of flow along the outside surface does not follow the rise and fall of the grooves and raised sections, indicating that these grooves were not hammered into the metal with a chasing tool. Instead, like MIT 5365, the grooves were most likely made with an engraving tool.

Sample MIT 5353 was further etched for two seconds with aqueous ferric chloride to reveal a microstructure characterized by very small grains with annealing twins and a light density deformation lines.

5.1.11e: Discussion

The ring is a tin bronze with a concentration of 10.5 weight percent tin. The tin composition is almost identical to MIT 5365. There is about 0.5 weight percent lead present in the ring. Again, like MIT 5365, the absence of lead in high concentration mirrors the alloy composition of bronze sheet metal from St. Lucia (Giumlia-Mair 1995).

The elongated gray copper sulfide inclusions and equiaxed grains with annealing twins and deformation lines show that the ring was subjected to several cycles of working and annealing. The ring was left slightly worked. The flow lines indicate that the outside surface of the ring was more heavily worked than the inside surface. This may explain why the inside surface appears rougher than the surface of ring MIT 5365. This roughness may be associated with the long line parallel to the longitudinal axis seen in the ring's external corrosion.

The flow lines beneath the decorative grooves at the outside surface do not follow the rise and fall of the grooves and raised sections, indicating that these grooves were not hammered into the metal with a chasing tool. Instead, like MIT 5365, the grooves were most likely made with an engraving tool.

5.1.11.f: Conclusions

- The flat finger ring has similar decorations to the flat arm ring, MIT 5365.
- The flat finger ring is a tin bronze with 10.54 weight percent tin and 0.5 weight percent lead. This alloy composition is very similar to that of MIT 5365.
- The ring's composition closely matches the composition of sheet bronze used for vessels at St. Lucia (Giumlia-Mair 1995)

- The metal was reduced to thin sheet through repeated cycles of working and annealing. The ring was left in a slightly worked state.
- The grooves and raised segments were made with an engraving tool.

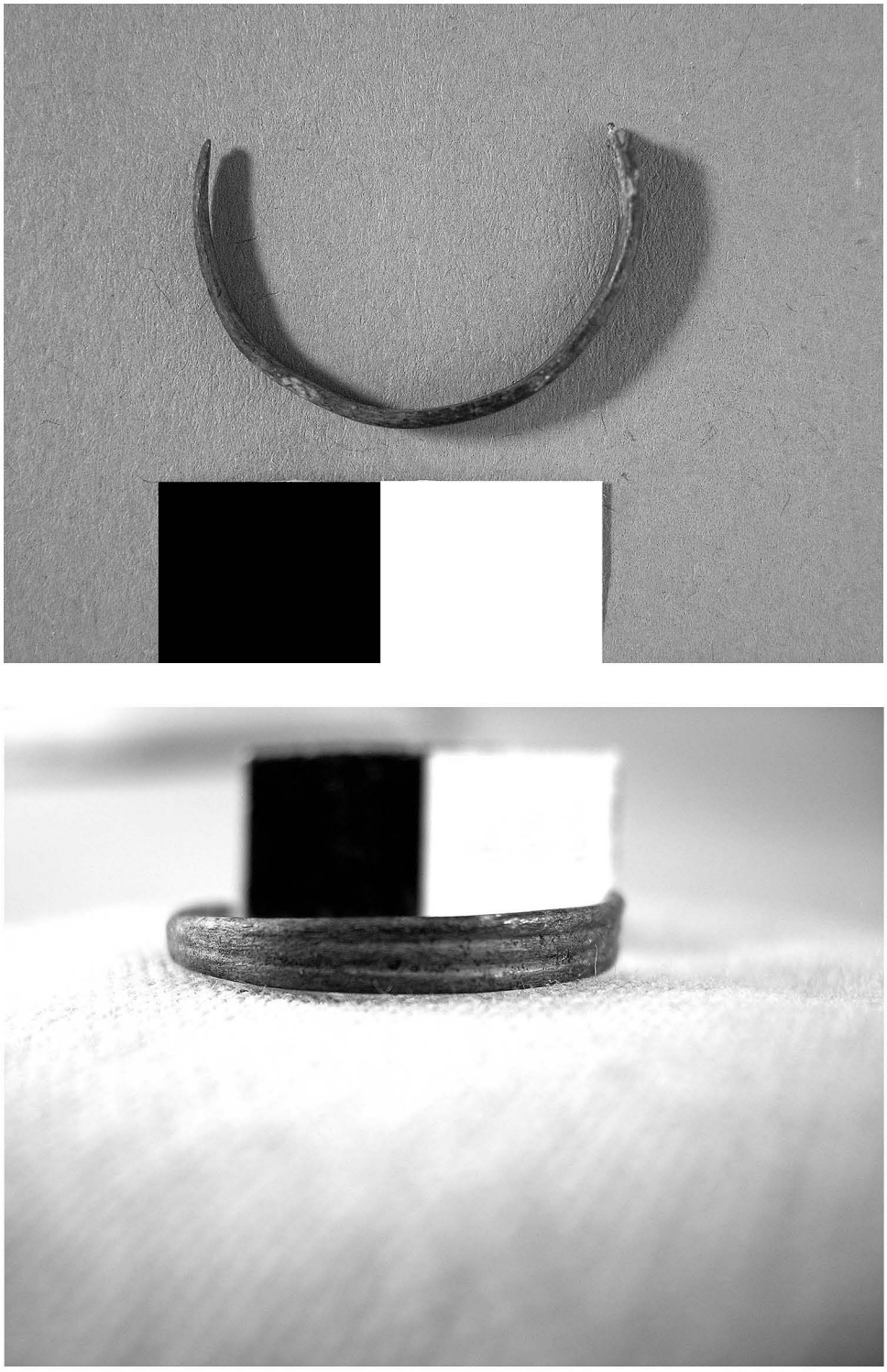

Figure 5.1.11.i: Flat finger ring. (MIT 5353/Peabody 40-77-40/13443). Photograph by E. Cooney.

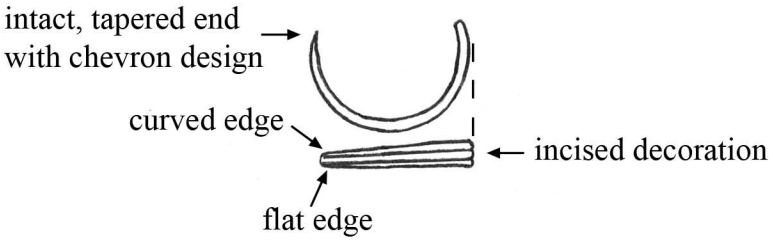

Figure 5.1.11.ii: Flat finger ring (MIT 5353). Key object features.

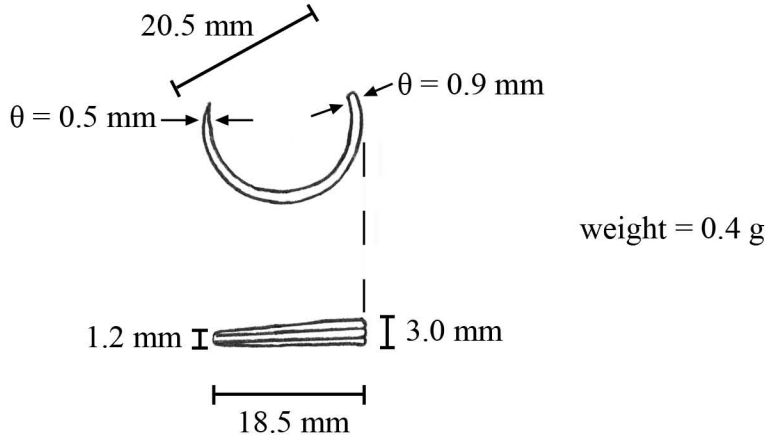

Figure 5.1.11.iii: Flat finger ring (MIT 5353). Drawing and measurements.

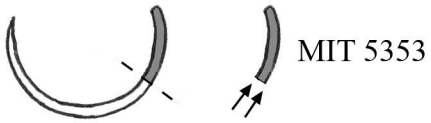

Figure 5.1.11.iv: Flat finger ring (MIT 5353). Sample MIT 5353 was removed for metallographic analysis and was mounted transversely as noted. Compositional analysis was determined with the electron microbeam probe.

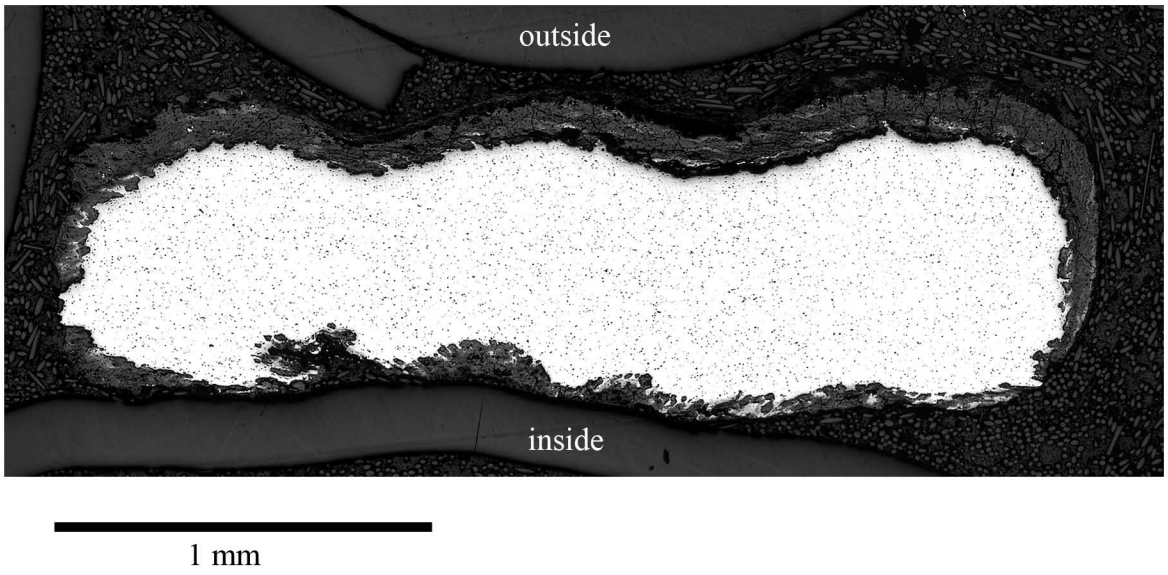

Figure 5.1.11.v: Flat finger ring (MIT 5353/40-77-40/13443). Transverse cross section, as polished. x50. The grooves comprising the ring's decoration can be seen in the ring's external corrosion product. (MIT Images 5353-01-02).

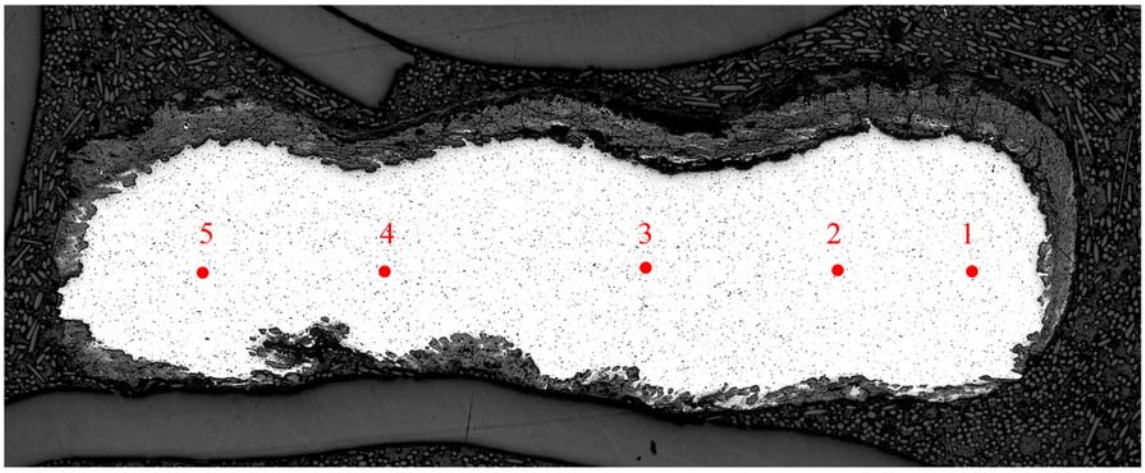

Electron Microbeam Probe Compositional Data

	Cu	Sn	Pb	Sb	As	Ni	Co	Ag	Fe
Pt 1	92.14	8.38	0.3922	n.d.	0.1448	0.3122	n.d.	n.d.	0.0027
Pt 2	89.27	11.2	0.829	0.1076	0.2374	0.3872	n.d.	0.1184	0.0125
Pt 3	90.11	9.67	0.159	0.0326	0.2482	0.3769	n.d.	0.0144	0.0104
Pt4	87.04	11.52	0.7377	0.1335	0.1496	0.3477	n.d.	0.1926	n.d.
Pt 5	89.7	11.93	0.1494	0.2951	0.3003	0.4168	n.d.	0.0737	n.d.
Average	**89.65**	**10.54**	**0.453**	**0.114**	**0.216**	**0.368**	**n.d.**	**0.080**	**0.005**

(values in weight %) n.d. = not determined

Figure 5.1.11.vi: Flat finger ring (MIT 5353/Peabody 40-77-40/13443).
Above: Points at which compositional data were taken by the electron microbeam probe.
Below: Electron microbeam probe compositional data from each point.

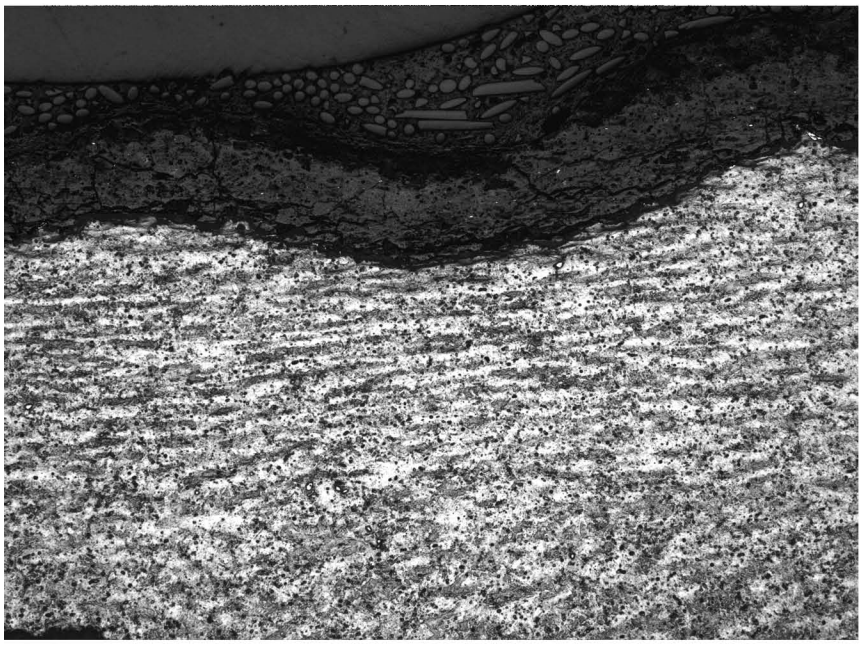

Figure 5.1.11.vii: Flat finger ring (MIT 5353/40-77-40/13443). Transverse cross section. Etch: 10 sec potassium dichromate. x100. The photomicrograph shows areas of compositional inhomogeneity oriented parallel to the ring's longitudinal axis. The metal close to the outside surface and directly beneath a groove was compressed more heavily than the metal close to the inside surface.(MIT Image 5353-06).

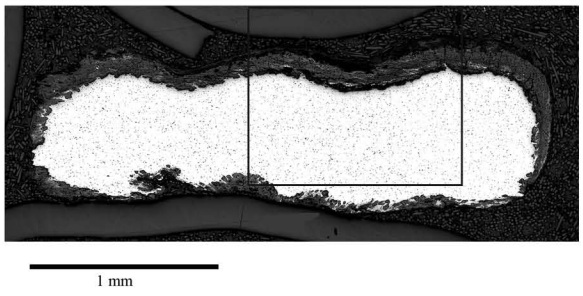

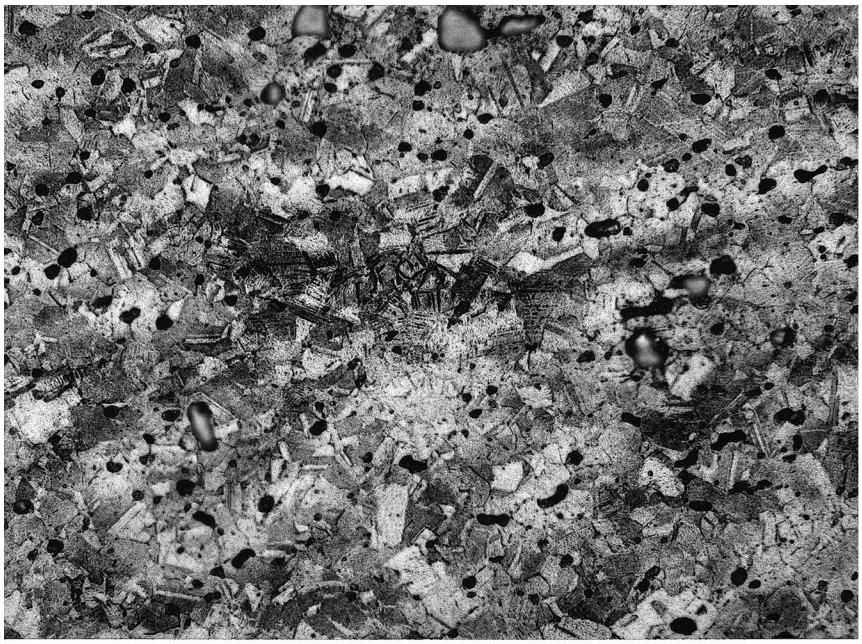

Figure 5.1.11.viii: Flat finger ring (MIT 5353/40-77-40/13443). Transverse cross section. Etch: 10 sec potassium dichromate and 2 sec ferric chloride. x200. Microstructural features of interest include equiaxed grains and annealing twins with a low density of deformation lines. (MIT Image 5353-08).

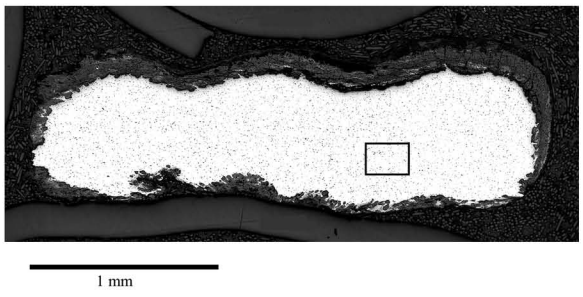

5.1.12: Segmented foot ring (MIT 5342/Peabody 40-77-40/13522)

5.1.12a: Provenance and Background

MIT 5342 (Figures 5.1.12.i and 5.1.12.ii), identified by Wells (1981) as fragments of a foot ring, came from Grave 47 of Tumulus IV.

Grave 47 was oriented southeast-northwest. It was 2.8 m long, 1.25 m wide, and was 2.3 m below the surface of the tumulus. The entire grave was lined with stones. Unburnt fragments of horse bones were found underneath a stone packing in the grave's northwest end, and burnt horse bones, including a horse mandible, were found under a stone packing in the grave's southeast end. The foot ring fragments were found mixed with the burnt bones, indicating that they were subject to the heat of a crematory fire.

Associated grave goods included 16 amber beads, a single glass bead, and a spindle whorl. Sherds of a tan colored ram's head rhyton were also recovered from the grave. According to Wells, the rhyton originates from the eastern Adriatic and is dated to the fourth or third century B.C.E (400-600 B.C.E) (1981). The presence of the ram's head rhyton makes Grave 47 one of the few roughly datable graves in Tumulus IV and at Stična as a whole.

There are two similar, intact, segmented foot rings from Grave 51 (Figure 5.1.12.iii). These intact foot rings are solid, closed, circular rings measuring 12.8 cm in diameter. They are both heavy, weighing 308.4 g and 329.8 g. Although from a cremation grave, MIT 5342 was chosen for metallographic analysis as it is the only fragmented foot ring in Tumulus IV.

5.1.12b: Initial Examination and Observations

The segmented foot ring was photographed (Figures 5.1.12.i and 5.1.12.ii), drawn to scale, measured, and observed (Figures 5.1.12.iv and 5.1.12.v).

There are five surviving fragments of the original foot ring. They do not fit together cleanly, indicating that fragments have been lost. Together the fragments weigh 132 g. Originally, MIT 5342 was most likely a closed ring of approximately the same size and weight as the two intact foot rings from Grave 51 (Figure 5.1.12.iii).

The fragments are structurally robust. They are solid and have a lenticular cross section. They are covered with a highly friable, dark and light green mottled corrosion product. Earthy accretions still adhere to the surface in some areas. Each fragment is decorated with segments and grooves. Each groove proceeds along the entire outside surface of the ring; the inside surface is ungrooved. The grooves and segments are not evenly spaced across the ring; their shapes and sizes differ on some fragments. Several fragments appear to have a seam that is proud of the metal surface along their inside surface. As the ring is solid, the presence of this seam suggests that the ring was cast to shape and that a seam was present in the mold in which the ring was cast.

Fragment A is 66.5 mm long. At one end its cross section is 11.1 mm wide and 9.8 mm thick, and at the other its cross section is 11.7 mm wide and 11.1 mm thick. Fragment A has a pronounced seam along its inside surface. The segments on Fragment A are evenly sized, and its grooves are evenly sized with a rounded concave, semi-annular shape. Fragment A weighs 40.2 g.

Fragment B is 64.8 mm long. At one end its cross section is 12.0 mm wide and 9.2 mm thick, and at the other its cross section is 11.2 mm wide and 9.2 mm thick. It has unevenly spaced and sized segments and grooves. The segments range is size from 5.8 mm in length to 4.8 mm in length. The grooves on Fragment B have differing widths and depths. Some are crudely shaped with abrupt, square-shaped ends while others are smoothly shaped with rounded, concave, semi-annular ends. There is a pronounced seam along its inside surface. Fragment B weighs 37.2 g.

Fragment C is 28.0 mm long. Its cross section is 11.5 mm wide and 9.9 mm thick. It has evenly spaced and sized segments, and its grooves are evenly sized with a rounded concave, semi-annular shape. No seam is visible on its inside surface. Fragment C weighs 15.6 g.

Fragment D is highly corroded, making its segments indistinct and difficult to distinguish. It is 28.2 mm long. At one end its cross section has a width of 10.6 mm with a thickness of 9.6 mm, and at its other end its cross section has a width of 11.0 mm and a thickness of 10.3 mm. It weighs 13.1 g.

Fragment E is 48.5 mm long. It is 9.8 mm thick, and its width ranges from 10.4 mm to 11.2 mm. Like Fragment B, it has unevenly spaced and sized segments and grooves and a pronounced seam along its inside surface. Fragment E weighs 25.9 g.

5.1.12c: Sampling

Fragment C was sampled twice with transverse cuts (Figure 5.1.12.vi). Sample MIT 5342a was taken for bulk composition analysis. Sample MIT 5342b was taken for metallographic analysis and was mounted transversely as noted. The fragment was highly metallic, and the metal was light gold in color.

5.1.12d: Bulk Composition Analysis

Bulk composition analysis shows that the segmented foot ring is a copper-lead-tin ternary alloy with the main alloying elements of lead at a concentration of 13.2 weight percent and tin at a concentration of 6.57 weight percent.

Other major, minor and trace elements include As (1.17%), Sb (1.05%), Ni (0.4920%), Ag (0.323%), Fe (0.054%), and Co (0.031%). Bulk composition analysis data are given in Table 5.1.12 and in the Appendix.

Table 5.1.12: Bulk Composition Analysis Data for MIT 5342 (Segmented Foot Ring)

	Sn	**Pb**	**Sb**	**As**	**Ni**	**Co**	**Ag**	**Fe**
ICP-ES	6.57	13.2	1.05	1.17	0.015	0.031	n.a.	0.054
INAA	3.80	n.a.	0.920	0.893	0.4920	0.0256	0.323	n.d.

(values in weight %) n.a. = not analyzed n.d. = not determined

5.1.12e: Metallographic Analysis

MIT 5342b was mounted as a transverse section. The as-polished section reveals a high density of porosities present in the sample, most of which are likely filled with lead (Figure 5.1.12.vii). The porosities outline dendritic structures. These porosities are not elongated or otherwise deformed, indicating that the ring was cast to shape and left as-cast without any further working.

The apparent right-hand side of the ring comes to a point (Figure 5.1.12.vii). This feature corresponds to the pronounced raised ridge (seam) observable on the inside

surface of the ring. Its presence indicates a discontinuity on the inside of the mold in which the ring was cast.

There is a large center-line shrinkage cavity in the center of the ring (Figures 5.1.12.vii and 5.1.12.viii). The center-line shrinkage cavity was formed during a casting operation, further indicating that the ring was cast to shape. This cavity is partially filled with gray copper sulfide inclusions. There is also a low density of gray copper sulfide inclusions and non-eutectoid green-blue copper corrosion product inclusions distributed homogenously throughout the sample.

The sample was etched lightly for two seconds with dilute aqueous ferric chloride to reveal compositional inhomogenities caused by microsegregation, or coring, during the casting process. These compositional inhomogeneities follow the dendritic structures outlined by the porosities and are not elongated or deformed in any way, again indicating that the metal was not worked after it was cast.

The sample was repolished and etched for three seconds with alcoholic ferric chloride to reveal a microstructure characterized by equiaxed grains and annealing twins (Figure 5.1.12.x). This microstructure coupled indicates that the ring was very lightly worked after casting, most likely to shore up its shape or fix a casting flaw.

5.1.12f: Discussion

The ring is made of a copper-lead-tin ternary alloy with the main alloying elements of lead at a concentration of 13.2 weight percent and tin at a concentration of 6.57 weight percent. The ring's microstructure indicates that it was cast to shape and very lightly worked after casting. Because the ring was a closed, solid ring, it needed to be cast into a round shape rather then hammered into a round shape like the open and semi-closed rings discussed previously.

A highly leaded tin-bronze alloy was used to make the ring because it was cast to shape. The alloy needed to serve no mechanical function, nor did the alloy need to permit further working of the ring after casting. The lead was most likely used as a "filler" material. The metal used to make the ring may have been recycled scrap bronze as the ring's alloy did not need to be carefully monitored, but the high concentration of lead was probably deliberate.

Because the foot ring was cast to shape, the unevenness of many of the grooves and segments on the foot ring is a product of unevenness in the mold in which the ring was cast. Similarly, the pronounced seam on the leg ring is a product of a discontinuity present in the original mold.

The composition of the ring would have made it fairly soft. This relative softness, coupled with the weight of the ring, indicate that the foot ring may have only been worn for decorative purposes during ritual use.

Similar as-cast objects at S. Lucia are also made of highly leaded tin bronze alloys. These cast objects do not exhibit any regular pattern of alloy composition, indicating that they may have been made using recycled bronze scrap (Giumlia-Mair 1995). Other as-cast, non-mechanically functioning objects from Stična, such as the rivets discussed in Sections 5.3.1 and 5.3.2 and the segmented ring belt attachment discussed in Section 5.3.4, also follow this pattern.

5.1.12g: Conclusions

- The foot ring is associated with a rhyton of eastern Adriatic origin dating to the fourth or third century B.C.E (Wells 1981).
- The foot ring is made of a copper-lead-tin ternary alloy with the main alloying elements of lead at a concentration of 13.2 weight percent and tin at a concentration of 6.57 weight percent.
- The foot ring was a closed ring. It was cast to shape and was only very lightly worked after having been cast.
- The high lead concentration is probably caused by the use of lead as a "filler" material in the alloy; the use of lead in such a high concentration was possible because the ring was cast to shape and left as-cast.
- The metal used to make the ring may have been recycled scrap bronze as the ring's alloy did not need to be carefully monitored, but the high concentration of lead was probably deliberate.
- The relative softness and weight of the ring indicate that it may have been worn only for decorative, ritual purposes.

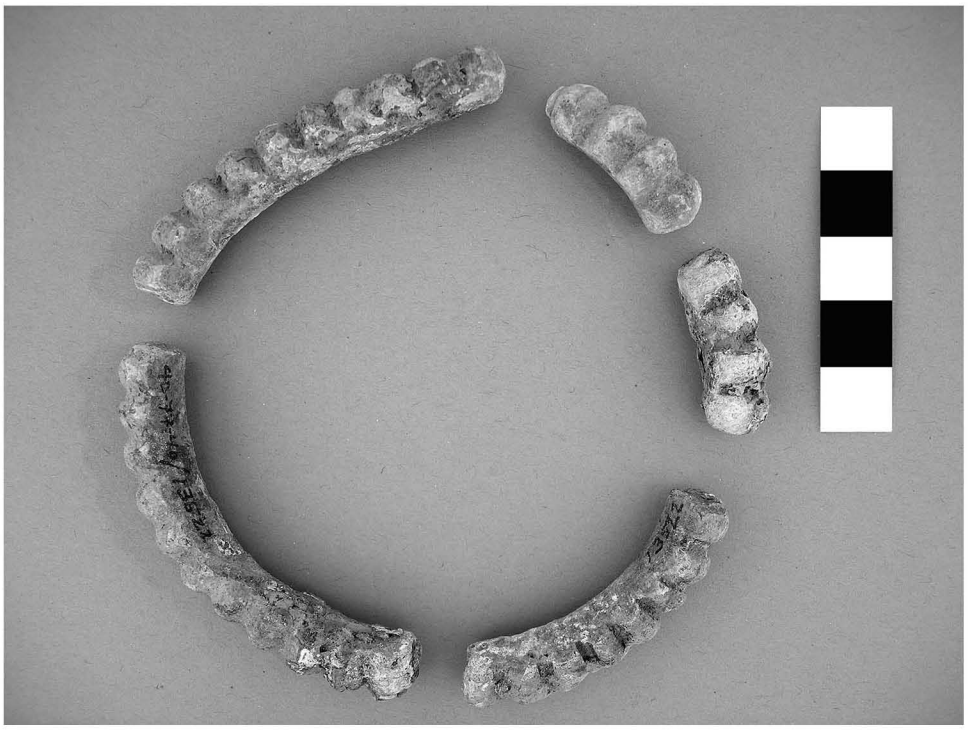

Figure 5.1.12.i: Segmented foot ring. (MIT 5342/Peabody 40-77-40/13522). Photograph by E. Cooney.

Figure 5.1.12.ii: Segmented foot ring, top view of fragment E. (MIT 5342/ Peabody 40-77-40/13522). Photograph by E. Cooney.

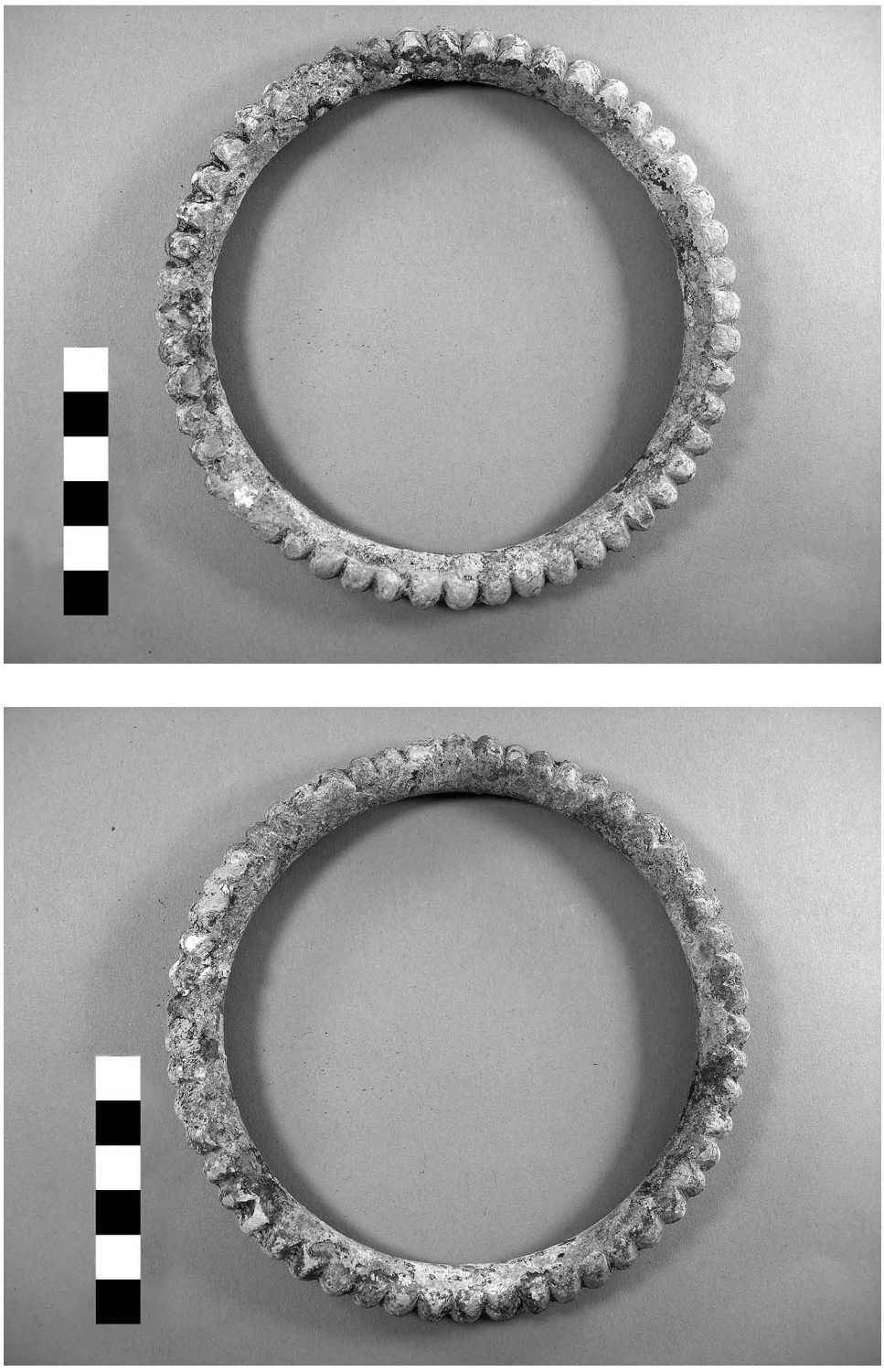

Figure 5.1.12.iii: Segmented foot rings. (Peabody 40-77-40/13550 and 40-77-40/13551). These foot rings from Grave 51 are intact, closed rings similar to MIT 5342. The solid foot rings weigh 308.4 g and 329.8 g respectively and are both 12.8 cm in diameter. Photographs by E. Cooney.

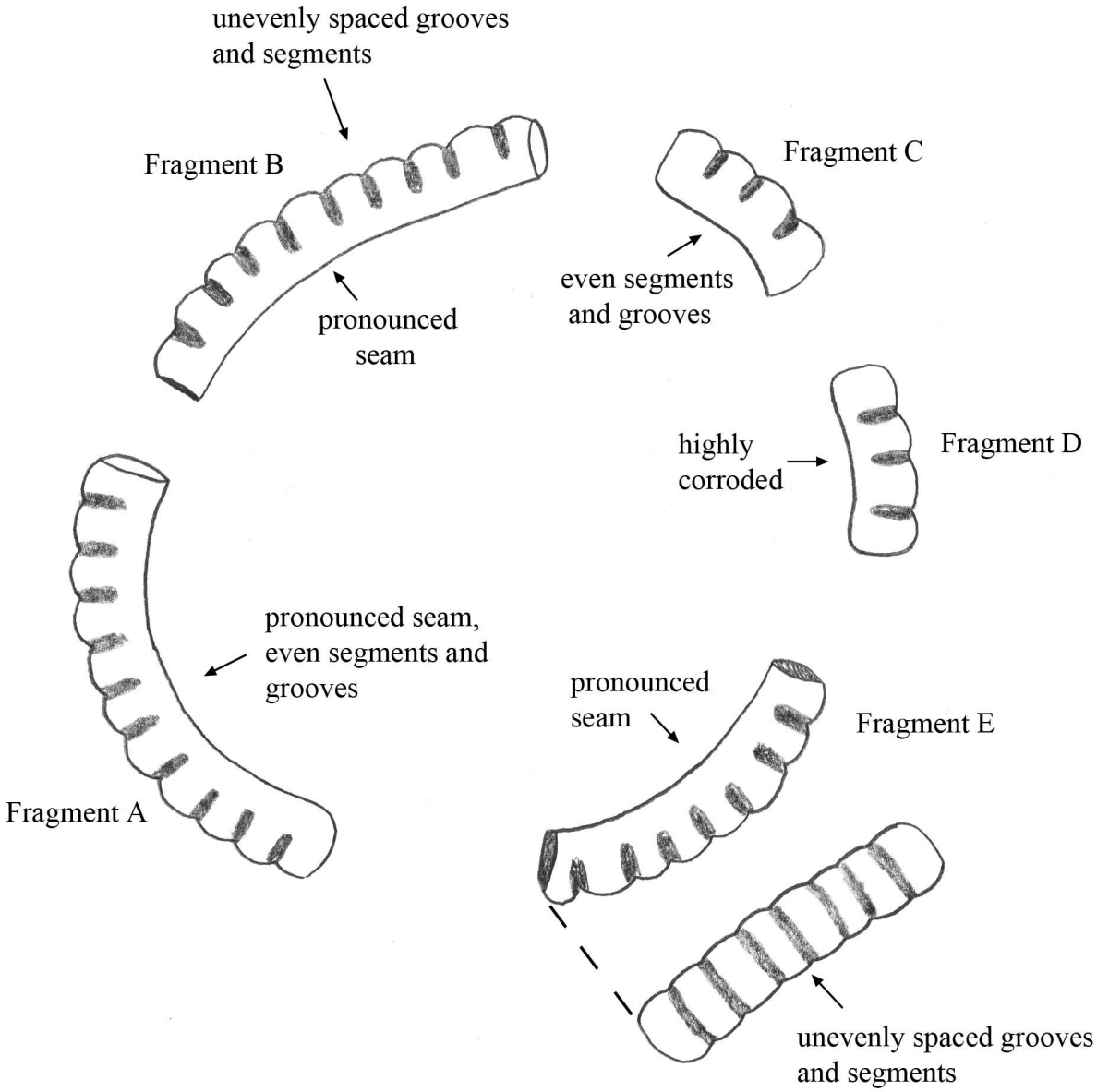

Figure 5.1.12.iv: Segmented foot ring (MIT 5342). Key object features.

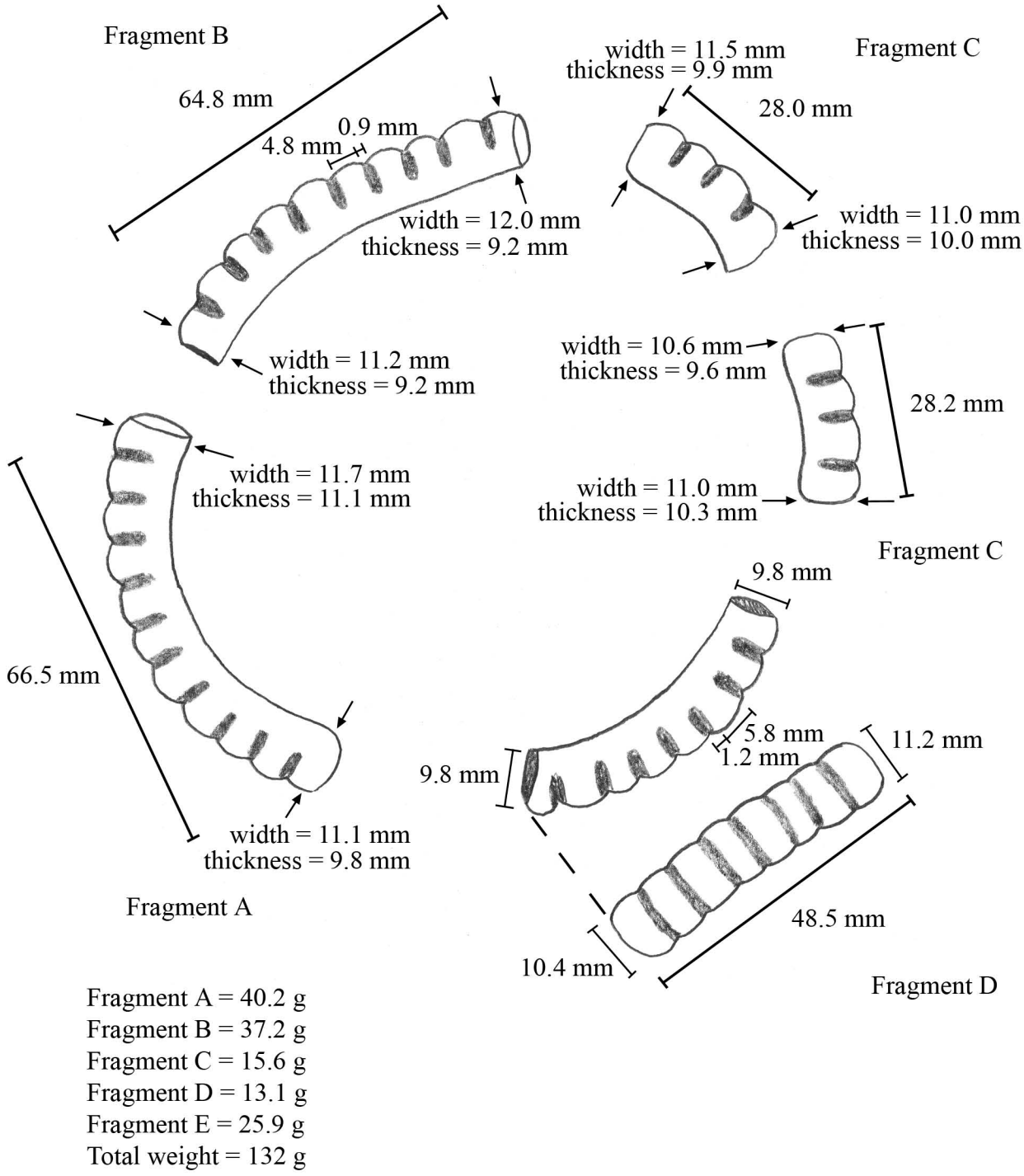

Fragment A = 40.2 g
Fragment B = 37.2 g
Fragment C = 15.6 g
Fragment D = 13.1 g
Fragment E = 25.9 g
Total weight = 132 g

Figure 5.1.12.v: Segmented foot ring (MIT 5342). Drawing and measurements.

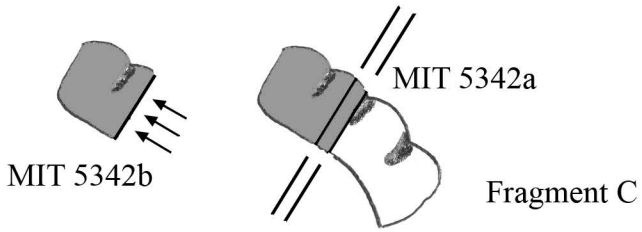

Figure 5.1.12.vi: Samples removed from segmented foot ring. Sample 5342a was removed for bulk composition analysis. Sample 5342b was removed for metallographic analysis and was mounted transversely as noted.

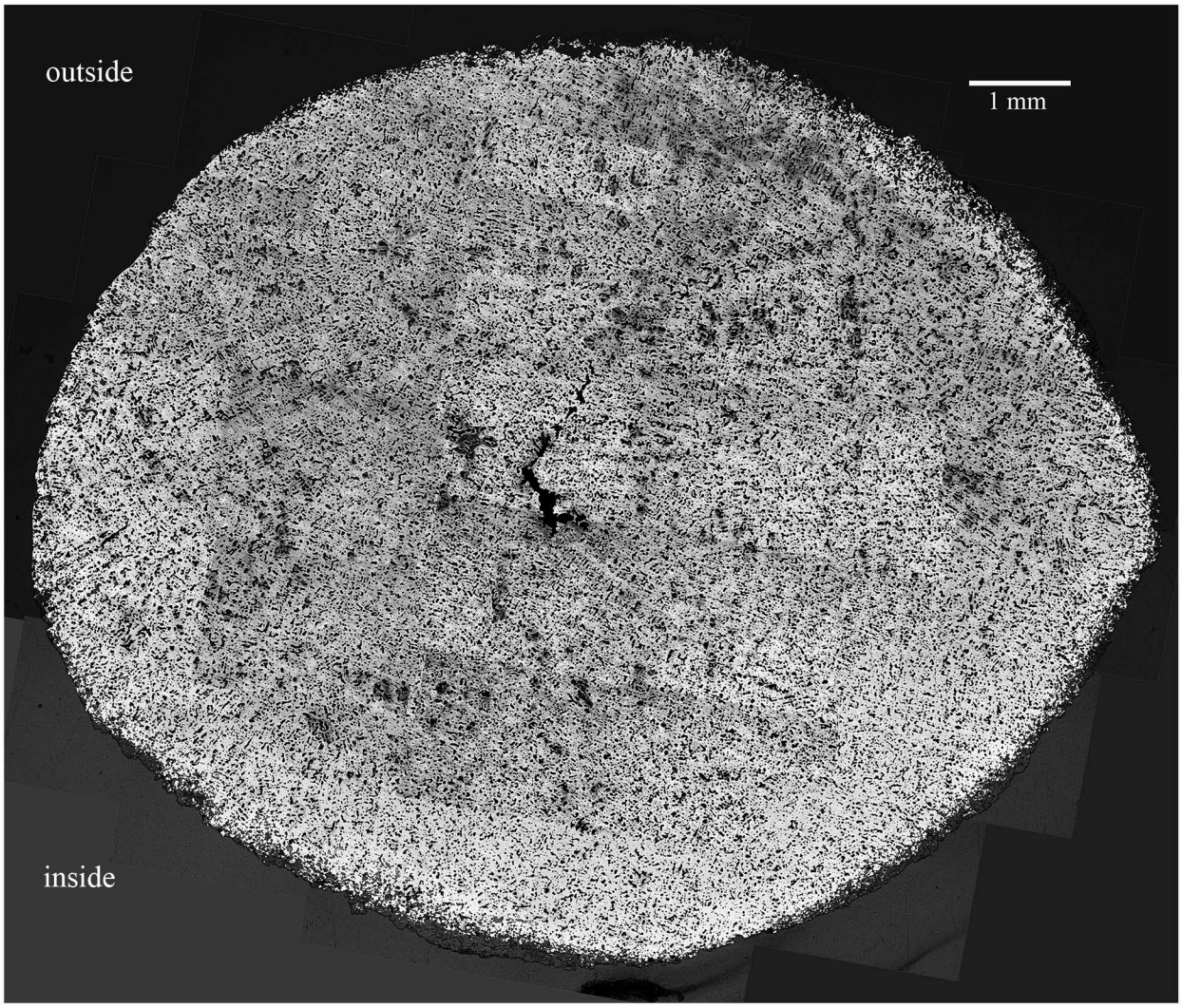

Figure 5.1.12.vii: Segmented foot ring (MIT 5342/Peabody 40-77-40/13522). Transverse cross section, as polished. Microstructural features of interest include a center line shrinkage cavity and porosities that outline primary dendrites. (MIT Images 5342b-001-034).

Figure 5.1.12.viii: Segmented foot ring (MIT 5342/Peabody 40-77-40/13522). Transverse cross section, as polished. x50. Microstrucutral features of interest include the large, center lines porosity partially filled with gray copper sulfide inclusions and porosities filled with lead outlining primary dendrities. (MIT Image 5342b-035).

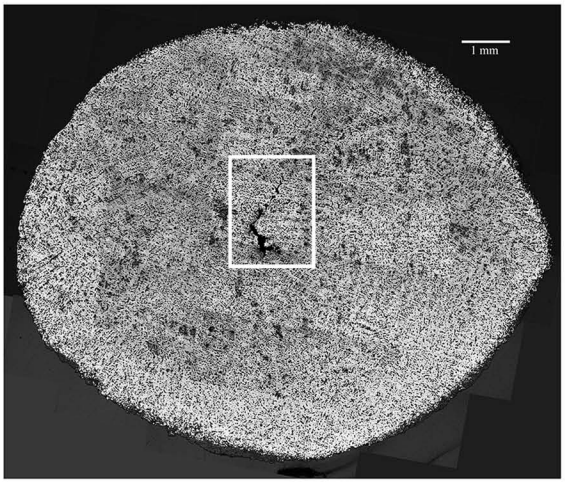

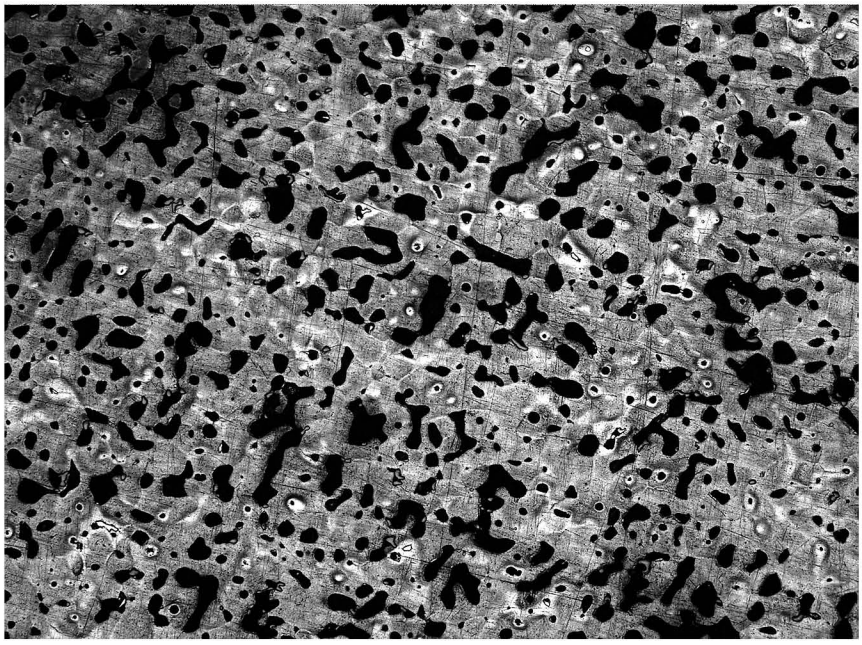

50 microns

Figure 5.1.12.ix: Segmented foot ring (MIT 5342/Peabody 40-77-40/13522). Transverse cross section. Etch: 2 sec dilute aqueous ferric chloride. x200. Microstructural features of interest include compositional inhomogeneities caused by segregation during the casting process. These compositional inhomogenities follow the shapes of the original dendrites.
(MIT Image 5342b-048).

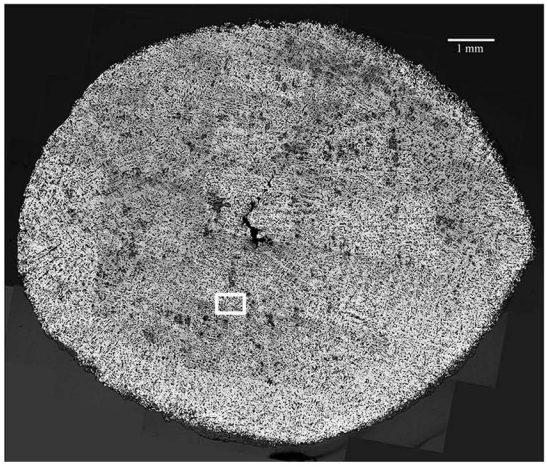

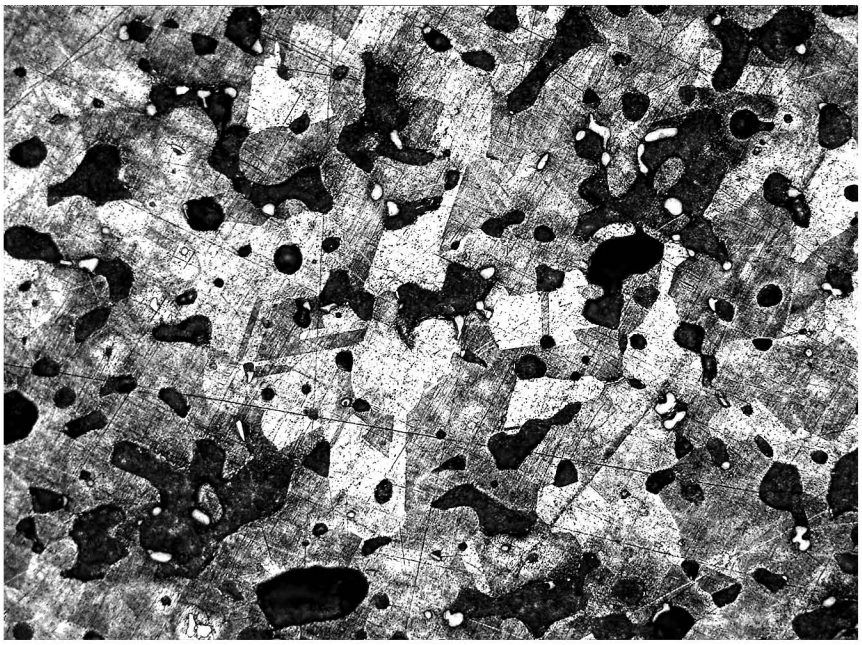

Figure 5.1.12.x: Segmented foot ring (MIT 5342/Peabody 40-77-40/13522). Transverse cross section. Etch: 3 sec alcholic ferric chloride. x500. Microstructural features of interest include equiaxed grains with annealing twins. Blue-green inclusions can also be seen homogenously distributed throughout the sample. (MIT Image 5342b-053.)

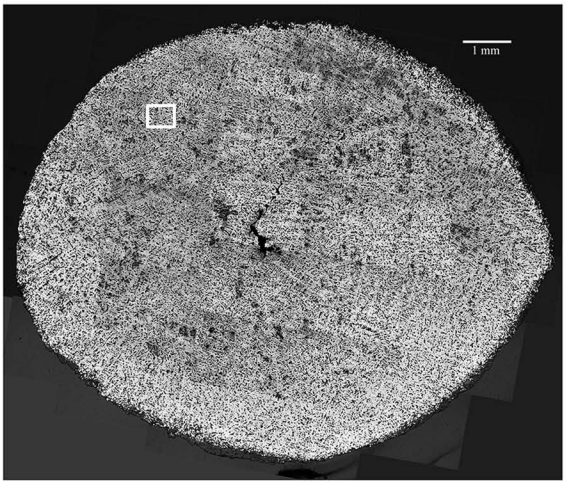

5.1.13: Hollow foot rings (not sampled)

Figure 5.1.13.i shows two segmented foot rings *in situ* in Grave 43 of Tumulus IV (Wells 1981). These two rings (Peabody 40-77-40/13510 and Peabody 40-77-40/13511) are shown in Figures 5.1.13.ii and 5.1.13.iii respectively.

This set of foot rings is similar to the set of foot rings from Grave 51 discussed in Section 5.1.12. Both sets of rings are about 12 cm in diameter, and both sets are segmented with semi-annular grooves. However, the foot rings from Grave 51 are solid, whereas the foot rings from Grave 43 are hollow. Peabody 40-77-40/13510 weighs 134.0 g, and Peabody 40-77-40/13511 weighs 141.0 g. The rings from Grave 51 weigh over twice as much (308.4 g and 329.8 g) as the hollow rings.

Peabody 40-77-40/13510 has a set of two seams that can be seen in Figure 5.1.13.ii. There is a seam running the length of the inside surface of the ring parallel to its longitudinal axis. This seam occurs at the juncture of the long edges of the rectangular piece of sheet metal bent round to form the hollow ring interior. There is a second seam running perpendicular to the ring's longitudinal axis where the two ends of the ring abut. The longitudinal seam on this foot ring is like the longitudinal seam seen on MIT 5366, discussed in Section 5.1.9.

The same two types of seam can be seen on Peabody 40-77-40/13511. This second ring in the pair has a series of holes in its outer surface revealing the hollow interior of the ring (Figure 5.1.13.iii). These two hollow foot rings were likely made in the same manner as MIT 5366.

Figure 5.1.13.i: Hollow foot rings. This photograph shows the hollow foot rings in Grave 43 (see preceding Figures 5.1.13i and 5.1.13ii) *in situ*. They were found together at the foot end of the grave. Copyright 2007: Harvard University, Peabody Museum, 40-77-40/14626.1.6.

Figure 5.1.13.ii: Hollow foot ring (Peabody 40-77-40/13510). This hollow foot ring from Grave 43 is 12 cm in diameter and weighs 134.0 grams. It is 12.5 mm wide and10.5 mm thick. The segments are 5.5 mm long and the grooves are approximately 1.5 mm wide. The longitudinal and transverse seams connecting the sides of the ring into a closed ring form can be seen clearly. Photograph by E. Cooney.

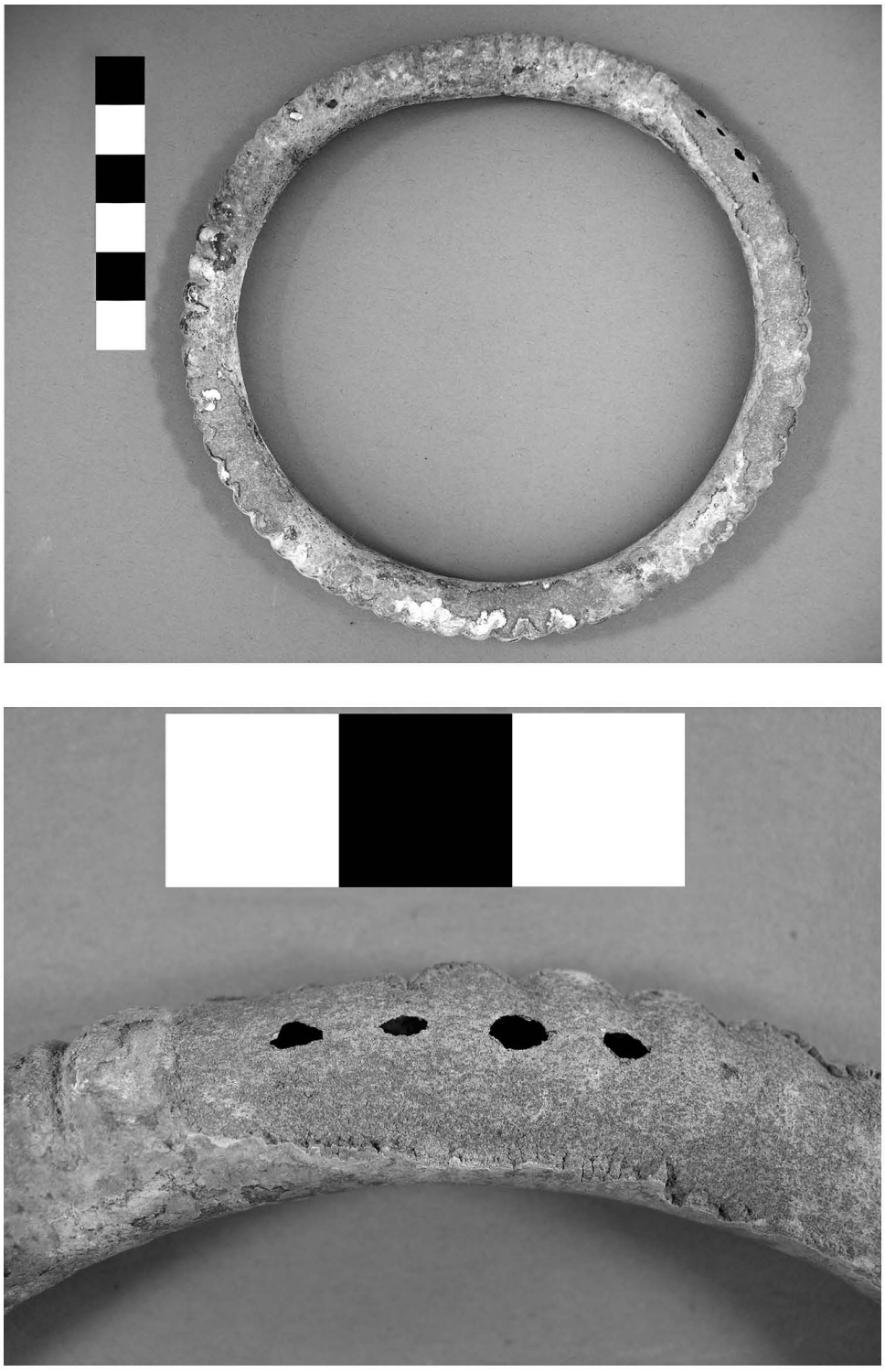

Figure 5.1.13.iii: Hollow foot ring (Peabody 40-77-40/13511). This hollow foot ring from Grave 43 is 12 cm in diameter and weighs 141.0 grams. It is 12.5 mm wide and 11.2 mm thick. The segments are 5.0 mm long and the grooves range from 1.5 to 2.0 mm in width. A few holes in a corroded area of the ring show that the foot ring is hollow. Photograph by E. Cooney.

5.2: Fibulae

There are 69 fibulae from Stična representing at least 11 distinct Hallstatt fibula types including dragon fibulae, shepherd's hook fibulae, certosa fibulae, leech fibulae, and serpentine fibulae. When compared to the rest of the tumuli at Stična, Tumulus IV does not contain a wide variety of fibula types; fourteen fibulae from at least five distinct fibula types are found in Tumulus IV. The fibula types represented are: serpentine (see Sections 5.2.1 and 5.2.2), navicular (see Section 5.2.3), dragon (Section 5.2.6), zoomorphic (Section 5.2.6), and shepherd's crook fibulae (the shepherd's crook fibulae are currently missing from the collection and were unable to be photographed). Many fibulae in Tumulus IV and at Stična as a whole are too fragmented to be assigned to a distinct fibula type (see section 5.2.4).

Given the limitations on fibula types in Tumulus IV, as wide a sample as possible was chosen for analysis. Three different fibula types were analyzed: two serpentine fibulae, one "knobbed" fibula which is too fragmented to be assigned to a distinct fibula type, and the spring and pin from a navicular fibula. A generic fibula spring was also analyzed. Both serpentine fibulae and the navicular fibula's spring and pin were sampled for bulk compositional and metallographic analyses. The knobbed fibula and the generic fibula spring were sampled for bulk compositional analysis.

5.2.1: Serpentine Fibula (MIT 5330/Peabody 40-77-40/13268)

5.2.1a: Provenance and Background

MIT 5330 (Figure 5.2.1.i), identified by Wells as a serpentine fibula, comes from Grave 2 of Tumulus IV (1981). It was found in conjunction with MIT 5339, the segmented leg ring discussed in Section 5.1.

Grave 2 was covered by a stone slab 0.85 m in diameter. The grave was 2.8 m long, 0.85 m wide, and 0.6 m deep. It contained some remains of a skeleton which was oriented east-west; no evidence of any crematory fires was recorded. Two segmented leg rings (MIT 5339 and an identical segmented ring) were found around the surviving leg bones. Other grave goods included transparent blue glass beads at the head end of the grave and a coarse ware urn and spindle whorl at the foot end.

There are six additional serpentine fibulae from Tumulus IV. Some serpentine fibulae, like MIT 5330, do not have a disc/fold stopper. Others, like the one discussed in section 5.2.2, do have a disc/fold stopper.

5.2.1b: Initial Examination and Observations

The serpentine fibula was photographed (Figure 5.2.1.i), drawn to scale, measured, and observed (Figures 5.2.1.ii and 5.2.1.iii).

The serpentine fibula, named for its curving body and characteristic saddle shaped bend, is broken into three fragments. The fibula was originally fashioned from one solid piece of metal. The fragments do not fit perfectly together, indicating that some small portions of the fibula may have been lost.

Fragment 1 contains the fibulae's pin catch and a decorative knob. It is 56.5 mm in length. The pin catch, 39.8 mm in length, is comprised of thin metal sheet 0.7 mm thick, curved into a concave groove to accommodate the pin. The decorative knob is cylindrical in shape, about 4.0 mm long with a radius of 4.5 mm. On one side of the knob there is a small hole 1.4 mm in diameter. The edges of this hole flare out slightly, indicating that it may have drilled. This fragment also contains a portion of the body of the fibula. This portion of the body has a circular cross section that starts with a radius of 2.5 mm and thins to a radius of 1.5 mm. Fragment 1 weighs 2.4 g.

Fragment 2 contains the bent bow of the fibula and the characteristic decorative saddle shaped bend of a serpentine fibula. The bow is on the side of the bend closest to the pin catch. Before the characteristic decorative bends the thickness of the fibula is 2.4 mm; within the bow the thickness is 4.8 mm. The fibula's bent bow is 22.1 mm wide, and the thickness at the bend is 2.6 mm. After the bend, the fibula starts tapering towards the pin, and the thickness of the fibula is reduced to 1.5 mm. Fragment 2 weighs 3.7 g.

Fragment 3 contains the intact end of the fibula's pin. The pin's thickness is reduced from 1.8 mm at the thickest end of this fragment to 1.4 mm thick at the pin's end. Fragment 3 weighs 0.8 g.

The fibula is structurally robust. The surface is covered with a smooth layer of mottled dark and light green corrosion product. This smooth layer of corrosion has been chipped away in some areas, revealing a layer of lighter green, friable corrosion product beneath. When observed under high magnification, a high density of deformation lines which were revealed through corrosion processes can be seen in this underlying layer of corrosion product. These deformation lines can be seen on every area of the fibula where the underlying layer of corrosion product has been revealed.

5.2.1c: Sampling

Two samples were removed from the fractured end of Fragment 3 as transverse sections (Figure 5.2.1.iv), one for bulk compositional analysis (MIT 5330a) and one for metallographic analysis (MIT 5330b). The fibula is highly metallic and the metal is light gold in color.

5.2.1d: Compositional Analysis

Bulk compositional analysis shows that the fibula is a copper alloy with the primary alloying element of tin at a concentration of 11.4 weight percent. The alloy is a leaded tin bronze. Other major and minor elements include Pb (1.53%), Sb (0.537%), As (0.485%), Ag (0.252%), and Ni (0.184%). Bulk compositional analysis data are shown in Table 5.2.1 and in the Appendix.

Table 5.2.1: Bulk Compositional Analysis Data for MIT 5330

	Sn	Pb	Sb	As	Ni	Co	Ag	Fe
ICP-ES	11.4	1.53	0.537	0.485	0.184	0.054	n.a.	0.018
INAA	10.4	n.a.	0.529	0.407	0.311	0.0591	0.252	n.d.

(values in weight %) n.a. = not analyzed n.d. = not determined

5.2.1e: Metallographic Analysis

MIT 5330b was mounted as a transverse section (Figure 5.2.1.iv).

As polished, the sample has a slightly oval, rounded cross section (Figure 5.2.1.v). There is little external corrosion, and the sample is highly porous. The pores vary in size, with slightly larger pores near the center of the sample. The pores are rounded and are not aligned in any way. The pores were most likely formed during a casting operation, suggesting that the metal stock from which the fibula was later fashioned was cast to shape. A few gray copper-sulfide inclusions with no apparent alignment or shape are scattered homogenously around the outer edges of the sample.

The sample was etched for 12 seconds with potassium dichromate and for 4 seconds with aqueous ferric chloride to reveal the microstructure which consists of equiaxed grains with bent annealing twins and a very high density of deformation lines (Figures 5.2.1.vi and vii.) The presence of equiaxed grains with bent annealing twins indicates that the object was worked and annealed at least once and probably multiple times during manufacture. Because the grains are not elongated in any discernable pattern, it is clear that the fibula's pin was worked around its total circumference. The high density of deformation lines and the bent annealing twins indicate that the fibula's pin was left in a worked condition.

There is a large cluster of smaller grains surrounded by larger grains near the sample's center. The presence of this cluster of smaller grains near the center of the sample is not readily explained. Deformation lines and bent annealing twins are uniformly distributed throughout the sample regardless of grain size.

5.2.1f: Discussion

Because this particular fibula was made from one single piece of metal, the same alloy needed to be used for the different functional parts of the fibula: the pin catch, the body of the fibula, and the pin. The bow of the fibula needed to be flexible enough to be

able to bend slightly during the fastening/unfastening process. At the same time, however, the pin needed to be hard enough to pierce the cloth garments and strong enough to withstand a load in tension without deforming as it held together hanging woolen garments. The body of the fibula had to be hard and robust, serving as an anchor for the fibula's pin, and the pin catch required metal malleable enough to be hammered thin and concave to hold the pin in place. The pin catch was strong so as not to buckle under the heavy load placed on the pin when fastened.

The choice of alloy for the fibula reflects its function. The pin is made from an approximately 11 weight percent Sn, leaded bronze. This tin alloy, when worked to the extent indicated by the pin's microstructure, is hard and strong enough to withstand the forces placed on the fibula. At the same time, although the elasticity of an 11 weight percent Sn alloy is much diminished in comparison with that of a low tin bronze, the bronze is not brittle. The 1.5 weight percent Pb was most likely added to aid in the casting process, and the antimony and arsenic in the alloy were likely present in the copper ore from which the metallic copper was smelted.

Interpretation of the microstructure indicates that the stock metal from which the fibula was fashioned was originally cast to shape and was subsequently subject to repeated cycles of cold-working and annealing to achieve the final shape of the fibula. Deformation lines revealed in the fibula's external corrosion product show that every area of the fibula was worked and left in a worked state. The bent annealing twins and high density of deformation lines in sample MIT 5330b show that the fibula pin was heavily worked after annealing and left in a heavily worked state.

The metal smith may have heavily worked the pin to reduce its thickness and to harden it for use as a pin so that it would not warp under the load of heavy cloth garments. The heavily worked structure may also stem from the slight bending and unbending of the pin portion of the fibula as the pin was fastened and unfastened from its pin catch during use. This is less likely, however, as the sampled portion of the pin was not close to any pivot point where the metal would have been subject to much bending.

The choice of alloy and manufacturing technique used to make this fibula closely resemble those used to make similar fibulae at S. Lucia at this same time (Guimlia-Mair 1998; Guimlia-Mair 1995).

5.2.1g: Conclusions

- The alloy choice, approximately 11 weight percent Sn and 1.5 weight percent Pb, reflects the fibula's intended use and manufacturing process. The body, pin, and pin catch of the fibula needed to be hard enough to hold heavy woolen robes in place at the same time as the bow of the fibula needed to be elastic enough to allow for repeated slight bending without breakage so the fibula could be fastened and unfastened. During manufacture the metal stock had to be easily castable.
- The metal stock from which the fibula was formed was cast roughly to shape and then worked to achieve the final shape of the fibula. The pin was heavily worked, most likely to harden the pin and to reduce it to its final shape. The pin's heavily worked structure may also stem from use wear, although this is less likely.

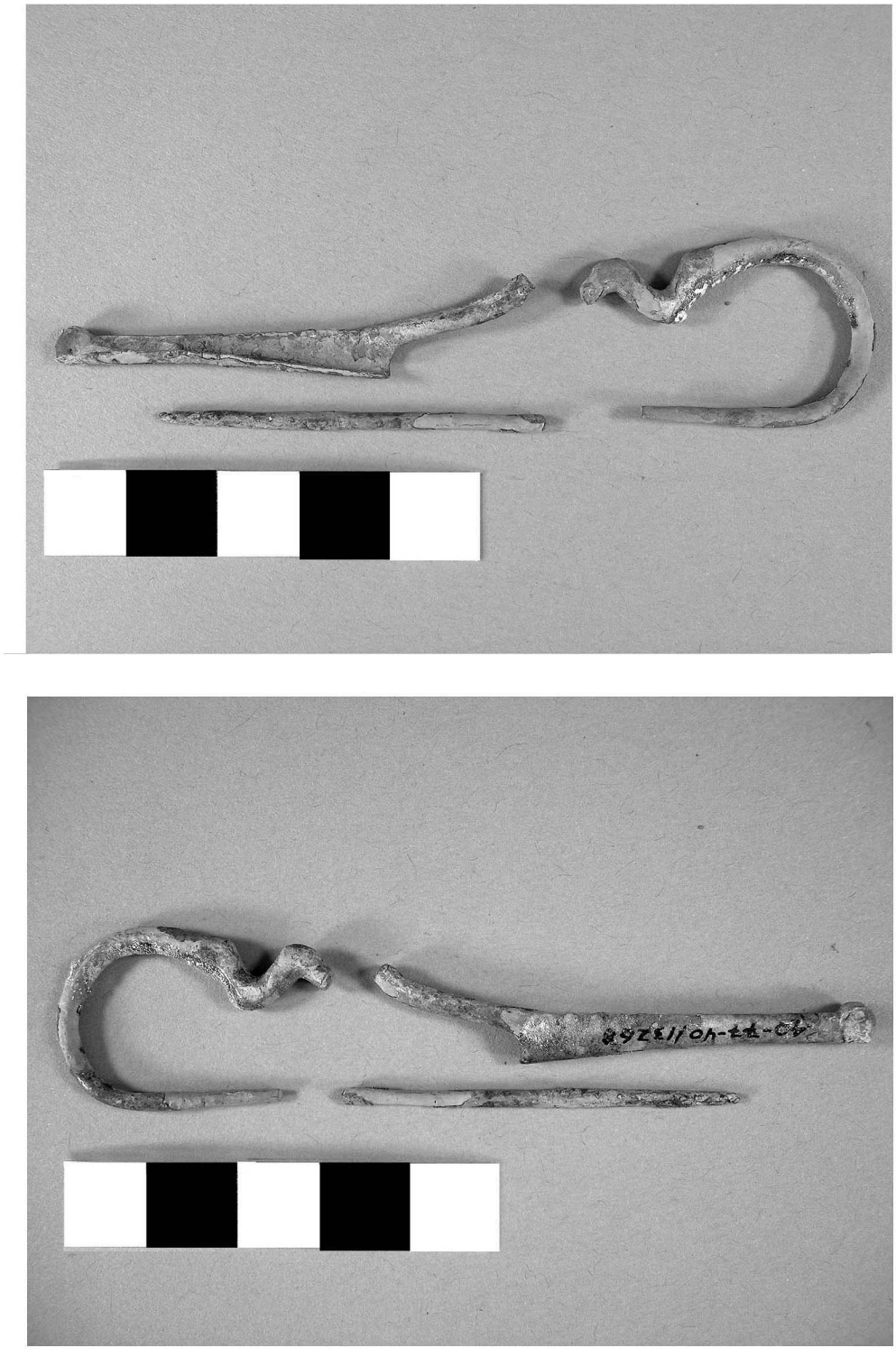

Figure 5.2.1.i: Serpentine fibula. (MIT 5330/Peabody 40-77-40/13268). Copyright 2007: President and Fellows of Harvard College.

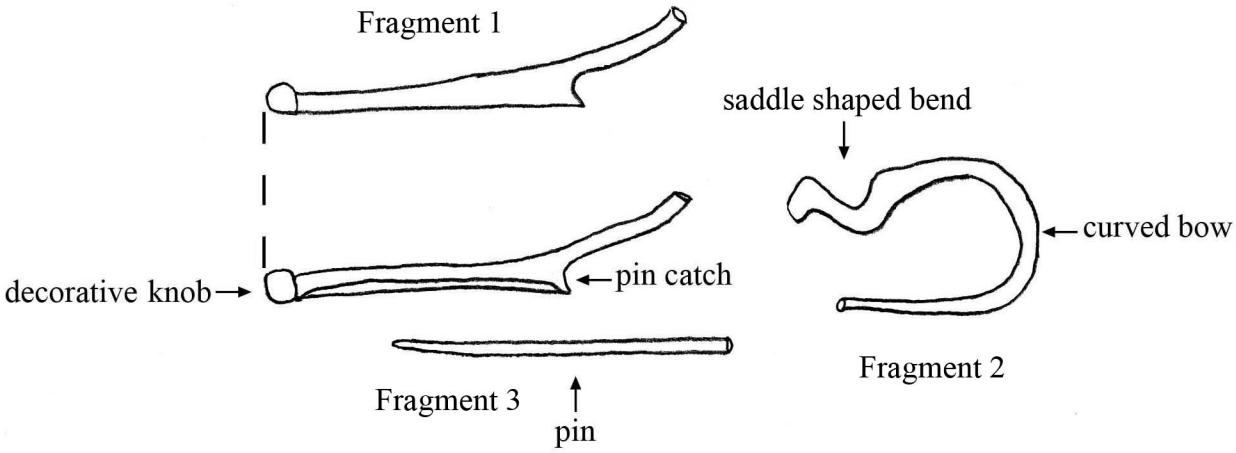

Figure 5.2.1.ii: Serpentine fibula (MIT 5330). Key object features.

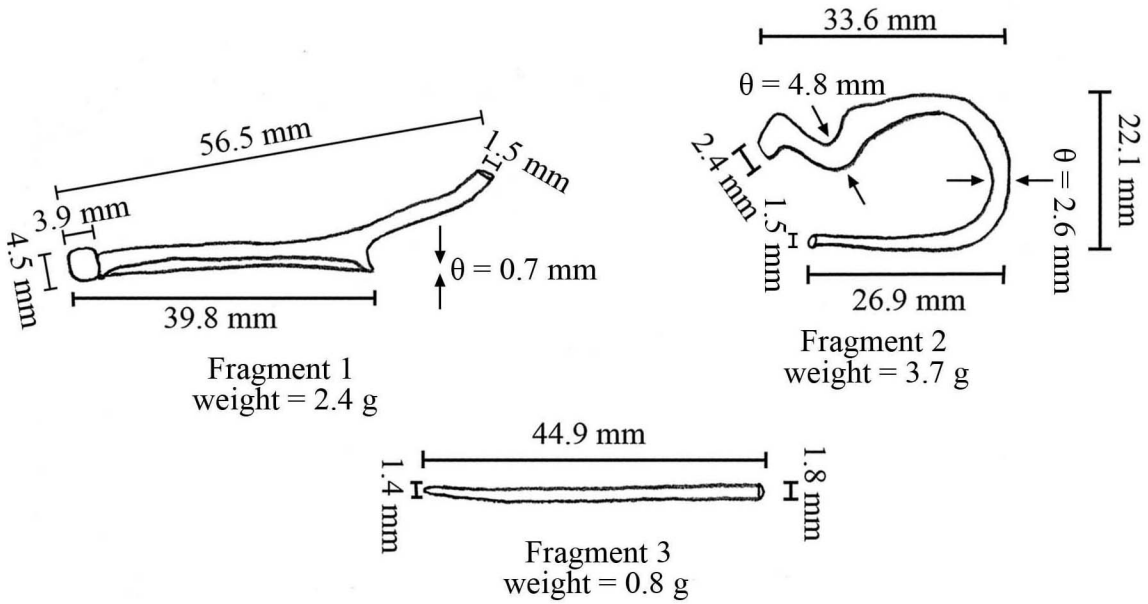

Figure 5.2.1.iii: Serpentine fibula (MIT 5330). Drawing and measurements.

Figure 5.2.1.iv

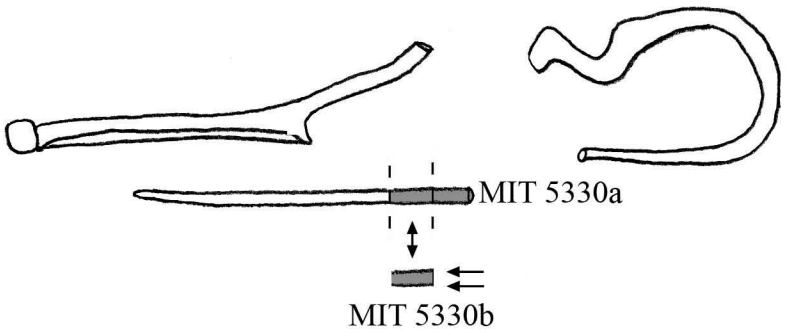

Figure 5.2.1.iv: Samples removed from Serpentine fibula. MIT 5330a was removed for bulk compositional analysis. MIT 5330b was removed for metallographic analysis and mounted transversely as noted.

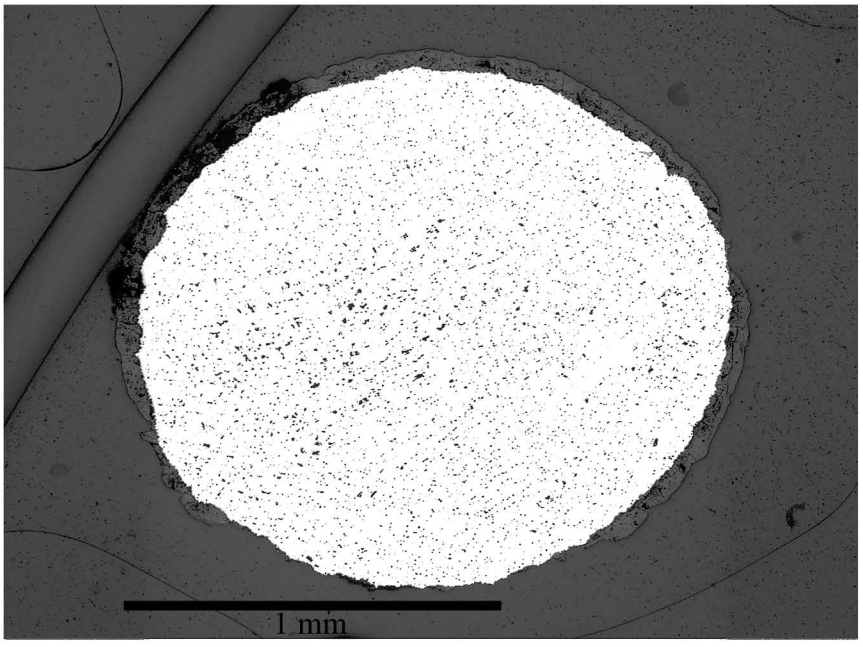

Figure 5.2.1.v: Serpentine fibula (MIT 5330/Peabody 40-77-40/13268). Transverse cross section, as polished. x50. Microstructural features of interest include homogenously distrubuted pores and thin layer of external corrosion product. (MIT Image 5330b-01.)

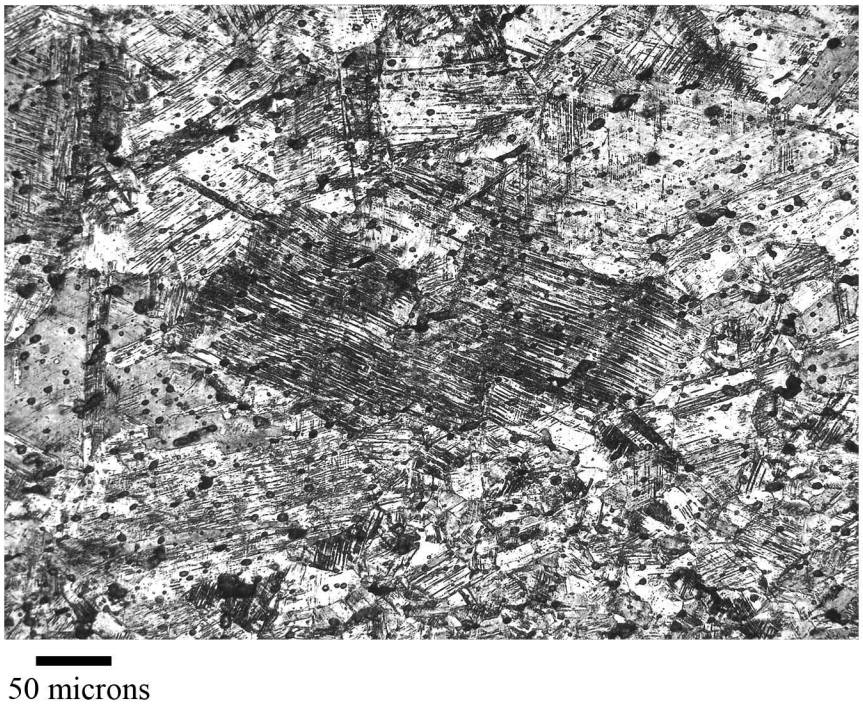

Figure 5.2.1.vi: Serpentine fibula (MIT 5330/Peabody 40-77-40/13268). Transverse cross section. Etch: 12 sec potassium dichromate and 4 sec aqueous ferric chloride. x200. Microstructural features of interest include equiaxed grains, bent annealing twins, and a high density of deformation lines throughout the sample (MIT Image 5330b-16.)

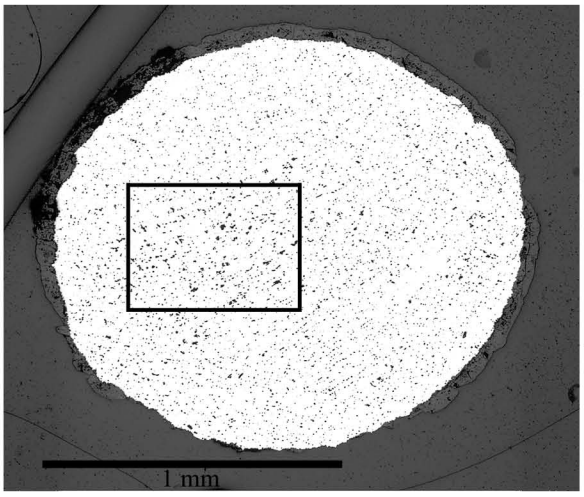

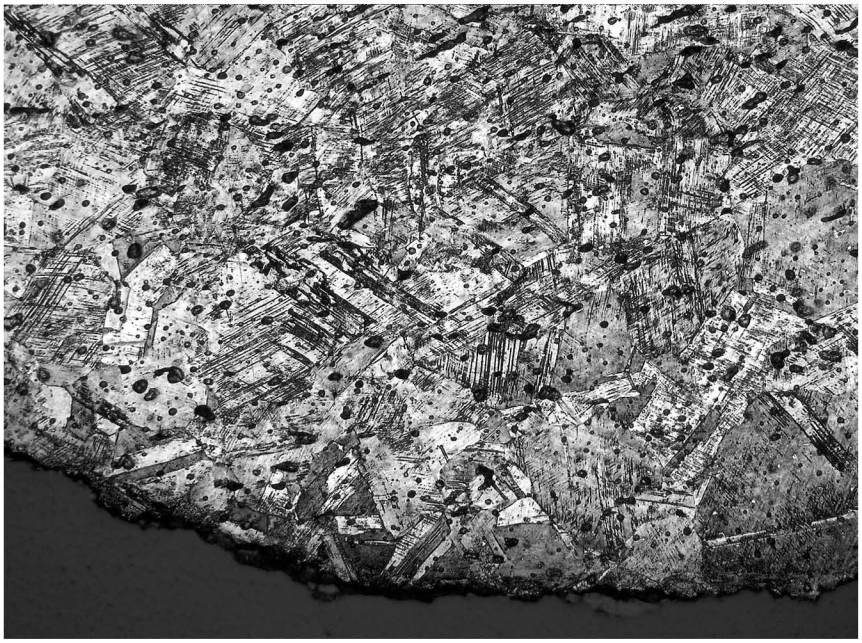

Figure 5.2.1.vii: Serpentine fibula (MIT 5330b/Peabody 40-77-40/13268). Transverse cross section. Etch: 12 sec potassium dichromate and 4 sec aqueous ferric chloride. x200. Microstructural features of interest include equiaxed grains, bent annealing twins, and a high density of deformation lines throughout the sample (MIT Image 5330b-18.)

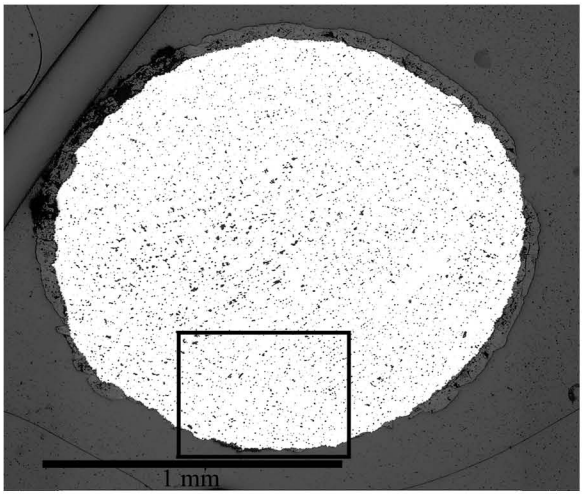

5.2.2: Serpentine fibula with disc (MIT 5352/Peabody 40-77-40/13555)

5.2.2a: Provenance and Background

MIT 5352 (Figure 5.2.2.i), identified by Wells (1981) as serpentine fibula with a stop disc, comes from Grave 53 of Tumulus IV. Grave 53 was 1.9 m below the surface of Tumulus IV.

Associated grave goods included two segmented bronze rings with overlapping ends, five colored glass beads, and sherds from a low, footed bowl with red-orange slip, decorated with raised horizontal bands and a band of graphite on the interior. These grave goods are very similar to those found in Grave 2 in conjunction with MIT 5330.

Two similar serpentine fibulae with discs are found in Graves 12 and 17 of Tumulus IV. The fibula from Grave 17 is almost entirely intact (Figure 5.2.2.ii). The discs, also referred to as fold stoppers, served to keep both the fibula and the woolen garments it held together in place while in use. When worn, only the external body of the fibula from the pin catch to the fold stopper would have been seen. The pin and interior of the pin catch would have been either beneath the garments or worn against the body, out of sight.

Serpentine fibulae are not the only Early Iron Age fibulae with fold stoppers. In studies of similar Early Iron Age fibulae with fold stoppers it has been shown that the stopper is usually made from a different alloy than the one used to make the body of the fibula. It is unclear if these stoppers were usually cast onto the bodies of the fibulae or if they were cast as separate parts and strung onto the pins (Guimlia-Mair 1995).

5.2.2b: Initial Examination and Observations

The serpentine fibula with disc was photographed (Figure 5.2.2.i), drawn to scale, measured, and observed (Figures 5.2.2.iii and 5.2.2.iv).

The serpentine fibula has lost its pin and pin catch. The surviving fragment contains the characteristic saddle shaped bend on its body, a curved bow, and a disc. The disc itself is fragmented and no longer retains its original edges.

The surviving fibula fragment is 51.4 mm long and weighs 6.4 g. It has a lenticular cross section that changes in area across the body of the fragment. The

fragmented edge furthest from the disc is 3.2 x 2.3 mm while the fragmented edge closest to the disc is 2.8 mm x 3.2 mm. The thickest portion of the fragment is at the saddle shaped bend where the dimensions are 4.0 x 4.5 mm. The fibula body is thicker above disc, the area of the body between the saddle shaped bend and the disc, which has a width of 3.5 mm, than it is below the disc, the area of the body between where the pin once was and the disc, which has a width of 3.0 mm. The surviving disc is vaguely oval shaped and measures10.0 x 9.5 mm. At its thickest point the disc is 1.6 mm thick.

The body of the fibula is structurally robust. It is covered with a thick layer of smooth corrosion product that is mottled dark green and brown in color. The area below the disc has been mostly cleaned of corrosion product. The disc is quite fragmented and appears to be entirely corroded at its outer edges. It too is covered in a thick layer of green and brown corrosion product. Due to the extent of the corrosion product, the method of the disc's attachment to the body of the fibula is unclear even when observed under magnification.

5.2.2c: Sampling

Two samples were removed from the serpentine fibula with transverse cuts (Figure 5.2.2.v), one for bulk compositional analysis of the fibula's body (MIT 5352a) and one for metallographic and electron microbeam probe analysis of the body and disc (MIT 5352b). The fibula is highly metallic and the metal is light gold in color.

5.2.2d: Bulk Compositional Analysis

Bulk compositional analysis shows that the fibula's body is made from a copper-tin alloy with tin present at a concentration of 10.9 weight percent. The alloy is a leaded tin bronze. Other major and minor elements include Pb (1.69%), As (0.187%), Sb (0.063%), Ni (0.061%), and Ag (0.056 %). Cobalt and iron are present in trace amounts. This composition is similar to the composition of MIT 5330. Bulk compositional analysis data are shown below in Table 5.2.2.i and in the Appendix.

Table 5.2.2i: Bulk Compositional Analysis Data for MIT 5352 (Fibula Body)

	Sn	**Pb**	**Sb**	**As**	**Ni**	**Co**	**Ag**	**Fe**
ICP-ES	10.9	1.69	0.063	0.187	0.058	0.011	n.a.	0.007
INAA	9.61	n.a.	0.045	0.166	0.0610	0.0170	0.056	n.d.

(values in weight %) n.a. = not analyzed n.d. = not determined

5.2.2e: Metallographic and Electron Microbeam Probe Analyses

MIT 5352b was mounted as a longitudinal section (Figure 5.2.2.v). It was ground halfway down to a point where both the body and the disc of the fibula were exposed *in situ*.

As-polished, the sample shows the curved body of the fibula surrounded by the disc on either side (Figure 5.2.2.vi). The juncture between the disc and the body of the fibula can be seen clearly, indicating that the disc was not cast onto the body of the fibula. The disc was fashioned independently of the fibula's body and was strung into place along the fibula's pin to its final position on the fibula's body.

The body and disc of the fibula are quite different in appearance in the as-polished sample (Figure 5.2.2.vii). The disc is noticeably more pinkish in color than the body, which is light gold. The disc has a very high density of small porosities while the body has a high density of larger porosities. In both the disc and the body the porosities are homogenously distributed and do not have any apparent alignment. Internal corrosion in the body of the fibula outlines equiaxed grains and deformation lines, while internal corrosion in the disc does not appear to have any defined structure. It is clear from the as polished sample that the body and disc are made of two different materials.

MIT 5352b was analyzed with an electron microbeam probe to determine the composition of the disc. The compositions of a series of six points across the disc whose locations are indicated in Figure 5.2.2.viii were determined and are shown in the table in Figure 5.2.2.viii. The average composition of the disc is given in Table 5.2.2.ii.

The fibula disc is a copper-tin-lead ternary alloy. The alloying elements tin and lead are present at a concentration of 7.5 weight % and 3.14 weight % respectively. The lower tin content in the disc causes it to have a pinker hue than the fibula's body.

Table 5.2.2.ii: Average Composition of Fibula Disc

Cu	Sn	Pb	Sb	As	Ni	Co	Ag	Fe
88.96	7.5	3.14	0.0118	0.38	0.057	0.0112	0.1138	0.0033

(all values in weight %)

The electron microbeam probe was also used to analyze the material at the juncture between the disc and the body of the fibula. Backscattered electron imaging showed that present along the entire length of the juncture between the disc and the body there are small amounts of two distinct materials, each of which is different in composition from both the disc and the body. These two distinct materials can be seen clearly in the backscattered electron image shown in Figure 5.2.2.ix and also in the color photomicrograph of the same area. Energy dispersive spectrometric (EDS) data spectra show that these two materials are almost pure Pb and almost pure Cu (Figure 5.2.2.x). The lead and copper are not metallurgically joined to either the disc or the fibula body. It is unclear exactly what function these materials had. The lead may have been introduced at the juncture to help keep the disc in place on the body of the fibula. It could have introduced as a solid and mechanically pushed down along the length of the juncture.

After analysis on the electron microbeam probe, MIT 5352b was etched for six seconds with potassium dichromate and for three seconds with aqueous ferric chloride. The enchants revealed that the disc has a dendritic, as-cast microstructure. Dendrites of the Cu-Sn alloy are surrounded by pores partially filled with Pb. Although the disc is not a high tin bronze, during the casting process segregation caused pools of eutectoid to be formed along the dendrites' outer edges and in the interdendritic spaces (Figure 5.2.2.xi.) The disc's microstructure shows that it was not worked or annealed after casting.

The fibula body's microstructure is characterized by equiaxed grains with deformation lines (Figure 5.2.2.xii). There is a higher density of deformation lines in the region above the disc than there is in the region below the disc (Figure5.2.2.xiii). The presence of equiaxed grains shows that the object was worked and annealed at least once and probably multiple times during manufacture.

The deformation lines probably stem mostly from use wear. As the pin was fastened and unfastened, the majority of the strain would have occurred in the area directly surrounding the disc, which serves as the pivot point. Many Early Iron Age

bronze fibulae with such discs have broken at the point directly above the disc because of the high strain (Guimlia-Mair 1995). Some deformation lines may also have come from the working of the body or from the stress placed on the body when the disc was strung along the pin to its final place on the body.

5.2.2f: Discussion

The choice of alloy used for the body of the fibula (approximately 11% Sn, 1.5% Pb) is virtually identical with that of MIT 5330 for the same reasons: the body of the fibula was made from a single alloy that needed to perform the functions of remaining hard yet somewhat elastic at the same time.

The disc, however, is made from a completely different alloy of 7.5% Sn and 3.14% Pb. The disc did not need to perform any mechanical function at all and could be made with less tin and more "filler" material like lead. Because tin was a scarce, non-local commodity, a metalsmith might have been reluctant to use a large amount of tin on such a tiny, non-mechanically functional part. At the same time, some tin needed to be used to keep the color golden. A disc of pure copper would have been very pink in color and a high contrast to the light gold of the fibula's body. Conversely, the smith may have wanted the slight color difference between the disc and the body as an accent for the piece.

The disc was cast and left in an as-cast condition. It was not cast onto the body of the fibula and was instead strung on. Lead and possibly copper were used to line the juncture, probably to help keep the disc in place on the body of the fibula. The join is mechanical, not metallurgical. The disc did not need to be worked to shape or worked hardened as it was made to be a tiny, non-mechanically functional part of the fibula.

The microstructure of the body of the fibula contains porosities and equiaxed grains with annealing twins that suggest it was originally cast to shape and was subsequently subject to several cycles of cold-working and annealing to achieve its final shape. It was probably left in a worked condition.

The high density of deformation lines in the body at the location of the disc most likely stems from use and repeated fastening/unfastening of the fibula.

5.2.2g: Conclusions

- The associated grave goods of MIT 5352 mirror those of MIT 5330.
- The alloy choice for the fibula's body, approximately 11 weight % Sn and 1.5 weight % Pb, reflects the fibula's intended use and manufacturing process. The body, pin, and pin catch of the fibula needed to be hard enough to hold heavy woolen robes in place at the same time that the bow of the fibula needed to be elastic enough to allow for repeated slight bending without breakage so it could be fastened and unfastened. During manufacture the stock metal had to be easily castable.
- The metal stock from which the fibula was formed was cast roughly to shape and then worked to achieve the final shape of the fibula.
- The alloy choice and manufacturing technique for the fibula's body are the same as those for MIT 5330.
- The alloy choice for the fibula's disc, approximately 7.5% Sn and 3% Pb, reflects its use as a non-mechanically functional part.
- The disc was cast and left in an as-cast condition, which also reflects its intended use as a non-mechanically functional part.
- The disc was strung onto the body of the fibula, and lead and copper were used as a mechanical means of insuring the disc remained in place.
- The fibula was used as intended and was fastened/unfastened many times prior to burial.

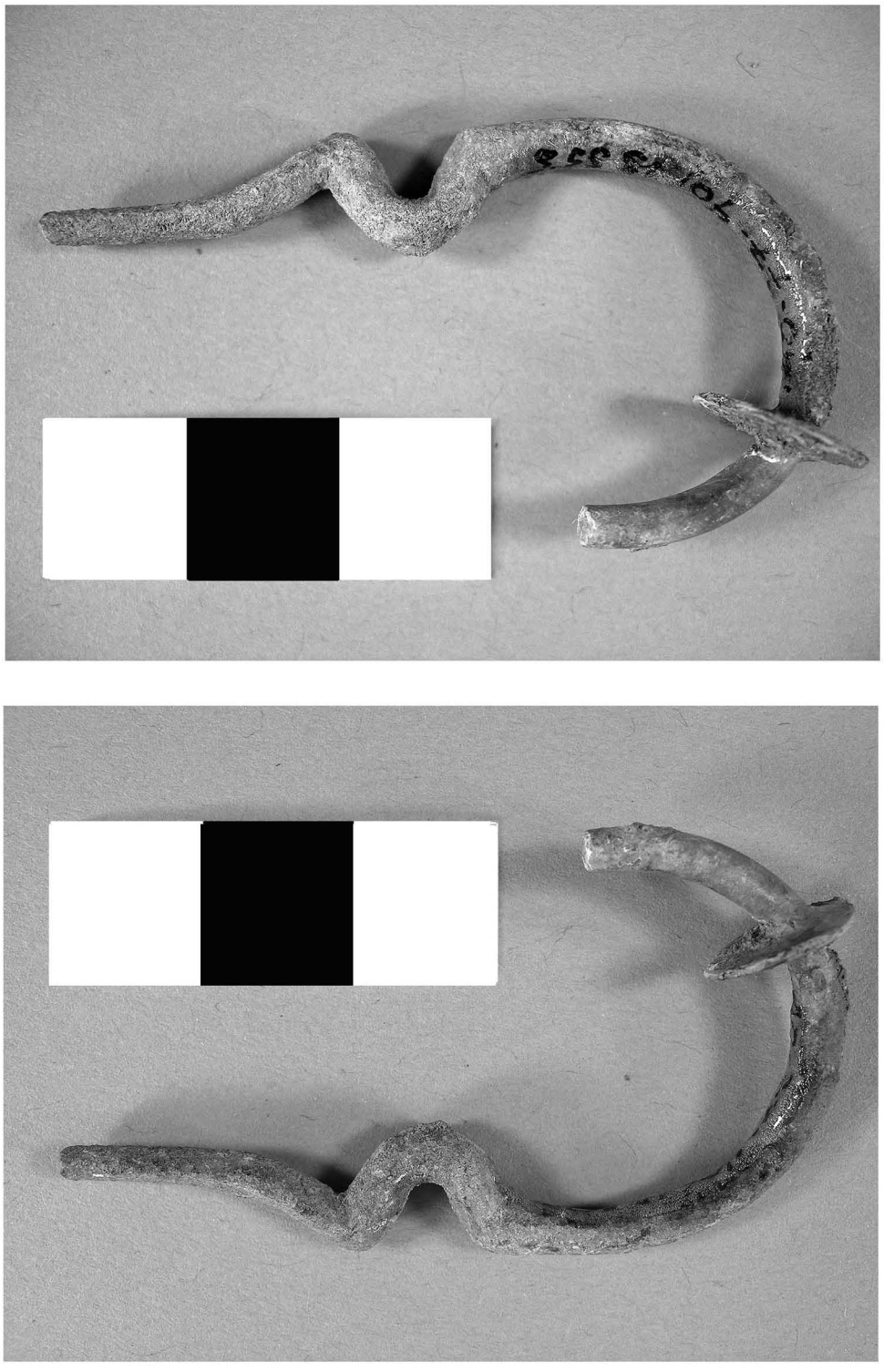

Figure 5.2.2.i: Serpentine fibula with disc. (MIT 5352/Peabody 40-77-40/13555). Photographs by E. Cooney.

5.2.2.ii: Serpentine fibula with disc (Peabody 40-77-40/13319). An additional serpentine fibula with an intact disc and pin catch from Tumulus IV, Grave 12. Photograph by E. Cooney.

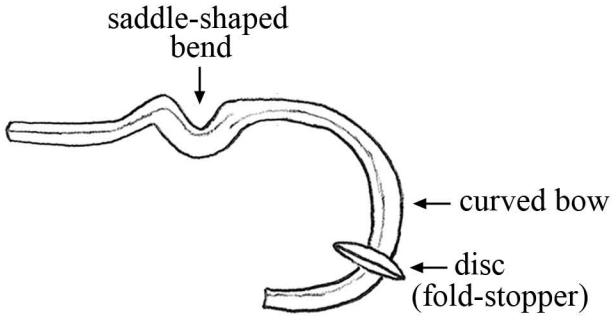

Figure 5.2.2.iii: Serpentine fibula with disc (MIT 5352). Key object features.

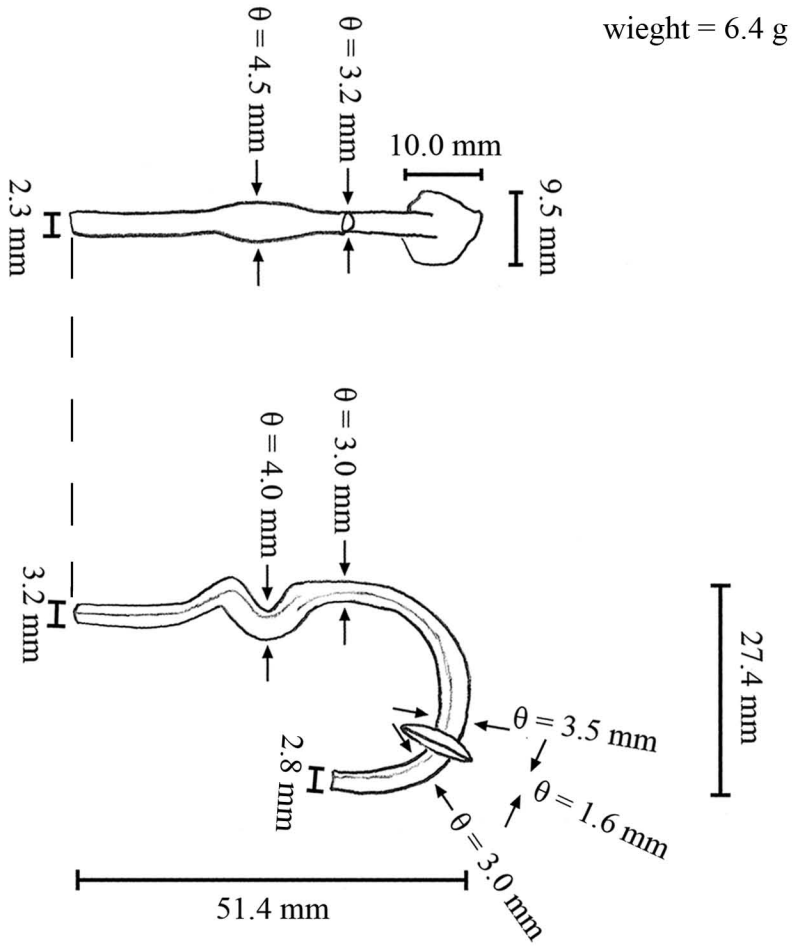

Figure 5.2.2.iv: Serpentine fibula with disc (MIT 5352). Drawing and measurements.

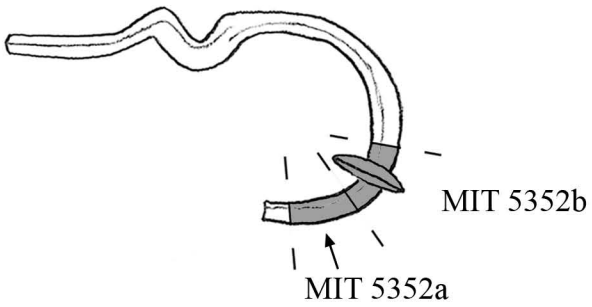

Figure 5.2.2.v: Samples removed from serpentine fibula with disc. MIT 5352a was removed for bulk compositional analysis. MIT 5352b was removed for metallographic analysis. It was mounted longitudinally and was ground down in the direction of the plane of the page until the curved body and the disc were exposed *in situ.*

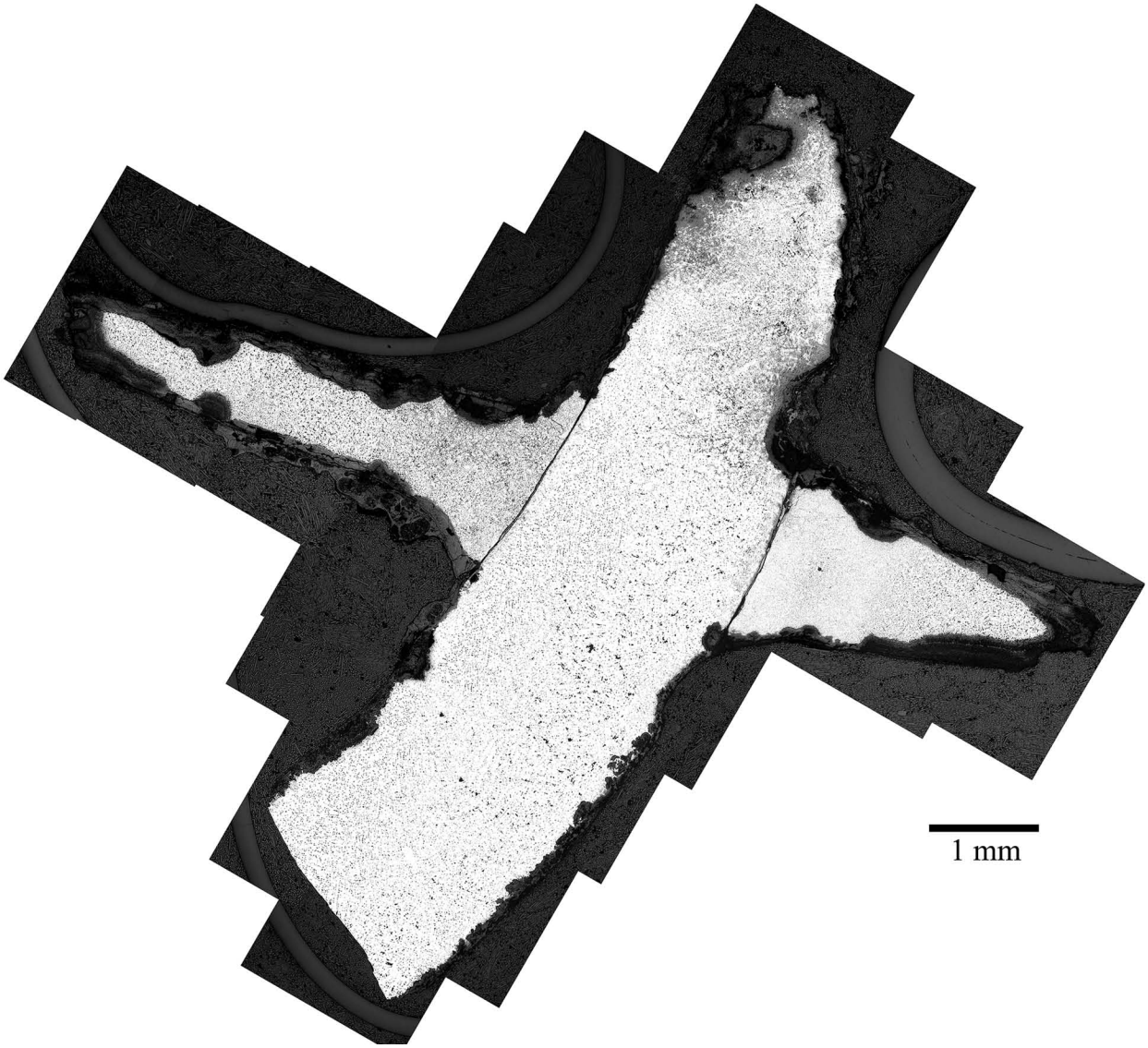

Figure 5.2.2.vi: Serpentine fibula with disc (MIT 5352/Peabody 40-77-40/13555.) Longitudinal cross section, as polished. Microstuctural features of interest include the juncture between the disc and the body of the fibula, a high density of porosities in both the body of the fibula and the disc, and the internal corrosion products outlining equiaxed grains with deformation lines in the body of the fibula. (MIT Images 5352b-01-17.)

Figure 5.2.2.vii: Serpentine fibula with disc (MIT 5352b/Peabody 40-77-40/13555). x50. Longitudinal cross section, as polished. Microstructural features of interest include the color difference between the body of the fibula and the disc. The disc is noticeably more pinkish in color than the body, which is a light gold. Other notable features are the join between the disc and the body, which appears to be filled with a thin layer of corrosion product, and the differences in pore size and arrangement in the disc and the body. The pores in the body are larger than in the disc and the density of pores is much greater in the disc than in the body. Finally, the internal corrosion present in the body outlines equiaxed grains and deformation lines. (MIT Image 5352b-30).

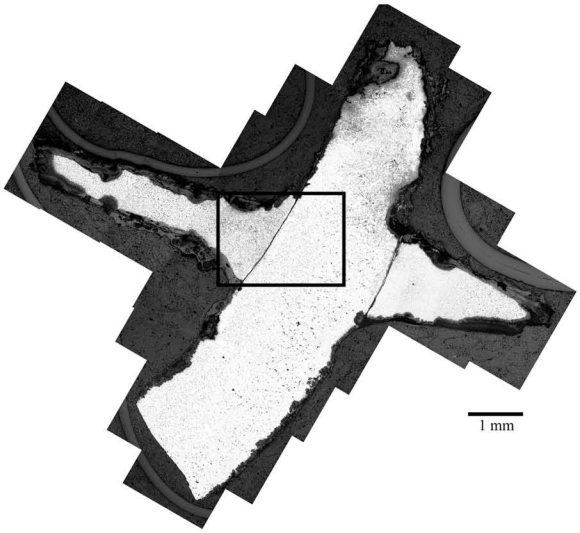

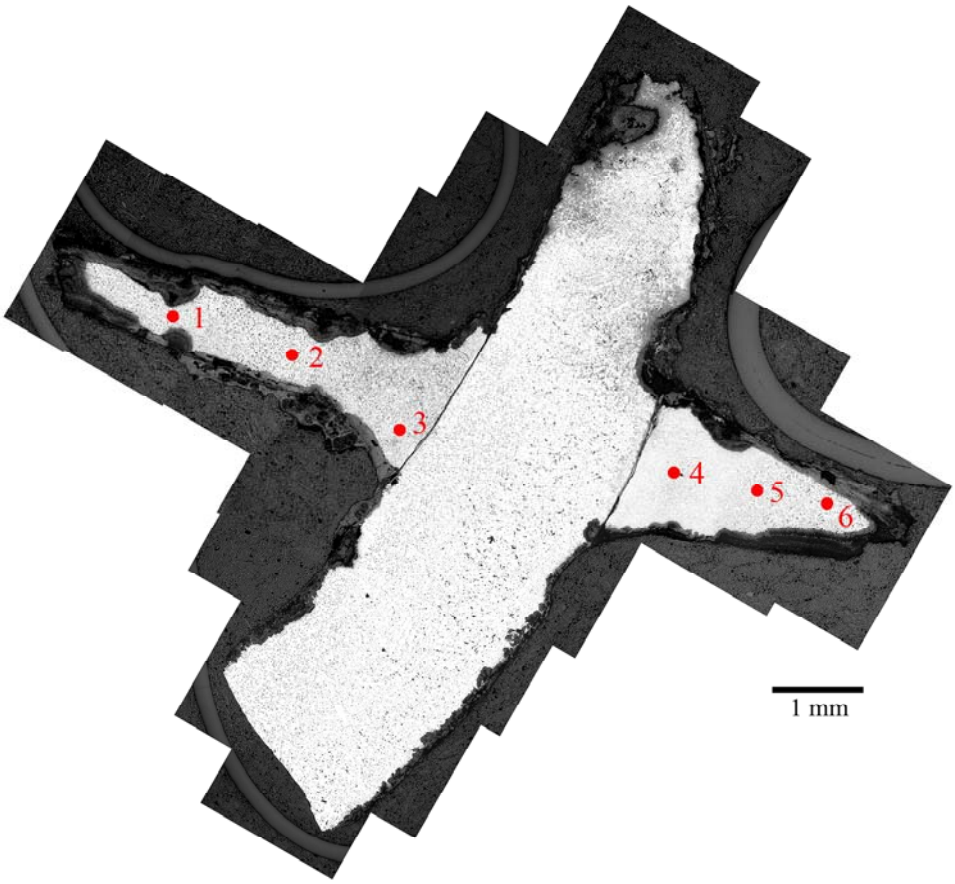

Electron Microbeam Probe Compositional Data

	Cu	Sn	Pb	Sb	As	Ni	Co	Ag	Fe
Pt 1	90.96	6.82	3.13	n.d.	0.402	0.058	0.002	0.037	n.d.
Pt 2	87.92	7.8	3.25	n.d.	0.3958	0.0587	0.0008	0.0867	n.d.
Pt 3	86.43	7.82	3.55	n.d.	0.3854	0.0774	0.0154	0.1935	0.012
Pt 4	91.73	7.51	2.17	0.0215	0.4001	0.0341	n.d.	0.1099	0.0083
Pt 5	88.05	7.8	4.72	0.0109	0.3134	0.0549	0.0348	0.2207	n.d.
Pt 6	88.65	7.09	2.02	0.0386	0.39	0.0584	0.014	0.035	n.d.
Average	**88.96**	**7.5**	**3.14**	**0.0118**	**0.38**	**0.057**	**0.0112**	**0.1138**	**0.0033**

(all values in weight %) n.d. = not determined

Figure 5.2.2.viii: Serpentine fibula with disc (MIT 5352b/Peabody 40-77-40/13555). **Above:** Points at which compositional data were taken by the electron microbeam probe. **Below:** Electron microbeam probe compositional data from each point.

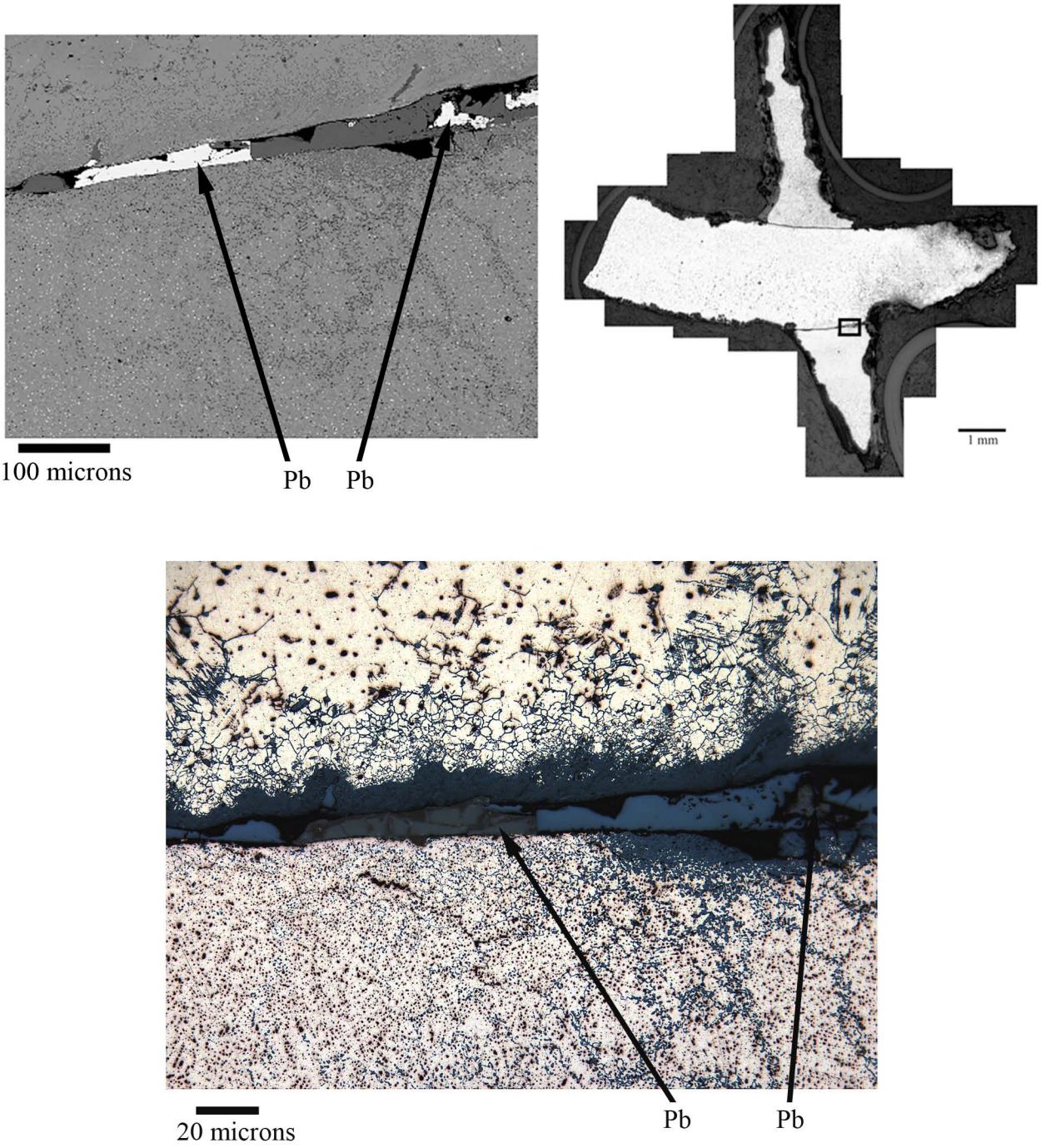

Figure 5.2.2. ix : Serpentine fibula with disc (MIT 5352b/Peabody 40-77-40/13555). Above: Backscattered electron image of material present in the juncture between the disc and the body of the fibula. The light-appearing material is pure lead. The dark-appearing material is copper corrosion product.
Below: Photomicrograph at x500 showing the lead and copper in the juncture. The lead is dark gray in color. The copper corrosion product is dark green. (MIT Image 5352b-28.)

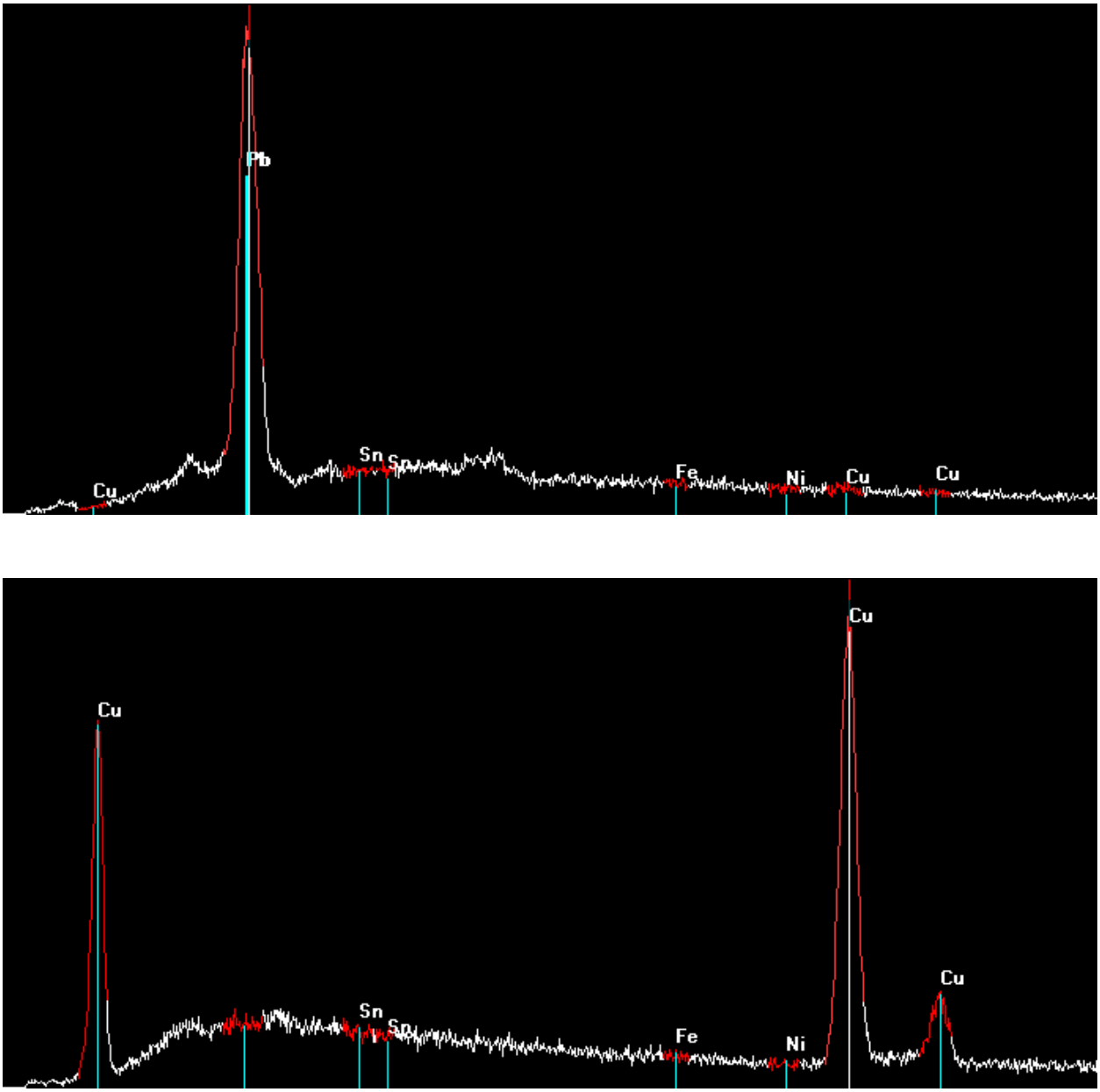

Figure 5.2.2.x: Serpentine Fibula with disc (MIT 5352b/Peabody 40-77-40/13555).
Above: EDS spectrum of the light-appearing material in the backscattered electron image of the juncture between the disc and the body of the fibula (see Figure 5.2.2.vii). The spectrum identifies this material as pure lead. This material appears gray in the preceding photomicrograph.
Below: EDS spectrum of the dark-appearing material in the backscattered electron image of the juncture between the disc and the body of the fibula. The spectrum identifies this material as pure copper. This material appears dark green in the preceding photomicrograph.

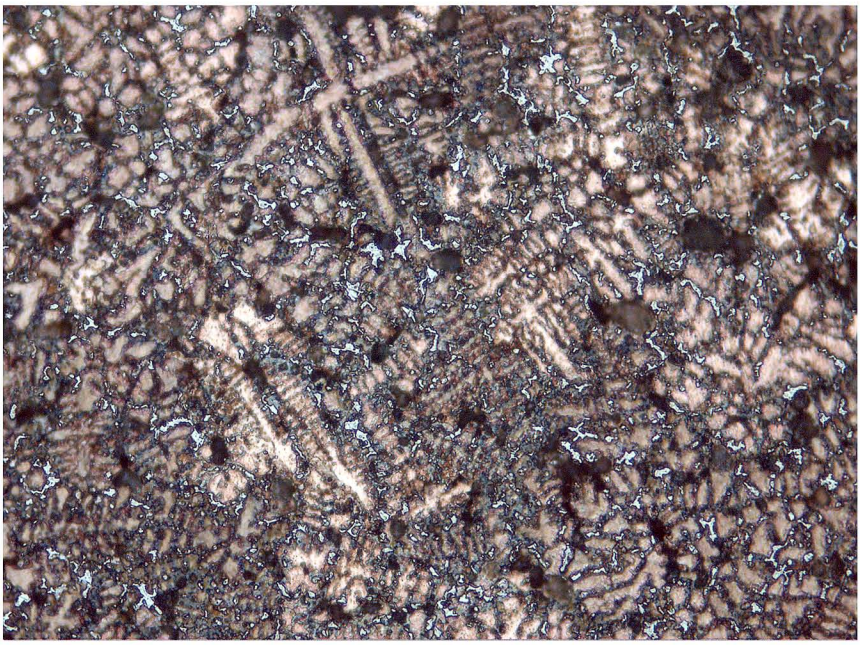

Figure 5.2.2.xi: Serpentine fibula with disc (MIT 5352/Peabody 40-77-40/13555). Longitudinal cross section. Etch: 6 sec potassium dichromate and 3 sec ferric chloride. x500. Microstructural features of interest in the disc include cored dendrites surrounded by pools of fine Cu-Sn eutectoid structures. (MIT Image 5352b-36).

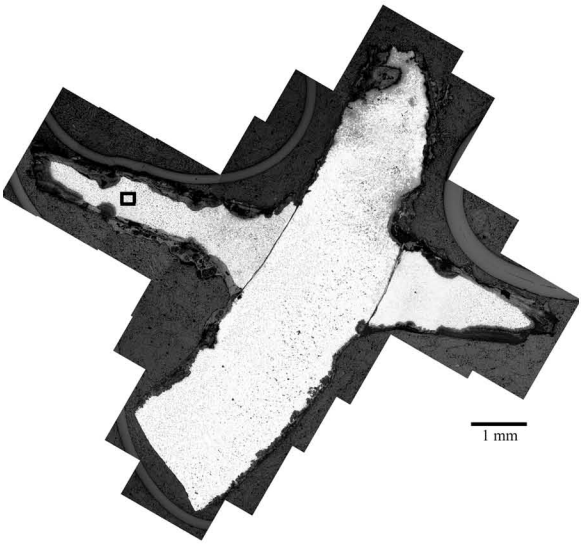

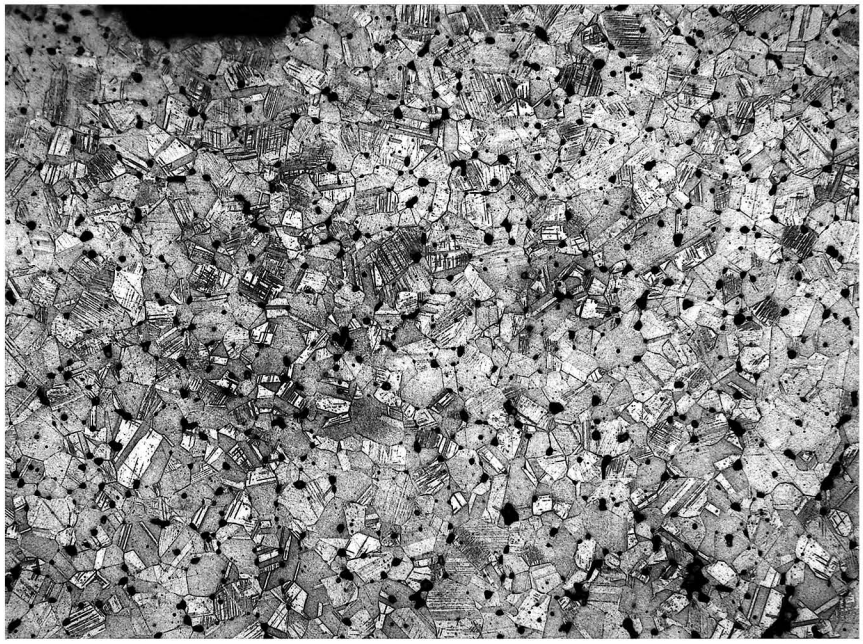

Figure 5.2.2.xii: Serpentine fibula with disc (MIT 5352/Peabody 40-77-40/13555). Longitudinal cross section. Etch: 6 sec potassium dichromate and 3 sec ferric chloride. x100. Microstructural features of interest in the fibula body include equiaxed grains with annealing twins and a medium density of deformation lines. (MIT Image 5352b-35).

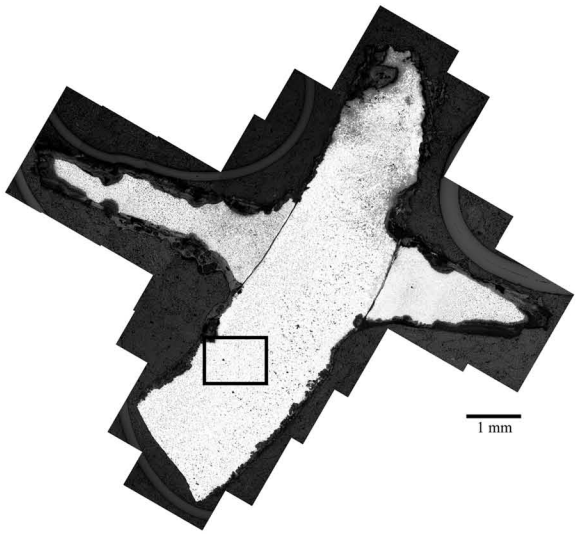

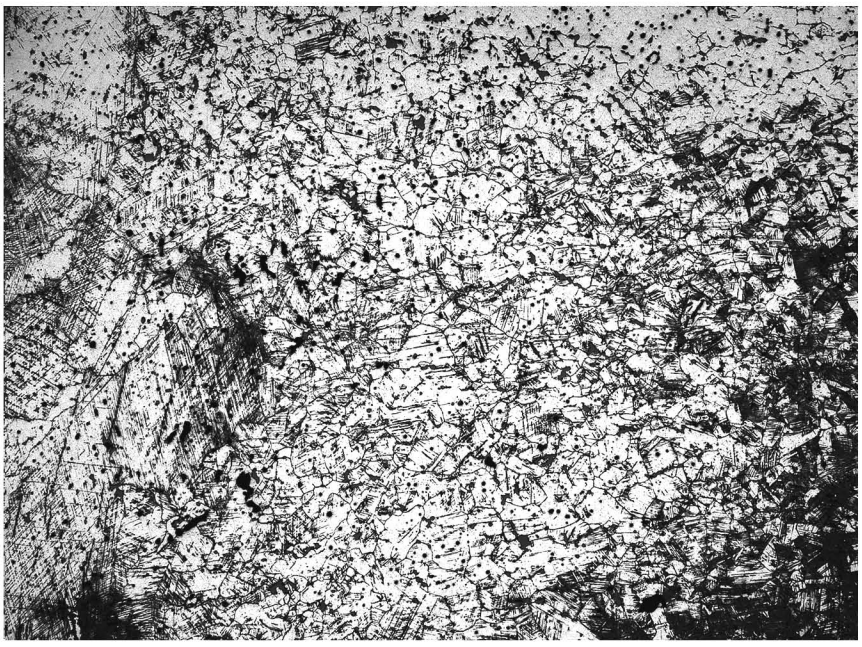

Figure 5.2.2.xiii: Serpentine fibula with disc (MIT 5352/Peabody 40-77-40/13555). Longitudinal cross section, as polished. x100. Microstructural features of interest in the fibula body include the high density of deformation lines in the body of the fibula after the disc. (MIT Image 5352b-31).

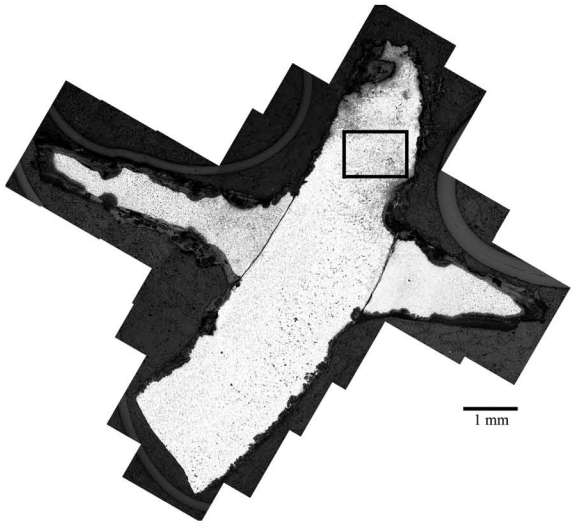

5.2.3: Navicular fibula (MIT 5348/Peabody 40-77-40/13285)

5.2.3a: Provenance and Background

MIT 5348 (Figures 5.2.3.i and 5.2.3.ii) is a fragmented navicular (boat-shaped) fibula from Grave 7 of Tumulus IV (Wells 1981). Grave 7 was 2.6 m long, 0.7 m wide, and was 1.1 m below the surface of the tumulus. Associated grave goods included 176 glass beads, 5 flat bronze beads, and sherds from a brownish-gray bowl.

MIT 5348 is one of five navicular fibulae from the Mecklenburg excavations at Stična.

5.2.3b: Initial Examination and Observations

The navicular fibula was photographed (Figures 5.2.3.i and 5.2.3.ii), drawn to scale, measured, and observed (Figures 5.2.3.iii and 5.2.4.iv).

The navicular fibula consists of two fragments. One fragment contains the fibula's body, and the other fragment contains portions of the fibula's spring and pin. It is not clear how the fibula pin and spring were attached to the fibula bow, although it can be assumed that the pin would have rested in the pin catch.

The fibula's body is made of one single bronze piece weighing 10.1 g. The body consists of a curved bow, which is decorated by two knobs, connected to a pin catch. The top of the pin catch is decorated with incised lines, and the end of the pin catch is adorned with a decorative knob. The bow of the fibula contains an iron rivet (Figure 5.2.3.v). This iron rivet is most likely evidence of a repair, although it could have been part of the original object. Bronze fibulae from other Early Iron Age Slovenian sites like St. Lucia were sometimes crudely repaired with iron rivets (Giumlia-Mair 1995).

The second fragment contains a portion of the fibula's pin and a portion of the coiled spring; this fragment weighs 3.5 g. The pin and spring are made from a single, long, thin piece of bronze 2.1 mm thick. The pin portion of this single bronze piece has a rectangular cross section, and the spring portion has a roughly circular cross section. The pin portion is 55.8 mm long. The coiled spring is oval shaped with a diameter measuring 10.0 mm. The portion of the coiled spring still intact is 10.7 mm wide.

The fragment containing portions of the pin and spring is structurally robust and is covered with a smooth, dark green corrosion product. A few cracks running perpendicular to the pin's longitudinal axis can be seen along the length of the pin.

5.2.3c: Sampling

The fragment containing portions of the fibula's spring and pin was sampled three times (Figure 5.2.3.vi). Sample MIT 5348a was removed from the pin portion for bulk composition analysis. Sample MIT 5348b was removed from the spring portion for metallographic analysis and was mounted longitudinally as noted. Sample MIT 5348c was removed from the pin portion for metallographic analysis and was mounted transversely as noted. The fragment was highly metallic, and the metal was light gold in color.

5.2.3d: Bulk Composition Analysis

Bulk compositional analysis shows that the metal comprising the fibula's spring and pin is a copper-tin alloy with the primary alloying element of tin at a concentration of 12.7 weight percent. The alloy is a high tin bronze. Other minor and trace elements include Pb (0.777%), As (0.375%), Sb (0.304 %), Ni (0.134%), Ag (0.118 %), and Co (0.0099%). Bulk compositional analysis data are shown in Table 5.2.3 and in the Appendix.

Table 5.2.3: Bulk Composition Analysis Data for MIT 5348 (Navicular Fibula Spring)

	Sn	**Pb**	**Sb**	**As**	**Ni**	**Co**	**Ag**	**Fe**
ICP-ES	12.7	0.777	0.304	0.375	0.089	0.008	n.a.	<0.005
INAA	11.4	n.a.	0.280	0.306	0.1340	0.0099	0.118	n.d.

(values in weight %) n.a. = not analyzed n.d. = not determined

5.2.3e: Metallographic Analysis

Sample MIT 5348c was taken from the pin portion of the fragment and was mounted as a transverse cross section. The as-polished cross section shows that the pin has an oval-shaped cross section (Figure 5.2.3.vii). Microstructural features of interest in the transverse cross section include a high density of small porosities homogenously distributed throughout the sample. MIT 5348c was etched for three seconds with

potassium dichromate and for two seconds with aqueous ferric chloride to reveal a microstructure characterized by equiaxed grains with annealing twins and a medium density of deformation lines (Figure 5.2.3.viii).

Sample MIT 5348b was taken from the spring portion of the fragment and was mounted longitudinally. As-polished, the longitudinal sample shows several surface cracks along the interior edge of the spring running perpendicular to the longitudinal axis of the metal (Figure 5.2.3.ix). These cracks are similar to the cracks on the pin portion of the spring noted during the initial examination, and they most likely stem from repeated flexing of the spring and pin. Other microstructural features of interest include a high density of small porosities homogenously distributed throughout the sample and elongated gray copper sulfide inclusions oriented parallel to the longitudinal axis of the metal.

MIT 5348b was etched for three seconds with potassium dichromate and for two seconds with aqueous ferric chloride to reveal a microstructure characterized by equiaxed grains with annealing twins and a high density of deformation lines (Figure 5.2.3.x). The density of deformation lines in the spring is significantly higher than in the pin.

5.2.3f: Discussion

The pin and spring are both made from a single piece of high tin bronze with a tin composition of 12.7 weight percent. It is unclear if lead, present at a concentration of 0.777 weight percent, was purposefully added to the alloy.

The high tin bronze alloy would have made the pin and spring hard but also fairly brittle. The alloy would have given the pin the strength to hold heavy woolen garments in place, but it also would have tended to fatigue and would have been more likely to fracture and break in bending as the fibula was fastened and unfastened. Over time, this repeated flexing of the pin and spring led to the cracks observable in the spring and along the pin.

The metal comprising the pin and coiled spring was originally cast. The metal was then subject to cycles of working and annealing to achieve the desired thickness and shape. After this thickness and shape were achieved, the spring was made by working a portion of the pin into a coil.

The spring and the pin were left in a worked condition. This would have made the pin and spring hard and strong, but it also would have made the metal brittle and more difficult to flex. The spring is more heavily worked than the pin. This may be due to use wear, as the spring would have been stressed more heavily than the pin as the metal was bent when the fibula was fastened and unfastened.

The tin concentration of the navicular fibula's pin and spring is higher than the tin composition of the serpentine fibulae discussed in Sections 5.2.1 and 5.2.2.

5.2.3g: Conclusions

- The pin and spring of the navicular fibula are made from a high tin bronze with a tin composition of 12.7 weight percent. It is unclear if lead, present at a concentration of 0.777 weight percent, was purposefully added to the alloy. The high tin bronze alloy would have made the pin and spring hard but also fairly brittle.
- The metal comprising the pin and spring was originally cast. The pin and spring were then worked to shape and left in a worked condition.
- The fibula was subject to large amounts of use wear that left the spring and pin cracked in some areas.

View A

View B

Figure 5.2.3.i: Navicular fibula, body. (MIT 5348/Peabody 40-77-40/13285). Photograph by E. Cooney.

Figure 5.2.3.ii: Navicular fibula, spring and pin. (MIT 5348/Peabody 40-77-40/13285). The pin is oriented with respect to the fibula bow in View A of Figure 5.2.3.i. Photograph by E. Cooney.

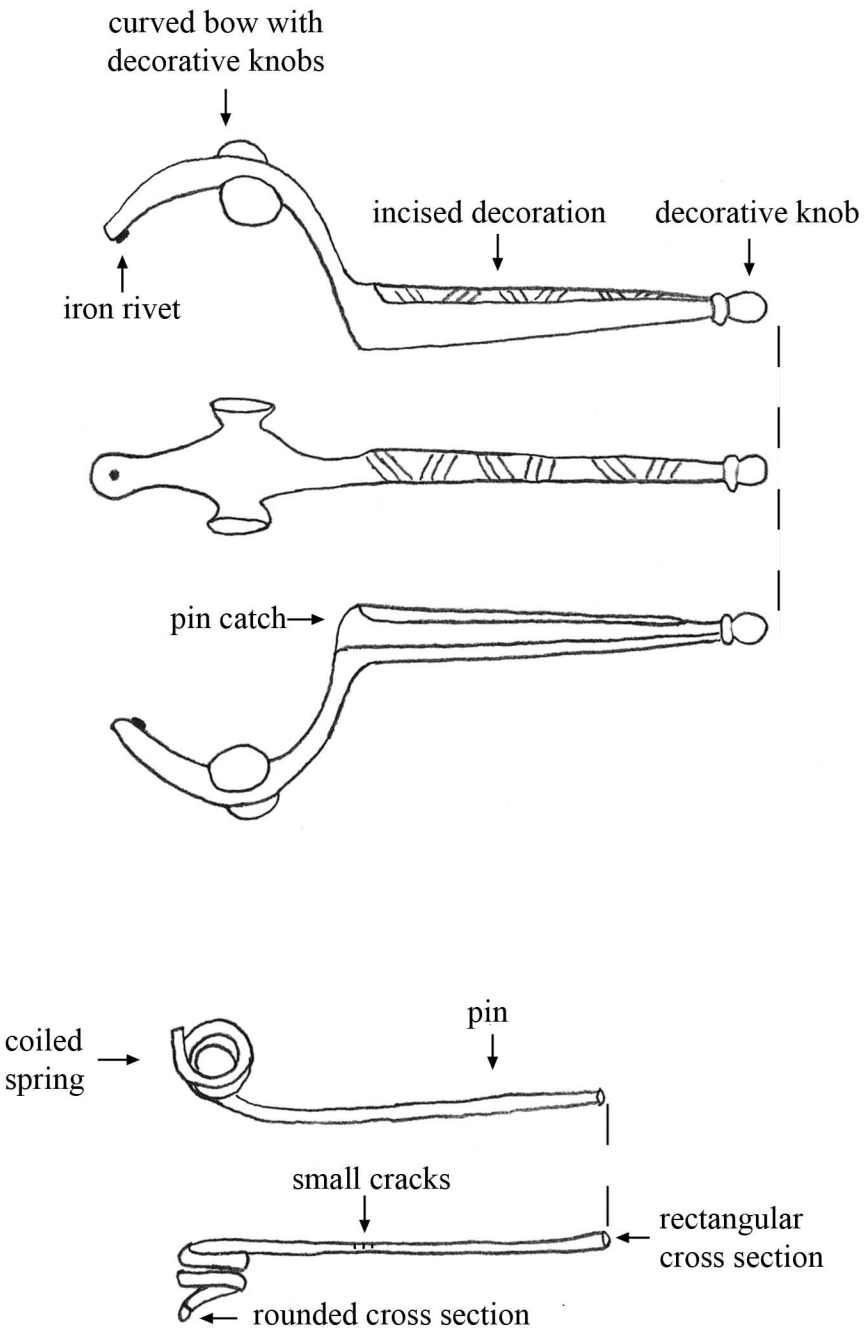

Figure 5.2.3.iii: Navicular Fibula (MIT 5348). Key Object Features.

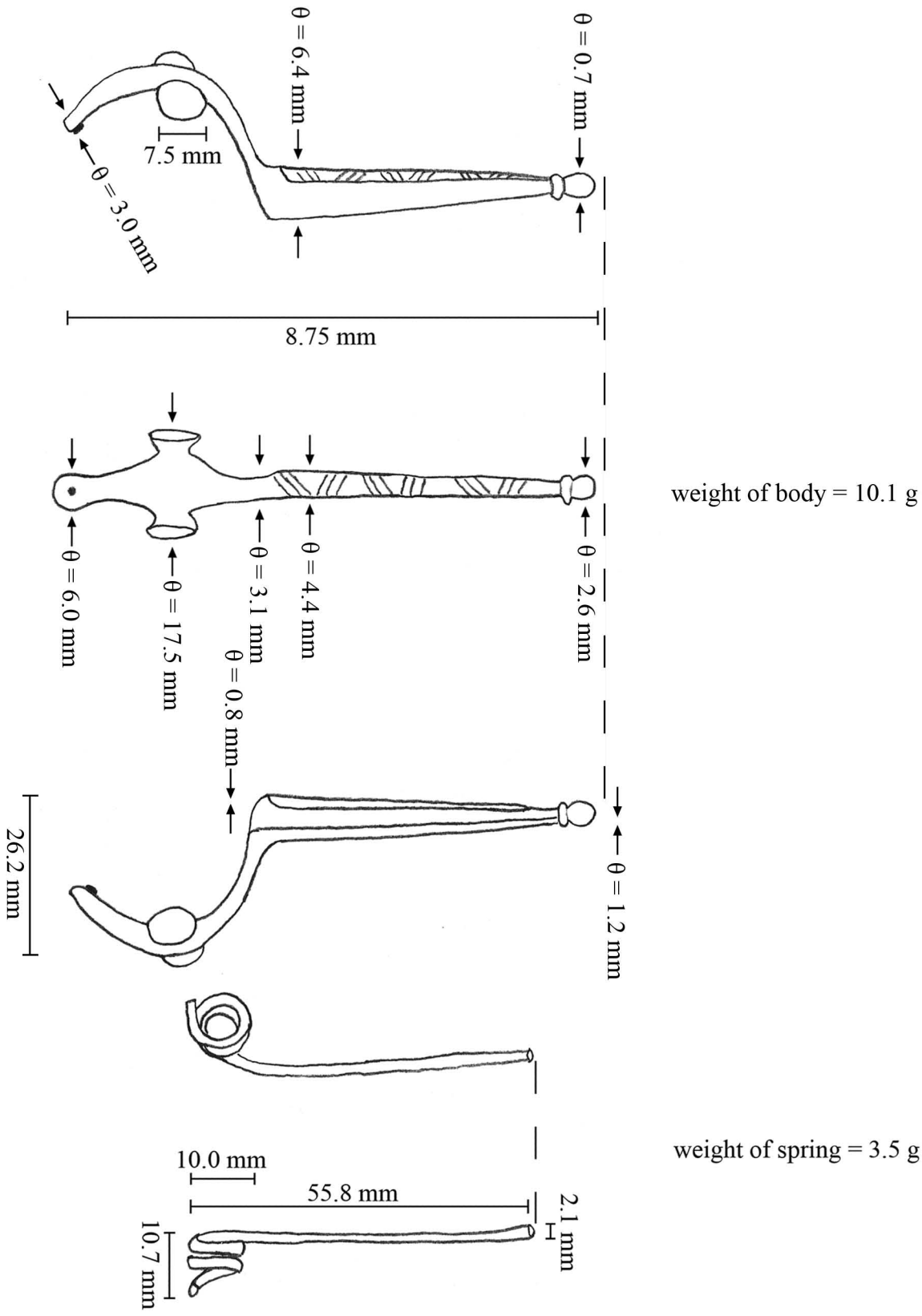

Figure 5.2.3.iv: Navicular fibula (MIT 5348). Drawing and measurements.

Figure 5.2.3.v: Close up of the iron rivet at the tip of the navicular fibula's curved bow. (MIT 5348/Peabody 40-77-40/13285).
Photograph by E. Cooney.

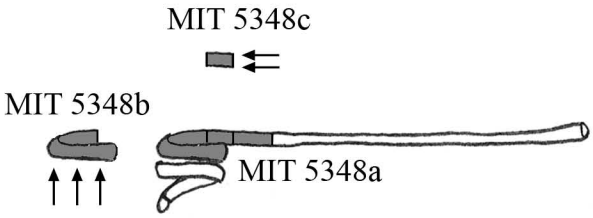

Figure 5.2.3.vi: Samples removed from navicular fibula. Sample MIT 5348a was removed for bulk composition analysis. Sample MIT 5348b was removed for metallographic analysis and was mounted longitudinally as noted. Sample 5348c was removed for metallographic analysis and was mounted transversely as noted.

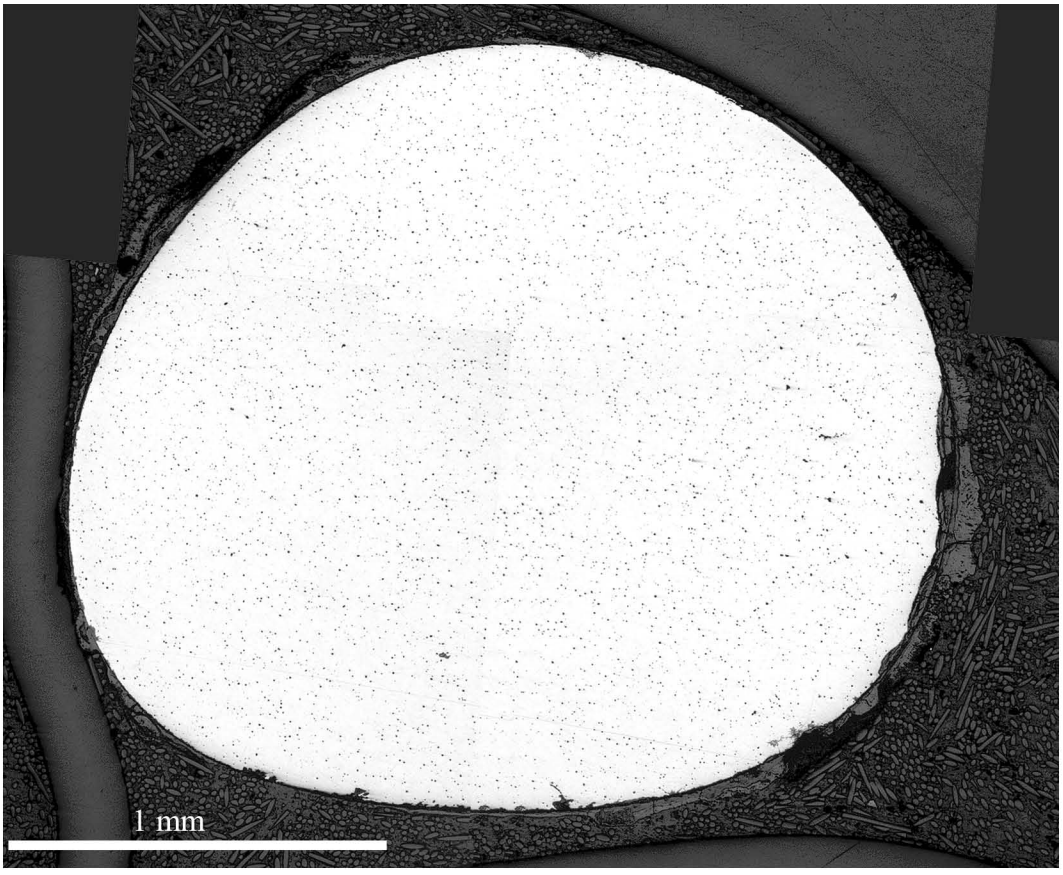

Figure 5.2.3.vii: Navicular fibula (MIT 5348/Peabody 40-77-40/13285). Transverse cross section, as polished. The spring has a roughly circular cross section. Microstructural features of interest include small porosities homogenously disributed throughout the sample. (MIT Images 5348c-01-03).

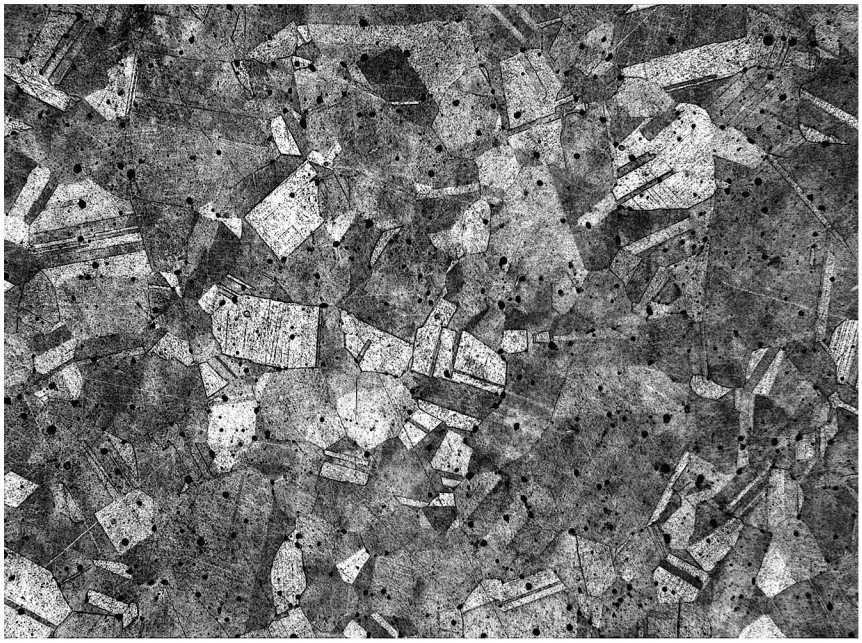

Figure 5.3.2.viii: Navicular fibula (MIT 5348/Peabody 40-77-40/13285). Transverse cross section. Etch: 3 sec potassium dichromate and 2 sec ferric chloride. x200. Microstructural features of interest include equiaxed grains with annealing twins and a medium density of deformation lines. (MIT Image 5348c-07).

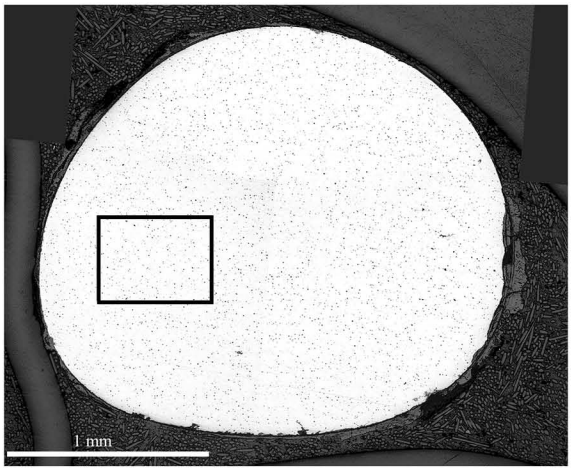

Figure 5.2.3.ix: Navicular fibula (MIT 5348/Peabody 40-77-40/13285). Longitudinal cross section, as polished. The longitudinal cross section shows that the metal has been coiled into an oval-shaped spring. Microstructural features of interest include small porosities homogenously distributed throughout the sample, elongated gray copper sulfide inclusions oriented parallel to the longitudinal axis, and a few surface cracks perpendicular to the longitudinal axis. These cracks most likely stem from repeated flexing of the spring (MIT Images 5348b-01-29).

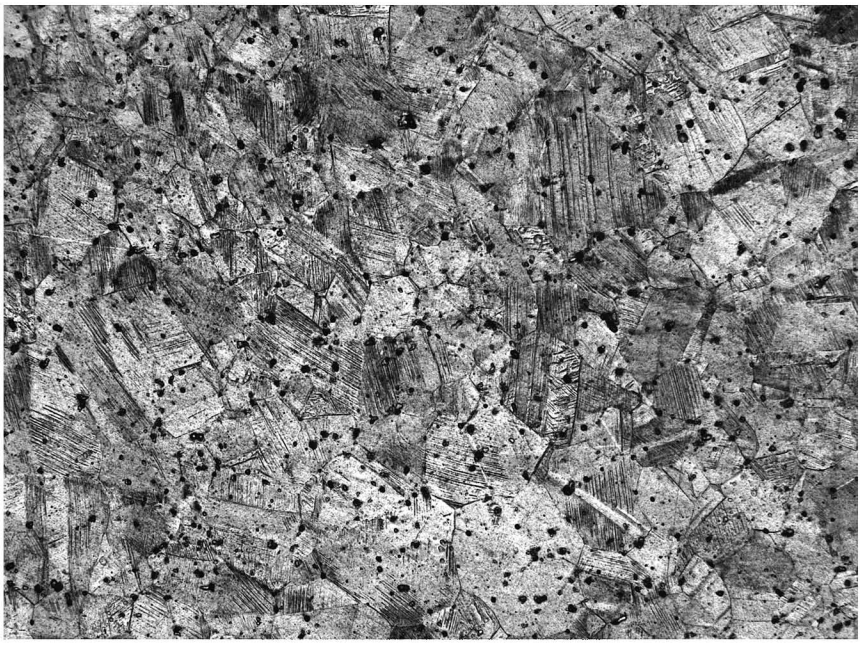

50 microns

Figure 5.3.2.x: Navicular fibula (MIT 5348/Peabody 40-77-40/13285). Longitudinal cross section. Etch: 3 sec potassium dichromate and 2 sec ferric chloride. x200. Microstructural features of interest include equiaxed grains with annealing twins and a high density of deformation lines. (MIT Image 5348b-33).

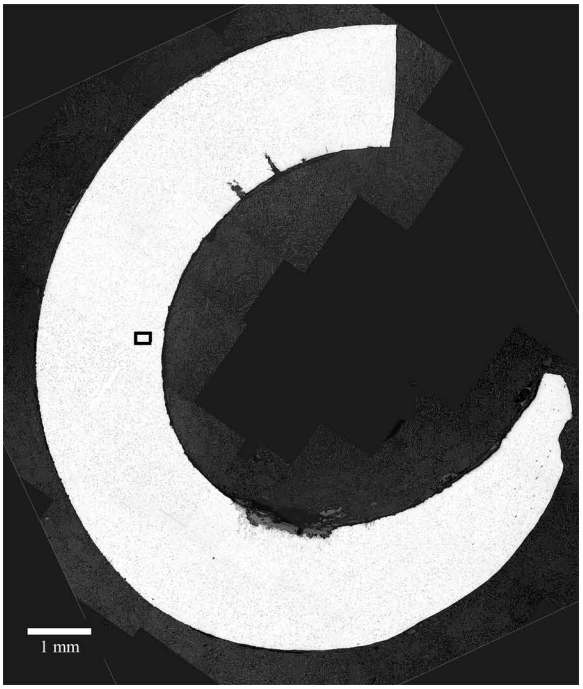

5.2.4: Knobbed fibula (MIT 5331/Peabody 40-77-40/13345)

5.2.4a: Provenance and Background

MIT 5331 (Figure 5.4.1.i) is identified by Wells (1981) as the "bow of a bronze fibula with a knob on top." It comes from Grave 17, which consists of a burned layer of earth 2.1 m below the surface of Tumulus IV. No skeletal remains are recorded.

Associated grave goods include a fragment of a serpentine fibula with disc, three fragmentary fibula springs (see section 5.2.5), fragments of a thin bronze ring, identified by the excavators as earrings, and twenty amber beads.

This knobbed fibula fragment is too fragmentary to assign to a specific fibula type. It is very likely that this fragment of fibula bow was originally part of the same fibula as the springs found in association with it.

5.2.4b: Initial Examination and Observations

The knobbed fibula bow was photographed (Figure 5.2.4.i), drawn to scale, measured, and observed (Figures 5.2.4.ii and 5.2.4.iii).

The surviving object consists of the bow of a fibula. The bow is decorated with a cone-shaped knob and with incised lines. The fragment is 34.0 mm in length. The knob is 5.0 mm tall and is 3.8 mm in diameter at its widest point. Under low magnification a small circular indentation can be seen on top of the knob. Incised lines perpendicular to the longitudinal axis of the bow separate a flared portion of the bow 10.7 mm wide from the thinner body of the fibula which is 4.0 mm wide at one fragmented end and 4.6 mm wide at the other fragmented end. The thickness of the bow ranges from 2.3 mm at one fragmented end to 0.6 mm at the other fragmented end. The fragment weighs 2.0 g.

The surviving fragment is fairly fragile. Although the knob and the main body appear to be structurally robust, the thin sheet 0.6 mm thick appears to be completely mineralized. The fibula is covered with a thick layer of smooth corrosion product that is mottled dark green and brown in color. A portion of the fibula has been cleaned of this layer of corrosion, revealing a layer of light green, friable corrosion product beneath. No evidence of manufacture or use wear is readily apparent.

5.2.4c: Sampling

One sample (sample MIT 5331) was removed from the fibula with transverse cuts (Figure 5.2.4.iv) for bulk compositional analysis. The fibula is fairly metallic and the metal is highly light gold in color.

5.2.4d: Bulk Compositional Analysis

Bulk compositional analysis shows that the fibula's body is made from a copper-tin-lead alloy with tin present at a concentration of 11.2 weight percent and lead at a concentration of 1.66 weight percent. The alloy is a tin bronze. Other major and minor elements include As (0.157%), Sb (0.053%), Ni (0.048%), Ag (0.020 %), Co (0.0192%) and Fe (0.13%). This alloy composition is similar to the compositions of the serpentine fibulae MIT 5330 and MIT 5352 discussed in sections 5.2.1 and 5.2.2. Bulk compositional analysis data are shown below in Table 5.2.4 and in the Appendix.

Table 5.2.4: Bulk Compositional Analysis Data for MIT 5331

	Sn	**Pb**	**Sb**	**As**	**Ni**	**Co**	**Ag**	**Fe**
ICP-ES	11.2	1.66	0.053	0.157	0.023	0.015	n.a.	0.007
INAA	10.5	n.a.	0.033	0.143	0.048	0.0192	0.020	0.13

(values in weight %) n.a. = not analyzed n.d. = not determined

5.2.4e: Conclusions

- The knobbed fibula bow is too fragmented to assign to a particular fibula type.
- The knobbed fibula bow may have originally been part of the same object as the fibula springs examined in section 5.2.5.
- The knobbed fibula bow is a leaded tin bronze with 11.2 weight percent Sn and 1.66 weight percent Pb.
- This alloy composition mirrors those of the serpentine fibulae from Tumulus IV examined in Sections 5.2.1 and 5.2.2, even though the knobbed fibula is from a different fibula typeset.

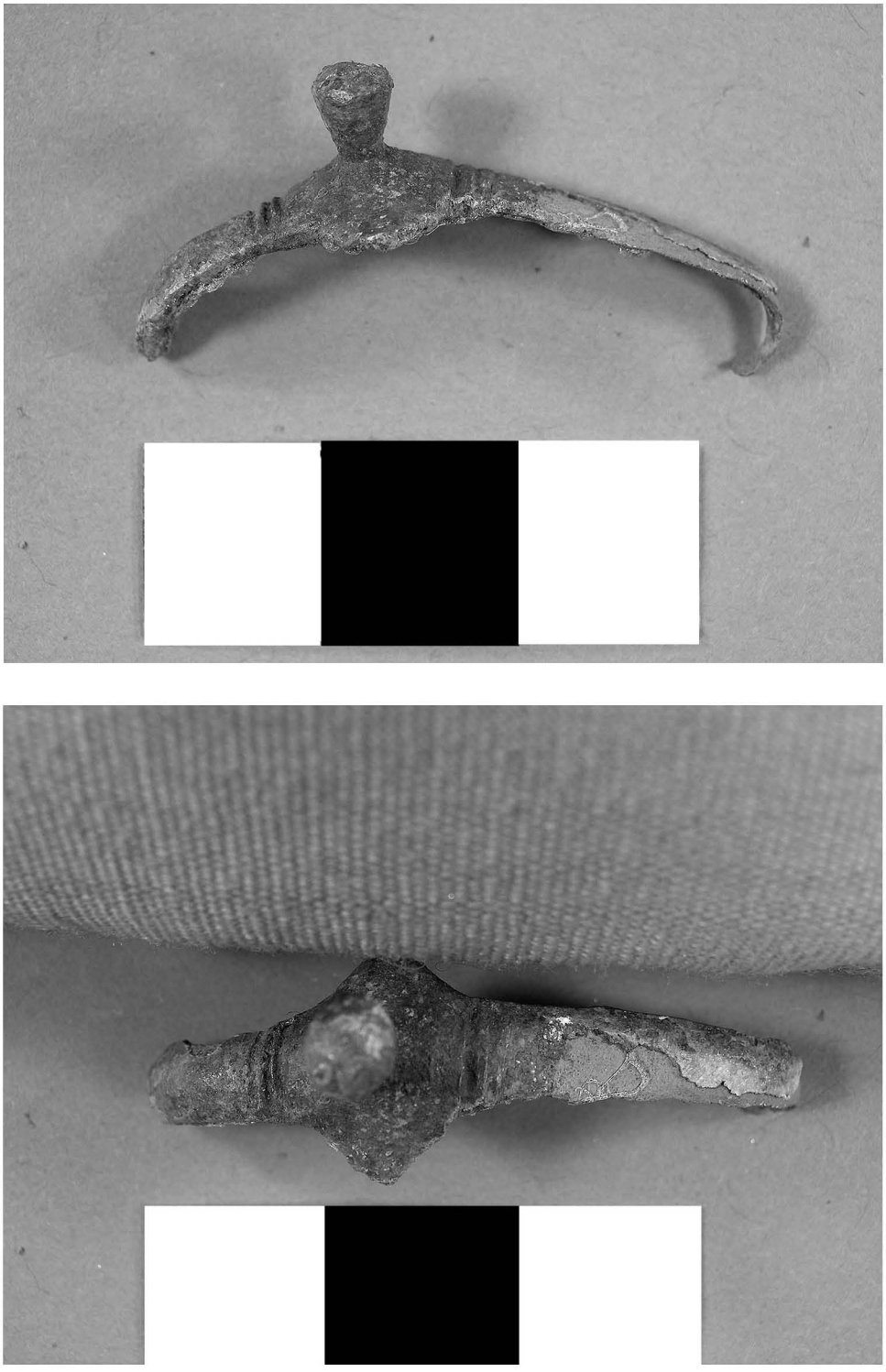

Figure 5.2.4.i: Knobbed fibula (MIT 5331/Peabody 40-77-40/13345). Photographs by E. Cooney.

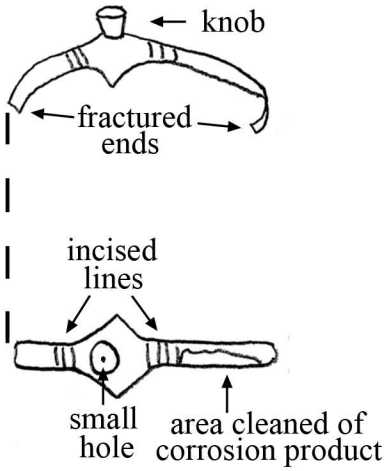

Figure 5.2.4.ii: Knobbed fibula (MIT 5331). Key object features

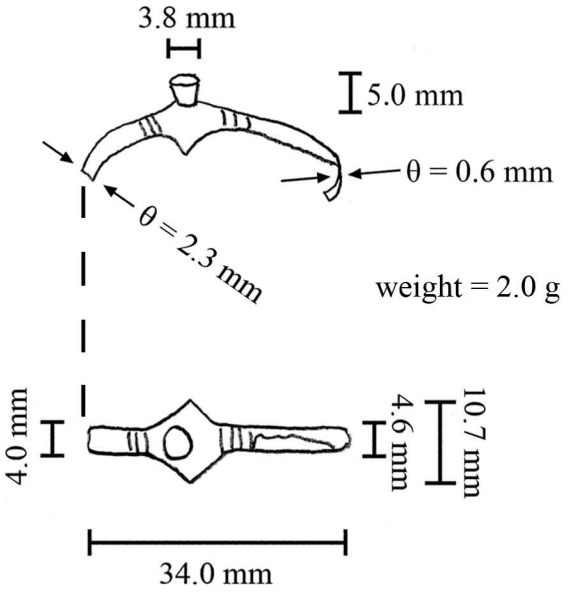

Figure 5.2.4.iii: Knobbed fibula (MIT 5331). Drawing and measurements.

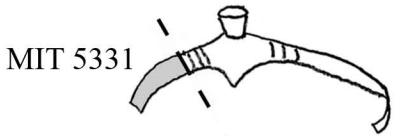

Figure 5.2.4.iv: Knobbed fibula (MIT 5331). Sample MIT 5331 was removed for bulk compositional analysis.

5.2.5: Fibula Springs (MIT 5332/Peabody 40-77-40/13346)

5.2.5a: Provenance and Background

MIT 5332 (Figure 5.2.5.i) is identified by Wells (1981) as "fragmentary springs from fibulae." These three spring fragments come from Grave 17 and are associated with the knobbed fibula discussed in Section 5.2.4. It is very likely that these spring fragments and the knobbed fibula bow were originally part of the same fibula.

Grave 17 consists of a burned layer of earth 2.1 m below the surface of Tumulus IV. No skeletal remains are recorded. Additional grave goods include a fragment of a serpentine fibula with disc, fragments of a thin bronze ring, identified by the excavators as earrings, and twenty amber beads.

5.2.5b: Initial Examination and Observations

The spring fragments were photographed (Figure 5.2.5.i), drawn to scale, measured, and observed (Figures 5.2.5.ii and 5.2.4.iii).

MIT 5332 includes three spring fragments. Each fragment consists of a thin strip of metal bent multiple times into a cylindrical column or coil.

Fragment A is 20.6 mm long and weighs 2.3 g. The diameter of the spring tapers from 7.3 mm at its widest point to 5.6 mm at its narrowest point. The metal strip making up the spring is 3.3 mm wide. At the spring's wider end the strip extends straight away from the spring.

Fragment B is 16.0 mm long and weighs 1.3 g. The diameter of the spring tapers from 6.0 mm to 5.7 mm. The metal strip making up the spring is 2.7 mm wide.

Fragment C is 11.9 mm long and weighs 0.7 g. Its diameter measures 5.7 mm and the metal strip making up the spring is 1.7 mm wide.

All the fragments are structurally robust. Fragment A is covered by a thick layer of dark green, smooth corrosion product. This corrosion product has been chipped away in some areas to reveal a lighter green, friable layer of corrosion product. The outer layer of corrosion has been cleaned from Fragment B. Fragment B is covered by an inner layer of light green corrosion product. In this corrosion product clusters of a secondary material can be seen. This secondary material is dark gray and is elongated parallel to the

longitudinal axis of the metal strip making the spring. Fragment C has been entirely cleaned of all external layers of corrosion product. It is dark in color, most likely because its metallic surface has been oxidized. Under magnification the same secondary material seen in Fragment B can be seen in Fragment C, aligned in the same way with the longitudinal axis of the metal strip.

5.2.5c: Sampling

One sample (sample MIT 5332) was removed from Fragment C (Figure 5.2.5.iv) for bulk compositional analysis. The spring is metallic and the metal is highly light gold in color.

5.3.5d: Bulk Compositional Analysis

Bulk compositional analysis shows that the fibula spring's body is made from a copper-tin-lead alloy with tin present at a concentration of 12.1 weight percent and lead present at a concentration of 5.22 weight percent. The alloy is a leaded tin bronze. Other major and minor elements include Ag (0.485%), Fe (0.25%), Sb (0.232%), As (0.219%), Ni (0.148%), and Co (0.009%). Bulk compositional analysis data are shown below in Table 5.2.5 and in the Appendix.

Table 5.2.5: Bulk Compositional Analysis Data for MIT 5332

	Sn	**Pb**	**Sb**	**As**	**Ni**	**Co**	**Ag**	**Fe**
ICP-ES	12.1	5.22	0.232	0.219	0.145	0.009	n.a.	0.01
INAA	9.27	n.a.	0.185	0.155	0.148	0.009	0.485	0.25

(values in weight %) n.a. = not analyzed n.d. = not determined

5.2.5e: Conclusions

- The spring fragments may originally have been part of the same fibula as the knobbed fibula bow discussed in section 5.2.4.
- The springs are made of a leaded tin bronze alloy with a composition of approximately 12 weight percent tin and 5 weight percent lead. This alloy has a higher tin content and a much higher lead content than that of the knobbed fibula. This suggests two alternate hypotheses: 1) The knobbed fibula and fragmented springs were originally part of one object. They were made separately and were

put together mechanically to form the final object in the same fashion as certosa and leech fibulae, or 2) the knobbed fibula and fragmented springs are from two separate objects.

- The high lead content coupled with the high tin content indicates that the springs were not designed to function elastically as springs. The high tin content makes the springs hard and reduces their elasticity. The high level of lead would have adversely affected any mechanical properties of the alloy such as hardness and elasticity. This suggests that the springs served a decorative function.
- The high tin content of the springs coupled with the high lead content indicate that the springs may have been made from melted down, recycled scrap bronze.
- The dark inclusions aligned in clusters and elongated parallel to the longitudinal axis of the sheet metal used to make the springs indicate that the metal comprising the springs was heavily worked before being coiled into its final shape as a spring.

Figure 5.2.5.i: Fibula spring (MIT 5332/Peabody 40-77-40/13346). Photograph by E. Cooney.

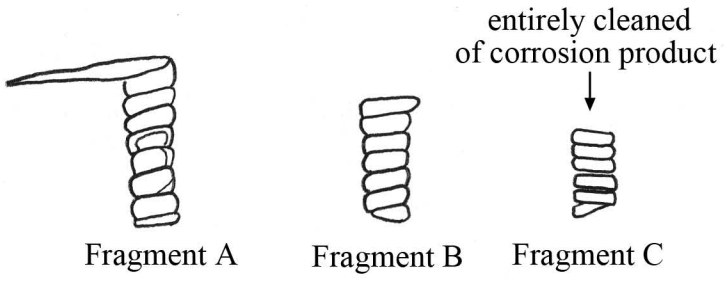

Figure 5.2.5.ii: Fibula spring (MIT 5332). Key object features.

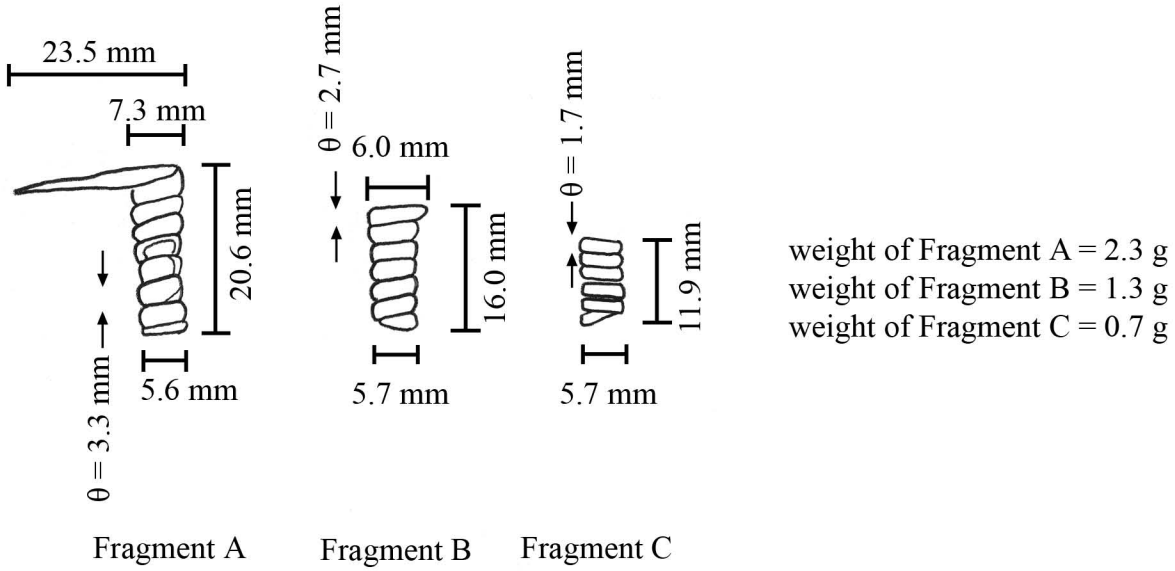

Figure 5.2.5.iii: Fibula spring (MIT 5332). Drawing and measurements.

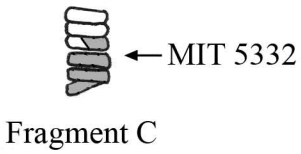

Figure 5.2.5.iv: Fibula spring (MIT 5332). Sample MIT 5332 was removed for compositional analysis.

5.2.6: Additional Fibula Types

5.2.6a: Dragon Fibula (Peabody 40-77-40/13447)

One example of a dragon fibula comes from Grave 32 of Tumulus IV (Figure 5.2.6.i). Wells describes this fibula as serpentine (1981:63, 178), but the Peabody Museum identifies it as a dragon fibula, and it more closely resembles dragon fibulae from other Early Iron Age sites than it does serpentine fibulae.

The dragon fibula's body has the characteristic saddle shaped bend and curved bow of a serpentine fibula, but it also has decorative items attached to its body. A tiny bird figurine, complete with incised wings, is riveted onto the fibula's bow. Also attached to the bow are four decorative horns (also called antennae) with large bulbous knobs. Two of these horns are attached with rivets, which can be seen clearly where one of the horns has broken off from the body (Figure 5.2.6.i). The front set of horns appears to be cast onto the body of the fibula. In addition to these decorative items, a large, incised fold stopper sits at the point where the pin and the bow of the fibula meet.

This dragon fibula's decorative horns and their attachment to the body of the fibula by means of rivets and casting closely resemble the dragon fibulae from St. Lucia (Guimlia-Mair 1995:65). Similar birds to the one found on this fibula are a recurring motif on other large bronze jewelry items such as fibulae and pendants from Stična and the other Slovenian Iron Age sites represented in the Mecklenburg collection.

The uniqueness of this dragon fibula in Tumulus IV is mirrored by the richness of the grave in which it was found. In addition to this dragon fibula, Grave 32 contained 190 amber beads, ear pendants, two earrings made of bronze wire, bronze spirals from a second set of earrings, a second *blumen* fibula, now missing, a small bronze ring, and a belt plate attachment. The belt attachment is discussed in Section 5.3.2, the bronze wire in Section 5.4.4, and the spirals in Section 5.4.5.

5.2.6b: Zoomorphic fibula (Peabody 40-77-40/13299)

One example of a zoomorphic fibula comes from Grave 10 of Tumulus IV (Figure 5.2.6.ii) Wells (1981: 57, 166). This fibula is of crossbow construction, meaning that the body of the fibula and the pin are mechanically put together and that the bow of

the fibula is perpendicular to the axle which holds the fibula's spring and the pin. The body of the fibula is completely intact, and the axle and spring are fragmented. The axle would have been placed perpendicular to the body of the fibula through the hole at the end of the bow, and there would have been a spring on either side of the axle for decorative effect. Similar fibulae with cross bow construction are found at Stična and at St. Lucia. If the knobbed fibula bow and the springs discussed in Sections 5.2.4 and 5.2.5 were indeed from the same fibula, it most likely was of crossbow construction.

The body of the fibula is decorated with a bronze animal head, most likely representing a deer. Zoomorphic representations of deer and horses are common motifs in large bronze jewelry items such as fibulae and pendants from Stična and the other Slovenian Iron Age sites represented in the Mecklenburg collection.

In addition to the zoomorphic fibula, Grave 10 also contained fragments of a belt plate with rivets and hooks, discussed in Section 5.3.1, an iron knife, and sherds of grayish-tan pottery.

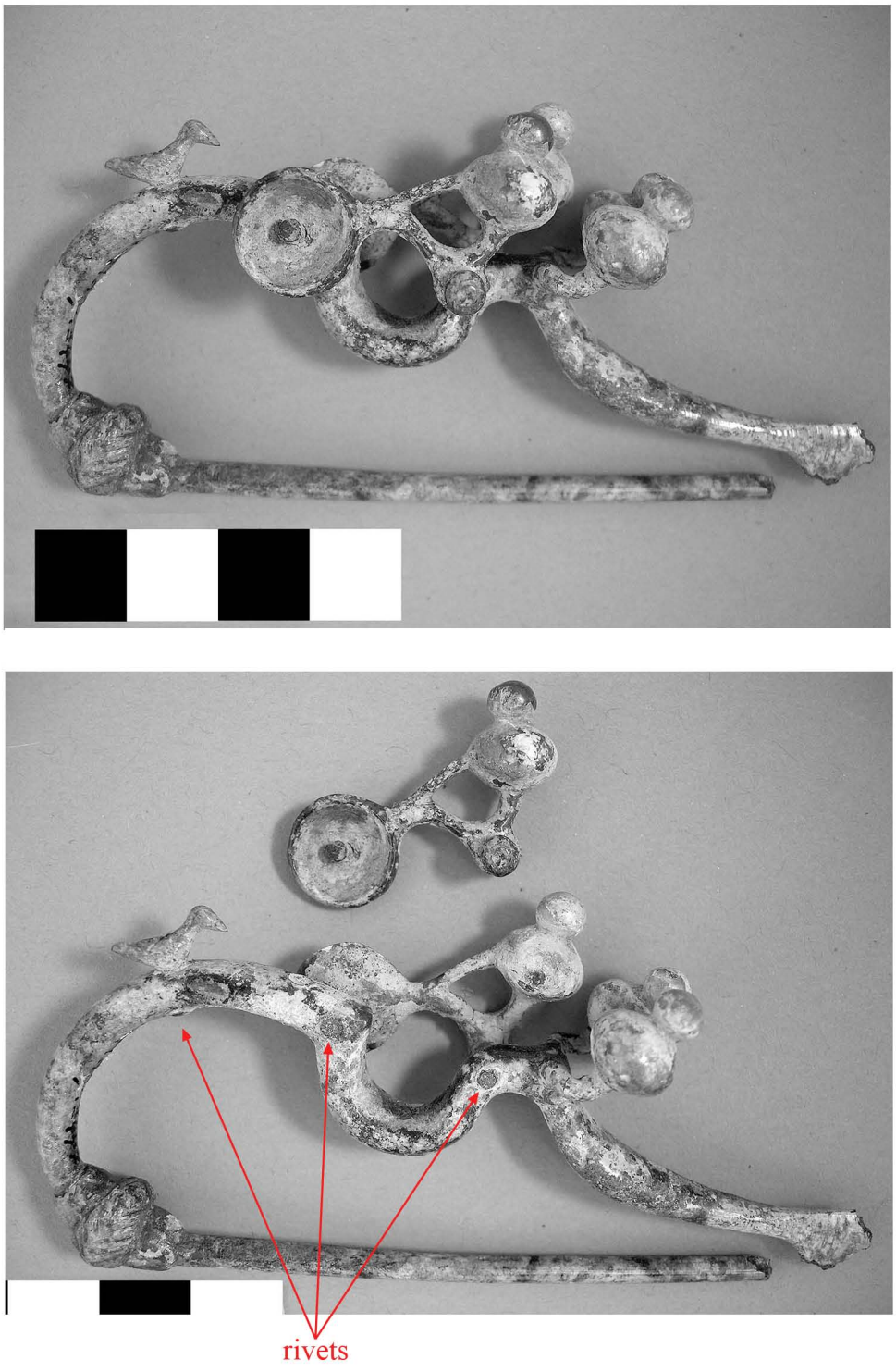

Figure 5.2.6.i: Dragon fibula (serpentine fibula with birds). (Peabody 40-77-40/13447).
Above: View with decorative horns *in situ.*
Below: View showing the rivets which attach the decorative horns to the body of the fibula. The rivet attaching the bird figure to the fibula can also be seen.

Figure 5.2.6.ii: Zoomorphic fibula. (Peabody 40-77-40/13299).
Photograph by E. Cooney.

5.3: Belt Plates and Attachments: Sheet, Rivets, Hooks, and Rings

After bronze rings and fibulae, the most prevalent types of bronze objects at Stična are belt plates and attachments. The belt plates consist of bronze sheet(s) held together mechanically by bronze rivets. Belt attachments are usually various shapes and sizes of bronze hooks, rings, and other attachments. The surviving plates and attachments are usually highly fragmentary. What remains of an object may consist of only small fragments of bronze plate and loose rivets. Six of the 50 reliable graves in Tumulus IV contain fragments of one or more bronze belt plates with bronze attachments. At least 39 objects comprising belt plates and various belt attachments come from the Mecklenburg excavations at Stična.

Four bronze objects from belt plate and attachment assemblages were analyzed for this study: a loose rivet (Section 5.3.1), a sheet metal belt attachment with a rivet *in situ* (Section 5.3.2), a hook belt attachment (Section 5.3.3), and a segmented ring belt attachment (Section 5.3.4). Several additional belt plates and attachments not sampled for analysis are shown in Section 5.3.5.

The loose rivet, sheet metal belt attachment, and the segmented ring belt attachment were all sampled for both bulk compositional analysis and for metallographic analysis. The hook was sampled only for bulk compositional analysis.

5.3.1: Rivets (MIT 5343/Peabody 40-77-40/13300)

5.3.1a: Provenance and Background

MIT 5343 (Figure 5.3.1.i) is part of at least one fragmented belt plate from Grave 10 of Tumulus IV (Wells 1981). In addition to the two rivets and the fragment of sheet metal shown in Figure 5.3.1.i, there are several small fragments of sheet metal, fragments of sheet metal with attached rivets, loose rivets, a fragmentary bronze ring attachment (MIT 5350, discussed in Section 5.3.4), a hollow hook/loop attachment, and an iron hook attachment (discussed in Section 5.3.6) associated with the belt plate. The sheet metal was too mineralized for analysis.

Grave 10 was found at a depth 0.45 m below the surface of the tumulus. There were several fragments of burnt bone found in association with the fragmented belt plate. In addition to the belt plate, associated grave goods included the zoomorphic fibula discussed in Section 5.2.6 and several sherds of grayish-tan pottery.

Although MIT 5343 was found in a context associated with burning, it was subject to metallographic analysis in order to provide a comparison between an *in situ* rivet such as the one examined in Section 5.3.2 and a loose rivet. There are well over 50 rivets of various shapes and sizes associated with belt plates, either loose or attached to sheet metal, in Tumulus IV. There were no loose rivets associated with any graves in which no evidence of burning was recorded.

5.3.1b: Initial Examination and Observations

The rivets were photographed (Figure 5.3.1.i), drawn to scale, measured, and observed (Figures 5.1.3.ii and 5.1.3.iii).

Two rivets are loose, but the small bits of fragmentary sheet metal still adhering to the stem of each rivet indicate that they were once attached to the sheet metal of a belt plate. Both rivets have large, bulbous heads and much thinner stems. Both the heads and the stems have circular cross sections.

Rivet A is 12.4 mm high. Its head is 7.1 mm high and has a diameter of 10.0 mm. Its stem is 5.3 mm high and has a diameter of 3.4 mm. It weighs 2.7 g. Rivet B is 12.2

mm high. Its head is 6.2 mm high and has a diameter of 9.6 mm. Its stem is 6.0 mm high and has a diameter of 3.8 mm. It weighs 2.5 g.

Both rivets are heavy and appear to be structurally robust. They are covered with a very thick layer of friable dark and light mottled green corrosion product. In areas this corrosion product has been chipped away, revealing a lighter green, friable corrosion product beneath. The fragments of sheet metal attached to the stems are completely mineralized and highly fragile. They appear to be adhering to the rivets' external corrosion product.

5.3.1c: Sampling

Rivet A was sampled for bulk compositional analysis. Its head was removed and identified as sample MIT 5343a (Figure 5.3.1.iv). Rivet B was sampled for metallographic analysis and analysis with the electron microbeam probe. It was taken in its entirety as sample MIT 5343b (Figure 5.3.1.iv). It was mounted longitudinally as indicated and was subsequently ground down until the center plane of the rivet was exposed.

5.3.1d: Bulk Composition Analysis

Bulk composition analysis shows that the rivet is made from a copper-lead-tin ternary alloy with lead present at a concentration of 14.4 weight percent and tin present at a concentration of 5.12 weight percent. The alloy is a highly leaded tin bronze. Other major and minor elements include As (1.06%), Sb (0.849%), Ni (0.397%), Ag (0.282%), Co (0.018%) and Fe (0.057%). Bulk composition analysis data are shown below in Table 5.3.1 and in the Appendix.

Table 5.3.1: Bulk Composition Analysis Data for MIT 5343 (Rivets)

	Sn	**Pb**	**Sb**	**As**	**Ni**	**Co**	**Ag**	**Fe**
ICP-ES	5.12	14.4	0.849	1.06	0.267	0.018	n.a.	0.057
INAA	3.91	n.a.	0.695	0.723	0.397	0.0147	0.282	n.d.

(values in weight %) n.a. = not analyzed n.d. = not determined

5.3.1e: Metallographic and Electron Microbeam Probe Analyses

MIT 5343b was mounted as a longitudinal section and was subsequently ground down until the center plane of the rivet was exposed.

As-polished, the entire longitudinal cross section of the rivet can be seen in Figure 5.1.3.v. The rivet is filled with dark inclusions and porosities, and these inclusions and porosities appear to outline dendritic structures. A few outlines of primary dendrites can be seen outlined in this way in the as-polished sample. A large center line porosity can be seen just below where the head and stem of the fibula meet. This was most likely caused by shrinkage of the metal during the casting process. The center line porosity and the dendrites outlined by the porosities indicate that the rivet was cast to shape and was not subsequently heavily worked.

The surface outline of the external corrosion product surrounding the still-metallic portion of the rivet indicates the original shape of the rivet. The external corrosion shows that the head of the rivet was quite angular, with the peak of the rivet coming to a cone-shaped point. The outline of the external surface of the rivet head shows several angular facets left by the blows of a hammer, but overall the surface configuration does not seem to indicate that the rivet was heavily hammered or otherwise deformed during attachment to the sheet metal, other than that the base of the stem appears to bulge slightly. The rivet metal must have been fairly soft and deformed readily with modest amounts of working.

MIT 5343b was analyzed with an electron microbeam probe to determine if the dark inclusions were mainly lead inclusions or porosities. Backscattered electron images and EDS spectra show that the majority of the dark material in the as-polished photomicrograph (Figure 5.3.1.v) is lead (Figures 5.3.1.vi and 5.3.1.vii). The lead, which appears bright in the backscattered images, appears to be filling porosities along the interdendritic spaces of the original casting. A few copper sulfide inclusions are also present.

MIT 5343b was etched for 6 seconds with potassium dichromate and for 2 seconds with aqueous ferric chloride. The etchants revealed a microstructure characterized by equiaxed grains with annealing twins (Figure 5.3.1.vii). A few deformation lines were observed near the base of the rivet's stem (Figure 5.3.1.ix). The high level of lead and additional minor elements in the alloy made etching difficult, so it

is unclear if the light density of deformation lines is limited to this area or if deformation lines are prevalent throughout the sample.

The equiaxed grains and annealing twins show that the rivet was annealed, but because this rivet was found associated with burnt bones this microstructure may stem from the heat of the crematory fire.

5.3.1f: Discussion

The rivet studied by metallography was likely cast to shape, and then lightly worked to even out the angular bends of its head and stem and in subsequent hammering through the beltplate.

The rivets contain a high concentration of lead (approximately 14 weight %) and a low concentration of tin (approximately 5 weight percent). This choice of alloy reflects the function of the rivet as a cast component of a belt plate. The rivet did not need to serve a mechanical purpose beyond either holding two pieces of sheet together and/or serving as a decorative detail. The lead was most likely used as a "filler" material. The metal used to make the rivet may have been recycled scrap bronze as the rivet's alloy did not need to be carefully monitored, but the high concentration of lead was probably deliberate.

The composition of the rivet also would have made it fairly soft. This may have helped attach it to sheet metal without damaging the sheet metal in the process. It also may have helped the smith to reshape the rivet's head if it were deformed while hammering it into place. The rivet's base bulges slightly, which likely occurred during hammering through the sheet metal to keep it in place.

The microstructure's equiaxed grains and annealing twins may be the product of recrystallization due to heating in a crematory fire.

Similar rivets and cast components of sheet metal vessels at St. Lucia are made of leaded bronze and do not exhibit any regular pattern of alloy composition, indicating that they may have been made using recycled bronze scrap. The amount of lead present in MIT 5343, however, is higher than the lead compositions reported for similar rivets and cast parts at St. Lucia (Giumlia-Mair 1995).

5.3.1g: Conclusions

- The rivet was roughly cast to shape and it was subject to light working to refined the shape and as it was hammered through the belt plate sheet metal.
- The high concentration of lead (about 14 weight percent) and low concentration of tin (about 5 weight percent) indicate that the alloy comprising the rivet is likely a mixture of scrap bronze and “filler” lead.
- The rivet did not serve a mechanical function beyond holding sheet together and/or serving as a decorative item. Its relative softness may have helped to minimize damage to the sheet metal when hammered into place on the belt plate.

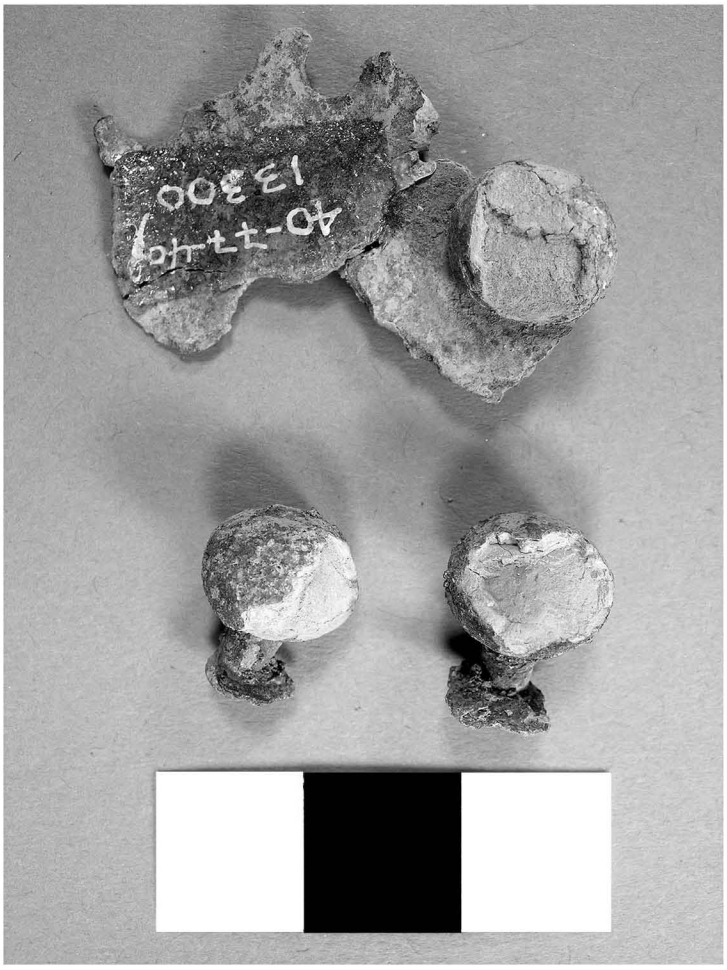

Figure 5.3.1.i: Rivets. (MIT 5343/Peabody 40-77-40/13300).
Photograph by E. Cooney

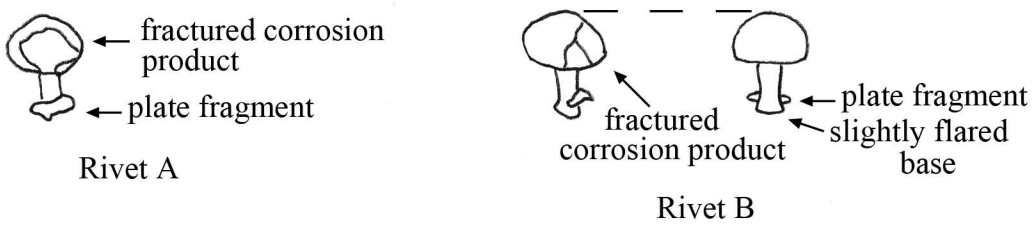

Figure 5.3.1.ii: Rivets (MIT 5343). Key object features.

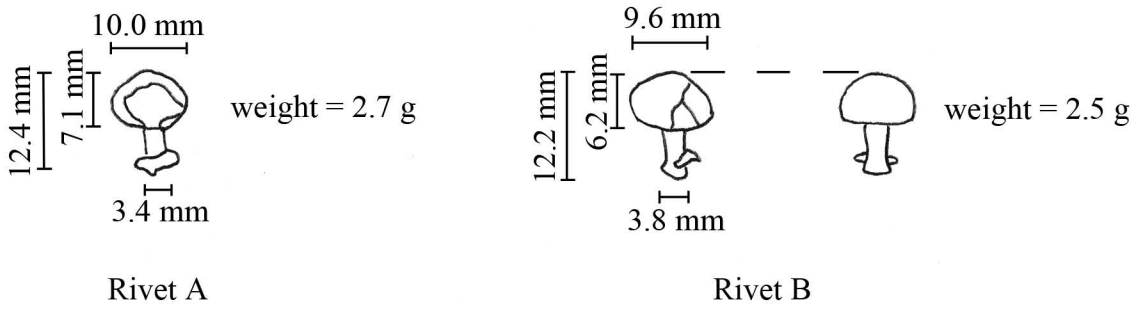

Figure 5.3.1.iii: Rivets (MIT 5343). Drawing and measurements.

Figure 5.3.1.iv: Rivets (MIT 5343). Samples removed from rivets.
MIT 5343a was removed from Rivet A for bulk compositional analysis.
Rivet B was taken in its entirety as MIT 5343b for metallographic analysis.
It was mounted longitudinally and ground down until the entire center plane of the rivet was exposed.

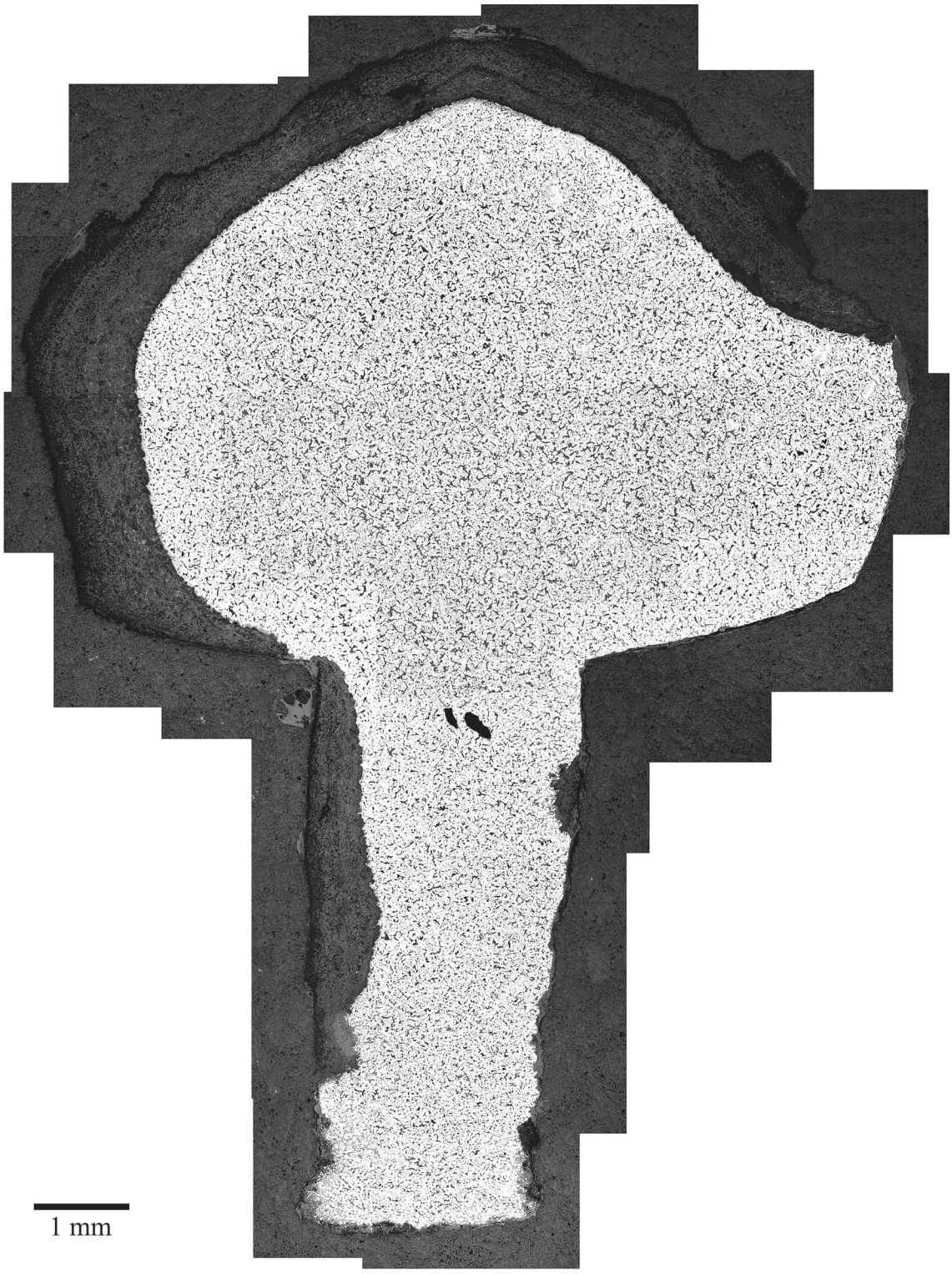

Figure 5.1.3.v: Rivets (MIT 5343/Peabody 40-77-40/13300.)
x 50. Longitudinal cross section, as polished. Microstructural features of interest include the high density of porosities, some of which outline the primary arms of dendrites, the shrinkage cavitiy in the center of the rivet, and the angular edges of the rivet's head outlined in the external corrosion product. (MIT Images 5343b-01-31.)

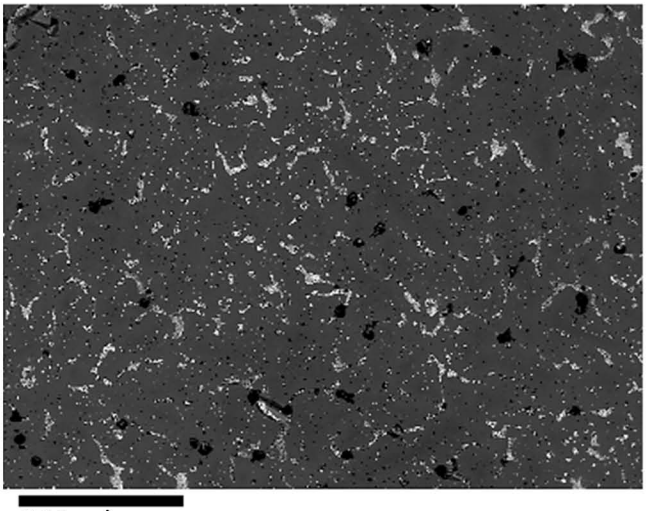

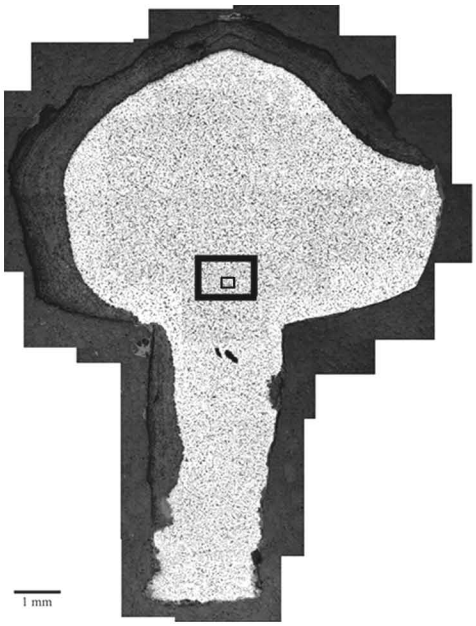

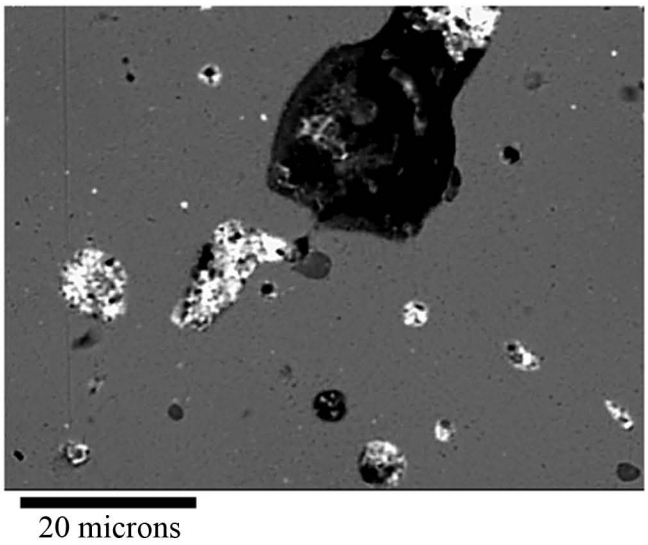

Figure 5.3.1.vi: Rivets (MIT 5343/Peabody 40-77-40/13300).
Above: Backscattered electron image showing the high density of lead that has segregated along the interdendritic spaces of the cast rivet. The lead appears bright in the image and the pores appear black.
Below: Backscattered electron image showing a close up of a pore (black) partially filled with lead (bright). The dark gray inclusions are copper sulfides.

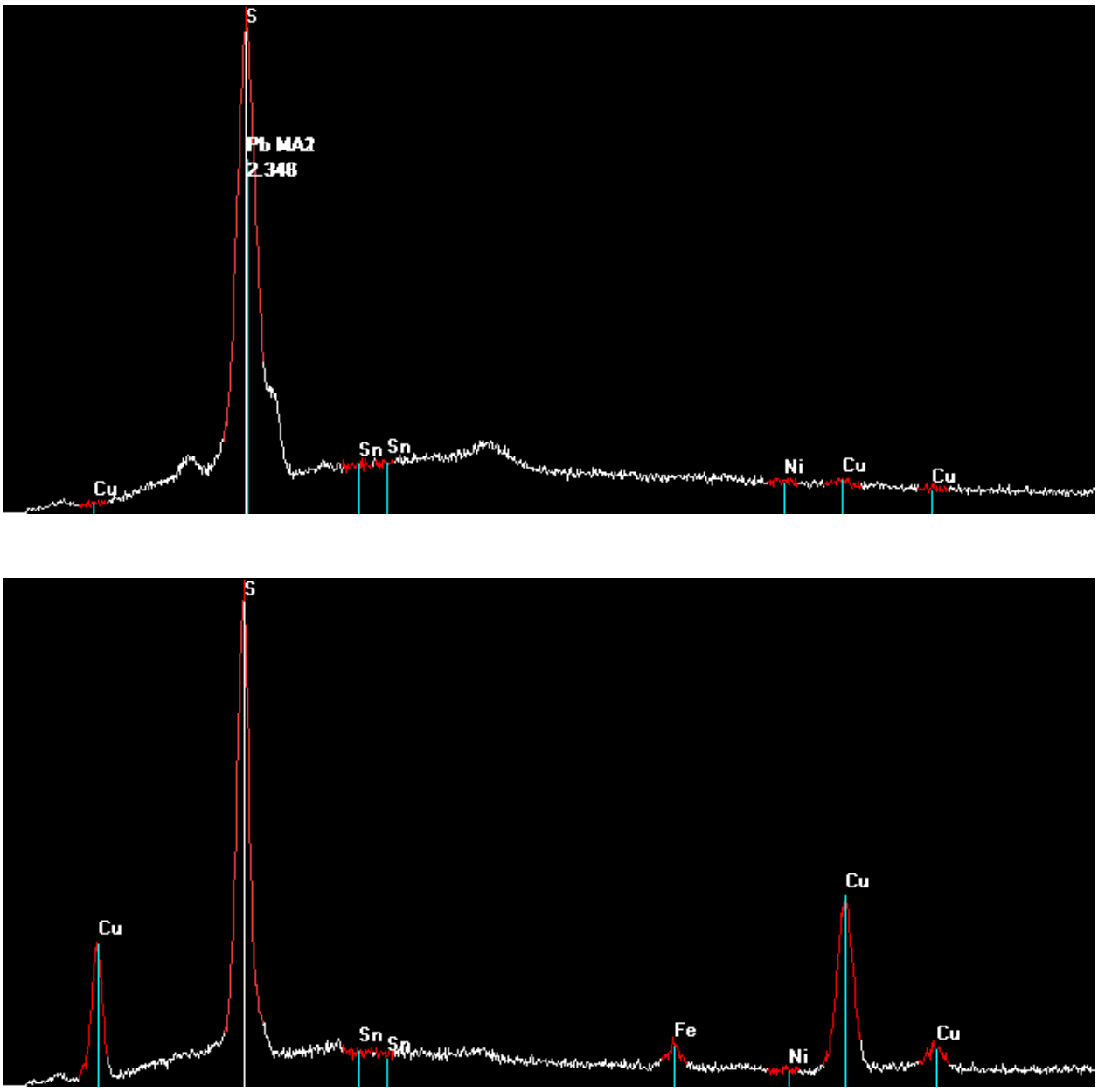

Figure 5.3.1.vii :Rivets (MIT 5343b/Peabody 40-77-40/13300).
Above: EDS spectrum of the light-appearing material in the backscattered electron image of the rivet (see Figure 5.3.1.vi). The spectrum identifies this material as a lead.
Below: EDS spectrum of the gray-appearing material in the backscattered electron image of the rivet. The spectrum identifies this material a copper sulfide.

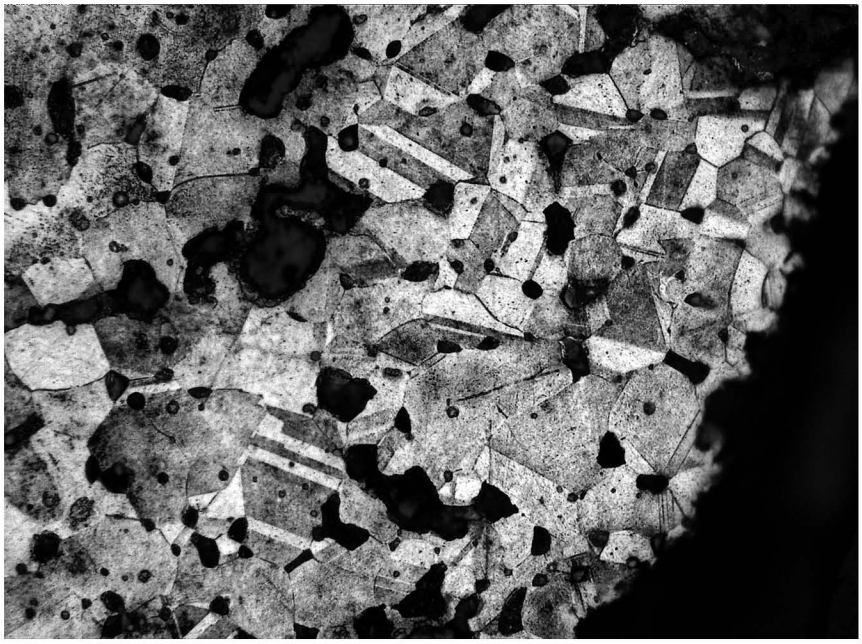

Figure 5.3.1.viii : Rivets (MIT 5343/Peabody 40-77-40/13300). Longitudinal cross section. Etch: 6 sec potassium dichromate, 2 sec aqueous ferric chloride. x500. Microstructural features of interest include the equiaxed grains and annealing twins at the point where the stem and head of the rivet meet. (MIT Image 5343b-33.)

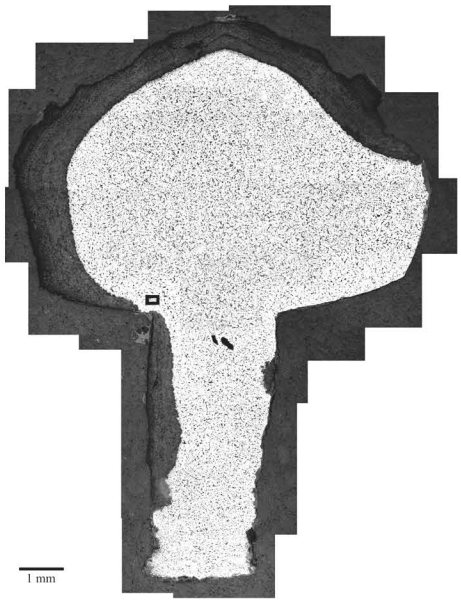

Figure 5.3.1.ix: Rivets (MIT 5343/Peabody 40-77-40/13300). Longitudinal cross section. Etch: 6 sec potassium dichromate, 2 sec aqueous ferric chloride. x500. Microstructural features of interest include the equiaxed grains and annealing twins at the base of rivet's stem. Some deformation lines are also present (MIT Image 5343b-36).

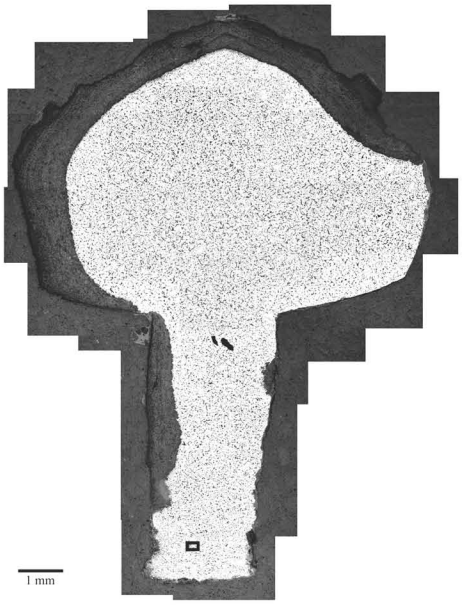

5.3.2: Belt Attachment (MIT 5368/Peabody 40-77-40/13448)

5.3.2a: Provenance and Background

MIT 5368 (Figure 5.2.3.i and 5.2.3.ii) from Grave 32 is identified as a belt plate attachment (Wells 1981). Grave 32 was covered and lined with stone slabs. It was 4.05 m long, 1.35 m wide, and its bottom was 2.45 m below the surface of the tumulus. The grave was lined with a layer of gray clay, and it was split down the center with a stone slab, leading the excavators to believe it was a double grave.

Grave 32 was especially rich. In addition to the belt attachment, Grave 32 contained 190 amber beads, ear pendants, two earrings made of bronze wire, bronze spirals from a set of earrings, a dragon fibula, a second *blumen* fibula, now missing, and a small bronze ring. The dragon fibula is discussed in Section 5.2.6, the bronze earring wire in Section 5.4.4, and the spirals in Section 5.4.5.

5.3.2b: Initial Examination and Observations

The belt attachment was photographed (Figures 5.2.3.i and 5.2.3.ii), drawn to scale, measured, and observed (Figures 5.2.3.iii and 5.2.3.iv).

The belt attachment consists of a single, thin bronze sheet folded over on itself and secured with two bronze rivets. The belt attachment is fragmented, and some pieces of sheet are missing. The sheet is decorated with a line of raised repoussé dots along one edge and with a spiral/wave pattern along its center made with impressed dots. The sheet is folded to create a loop through which a circular, closed, segmented ring has been secured. The ring has semi-annular grooves that meet each other at a center line. A similar ring belt attachment, MIT 5350, is discussed in Section 5.3.4.

The flat sheet portion of the belt attachment is 54.0 mm long and 11.9 mm wide. The loop portion is 9.5 mm long, 18.6 mm high, and 7.0 mm wide. The sheet is 0.7 mm thick. The rivets have an oval-shaped head with a cross section measuring 5.7 x 5.1 mm. The rivets have different size oval-shaped stems, one with a stem cross section measuring 3.7 x 3.2 mm and the other with a stem cross section measuring 3.5 x 3.2 mm. One rivet is 8.7 mm tall and the other rivet is 9.1 mm tall. The ring has a diameter of 23.3 mm, a width of 3.5 mm, and a thickness of 4.7 mm. The belt attachment weighs 13.7 g.

The belt attachment is covered with a thin layer of friable dark and light green mottled corrosion product, and it appears to be structurally robust.

5.3.2c: Sampling

Sample MIT 5368 was removed with a single transverse cut (Figure 5.3.2.v). It was mounted transversely as noted and was ground down until the center plane of the rivet could be seen *in situ* with the sheet. The belt attachment was highly metallic, and the metal was light gold in color.

5.3.2d: Metallographic and Electron Microbeam Probe Analyses

Sample MIT 5368 was mounted as a transverse section and was ground down until the rivet and sheet were exposed together *in situ.*

The as-polished transverse cross section (Figure 5.3.2.vi) shows the rivet and sheet together *in situ*. The rivet and sheet are not noticeably different in color. The rivet is filled with dark inclusions and porosities, and these inclusions and porosities appear to outline dendritic structures. Primary dendrites can be seen outlined in this way in the as-polished sample, indicating that the rivet was cast. The sheet metal also has a high density of porosities, and they are slightly elongated. At the apparent right of the upper sheet the raised repoussé decoration can be seen.

The outline of the rivet and the sheet can be clearly seen. The rivet was tapped or pushed through a hole in the sheet; the juncture between the rivet and upper sheet can be seen at the rivet's apparent left (Figure 5.3.2.vii). The porosities in the rivet around this juncture are elongated, indicating that the rivet was heavily worked at this point as a result of compression of the metal as it passed through the hole. The base of the rivet's stem is split, and the porosities at the base are deformed and elongated, indicating that the rivet stem was hammered inward towards the lower sheet after the rivet was in place to secure it. The force of punching a hole through the sheet for the rivet and/or of hammering the rivet through the sheet forced the bottom sheet to warp slightly.

The transverse cross section was analyzed with the electron microbeam probe to determine the composition of the rivet and sheet. The composition was determined of a series of twelve points (given in the table in Figure 5.3.2.viii), six across the rivet and six

across the sheet; their locations are indicated in Figure 5.3.2.viii. The average composition of the six rivet points and the six sheet points is given below in Table 5.3.2.

Table 5.3.2: Average Composition of Rivet and Sheet, MIT 5368

	Cu	**Sn**	**Pb**	**Sb**	**As**	**Ni**	**Co**	**Ag**	**Fe**
Rivet Average	85.28	3.34	8.89	0.50	0.970	0.331	0.013	0.388	0.284
Sheet Average	88.57	8.04	1.86	n.d.	0.134	1.147	0.013	0.044	0.021

(all values in weight %) n.d. = not determined

The sheet is a leaded tin bronze with a tin composition of approximately 8 weight percent and a lead composition of approximately 1.8 weight percent. The tin concentration is slightly lower and the lead concentration slightly higher in this sheet than in the rings made of bronze sheet discussed in Section 5.1.

The rivet is a highly leaded, low tin bronze with a lead composition of 8.89 weight percent and a tin composition of approximately 3.34 weight percent. Due to the inhomogeneous presence of lead in the sample, which is discussed below, the composition of lead is probably underreported. The low tin and high lead composition is similar to the composition of MIT 5343, the loose rivet discussed in Section 5.3.1, which has a tin concentration of 5.12 weight percent and a lead concentration of over 14 weight percent.

Figure 5.3.2.ix shows a backscattered electron image of the rivet. The bright-appearing material is lead, which is inhomogeneously present throughout the bulk of the rivet in porosities and in interdendritic spaces. Due to the inhomogeneous presence of lead in the sample, the composition of lead is probably higher than the average 8.89 weight percent determined by the electron microbeam probe.

The sample was etched for five seconds with potassium dichromate and for two seconds with aqueous ferric chloride. The microstructure of the sheet is characterized by equiaxed grains with annealing twins and a high density of deformation lines (Figure 5.3.2.x), indicating that the sheet was subject to several cycles of working and annealing and that it was left in a worked state. In the metal that comprises the raised, repoussé decoration of the sheet, the equiaxed grains are elongated and the annealing twins are bent (Figure 5.3.2.xi), indicating that this area of the sheet was subject to intense working

when the decoration was made. The raised decoration was made with a chasing tool that compressed the metal.

The microstructure of the rivet is characterized by cored dendrites (Figure 5.3.2.xii), indicating that the rivet was left as-cast.

5.3.2e: Discussion

The rivet and sheet that make up the belt attachment are made of different alloys and were fabricated differently.

The rivet is a highly leaded, low tin bronze with a lead composition of 8.89 weight percent and a tin composition of approximately 3.34 weight percent. The lead composition is probably underreported. The rivet has an as-cast structure. Elongation of its porosities at the points where the rivet meets the sheet and at the base of the rivet's stem indicates that the rivet was lightly hammered to place it into and secure it in the sheet. Because the rivet would have been relatively soft compared to the sheet, the hole in the sheet through which the rivet was pushed was punched prior to insertion of the rivet.

This rivet is very similar to the loose rivet discussed in Section 5.3.1. The choice of a highly leaded, low tin bronze for both rivets reflects the function of the rivet as a cast component of a belt plate. The rivet did not need to serve a mechanical purpose beyond merely maintaining two pieces of sheet together rigidly, and it also served as a decorative detail. The lead was most likely used as a "filler" material. The metal used to make the rivet may have been recycled scrap bronze as the rivet's alloy did not need to be carefully monitored, but the high concentration of lead was probably deliberate. Similar rivets and cast components of sheet metal vessels at S. Lucia are made of leaded bronze and do not exhibit any regular pattern of alloy composition, indicating that they may have been made using recycled bronze scrap (Giumlia-Mair 1995).

The sheet is a leaded tin bronze with a tin composition of approximately 8 weight percent and a lead composition of approximately 1.8 weight percent. The tin concentration is slightly lower and the lead concentration slightly higher in this sheet that in the bronze sheet used to fashion the rings discussed in Section 5.1. The tin and lead concentrations of the sheet distinguish it from objects made of bronze sheet from S.

Lucia, the majority of which contain between 9-13 weight percent tin with less than 0.5 weight percent lead (Giumlia-Mair 1995). However, the tin concentration is high enough so that the sheet would have been significantly harder than the rivet, especially when left in a worked condition.

The sheet was subject to several cycles of working and annealing, and it was left in a worked state. These cycles of working and annealing were necessary to reduce the metal to thin sheet while avoiding brittleness. It was left worked so as to be hard enough to withstand use as a belt attachment. The raised, repoussé decoration was made with a chasing tool after the sheet had been worked to its desired thickness.

5.3.2f: Conclusions

- The rivet and sheet making up the belt attachment are made of different alloys and were manufactured differently.
- The rivet is a highly leaded, low tin bronze with a lead composition of 8.89 weight percent and a tin composition of approximately 3.34 weight percent. It has an as-cast structure.
- The sheet is a leaded tin bronze with a tin composition of approximately 8 weight percent and a lead composition of approximately 1.8 weight percent; it was subject to several cycles of working and annealing to reduce it to a thin sheet and it was left in a worked state.
- The raised decoration on the sheet's surface was made with a chasing tool after the desired sheet thickness had been achieved.
- A hole was punched through the sheet to accept the rivet. The rivet was then hammered gently or pressed into place and secured by hammering the base of the rivet stem so that the stem bulged slightly.
- The alloy and fabrication of the rivet are similar to those of the rivet discussed in Section 5.3.1, MIT 5343. The high concentration of lead and low concentration of tin indicate that the alloy comprising the rivet is likely a mixture of scrap bronze and "filler" lead. Such an alloy would have been suitable for a rivet that did not serve a mechanical function beyond holding sheet together while, at the same time, providing decorative detail.

Figure 5.3.2.i: Belt attachment. (MIT 5368/Peabody 40-77-40/13448). Photograph by E. Cooney.

Figure 5.3.2.ii: Belt attachment, detail of repoussé and impressed spiral pattern. (MIT 5368/Peabody 40-77-40/13448). Photograph by E. Cooney.

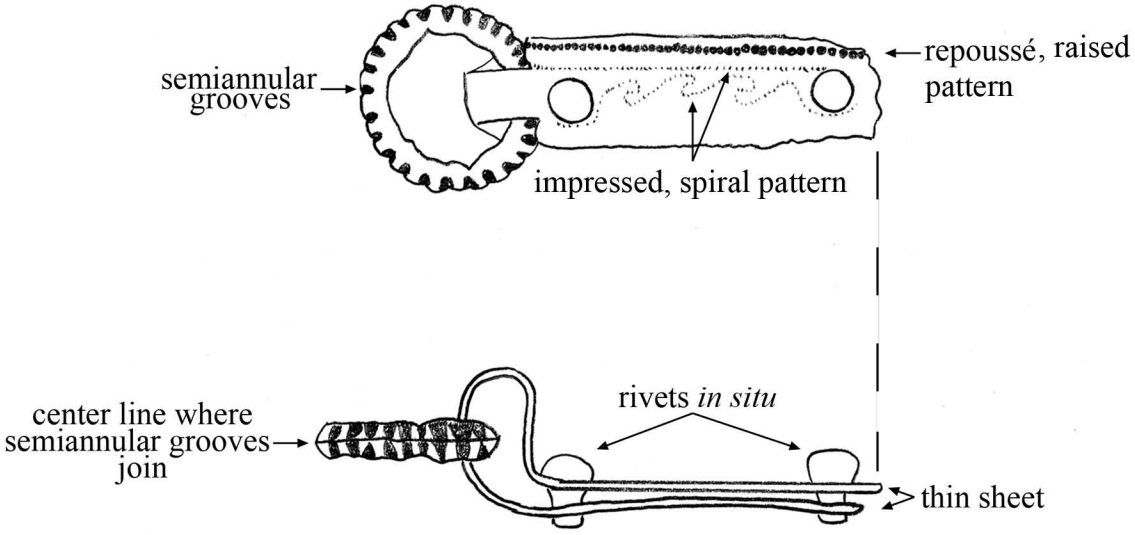

Figure 5.3.2.iii: Belt attachment (MIT 5368). Key object features.

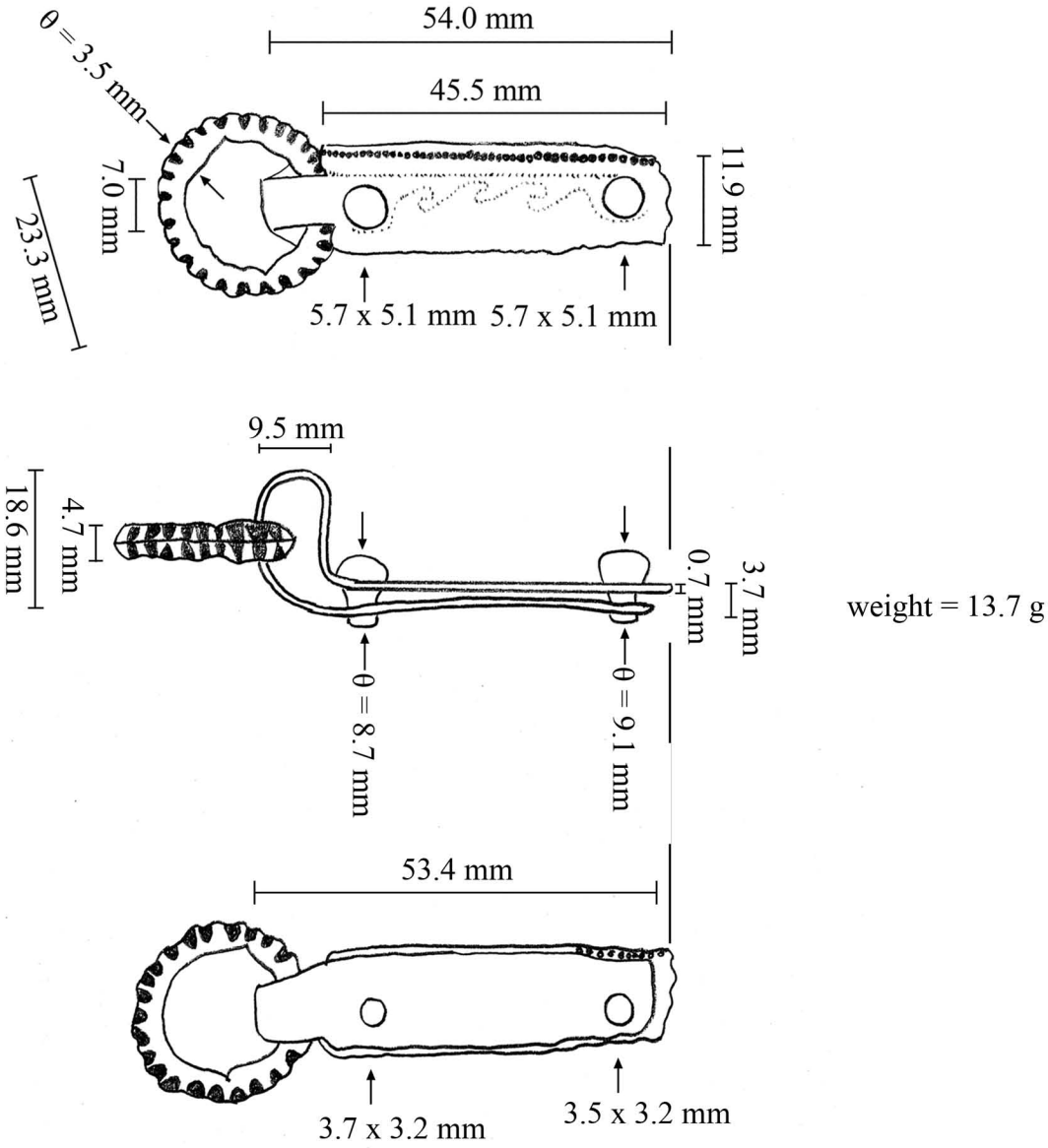

Figure 5.3.2.iv: Belt attachment (MIT 5368). Drawing and measurements.

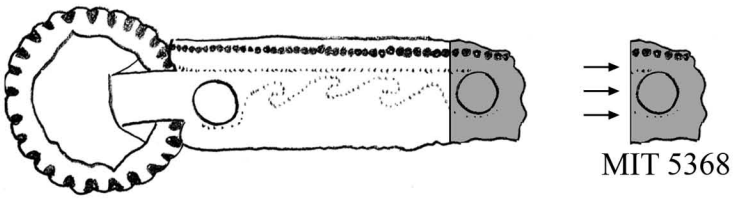

Figure 5.3.2.v: Sample removed from belt attachment. Sample MIT 5368 was removed for metallographic analysis and compositional analysis with the electron microbeam probe and was mounted transversely as noted.

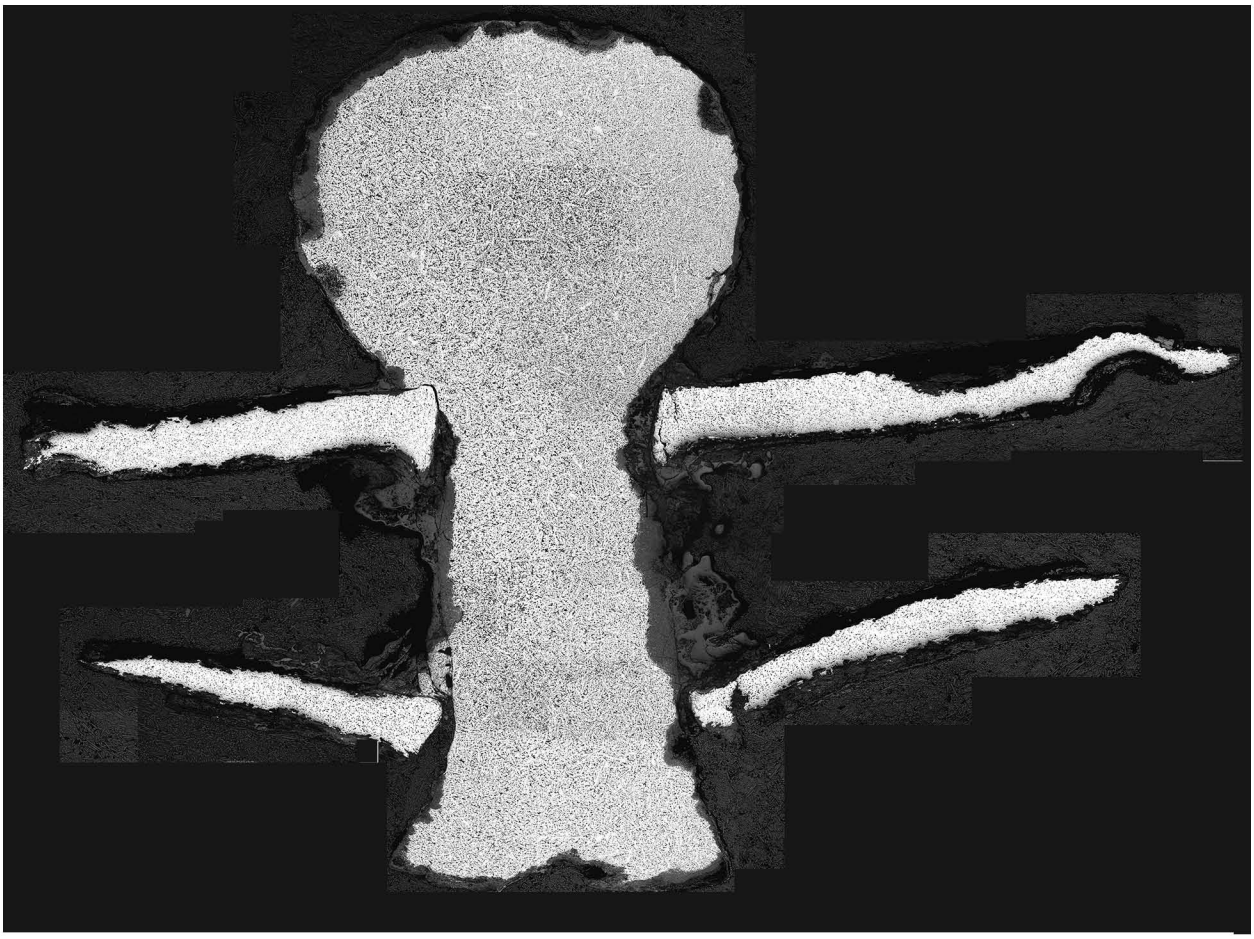

Figure 5.3.2.vi: Belt attachment (MIT 5368/Peabody 40-77-40/13448). Transverse cross section, as polished. Microstructural features of interest include the juncture between the rivet and the sheet metal, the raised repoussé decoration in the apparent upper right of the sheet metal, and the high density of porosities in both the sheet metal and the rivet. Porosities in the rivet outline the primary arms of individual dendrites. (MIT Images 5368-29-61).

Figure 5.3.2.vii: Belt attachment (MIT 5368/Peabody 40-77-40/13448).
Transverse cross section, as polished. x 50. Inclusions and porosities in the bulk of the rivet outline dendritic structures. These inclusions and porosities are elongated at the juncture between the rivet and sheet, indicating that the rivet was heavily worked at this point. The sheet has a high density of porosities elongated parallel to the sheet's longitudinal axis. (MIT Image 5368-35).

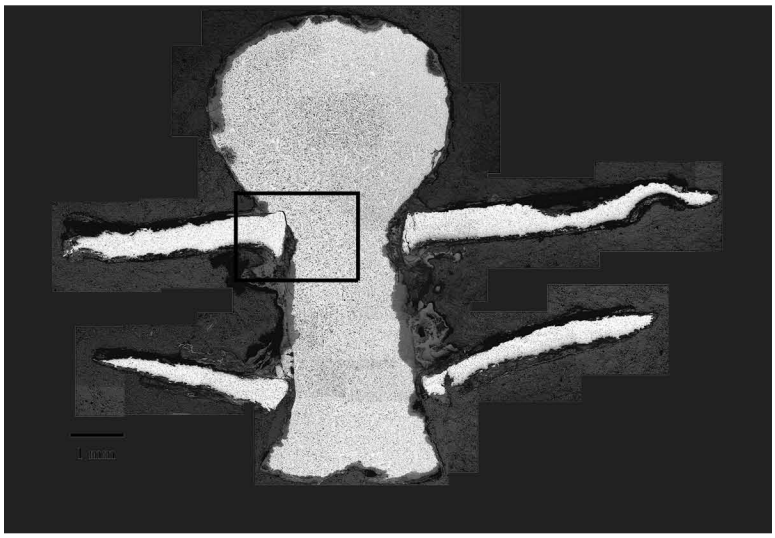

Electron Microbeam Probe Compositional Data

	Cu	Sn	Pb	Sb	As	Ni	Co	Ag	Fe
Pt 1	84.08	3.73	10.93	0.6899	0.9814	0.3534	0.0186	0.2722	0.321
Pt 2	89.08	3.07	6.1	0.2953	0.8766	0.3637	n.d.	0.1315	0.2459
Pt 3	94.8	2.82	2.18	0.234	0.9019	0.337	n.d.	0.0433	0.2988
Pt 4	88.78	2.87	6.12	0.3511	0.8684	0.2849	0.0257	0.4635	0.2484
Pt 5	84.55	3.71	8.37	0.5911	1.1267	0.349	0.0241	0.5136	0.3536
Pt 6	70.41	3.83	19.61	0.815	1.0628	0.2981	0.0107	0.904	0.2339
Rivet Average	**85.28**	**3.34**	**8.89**	**0.50**	**0.970**	**0.331**	**0.013**	**0.388**	**0.284**
Pt 7	88.48	10.33	1.261	n.d.	0.2297	1.2235	0.0096	0.0576	0.0072
Pt 8	87.3	7.23	3.98	n.d.	0.1379	1.1135	0.0206	0.0063	0.0277
Pt 9	88.82	8.06	1.434	n.d.	0.1344	1.1052	0.0083	0.0536	n.d.
Pt 10	88.51	7.75	1.125	n.d.	0.1056	1.2736	0.0236	0.0023	0.0761
Pt 11	85.78	8.93	3.04	n.d.	0.148	0.9749	0.0095	0.1422	0.0087
Pt 12	92.53	5.93	0.3385	n.d.	0.0467	1.1887	0.0084	n.d.	0.0077
Sheet Average	**88.57**	**8.04**	**1.86**	**n.d.**	**0.134**	**1.147**	**0.013**	**0.044**	**0.021**

(all values in weight %) n.d. = not determined

Figure 5.3.2.viii: Belt Attachment (MIT 5368/Peabody 40-77-40/13448).
Above: Points at which compositional data were taken by the electron microbeam probe.
Below: Electron microbeam probe compositional data from each point in the rivet and in the sheet.

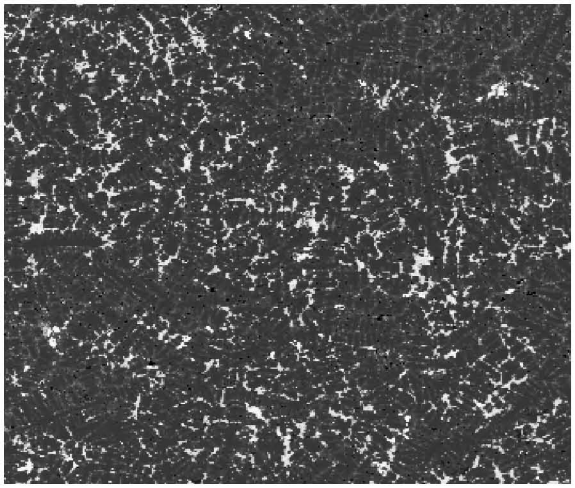

Figure 5.3.2.ix: Belt attachment (MIT 5368/Peabody 40-77-40/13448). Backscattered electron image showing lead, which appears bright, inhomogenously distributed throughout the interdendritic spaces and porosities of the rivet.

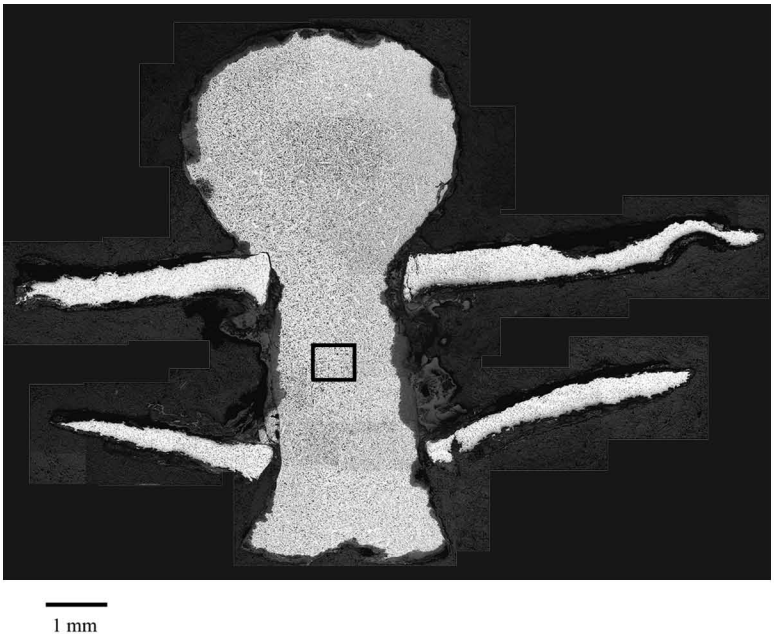

50 microns

Figure 5.3.2.x: Belt attachment (MIT 5368/Peabody 40-77-40/13448). Transverse cross section. Etch: 5 seconds potassium dichromate and 3 seconds ferric chloride. x200. Microstructural features of interest in the sheet include equiaxed grains with annealing twins and a high density of deformation lines. (MIT Image 5368-63).

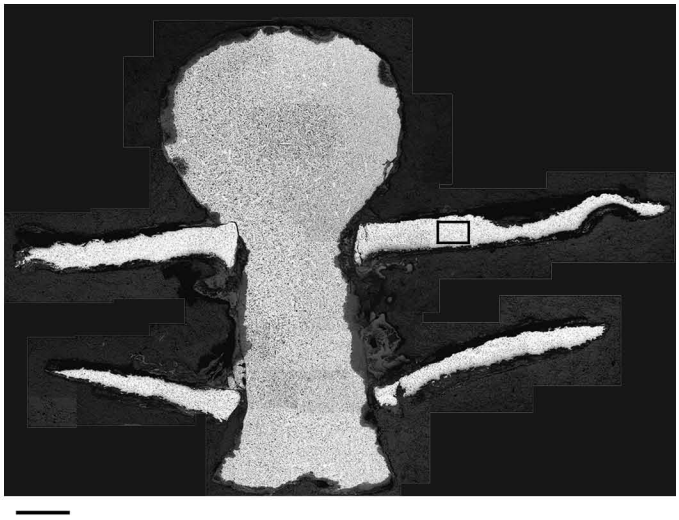

1 mm

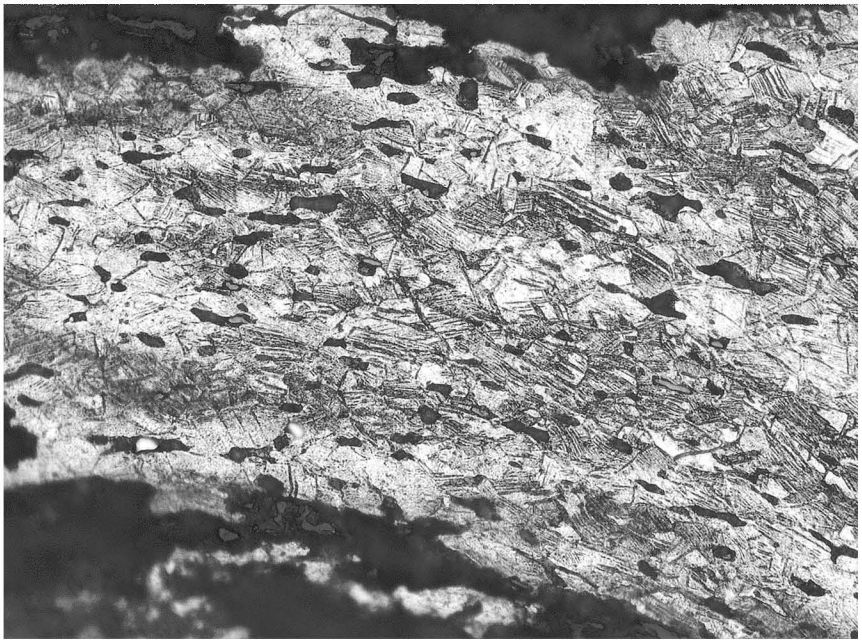

Figure 5.3.2.xi: Belt Attachment (MIT 5368/Peabody 40-77-40/13448). Transverse cross section. Etch: 5 sec potassium dichromate and 2 sec ferric chloride. x500. Microstructrual features of interest include elongated grains with bent annealing twins and a high density of deformation lines in the metal making up the raised decoration in the sheet. (MIT Image 5368-65.)

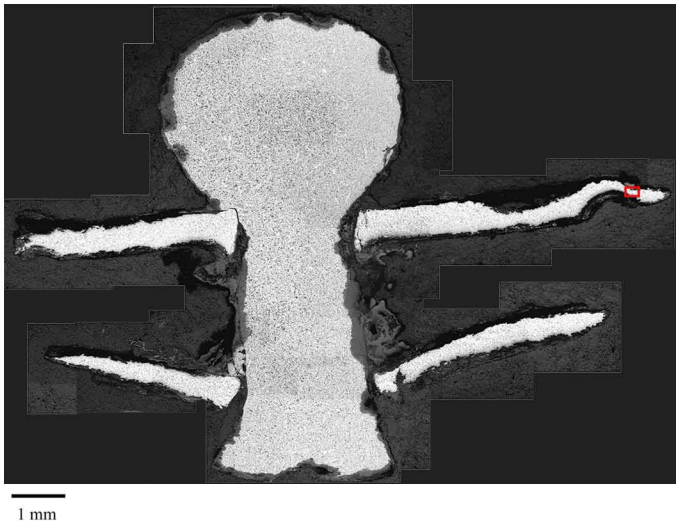

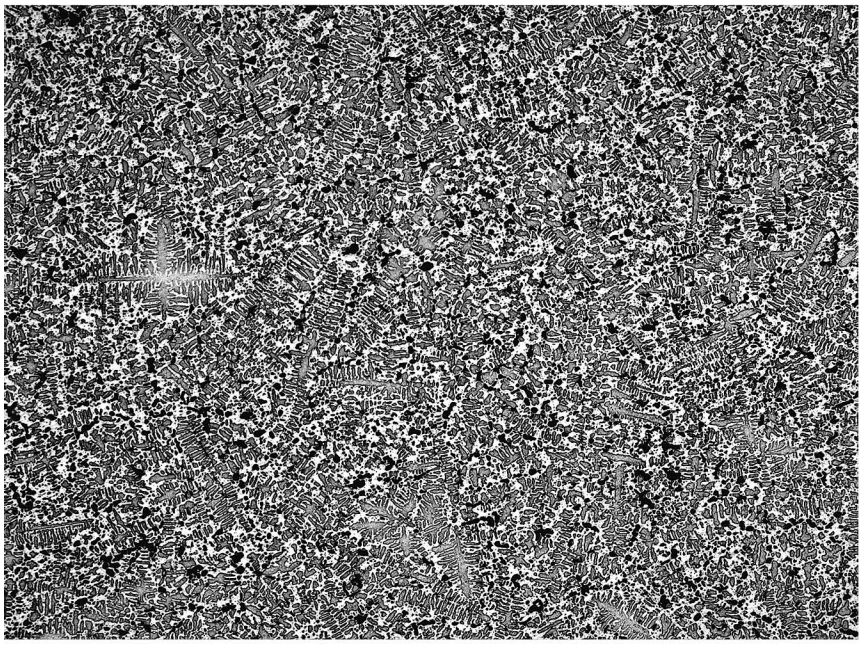

100 microns

Figure 5.3.2.xii: Belt attachment (MIT 5368/Peabody 40-77-40/13448). Transverse cross section. Etch: 5 seconds potassium dichromate and 3 seconds ferric chloride. x100. Microstructural features of interest include an as-cast structure with cored dendrites in the rivet. (MIT Image 5368-64).

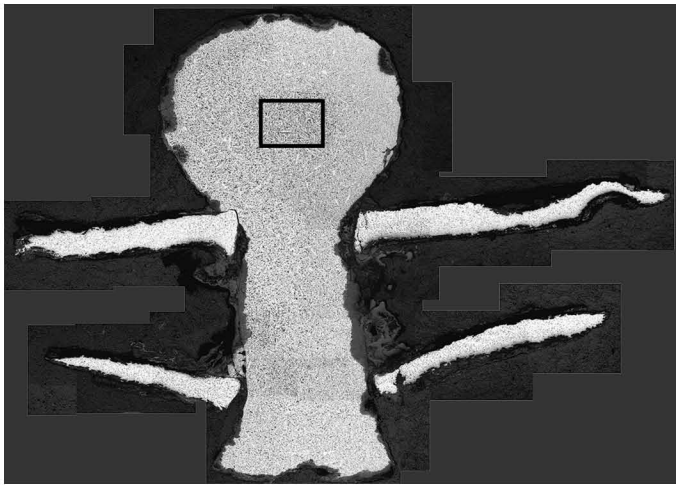

1 mm

5.3.3: Hook (MIT 5345/Peabody 40-77-40/13483)

5.3.3a: Provenance and Background

MIT 5345 (Figures 5.3.3.i and 5.3.3.ii), identified by Wells as a bronze hook (1981) came from Grave 40. Grave 40 was a cremation grave 2.1 m below the surface of the tumulus and oriented southeast-northwest. MIT 5345 is part of a belt plate assemblage of which other surviving pieces include fragments of sheet bronze with and without rivets, sheet with a band and hook of iron, a hollow bronze hook with rivet, and a small segmented bronze ring belt attachment (MIT 5350, discussed in Section 5.3.4).

Associated grave goods include two hollow bronze rings, one of which is MIT 5366, discussed in Section 5.1.9, an iron spearhead, sherds of at least four different pottery vessels, and a spindle whorl.

A similar solid hook belt attachment is found in Grave 36 (Figure 5.3.3.iii). There are other solid belt hooks from other tumuli at Stična as well.

5.3.3b: Initial Examination and Observations

The hook was photographed (Figures 5.3.3.i and 5.3.3.ii), drawn to scale, measured, and observed (Figures 5.3.3.iv and 5.3.3.v).

The hook is fragmented and has several component parts. It is constructed from two sheets of metal riveted together with two rivets of different sizes. The actual hook, now broken off from the sheet, was attached to the bottom of the two sheets. It was made by bending the sheet into a hook shape. Figure 5.3.3.ii shows the hook *in situ* as MIT 5345 would have looked from the side when the hook was still attached to its sheet metal.

The area on the hook fragment that was immediately adjacent to the rivet can still be seen (Figure 5.3.3.iv). The hook end is completely mineralized and has a hairline fracture running longitudinally through its center. This crack stops near the more metallic area of the hook fragment closer to the fragmented edge. The fragment is 17.6 mm long and is 9.6 mm wide at the end once attached to the sheet and 6.4 mm wide at the actual hook end. The sheet that forms the hook is 1.5 mm thick. The hook weighs 1.1 g.

The fragment with the attached rivets that hold together the two bronze sheets is 26.8 mm long. It weighs 7.7 g.

The top sheet is 11.8 mm wide at the edge adjacent to the hook fragment and is 13.8 mm wide at the opposite edge. The edge adjacent to the hook fragment appears to be an original edge. The top sheet is 0.8 mm thick.

The bottom sheet is slightly narrower than the top sheet at the point where the hook fragment was once attached, but at the opposite end they are the same width. The bottom sheet is 1.2 mm thick.

One rivet is much larger than the other. The larger one is 10.4 mm high with a head diameter of 11.1 mm and a stem diameter of 4.6 mm. The smaller one is 9.5 mm high with a head diameter of 7.7 mm and a stem diameter of 4.1 mm. Overall, the head to stem ratio of these rivets is higher than the head to stem ratio of other rivets examined at Stična.

The sheet metal making up both the hook fragment and the fragment with the rivets appeared upon initial examination to be mineralized. The rivets appeared to be structurally quite robust. The entire object was covered with a smooth dark and light green mottled corrosion product. In areas where this corrosion product was removed, a layer of friable dark green corrosion product was visible.

Under low power magnification, some scratches and striations were visible in the corrosion product on the underside of the hook fragment and on the top of the fragment with rivets. These striations most likely came from post-excavation cleaning.

5.3.3c: Sampling

Sample MIT 5345 was removed from the hook fragment via a transverse cut for bulk compositional analysis (Figure 5.3.3.vi). The fragment was surprisingly metallic and the metal was light gold in color.

5.3.3d: Bulk Compositional Analysis

Bulk compositional analysis shows that the hook is a copper-tin-lead alloy with the primary alloying element of tin at a concentration of 13.6 weight percent. The alloy is a high tin leaded bronze with the lead present at a concentration of 2.88 weight percent. Other major and minor elements include As (0.359%), Sb (0.225%), Ni (0.139%), Ag

(0.093%), and Fe (0.047%). Bulk compositional analysis data are shown in Table 5.3.3 and in the Appendix.

Table 5.3.3: Bulk Compositional Analysis Data for MIT 5345

	Sn	**Pb**	**Sb**	**As**	**Ni**	**Co**	**Ag**	**Fe**
ICP-ES	13.6	2.88	0.225	0.359	0.139	0.038	n.a.	0.047
INAA	12.8	n.a.	0.221	0.322	0.199	0.0456	0.093	n.d.

(values in weight %) n.a. = not analyzed n.d. = not determined

5.3.3e: Conclusions

- The alloy comprising the sheet from which the hook is made is a high tin leaded bronze. The high tin content was needed to make the sheet hard. The hook especially needed to be hard if it was engineered to suspend an item in tension.
- The lead composition of the hook is slightly higher than the range reported for items made of sheet metal at St. Lucia (Giumlia-Mair 1995.)

Figure 5.3.3.i: Solid hook, front and back. (MIT 5345/Peabody 40-77-40/13483). Photographs by E. Cooney.

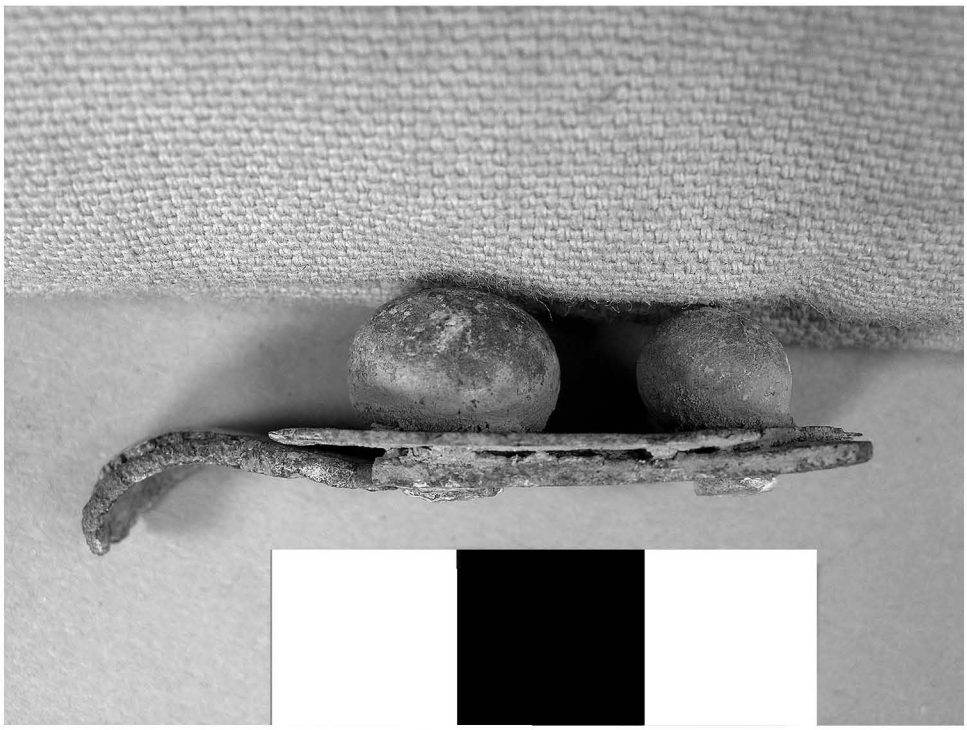

Figure 5.3.3.ii: Solid hook, side. (MIT 5345/Peabody 40-77-40/13483).
Photograph by E. Cooney. Copyright 2007: President and Fellows of Harvard College.

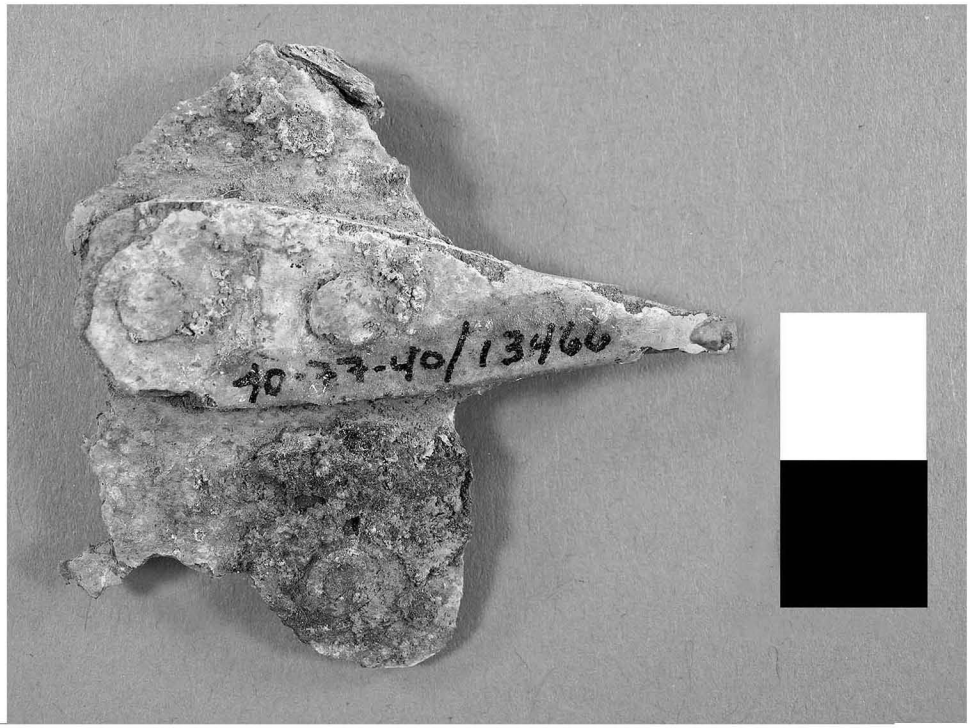

Figure 5.3.3.iii: Solid hook belt attachment (Peabody 40-77-40/13400.)
An additional solid bronze hook attached to bronze sheet with rivets.
Photograph by E. Cooney. Copyright 2007: President and Fellows of Harvard College.

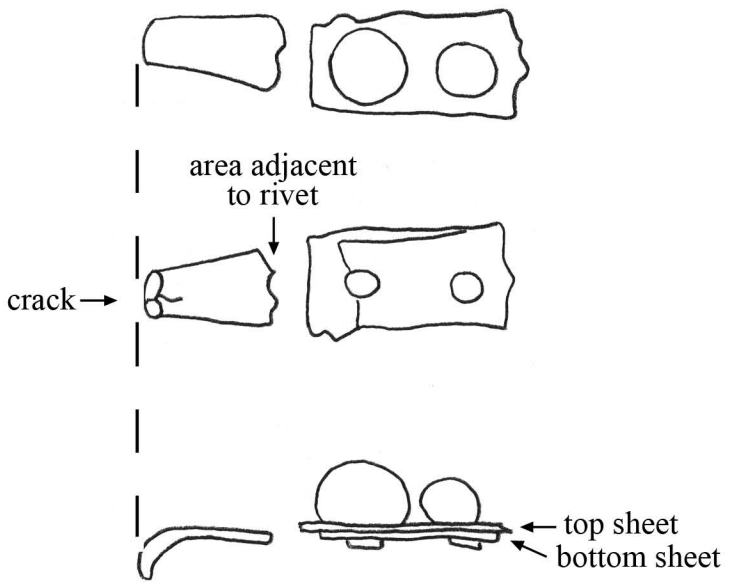

Figure 5.3.3.iv: Solid hook (MIT 5345). Key object features.

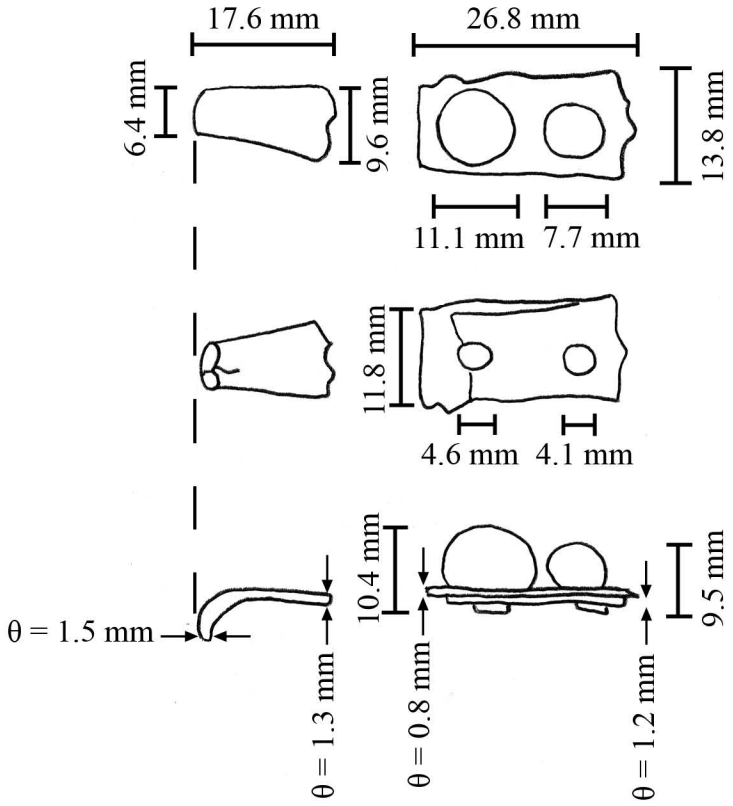

Figure 5.3.3.v: Solid hook (MIT 5345). Drawing and measurements.

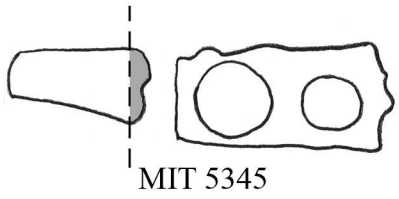

Figure 5.3.3.vi: Solid hook (MIT 5345). Sample MIT 5345 was removed for bulk compositional analysis.

5.3.4: Segmented ring belt attachment (MIT 5350/Peabody 40-77-40/13488)

5.3.4a: Provenance and Background

MIT 5350 (Figure 5.3.4.i), a segmented ring belt attachment, came from Grave 40, which is discussed in detail in Section 5.3.3. There are several other intact, segmented solid ring belt attachments in Tumulus IV, two of which are still attached to the belt loop. These include the segmented ring belt attachment, which is part of the belt plate attachment MIT 5368, discussed in Section 5.3.2.

5.3.4b: Initial Examination and Observations

The segmented ring belt attachment was photographed (Figure 5.3.4.i), drawn to scale, measured, and observed (Figures 5.3.4.ii and 5.3.4.iii).

The segmented ring is a circular, closed ring with a diameter measuring 24.1 mm. The ring varies in width from 5.0 to 5.2 mm and in thickness from 3.5 mm to 5.2 mm. The ring weighs 5.8 g.

The majority of the ring is covered with a friable, dark green corrosion product. A few areas are not covered with this corrosion product and are dark in color with a smooth texture. It is unclear if this dark, smooth material is oxidized metal or another substance. One of the areas covered by this dark, smooth material is highly mineralized and is fragmented. The ring is missing a 6.1 mm long piece from the fragmented area.

The segments are bulbous and evenly sized; they are 2.3 mm long. Each groove proceeds along the entire outside surface of the ring; the inside surface is ungrooved and smooth. The grooves have a rounded, concave, semi-annular shape and are 1.5 mm wide.

One particular groove immediately adjacent to the fragmented area present in the dark, smooth material is unlike the other grooves. Under low magnification it can be seen that this particular groove is crudely made; it does not have a rounded, concave, semi-annular shape, and it appears to have been roughly engraved into the material.

With the exception of the fragmented area, the ring appears to be structurally robust.

5.3.4c: Sampling

The ring was sampled twice (Figure 5.3.4.iv). Sample MIT 5350a was removed for bulk composition analysis. Sample MIT 5350b was removed for metallographic analysis and was mounted longitudinally as noted. The ring was fairly metallic, and the metal was light gold in color.

5.3.4d: Bulk Composition Analysis

Bulk composition analysis data show that the segmented ring belt attachment is a ternary copper-lead-tin alloy with lead present at a concentration of 18.7 weight percent and tin present at a composition of 9.38 weight percent. Other major, minor and trace elements include Sb (1.46%), As (1.36%), Ni (0.763%), Ag (0.404%), Co (0.041%), and Fe (0.073%). Bulk composition analysis data are given in Table 5.3.4 and in the Appendix.

Table 5.3.4: Bulk Composition Analysis Data for MIT 5350 (Ring Belt Attachment)

	Sn	**Pb**	**Sb**	**As**	**Ni**	**Co**	**Ag**	**Fe**
ICP-ES	9.38	18.7	1.46	1.36	0.505	0.041	n.a.	0.073
INAA	6.33	n.a.	0.210	n.a.	0.7630	0.0332	0.404	n.d.

(values in weight %) n.a. = not analyzed n.d. = not determined

5.3.4e: Metallographic Analysis

The sample was mounted longitudinally as noted. The as-polished longitudinal sample is shown in Figure 5.3.4.v. The contours of the evenly sized and spaced segments and grooves can be seen outlined in the external corrosion product. The single, crudely shaped groove cannot be seen in the longitudinal cross section.

The sample has a high density of porosities, most of which are filled with lead. These porosities range in size from very small to large, and they are not homogenously distributed throughout the sample. The majority of the large and medium sized porosities are located towards the outside surface of the ring. The metal close to the inside surface has only very small porosities. The porosities appear to outline large grains.

The sample was etched for three seconds with potassium dichromate and for one second with ferric chloride to reveal an as-cast microstructure (Figure 5.3.4.vi). Highly

cored dendrites are surrounded by pools Cu-Sn eutectoid and large, spherical porosities filled with lead. The cored dendrites and eutectoid do not appear to be elongated or deformed in any way, indicating that the ring was left as-cast.

The low density of porosities at the ring's inside surface may have been a result of the orientation of the mold as the molten metal solidified. The porosities and liquid lead rose to the outside surface as the metal froze in the mold.

The entire longitudinal sample is made of the same material, indicating that the "dark" material observed on the ring's exterior surface is simply oxidized metal.

5.3.4f: Discussion

The segmented ring belt attachment is a ternary copper-lead-tin alloy with lead present at a concentration of 18.7 weight percent and tin present at a composition of 9.38 weight percent. The ring was cast to shape and left as-cast. Thus, the segments and grooves visible in the longitudinal cross section were part of the mold in which the ring was cast.

However, no groove is present in the longitudinal cross section at the point where the "crude" groove was present on the outside surface. A flaw in the mold or casting operation most likely failed to cast a segment and groove at this point during the casting process. The metalsmith needed to engrave a shallow groove into the ring —the "crude" groove observed on the ring's surface—so that this flaw did not ruin the ring's segmented decoration.

A highly leaded tin-bronze alloy was used to make the ring, which was cast to shape and left as-cast. The lead was most likely used as a "filler" material. The metal used to make the ring may have been recycled scrap bronze as the ring's alloy did not need to be carefully monitored, but the high concentration of lead was probably deliberate.

Similar as-cast objects at S. Lucia are also made of highly leaded tin bronze alloys. These cast objects do not exhibit any regular pattern of alloy composition, indicating that they may have been made using recycled bronze scrap (Giumlia-Mair 1995). Similar as-cast objects from Stična, such as the solid segmented foot ring

discussed in Section 5.1.12 and the rivets discussed in Section 5.3.1 and 5.3.2, also exhibit a high lead content.

5.3.4g: Conclusions

- The segmented ring belt attachment is a ternary copper-lead-tin alloy with lead present at a concentration of 18.7 weight percent and tin present at a composition of 9.38 weight percent.
- The ring was cast to shape and left as-cast.
- The "crude" groove observed on the ring's exterior surface was engraved by the metalsmith because a casting flaw had failed to cast a groove into the ring at this point.
- The high lead concentration is probably caused by the use of lead as a "filler" material in the alloy; the use of lead in such a high concentration was possible because the ring was cast to shape and left as-cast.

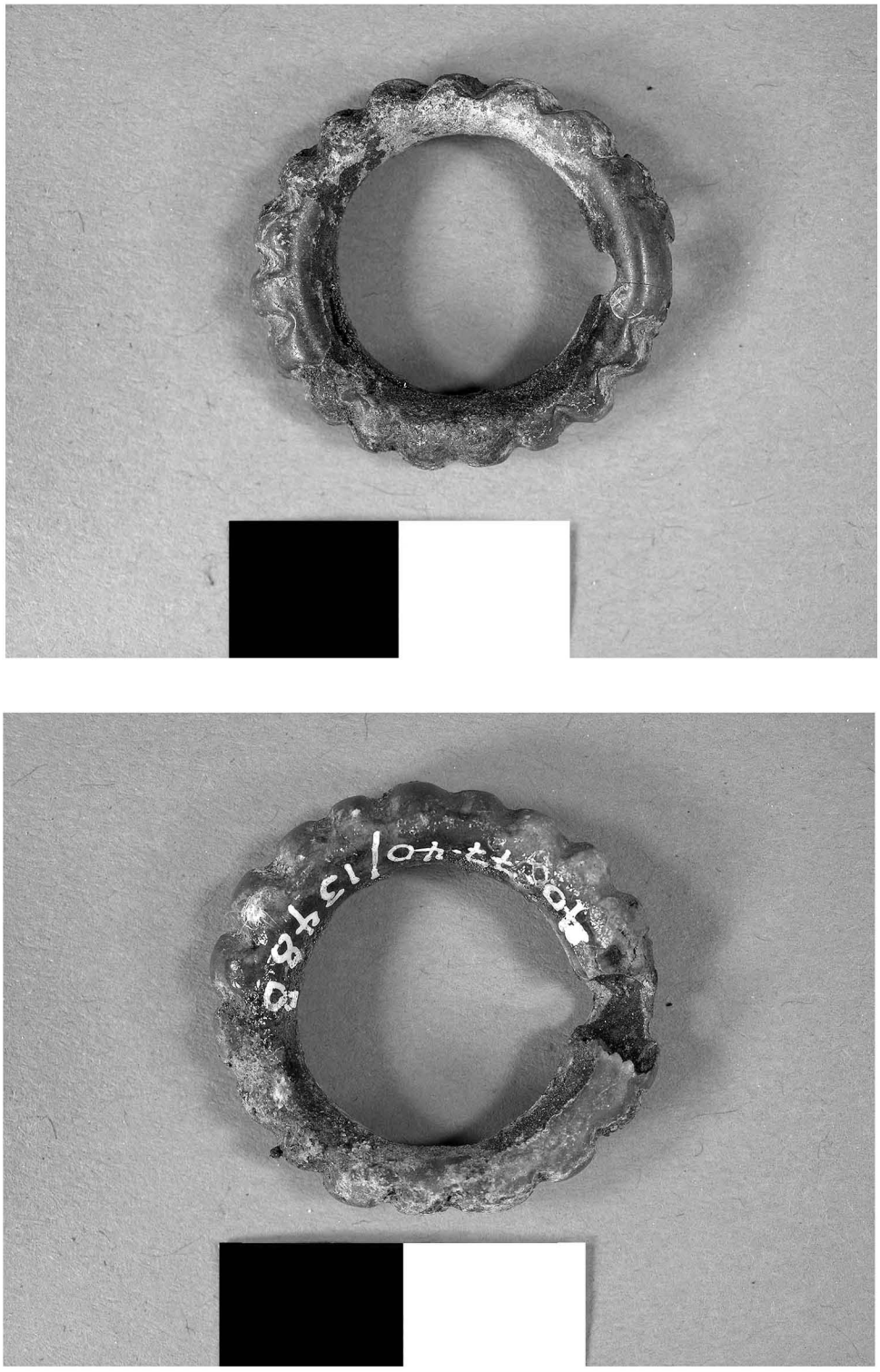

Figure 5.3.4.i: Segmented ring belt attachment. (MIT 5350/Peabody 40-77-40/13488). Photograph by E. Cooney.

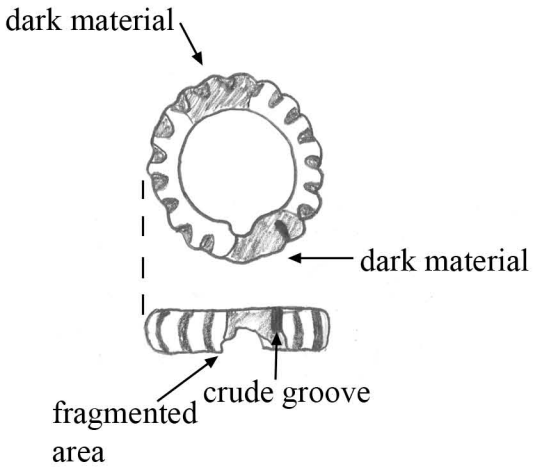

Figure 5.3.4.ii: Segmented ring belt attachment (MIT 5350). Key object features.

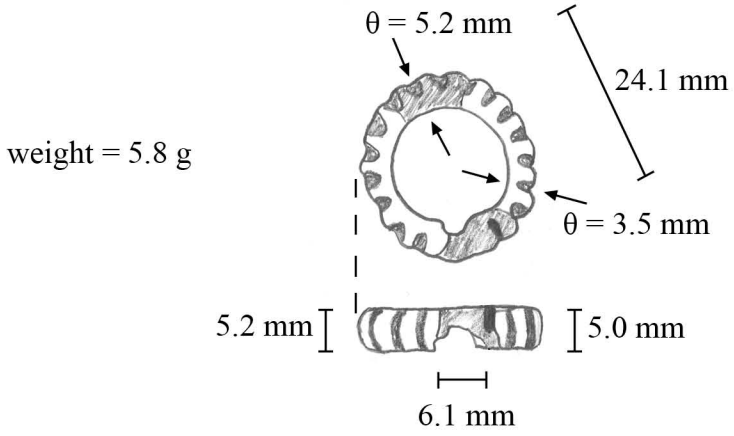

Figure 5.3.4.iii: Segmented ring belt attachment (MIT 5350). Drawing and measurements.

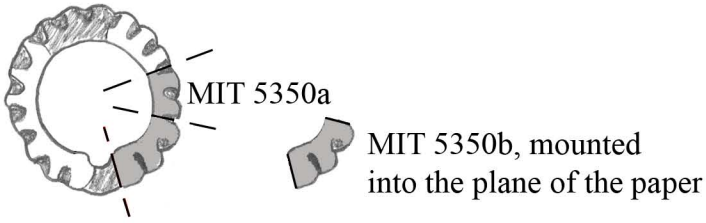

Figure 5.3.4.iv: Samples removed from segmented ring belt attachment. Sample MIT 5350a was removed for bulk composition analysis. Sample MIT 5350b was removed for metallographic analysis and was mounted longitudinally into the plane of the paper.

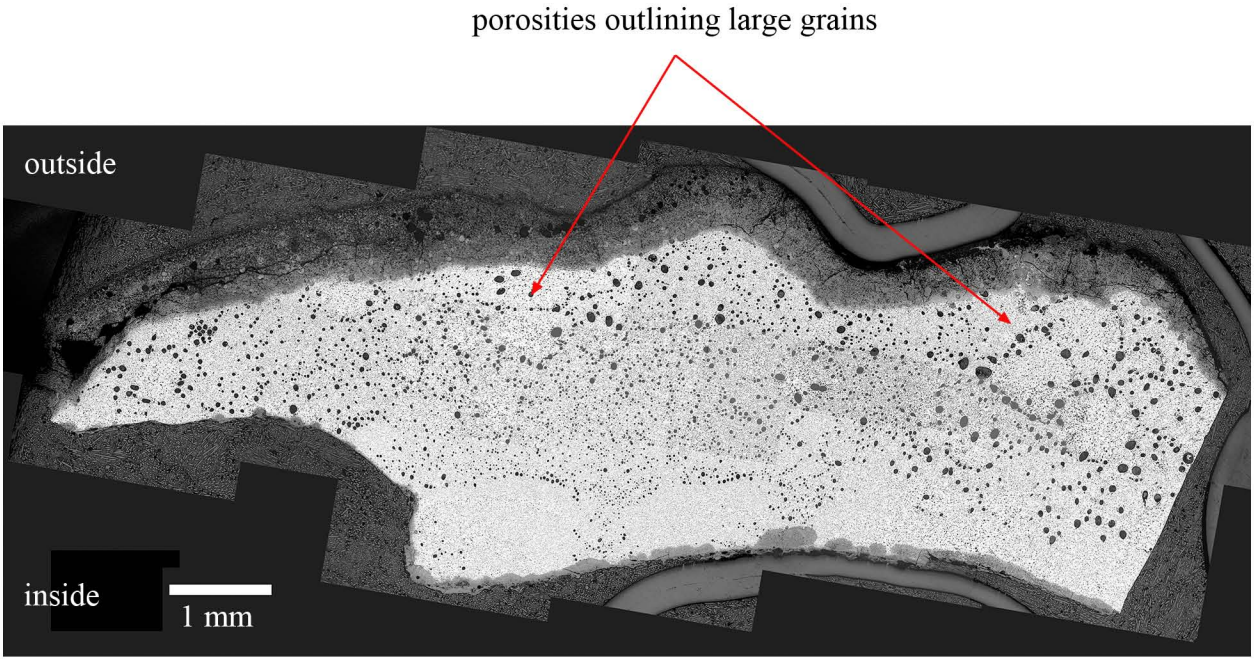

Figure 5.3.4.v: Segmented ring belt attachment (MIT 5350/Peabody 40-77-40/13488). Longitudinal cross section, as polished. The segments and grooves can be seen outlined in the external corrosion product. Other microstructural features of interest include large spherical porosities filled with lead. The porosities appear to outline large grains. (MIT Images 5350b-01-21).

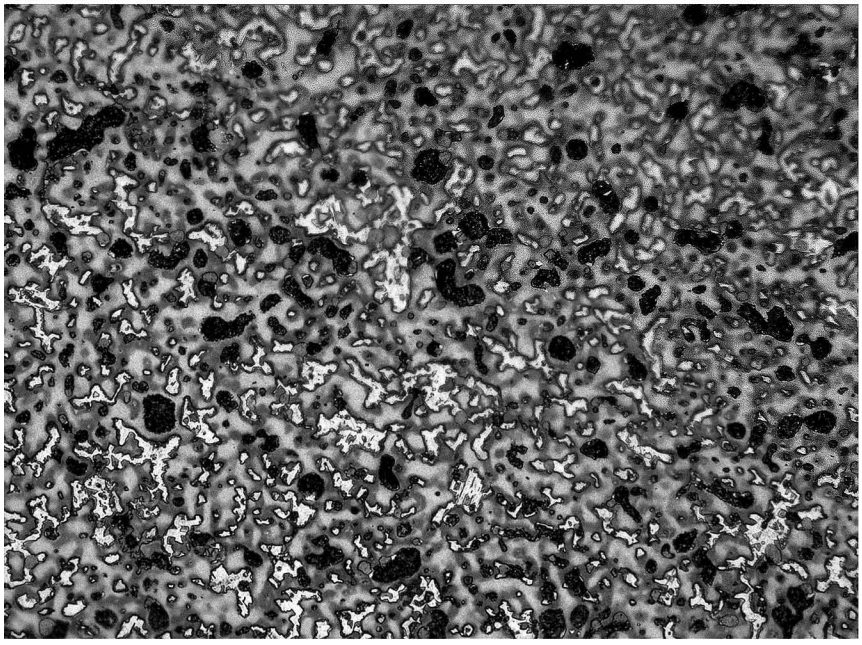

Figure 5.3.4.vi: Segmented ring belt attachment. (MIT 5350/Peabody 40-77-40/13488). Longitudinal cross section. Etch: 3 sec potassium dichromate and 1 sec ferric chloride. x500. Microstructural features of interest include highly cored dendrites surrounded by eutectoid, which appears bright in the photomicrograph, and large, spherical porosities filled with lead, which appears black in the photomicrograph. (MIT Image 5350b-22).

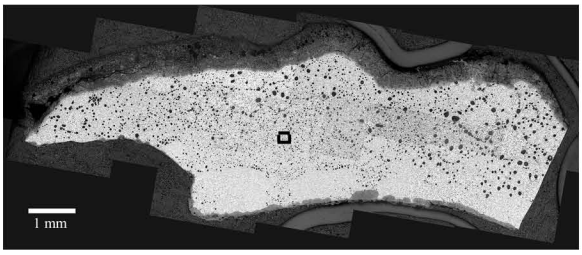

5.3.5: Additional Belt Plates and Attachments

5.3.5a: Incised belt plate (Peabody 40-77-40/13332)

This large, incised belt plate (Figure 5.3.5.i) came from Grave 16 of Tumulus IV. It is made of thin bronze sheet and has incised lines decorating its outer edges. The holes which once held the attached rivets are still intact on one side of the belt plate. These holes have edges that flare to the opposite side of the plate, indicating that they were punched through the sheet prior to insertion of the rivets.

Grave 16 was unusually rich in iron weapons, and it contained horse bones. It is oriented east-west and was 1.8 m below the surface of the tumulus. Its dimensions are 3.5 x 1.3 x 0.7 m. The four walls were lined with 21 stones. At the foot end of the grave were two iron spearheads and an iron celt. At the head end were bones from an adult horse, including teeth, hooves, and foot bones. Also associated with the grave were two urns with lids (Wells 1981).

5.3.5b: Belt attachment (Peabody 40-77-40/13350)

This bronze belt attachment (Figure 5.3.5.ii) from Grave 18 is comprised of a thin bronze sheet folded in half and secured with iron rivets. It has a hole in its center which may at one point have held a rivet. This attachment is one of the few bronze objects at Stična with components of wrought iron. Bronze fibulae from other Early Iron Age Slovenian sites like S. Lucia were sometimes repaired with iron rivets (Giumlia-Mair 1995), and the navicular fibula discussed in Section 5.2.3 also contains an iron rivet. However, it is unclear if the iron rivets here indicate a repair or if they were part of the piece originally.

Associated grave goods included several other fragments of belt attachments, two segmented ring belt attachments, one with small bits of leather still adhering to it, two pairs of bronze tweezers (MIT 5329 and MIT 5333, discussed in Sections 5.4.1 and 5.4.2 respectively), and some pottery sherds (Wells 1981).

5.3.5c: Belt attachment (Peabody 40-77-40/13407)

This bronze belt attachment (Figure 5.3.5.iii) from Grave 27 consists of a handle-like object attached to metal sheets via riveting. The two ends of the handle serve as the rivets. The exterior sheet is circular and appears to be intact. It most likely served to hold the interior sheet and the handle in place together.

Wells describes this object as a "three-sided ornament on a fragmentary belt attachment" (1981). This type of belt attachment is unique in the Mecklenburg collection from Stična. Associated belt attachments included a "weapon" ring, discussed below in Section 5.3.5d, and an additional sheet bronze belt attachment with rivets. Other grave goods included iron knives, a bronze "lump" (MIT 5347, discussed in Section 5.4.7), a fragment of a bronze ring and several fibula fragments.

5.3.5d: "Weapon" ring belt attachment. (Peabody 40-77-40/13408)

This circular bronze ring (Figure 5.3.5.iv) from Grave 27 was found in association with the belt attachment discussed above. It is described by Wells as a "weapon" ring (Wells 1981), and it would have been used to suspend weapons or other objects from the belt. Four of the six graves with belt plates and belt attachments in Tumulus IV have similar circular rings.

5.3.5e: Iron hook belt attachment

This hook belt attachment (Figure 5.3.5.v) from Grave 10 is made from wrought iron. It was found in association with the belt plate and attachment assemblage discussed in Sections 5.3.1 and 5.3.4. It is the only iron hook found in the Mecklenburg excavations at Stična.

5.3.5f: Hollow hook/loop belt attachment (Peabody 40-77-40/13467)

This hollow hook/loop belt attachment (Figure 5.3.5.vi) came from Grave 36. It is made from bronze sheet folded over on itself and curved to make a hollow hook/loop. It was attached to the belt plate with a bronze rivet.

This hollow hook was associated with the solid hook attachment shown in Figure 5.3.3.iii and with a circular bronze ring similar to the "weapon" ring discussed above.

Other associated grave goods included an urn and 30 blue glass beads (Wells 1981). A similar hollow hook/loop was found in Grave 10.

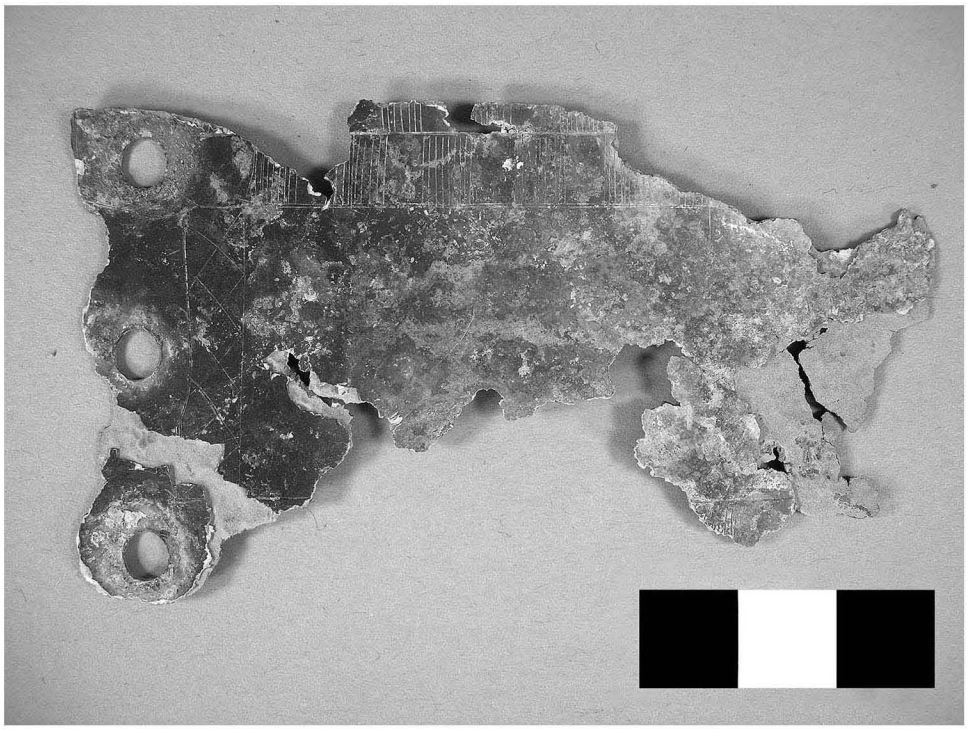

Figure 5.3.5.i: Incised belt plate. (Peabody 40-77-40/13332).
This belt plate comes from Grave 16 and is comprised of thin bronze sheet. Incised decorations surround the edges of the plate. The holes which once held bronze rivets are also visible. Photograph by E. Cooney.

Figure 5.3.5.ii: Belt attachment (Peabody 40-77-40/13350). This belt attachment from Grave 18 consists of a single sheet of bronze folded in half. The two halves are fasted together with iron rivets. Photograph by E. Cooney.

Figure 5.3.5.iii: Belt attachment. (Peabody 40-77-40/13407). This belt attachment from Grave 27 consists of a bronze handle-like object attached to metal sheets via riveting. The two ends of the handle serve as the rivets. The exterior sheet is circular and appears to be intact. It most likely served to hold the interior sheet and the handle in place together. Photograph by E. Cooney.

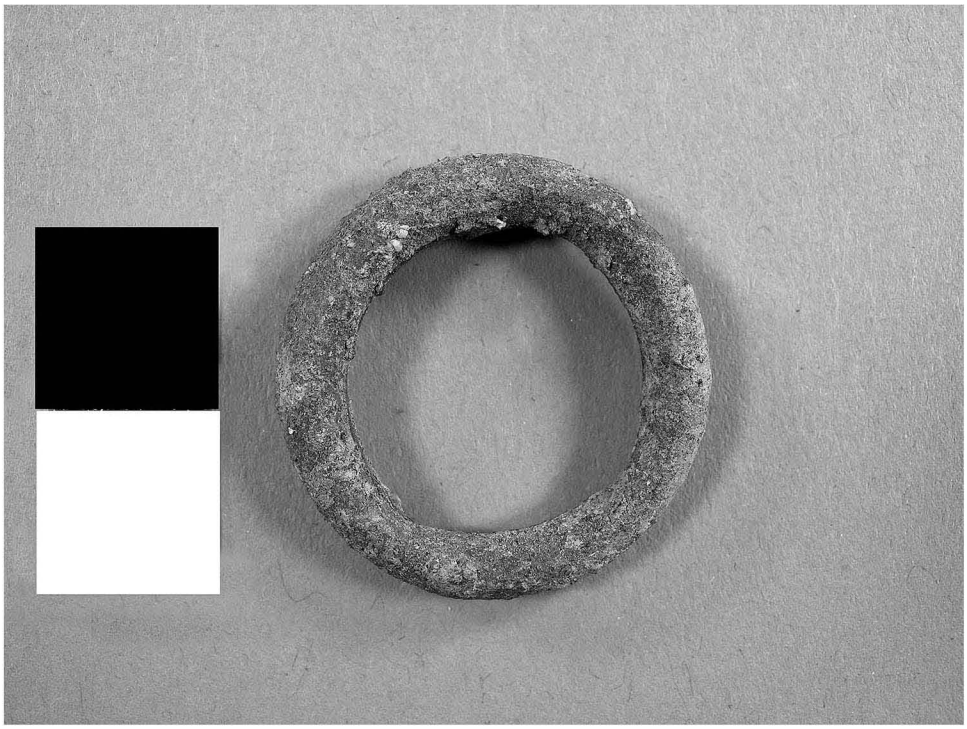

Figure 5.3.5.iv: "Weapon" ring belt attachment. (Peabody 40-77-40/13408). This circular bronze ring belt attachment was found in Grave 27. Photograph by E. Cooney.

Figure 5.3.5.v: Iron hook belt attachment. (Peabody 40-77-40/13303). This hook belt attachment from Grave 10 is wrought from iron. Photograph by E. Cooney.

Figure 5.3.5.vi: Hollow hook/loop belt attachment. (Peabody 40-77-40/13467). This hollow hook/loop belt attachment comes from Grave 36. It is made from bronze sheet folded over on itself and curved to make a hollow hook/loop. It was attached to the belt plate with a bronze rivet. Photograph by E. Cooney.

5.4: Miscellaneous Objects

There are many bronze objects in the Mecklenburg collection from Stična that do not fall into the categories of rings, fibulae, and belt plates and attachments. Many of these are jewelry items such as necklaces, pendants, beads, earrings, and earring wire. Other bronze objects, though most likely still serving a decorative and/or ritual function, are warfare related: sheet bronze helmets, including a double crested helmet, weapon sockets, a bronze cuirass, and horse bridal knobs. Other miscellaneous bronze objects include several vessels made from sheet bronze, a solid bronze figurine, nails, clamps, spatulas, hundreds of bronze buttons, and lumps of metal or ingots.

Tumulus IV does not contain a representative example of every type of bronze object found during the Mecklenburg excavations at Stična, so many important types of objects such as helmets, vessels made from sheet bronze, and utilitarian objects like nails were not analyzed.

Seven "miscellaneous" objects from Tumulus IV were sampled. These objects include two spatulas (Sections 5.4.1 and 5.4.2), an earring (Section 5.4.3), earring wire (Section 5.4.4), earring spirals (Section 5.4.5), buttons (Section 5.4.6), and a metal lump or ingot (Section 5.4.7). Several additional objects not available for sampling are discussed in Section 5.4.8.

The spatulas and the metal lump were sampled for bulk compositional analysis only. The earring wire, spirals, and buttons were sampled for both metallographic analysis and bulk compositional analysis. The earring was sampled for metallographic analysis with compositional analysis on the electron microbeam probe.

5.4.1: Tweezers (MIT 5329/Peabody 40-77-40/13353)

5.4.1a: Provenance and Background

MIT 5329 (Figure 5.4.1.i), identified by Wells as a fragmented pair of tweezers (1981), came from Grave 18. Grave 18 contained a burned area, and no skeletal remains were recorded.

Associated grave goods included a fragment from a second pair of tweezers (MIT 5333, discussed below in Section 5.4.2), an assemblage of belt plates and attachments (discussed in Section 5.3.5b), an iron celt, and pottery sherds from a brown vessel.

The two tweezers from Grave 18, MIT 5329 and MIT 5333, are the only two tweezers from Tumulus IV. One other pair of tweezers was found during Mecklenburg's excavations at Stična. The only mention of tweezers at S. Lucia is a small, nonfunctional pair attached to a dragon fibula (Giumlia-Mair 1995; Giumlia-Mair 1998).

5.4.1b: Initial Examination and Observations

The fragmented tweezers were photographed (Figure 5.4.1.i), drawn to scale, measured, and observed (Figures 5.4.1.ii and 5.4.1.iii).

The pair of tweezers has broken into two blade fragments. They do not appear to fit together exactly, indicating that the hinge section of the tweezers is missing. Neither fragment has an intact tip or portion of the hinge. Both Fragment A and B have incised lines decorating the blade. These lines are faint and are best seen under low magnification. Fragment A has a crack running transversely across the blade at the end opposite the tip. The crack does not go all the way through the thickness of the fragment.

Fragment A is 56.7 mm long, 13.2 mm wide and 0.7 mm thick at the end nearest the tip and 5.1 mm wide, and 2.2 mm thick at the end nearest the hinge. It weighs 4.1 g. Fragment B is 67.5 mm long, 15.7 mm wide and 0.9 mm thick at the end nearest the tip, and 4.8 mm wide and 2.3 mm thick at the end nearest the hinge. It weighs 5.6 g.

The areas near what would have been the hinge of the spatula are structurally robust, but the thin areas close to the tips of the fragments are fragile and appear to be completely mineralized. The fragments are covered in a dark green and brown mottled corrosion product.

5.4.1c: Sampling

Sample MIT 5329 was removed from Fragment A transversely at the hinge end for bulk compositional analysis (Figure 5.4.1.iv). During sampling the fragment fractured along the crack present at this location. The cut sample revealed that the crack had been caused by a flaw in the casting of the tweezers; there was a large internal cavity 2.5 mm wide and 1 mm high in the metal right at the crack. Despite the crack the metal was still fairly metallic and was light gold in color.

5.4.1d: Bulk Composition Analysis

Bulk composition analysis shows that the pair of tweezers is a copper-tin-lead alloy with primary alloying elements of tin at a concentration of 7.5 weight percent and lead at 6.47 weight percent. The alloy is a highly leaded tin bronze. Other minor elements include As (0.204%), Sb (0.13%), Ni (0.058%), Ag (0.071%), Co (0.027%), and Fe (0.16%). Bulk compositional analysis data are shown in Table 5.4.1 and in the Appendix.

Table 5.4.1: Bulk Compositional Analysis Data for MIT 5329

	Sn	**Pb**	**Sb**	**As**	**Ni**	**Co**	**Ag**	**Fe**
ICP-ES	7.55	6.47	0.13	0.204	0.058	0.027	n.a.	0.008
INAA	7.22	n.a.	0.120	0.175	0.0749	0.0317	0.071	0.16

(values in weight %) n.a. = not analyzed n.d. = not determined

5.1.4e: Conclusions

- The alloy comprising the pair of tweezers is a copper-tin-lead alloy with tin and lead concentrations of 7.5 and 6.47 weight percent respectively.
- The high level of lead indicates that the alloy was not designed to be hammered extensively nor to be particularly hard. This suggests that the tweezers were not intended for actual use.
- The large internal shrinkage cavity indicates that the tweezers were at least cast somewhat to shape. It also indicates that the tweezers were not hammered extensively near the hinge end as the casting flaw would have been exposed upon hammering.

Figure 5.4.1.i: Tweezers. (MIT 5329/Peabody 40-77-40/13353).
Photograph by E. Cooney.

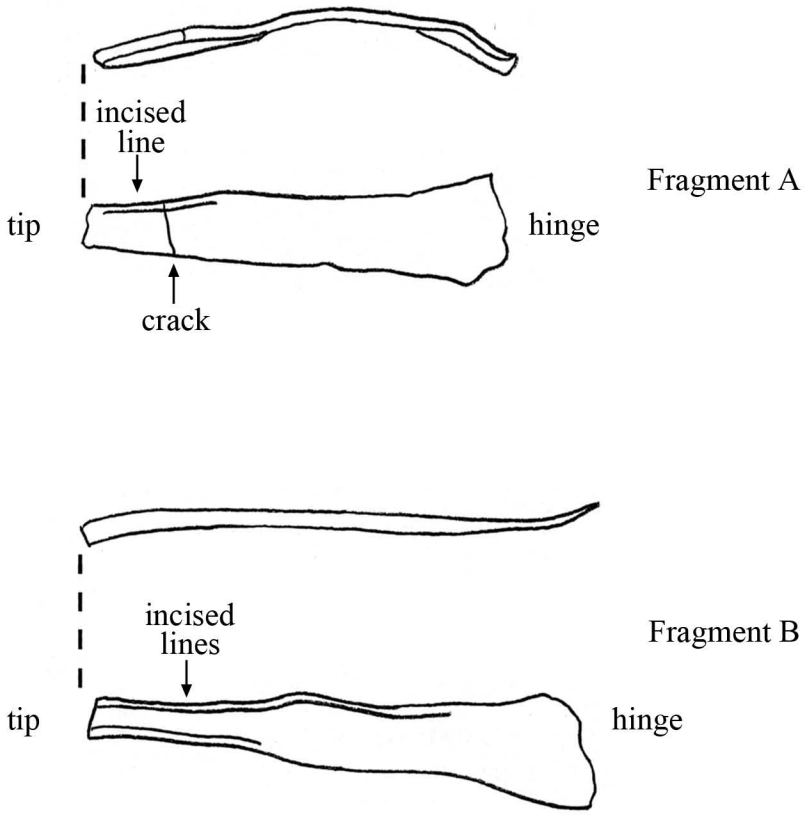

Figure 5.4.1.ii: Tweezers (MIT 5329). Key object features.

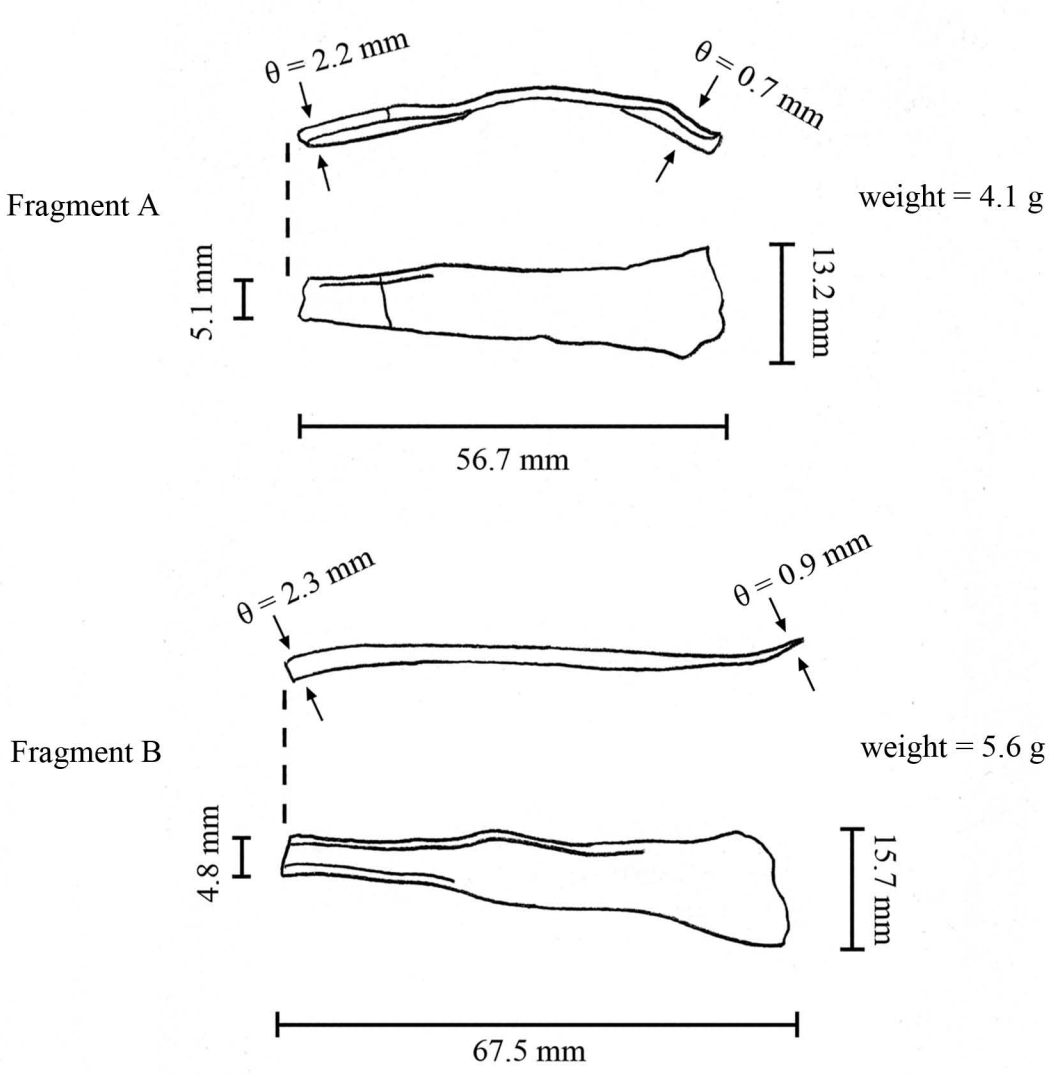

Figure 5.4.1.iii: Tweezers. (MIT 5329). Drawing and measurements.

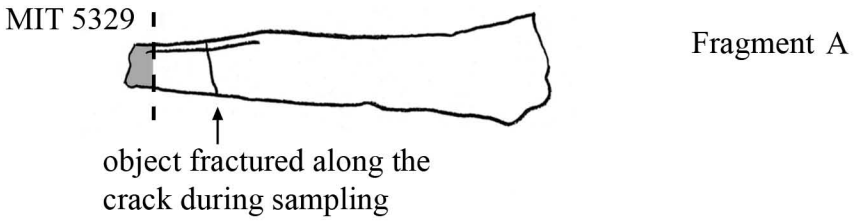

Figure 5.4.1.iv: Tweezers (MIT 5329). Sample MIT 5329 was removed for bulk compositional analysis.

5.4.2: Tweezers (MIT 5333/Peabody 40-77-40/13354)

5.4.2a: Provenance and Background

MIT 5333 (Figure 5.4.12.i), identified by Wells as a fragmented pair of tweezers (1981), came from Grave 18. It was associated with MIT 5329 (Section 5.4.1) and the same grave assemblage from Grave 18.

5.4.2b: Initial Observation and Background

The fragmented tweezer was photographed (Figure 5.4.2.i), drawn to scale, measured, and observed (Figures 5.4.2.ii and 5.4.2.iii). MIT 5333 is one fragmented half of a pair of tweezers. It is highly corroded and appears to be metallic only at its tip end. Its hinge end is fractured and bent at a high angle to the rest of the body. It is covered with friable dark green and brown accretions and friable corrosion product. At the tip end two incised decorative lines can be seen under low magnification.

The fragmented half is 65.8 mm long, 22.7 mm wide and 1.7 mm thick at the point nearest the hinge, and 6.6 mm wide and 2.2 mm thick at the tip end. It weighs 9.0 grams.

5.4.2c: Sampling

The tweezer fragment was sampled adjacent to its hinge end (Figure 5.4.2.iv). Care was taken to avoid the incised decoration and the highly corroded area adjacent to the sample. Sample MIT 5333 was taken for bulk compositional analysis. The sample was taken from a highly metallic area and the metal was light gold in color

5.4.2d: Bulk Compositional Analysis

Bulk compositional analysis shows that the tweezer is a copper-tin-lead alloy with primary alloying elements of tin at a concentration of 4.79 weight percent and lead at 3.5 weight percent. The alloy is a leaded, low tin bronze. Other major and minor elements include, Fe (0.61%), Sb (0.348%), As (0.253%), Ni (0.200%), Ag (0.200%), and Co (0.0219%). Bulk compositional analysis data are shown in Table 5.4.2 and in the Appendix.

Table 5.4.2: Bulk Compositional Analysis Data for MIT 5333

	Sn	Pb	Sb	As	Ni	Co	Ag	Fe
ICP-ES	4.79	3.5	0.341	0.253	0.195	0.016	n.a.	0.14
INAA	4.69	n.a.	0.348	0.225	0.200	0.0219	0.200	0.61

(values in weight %) n.a. = not analyzed n.d. = not determined

5.4.2e: Conclusions

- The alloy comprising the pair of tweezers is a copper-tin-lead alloy with tin and lead concentrations of 4.79 and 3.5 weight percent respectively. The alloy is a leaded, low tin bronze.
- The low tin content of the alloy made these tweezers relatively soft and elastic. . The tweezers may have been designed to bend together easily and to separate again in order to grasp an object, but the softness of the alloy may not have imparted sufficient hardness to the tweezers for regular use and the grasping of hard objects.
- MIT 5333 has an alloy composition very different from that of its companion pair of tweezers in Grave 18, MIT 5329. MIT 5333 has tin and lead concentrations approximately three weight percent less than the concentrations of both elements in MIT 5329, which has a tin concentration of about 7.5 weight percent and a lead concentration of about 6.5 weight percent.

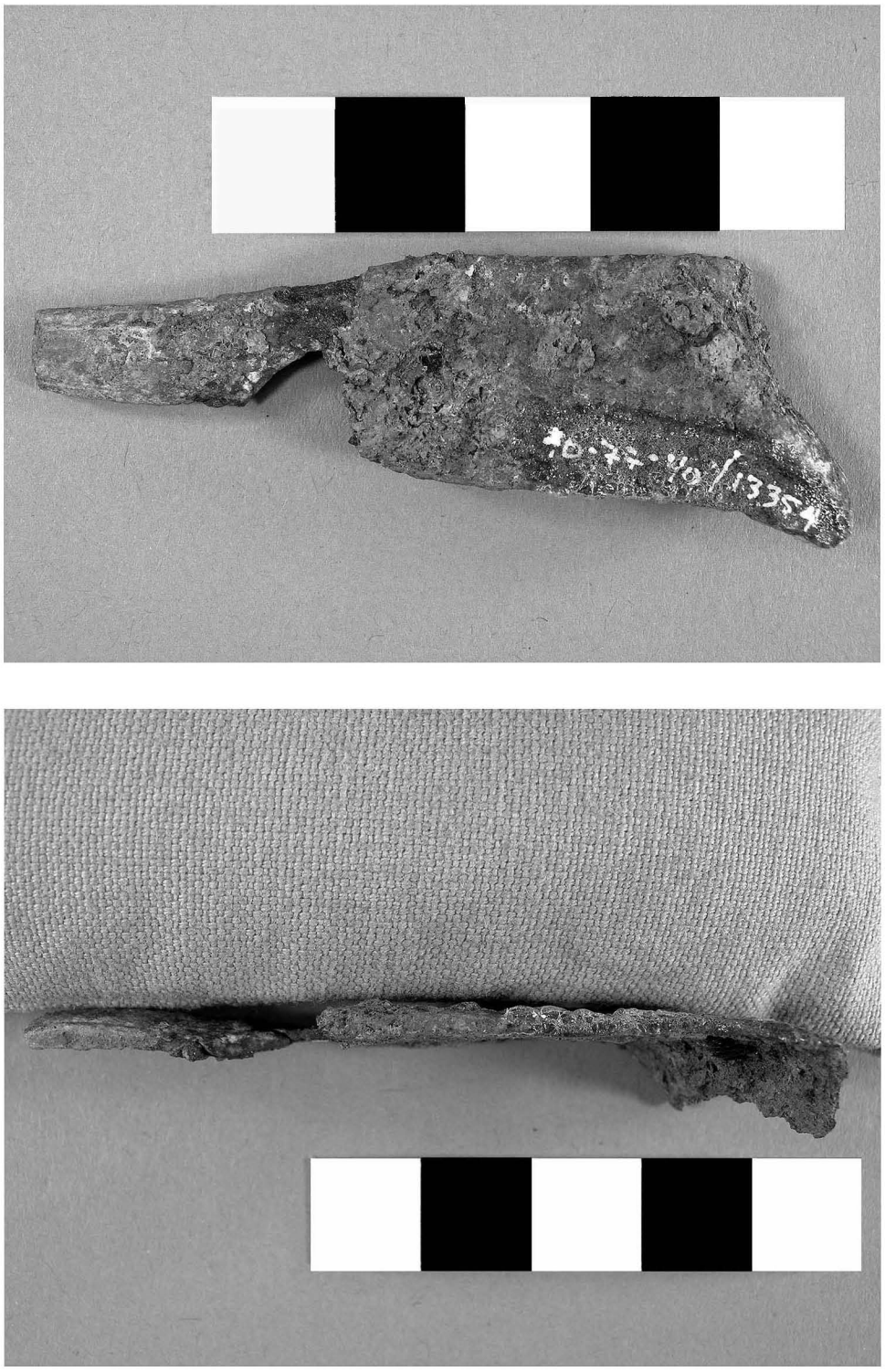

Figure 5.4.2.i: Tweezers. (MIT 5333/Peabody 40-77-40/13354).
Photograph by E. Cooney.

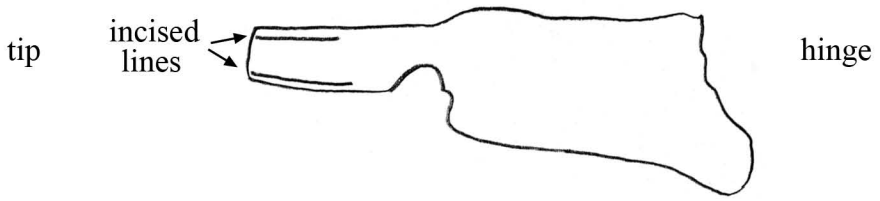

Figure 5.4.2.ii: Tweezers (MIT 5333). Key object features.

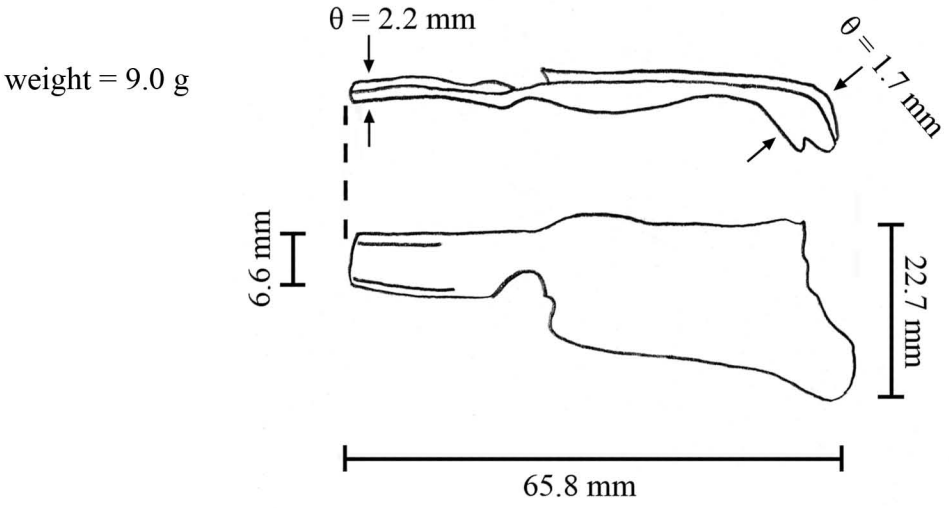

Figure 5.4.2.iii: Tweezers (MIT 5333). Drawing and Measurements.

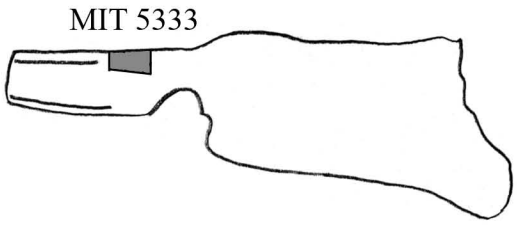

Figure 5.4.2.iv: Tweezers (MIT 5333). Sample MIT 5333 was removed for bulk compositional analysis.

5.4.3: Earring (MIT 5367/Peabody 40-77-40/13387)

5.4.3a: Provenance and Background

MIT 5367 (Figure 5.4.3.i), a fragmented earring, came from Grave 22 (Wells 1981). Grave 22 was 3.5 m long, 0.9 m wide, and was 1.1 m below the surface of the tumulus. Seventy-two amber beads and at least three, similar, badly preserved earrings were recovered from Grave 22. These earrings are described by Wells as " band earrings decorated with repoussé lines and dots" (1981:60).

5.4.3b: Initial Examination and Observations

The fragmented earring was photographed (Figure 5.4.3.i), drawn to scale, measured, and observed (Figures 5.4.3.ii and 5.4.3.iii).

The earring is broken into several very small, highly mineralized fragments. These fragments are mostly small pieces of thin sheet decorated with repoussé lines and dots. Two fragments are diagnostic. One diagnostic fragment consists of thin sheet folded into a tube to create a long, curved earring wire. A hole in a completely mineralized portion of the wire shows that the wire is hollow. The other diagnostic fragment appears to be part of the earring catch; it contains a small hole through which the earring wire would have been placed to secure the earring in place in the ear.

The fragment of sheet with the earring wire is highly mineralized and weighs 0.6 g. At its widest point the fragment is 3.5 mm long, and the sheet is 0.3 mm thick. The earring wire is 1.2 mm thick. The earring catch plate is also highly mineralized. It is 16.9 mm long, 8.0 mm wide, and the sheet is 0.4 mm thick. The catch hole has a diameter of 1.7 mm. The catch plate weighs 0.3 g.

5.4.3c: Sampling

The earring wire was sampled with two transverse cuts for metallographic analysis (Figure 5.4.3.iv) and was mounted transversely as noted. Composition analysis was carried out with the electron microbeam probe.

5.4.3d: Metallographic and Electron Microbeam Probe Analyses

The transverse cross section of the earring wire shows that the wire is a hollow tube made from a single piece of sheet folded over onto itself (Figure 5.4.3.v). The sheet is very thin; it is less than 200 microns thick. Microstructural features of interest include a medium density of porosities and gray copper sulfide inclusions oriented parallel to the longitudinal axis of the sheet comprising the earring.

The as-polished sample was analyzed with an electron microbeam probe to determine its composition. The composition of a series of five points across the longitudinal section whose locations are indicated in Figure 5.4.3vi was determined, and the average value of the six is given in the table in Figure 5.4.3.vi. The average composition of the earring is given below in Table 5.4.3.

Table 5.4.3: Average Composition of MIT 5367

	Cu	**Sn**	**Pb**	**Sb**	**As**	**Ni**	**Co**	**Ag**	**Fe**
Average	91.76	7.61	0.164	n.d	0.028	0.017	0.007	n.d	0.028

(all values in weight %) n.d.= not determined

The earring is a tin bronze with tin present at a concentration of 7.61 weight percent. Lead was not purposefully added to the alloy.

The earring was etched for three seconds with potassium dichromate and for one second with aqueous ferric chloride to reveal flow lines, elongated areas of compositional inhomogeneities, oriented parallel to the longitudinal axis of the sheet (Figure 5.4.3.vii). These flow lines indicate that the sheet was heavily worked perpendicular to its longitudinal axis. Other microstructural features of interest include equiaxed grains with annealing twins and a high density of deformation lines (Figure 5.4.3.viii).

5.4.3e: Discussion

The earring wire is made from thin sheet less than 200 microns thick rolled into a hollow tube. The wire is a tin bronze with a tin concentration of 7.61 weight percent; it was not purposefully alloyed with lead. The concentration of tin present in the sheet's alloy would have made the sheet hard but still malleable and flexible. This combination of mechanical properties is ideal for an earring wire that would have been subject to frequent bending as the earring was placed in and removed from the earlobe.

The earring's microstructure shows that it was subject to several cycles of working and annealing to reduce the sheet to its desired thinness. It was left in a worked condition, most likely to harden the sheet.

5.4.3f: Conclusions

- The earring wire is made from thin sheet less than 200 microns thick rolled into a hollow tube.
- The earring is a tin bronze with a tin concentration of 7.61 weight percent.
- The thin sheet comprising the earring was subject to several cycles of working and annealing to reduce the sheet to its desired thinness, and it was left in a worked condition.

Figure 5.4.3.i: Earring. (MIT 5367/Peabody 40-77-40/13387).
Photograph by E. Cooney.

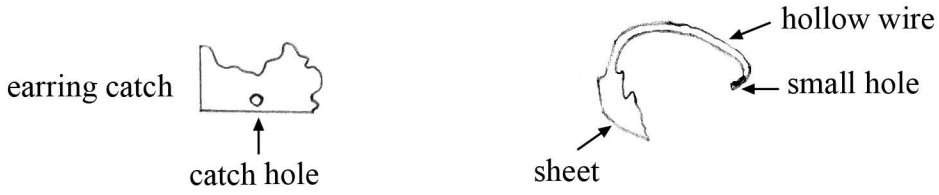

Figure 5.4.3.ii: Earring (MIT 5367). Key object features.

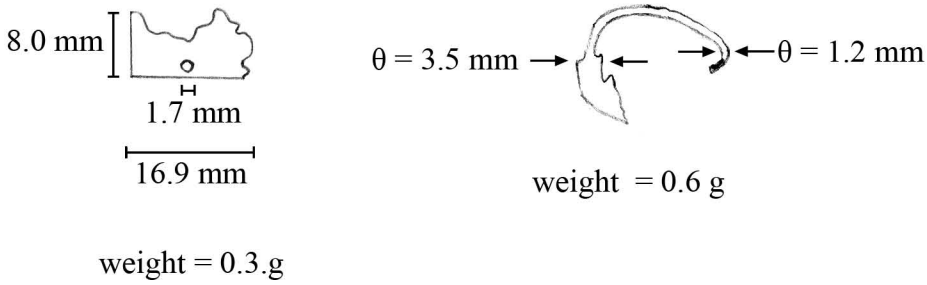

Figure 5.4.3.iii: Earring (MIT 5367). Drawing and measurements.

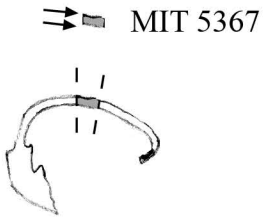

Figure 5.4.3.iv: Sample MIT 5367 was removed from the earring with transverse cuts and was mounted transversely as noted.

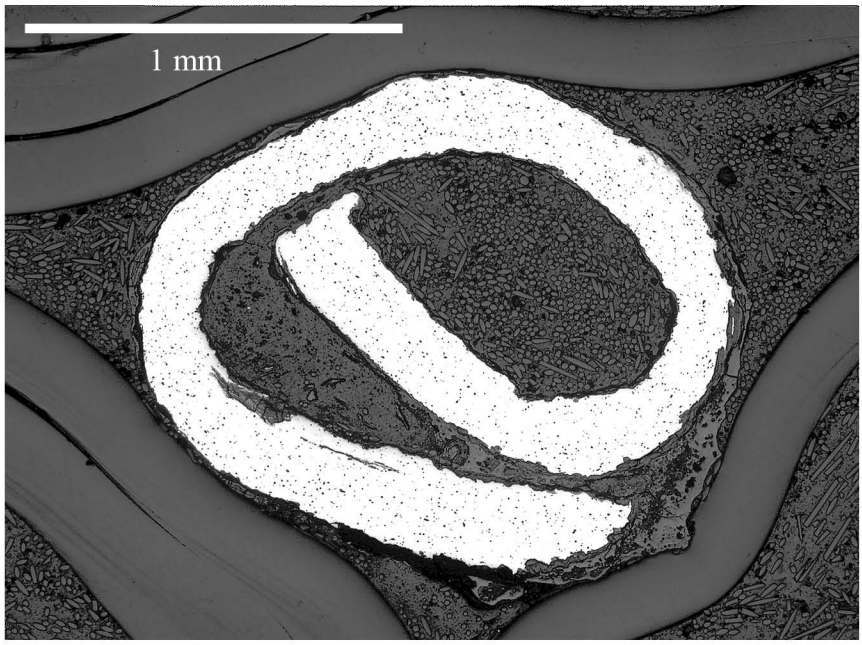

Figure 5.4.3.v: Earring (MIT 5367/Peabody 40-77-40/13387). Transverse cross section, as polished. x50. Microstructural features of interest include a medium density of porosities and gray copper sulfide inclusions oriented parallel to the longitudinal axis of the sheet comprising the earring. An elongated internal fracture can also be seen. (MIT Image 5367-01.)

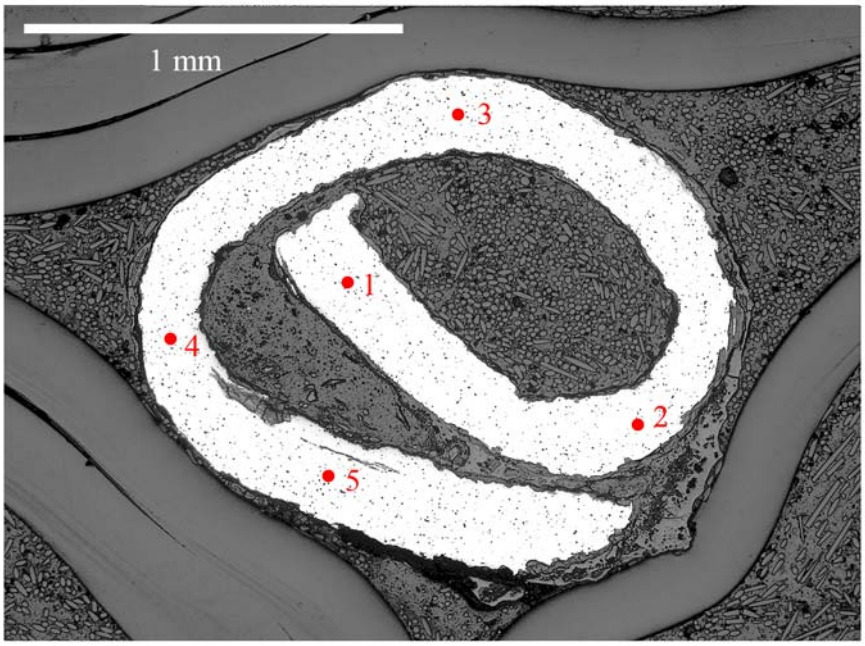

Electron Microbeam Probe Compositional Data

	Cu	Sn	Pb	Sb	As	Ni	Co	Ag	Fe
Pt 1	91.89	7.3	n.d.	n.d.	n.d.	0.034	n.d.	n.d.	0.016
Pt 2	91.73	8.1	0.114	n.d.	0.093	n.d.	0.033	n.d.	0
Pt 3	88.99	8.89	0.355	n.d.	0.048	n.d.	n.d.	n.d.	0
Pt 4	94.16	6.99	0.252	n.d.	n.d.	0.05	n.d.	n.d.	0.095
Pt 5	92.02	6.77	0.098	n.d.	n.d.	n.d.	n.d.	n.d.	0.028
Average	**91.76**	**7.61**	**0.164**	**n.d**	**0.028**	**0.017**	**0.007**	**n.d**	**0.028**

(all values in weight %) n.d.= not determined

Figure 5.4.3.vi: Earring (MIT 5367/Peabody 40-77-40/13387)
Above: Points at which compositional data were taken by the electron microbeam probe.
Below: Electron microbeam probe compositional data from each point.

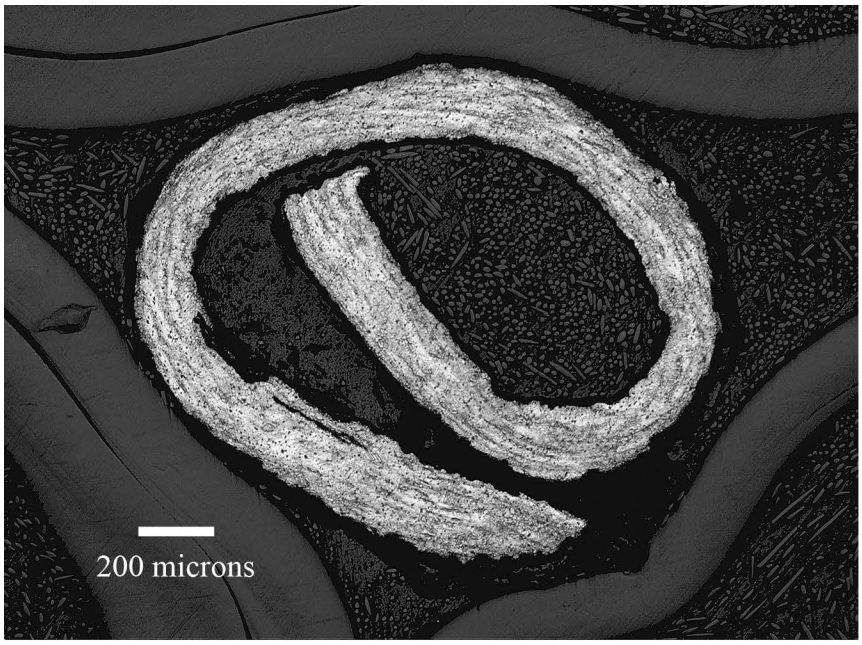

Figure 5.4.3.vii: Earring (MIT 5367/Peabody 40-77-40/13387). Transverse cross section. Etch: 3 sec potassium dichromate and 1 sec ferric chloride. x50. Microstructural features of interest include elongated areas of compositional inhomogeneities oriented parallel to the longitudinal axis of the sheet. (MIT Image 5367-04.)

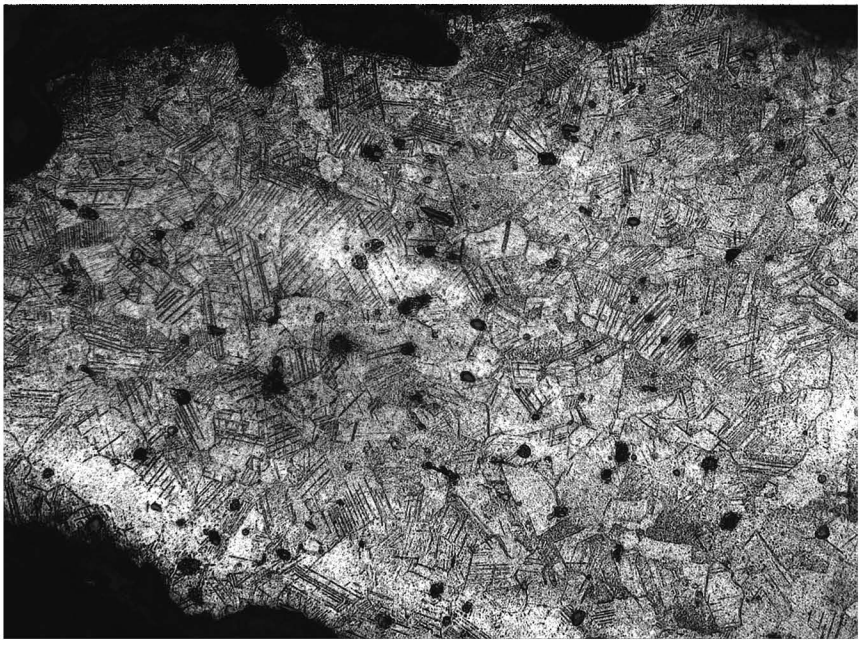

20 microns

Figure 5.4.3.viii: Earring (MIT 5367/Peabody 40-77-40/13387). Transverse cross section. Etch: 3 sec potassium dichromate and 1 sec ferric chloride. x500. Microstructural features of interest include equiaxed grains with annealing twins and a high density of deformation lines (MIT Image 5367-07.)

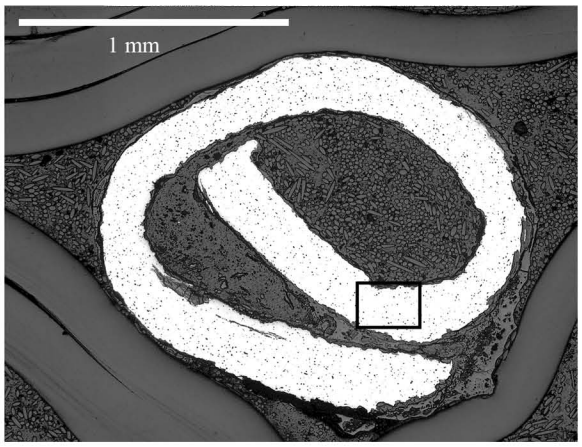

5.4.4: Earring Wire
(MIT 5337/Peabody 40-77-40/13450 and MIT 5351/Peabody 40-77-40/13451)

5.4.4a: Provenance and Background

MIT 5337 (Figure 5.4.4i) and MIT 5351 (Figure 5.4.4.ii) are two sets of fragmented earring wires from Grave 32 (Wells 1981). According to Wells, these sets of wire came from a pair of large earrings. Because they are associated with one single object they are discussed together here.

Grave 32 was an especially rich double grave, and it is discussed in detail in Section 5.3.2. Associated grave goods include the dragon fibula discussed in Section 5.2.6, the belt plate attachment discussed in Section 5.2.3, and the spirals discussed in Section 5.4.5. The sets of earring wire and the spirals may have been associated with the same set of earrings.

These sets of earring wire are unique in the Mecklenburg excavations at Stična.

5.4.4b: Initial Examination and Observations

MIT 5337 and MIT 5351 are two groups of fragmented bronze wire. MIT 5337, MIT 5351, and the specific wire fragments chosen for sampling were photographed (Figures 5.4.4.i and 5.4.4.ii), drawn to scale, measured, and observed (Figures 5.4.4.iii and 5.4.4.iv).

MIT 5337 consists of several fragments of twisted wire (Figure 5.4.4.i). Some of these fragments have a right-handed, S-twist, and others have a left-handed, Z-twist. A few of the fragments have been bent in half or have what appear to be looped ends, suggesting that, when intact, the object consisted of a single, long wire bent over on itself several times. The wire fragments are covered in a smooth layer of greenish corrosion product that has been chipped away in some areas to reveal the dark, oxidized metal surface beneath.

The fragment chosen for sampling is 60.1 mm long. Where the corrosion product has chipped away the wire is 1.1 mm thick; where the corrosion product is intact the wire is 1.5 mm thick. The wire fragment weighs 0.7 g.

MIT 5351 consists of several fragments of cylindrical wire. Two of these fragments have ends where the cylindrical wire is twisted together with a second piece of wire in a left-handed, Z-twist (Figure 5.4.4.ii). When observed under low magnification it is clear that original, cylindrical wire is twisted together with a second piece of wire to create the twist. The cylindrical wire fragments are all covered with a thick layer of greenish, smooth corrosion product, with the exception of the fragment chosen for sampling, which has been mostly cleaned of corrosion product.

The fragment chosen for sampling is comprised primarily of cylindrical wire with a second piece of flat wire twisted onto one end. This twist can be clearly seen because of the thick, bright green corrosion product that has formed in the juncture between the two twisted wires (Figure 5.4.4.ii). The wire fragment is 64.7 mm long and the twisted area of the wire is 19.4 mm long. The cylindrical wire is 1.3 mm thick; where the two wires are twisted together the resulting twist is 1.5 mm thick. The fragment weighs 1.2 g.

5.4.4c: Sampling

MIT 5337 was sampled three times (Figure 5.4.4.v). Sample MIT 5337a was removed for bulk composition analysis. Sample MIT 5337b was removed for metallographic analysis and was mounted longitudinally as noted. Sample MIT 5337c was removed for metallographic analysis and was mounted transversely as noted. The wire was highly metallic, and the metal was light gold in color.

MIT 5351 was also sampled three times (Figure 5.4.4.vi). Sample MIT 5351a was removed from the untwisted end of the fragment for bulk composition analysis. Sample MIT 5351b was removed for metallographic analysis and was mounted transversely as noted. Sample MIT 5351c was removed for metallographic analysis and mounted longitudinally as noted. The metal was highly metallic, and the metal was light gold in color.

5.4.4d: Bulk Composition Analyses

MIT 5337, the twisted earring wire, is a tin bronze with a tin composition of 10.5 weight percent. Other minor and trace elements include Fe (0.50%), Pb (0.492%), As

(0.222%), Sb (0.174%), Ni (0.171%), Ag (0.097%), and Co (0.04%). Bulk composition analysis data are shown below in Table 5.4.4.i and in the Appendix.

Table 5.4.4.i: Bulk Composition Analysis Data for MIT 5337 (Twisted Earring Wire)

	Sn	Pb	Sb	As	Ni	Co	Ag	Fe
ICP-ES	10.5	0.492	0.174	0.222	0.135	0.037	n.a.	0.314
INAA	10.1	n.a.	0.149	0.175	0.171	0.0401	0.097	0.50

(values in weight %) n.a. = not analyzed n.d. = not determined

MIT 5351, the cylindrical earring wire, is a tin bronze with a tin composition of 12.9 weight percent. Other minor and trace elements include Fe (0.47%), Pb (0.436%), Ni (0.137%), As (0.119%), Sb (0.115%), Co (0.089%), and Ag (0.061%). Bulk composition analysis data are shown below in Table 5.4.4.ii and in the Appendix.

Table 5.4.4.ii: Bulk Composition Analysis Data for MIT 5351 (Cylindrical Wire)

	Sn	Pb	Sb	As	Ni	Co	Ag	Fe
ICP-ES	12.9	0.436	0.115	0.119	0.094	0.078	n.a.	0.189
INAA	12.6	n.a.	0.104	0.114	0.1370	0.0886	0.061	0.47

(values in weight %) n.a. = not analyzed n.d. = not determined

5.4.4e: Metallographic Analyses

MIT 5337b and 5337c were mounted for metallographic analysis. The as-polished longitudinal and transverse cross sections are shown in Figure 5.4.4.vii. The outline of the twisted wire can be seen in the external corrosion product of the longitudinal cross section. The diamond-shaped transverse cross section with four distinct facets can be seen in the as-polished photomicrograph of sample MIT 5337c. Other microstructural features of interest include small porosities homogenously distributed throughout the sample. These porosities and elongated gray copper sulfide inclusions oriented parallel to the wire's longitudinal axis can be seen in the longitudinal cross section (Figure 5.4.4.viii). It is clear that the wire is made from one single, solid piece, and that it was worked extensively perpendicular to its longitudinal axis.

The longitudinal and transverse cross sections were both etched for four seconds with potassium dichromate and for two seconds with aqueous ferric chloride. The longitudinal cross section's microstructure is characterized by small, equiaxed grains

with annealing twins (Figure 5.4.4.ix). The transverse cross section's microstructure is characterized by clusters of small, equiaxed grains with annealing twins surrounded by larger equiaxed grains with annealing twins. The clusters of smaller grains are homogenously distributed throughout the sample (Figure 5.4.4.x). A low density of deformation lines is also present.

The wire was subject to several cycles of working and annealing to reduce it to its desired thickness and to twist it, and it was left in an annealed state. The low density of deformation lines most likely comes from use wear and/or bending of the wire into the final earring shape.

MIT 5351b and MIT 5351c were mounted for metallographic analysis. The as-polished longitudinal and transverse cross sections are shown in Figure 5.4.4.xi.

The longitudinal cross section shows two pieces of wire twisted together. The junctures between the wires can be seen in the corrosion product. The wire itself is highly corroded in a few areas. Small porosities are homogenously distributed throughout the wires, and elongated gray copper sulfide inclusions are aligned parallel to the angle of the twist.

The transverse cross section shows the two pieces of wire twisted together and the great difference in shape between the two wire components: one is roundish, and the other is flat. The larger, roundish wire is the cylindrical wire that was subject to bulk composition analysis. The thinner, flat wire is the piece mechanically twisted together with the cylindrical wire to create the composite twist. The juncture between the two wires can be seen in the corrosion product between the two. The smaller piece is more heavily corroded than the larger piece.

Sample MIT 5351c, the transverse cross section, was analyzed on the electron microbeam probe to determine the composition of the thinner piece of wire. The composition of a series of five points across the smaller piece whose locations are indicated in Figure 5.4.4.xii was determined, and the average value of the five is given in the table in Figure 5.4.4.xii. The average composition of the smaller wire piece is given below in Table 5.4.4.iii.

Table 5.4.4.iii: Average Composition of the smaller wire piece, MIT 5351

	Cu	Sn	Pb	Sb	As	Ni	Co	Ag	Fe
Average	88.57	12.71	0.139	n.d.	0.053	0.101	0.063	n.d.	0.224

(all values in weight %) n.d.= not determined

The thinner piece of wire is a tin bronze with an average tin composition of 12.7 weight percent. This composition is almost identical to the composition of the larger wire piece, indicating that the larger, cylindrical wire and the thinner piece of wire twisted with it are made from the same alloy. To insure that this twist was mechanical and not metallurgical, the juncture between the two wires was analyzed with the electron microbeam probe (Figure 5.4.4.xiii). The probe detected only copper-tin corrosion product at the juncture, indicating that the twist is a purely mechanical means of attaching two pieces of wire to each other.

The longitudinal and transverse cross sections were both etched for six seconds with potassium dichromate and for two seconds with aqueous ferric chloride. The longitudinal cross section's microstructure is characterized by small, equiaxed grains with annealing twins (Figure 5.4.4.xiv). The transverse cross section is also characterized by small, equiaxed grains; both the larger and smaller wire pieces have a similar microstructure (Figure 5.4.4.xv). Only a few deformation lines can be seen along the edges of the smaller piece of wire. Both pieces of wire were subject to several cycles of working and annealing. After they were twisted together the wire was annealed and it was left in an annealed state. The low density of deformation lines most likely comes from use wear and/or bending of the wire into the final earring shape.

5.4.4f: Discussion

MIT 5337 is a made of a tin bronze alloy with 10.5 weight percent tin. It has less than 0.5 weight percent lead. The wire was probably worked and annealed several times to reach its desired thickness. It was then twisted, and most likely annealed several times during twisting, as a 10.5 weight percent tin bronze is somewhat hard and brittle. The wire was left in an annealed state, and the few deformation lines present were probably caused by use wear and/or by bending the wire into its final configuration in the earring.

MIT 5351 consists of two wires twisted together. There is no trace of a metallurgical join between the two wire pieces, indicating that they were attached mechanically through twisting. The larger, cylindrical wire is a tin bronze with a tin composition of 12.9 weight percent. The alloy contains less than 0.5 weight percent lead. The thinner, flat wire has an average tin composition of 12.7 weight percent and a lead composition of less than 0.5 weight percent, almost identical to that of the larger wire.

These two pieces of wire are made of the same alloy, and the smaller piece of wire is probably a flattened piece of wire similar to the majority of the wire making up MIT 5351. If the twist were purely for decorative effect, a more effective use of the bronze metal would have been simply to twist the cylindrical wire as MIT 5337 was twisted. This leads to the conclusion that the twist served as a mechanical device to attach two separate pieces of wire together.

The two wires comprising MIT 5351 were worked and annealed several times to reach their desired thicknesses. They were then twisted together, annealed again, and left in an annealed state. The few deformation lines present in the wire are most likely caused by use wear and/or bending the wire into its final configuration in the earring.

MIT 5337 and MIT 5351 have slightly different alloy compositions. It is unclear if this was intentional, just as it is unclear how these two wire types were related to one another in the original earring. The slightly lower tin composition in MIT 5337 may have made it slightly easier to twist than MIT 5351.

5.4.4.g: Conclusions

- MIT 5337, the twisted earring wire, is a tin bronze with a composition of 10.5 weight percent tin. The wire was worked and annealed several times to reach its desired thickness. It was then twisted, annealed, and left in an annealed state.
- MIT 5351 consists of two wires mechanically twisted together. Both wires are made of a high tin bronze with approximately 13 weight percent tin. They appear to be made from the same alloy.
- The two wires that make up MIT 5351 were worked and annealed several times to reach their desired thicknesses. They were then twisted together, annealed again, and left in an annealed state.

- The twist found in MIT 5351 served as a mechanical device to attach two separate pieces of wire together.
- It is unclear how MIT 5337 and MIT 5351 were related to one another in the original earring.

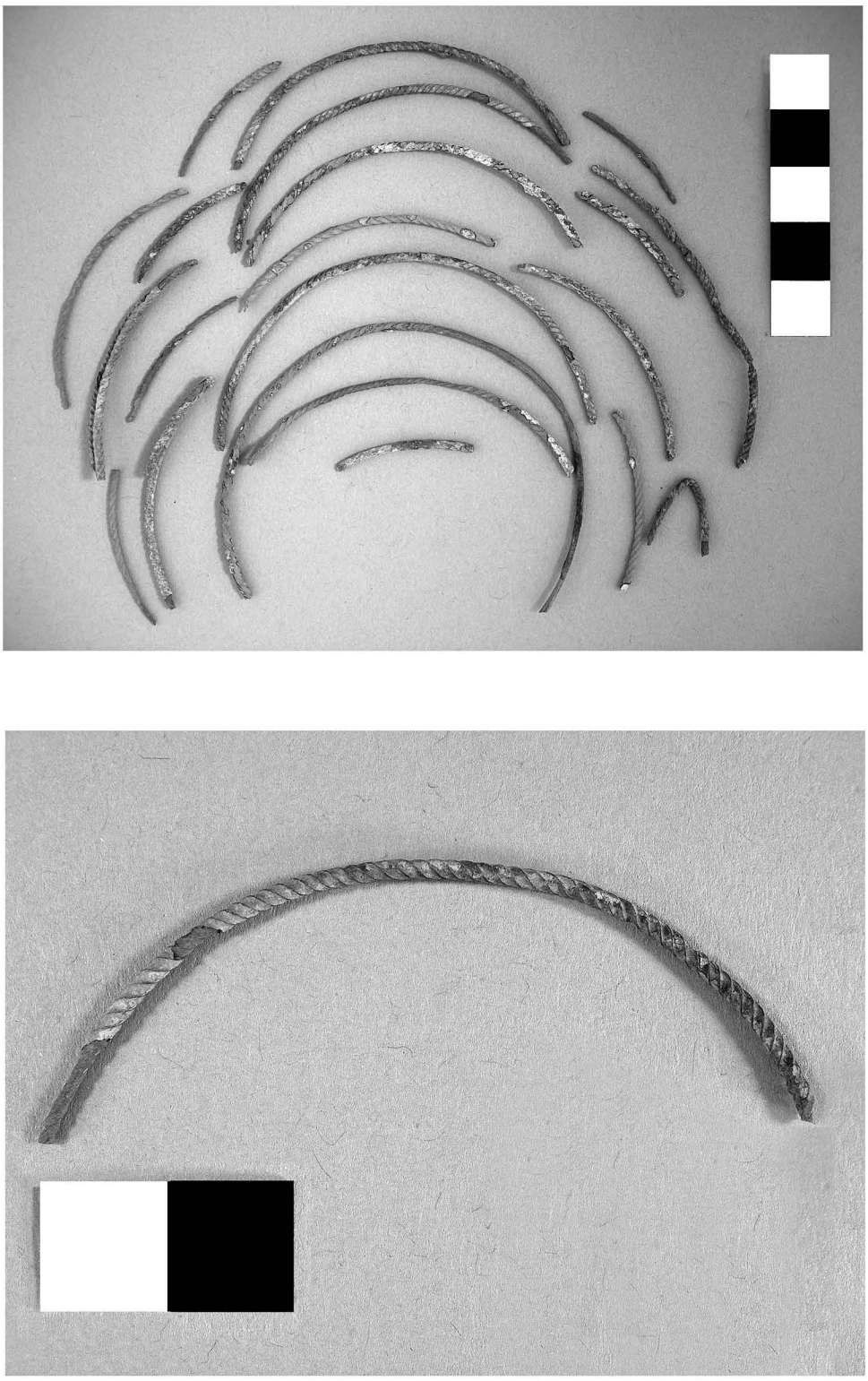

Figure 5.4.4.i: Earring wire (MIT 5337/Peabody 40-77-40/13450).
Above: Earring wire fragments. Below: Fragment chosen for sampling.
Photographs by E. Cooney.

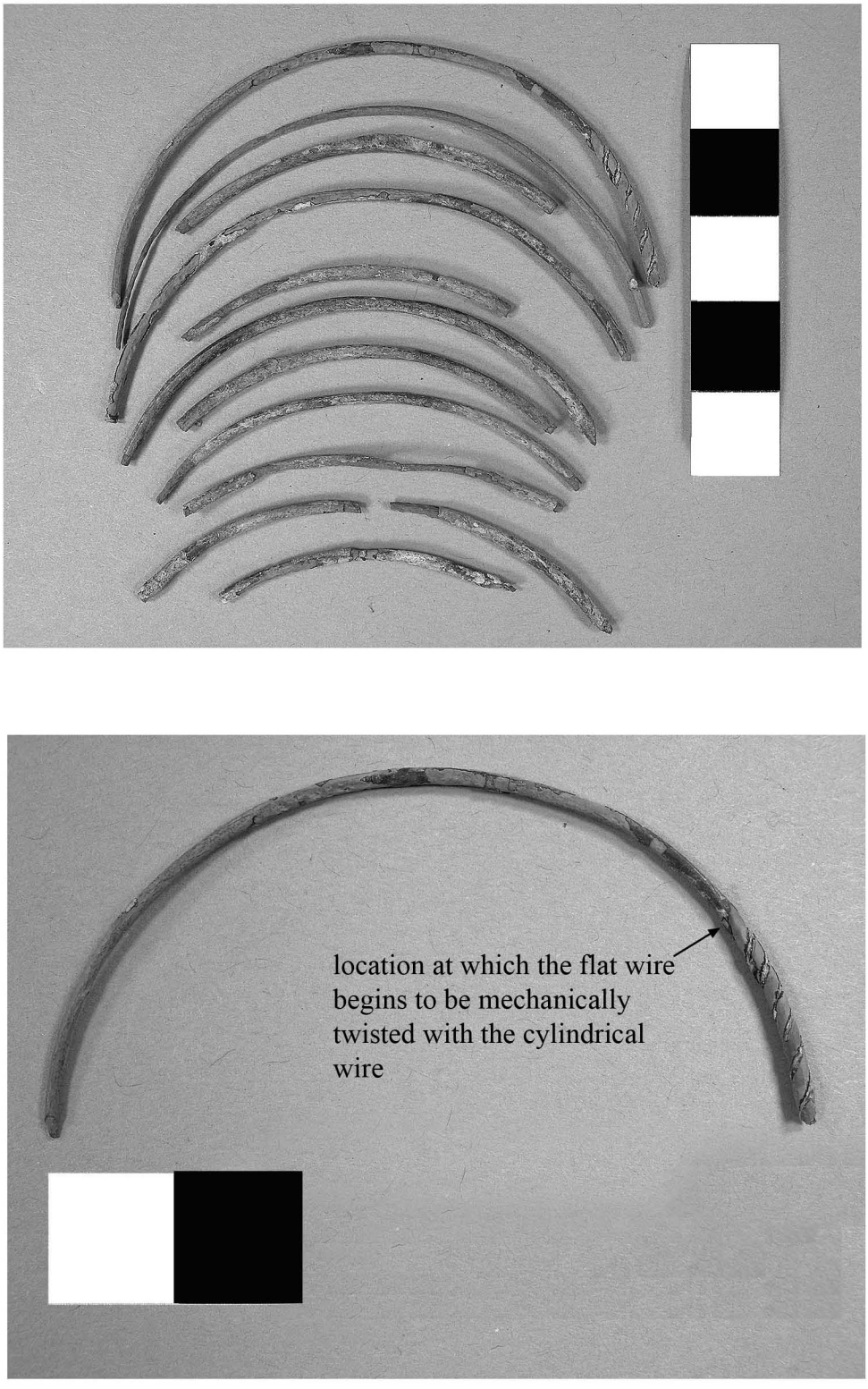

Figure 5.4.4.ii: Earring wire (MIT 5351/Peabody 40-77-40/13451).
Above: Cylindrical earring wire fragments. Below: Twisted fragment chosen for sampling.
Photographs by E. Cooney.

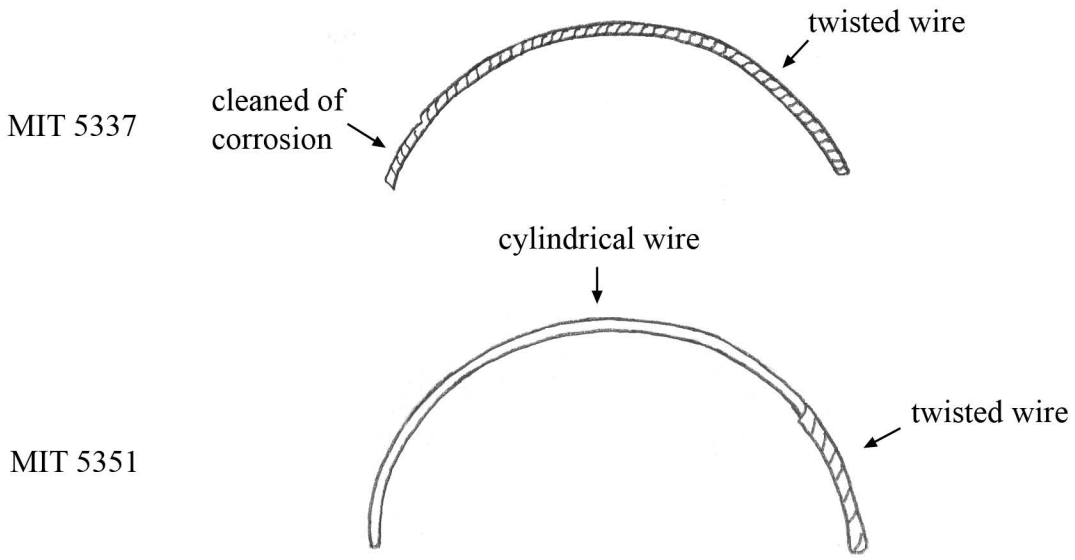

Figure 5.4.4.iii: Earring wire (MIT 5337 and MIT 5351). Key object features.

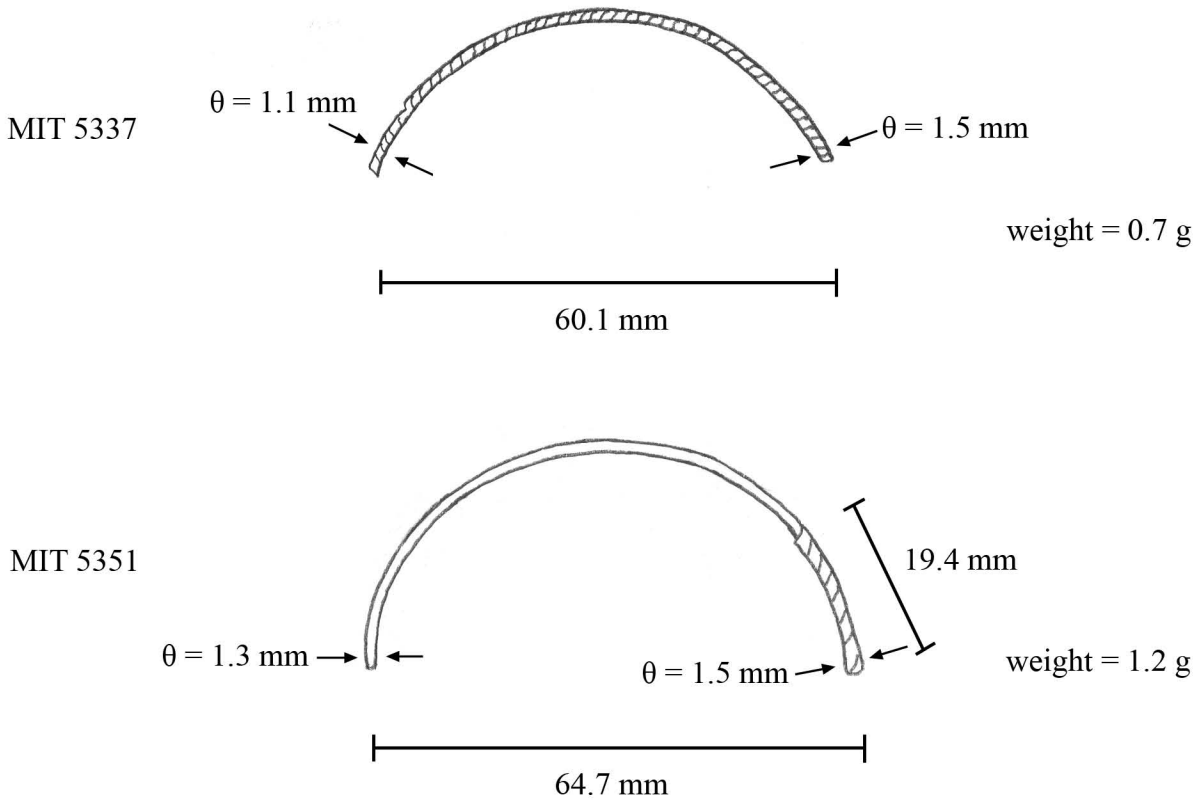

Figure 5.4.4.iv: Earring wire (MIT 5337 and MIT 5351). Drawing and measurements.

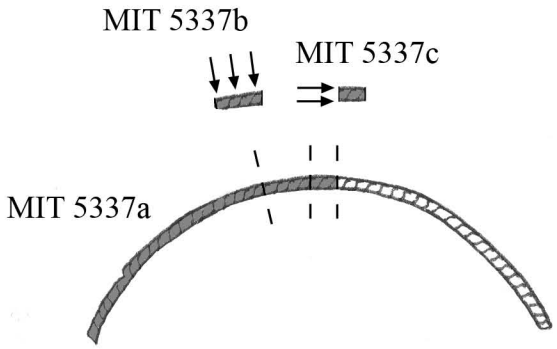

Figure 5.4.4.v: Samples removed from MIT 5337. Sample MIT 5337a was removed for bulk composition analysis. Sample MIT 5337b was removed for metallographic analysis and was mounted longitudinally as noted. Sample MIT 5337c was removed for metallographic analysis and was mounted transversely as noted.

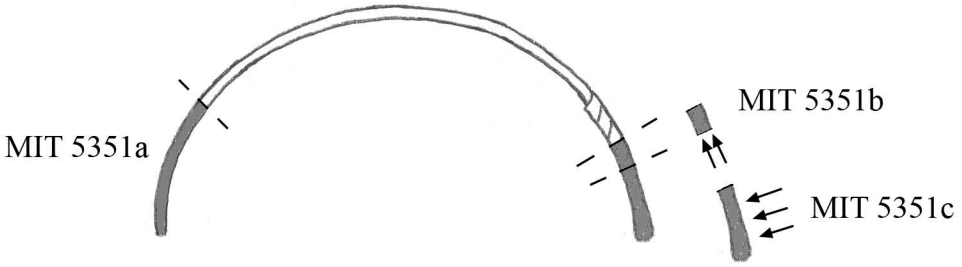

Figure 5.4.4.vi: Samples removed from MIT 5351. Sample MIT 5351a was removed for bulk compositon analysis from the cylindrical end of the wire. Sample MIT 5351b was removed for metallographic analysis from the twisted portion of the wire and was mounted transversely as noted. Sample MIT 5351c was removed for metallographic analysis from the twisted portion of the wire and was mounted longitudinally as noted.

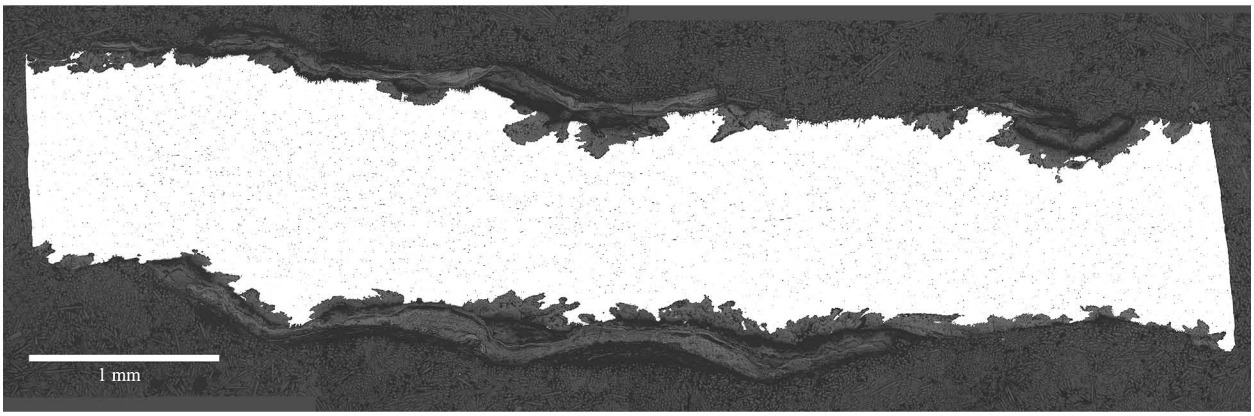

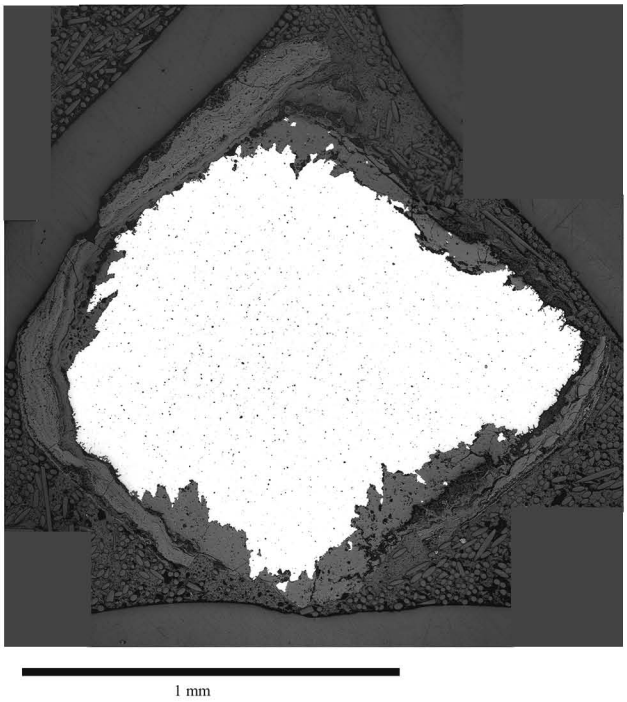

Figure 5.4.4.vii: Twisted earring wire (MIT 5337/Peabody 40-77-40/13450).
Above: Longitudinal cross section (Sample MIT 5337b) as polished.
The twisted contour of the wire can be seen in the external corrosion product (MIT Images 5337b-01-05)..
Below: Transverse cross section (Sample MIT 5337c) as polished.
The original, somewhat diamond-shaped cross section of the twisted wire can be seen in the external corrosion product. Other microstructural features of interest include small porosities homogenously distributed throughout the sample. (MIT Images 53337c-01-05).

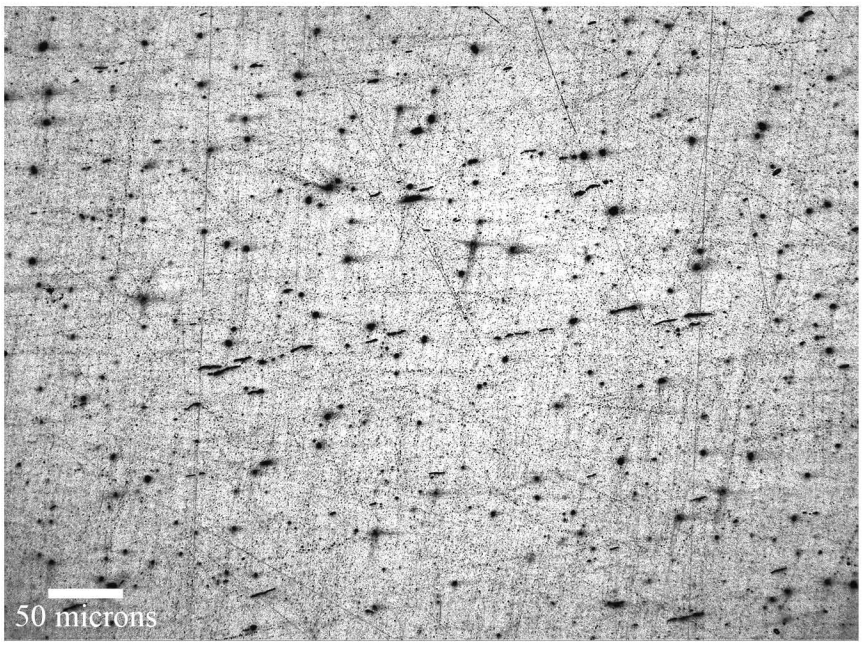

Figure 5.4.4.viii: Twisted earing wire (MIT 5337/Peabody 40-77-40/13450). Longitudinal cross section, as polished. x200. Microstructural features of interest include small porosities homogenously distributed throughout the sample and elongated gray copper sulfide inclusions oriented parallel to the wire's longitudinal axis. (MIT Image 5337b-06).

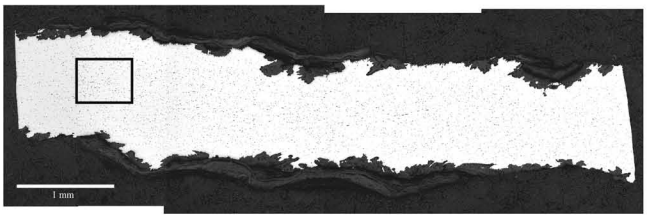

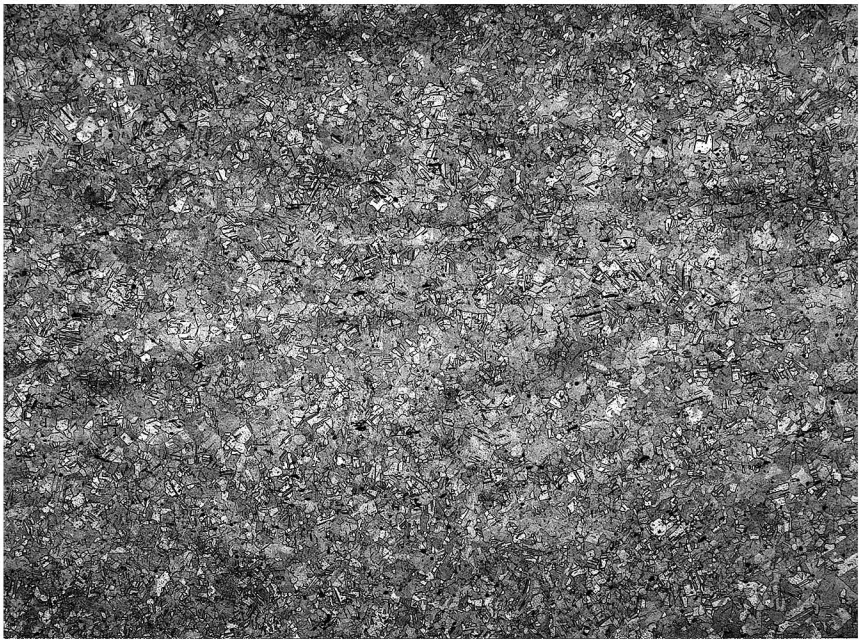

Figure 5.4.4.ix: Twisted earring wire (MIT 5337/Peabody 40-77-40/13450). Longitudinal cross section (MIT 5337b). Etch: 4 sec potassium dichromate and 2 sec ferric chloride. x100. Microstructural features of interest include small, equiaxed grains with annealing twins. (MIT Image 5337b-34).

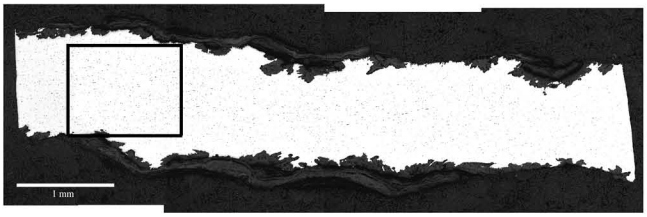

50 microns

Figure 5.4.4.x: Twisted earring wire (MIT 5337/Peabody 40-77-40/13450). Transverse cross section (MIT 5337c). Etch: 4 sec potassium dichromate and 2 sec ferric chloride. x200. Microstructural features of interest include clusters of very small, equiaxed grains with annealing twins surrounded by larger equiaxed grains with annealing twins. The clusters of smaller grains are homogenously distributed throughout the sample (MIT Image 5337c-11).

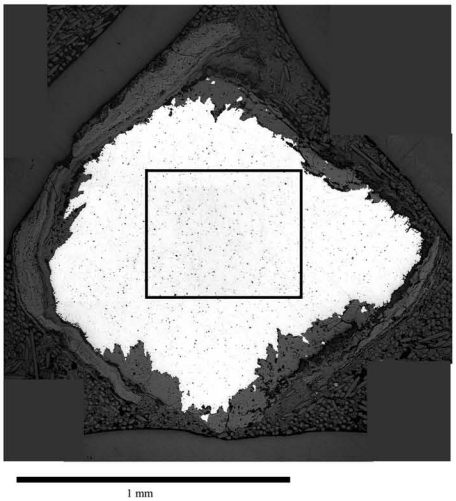

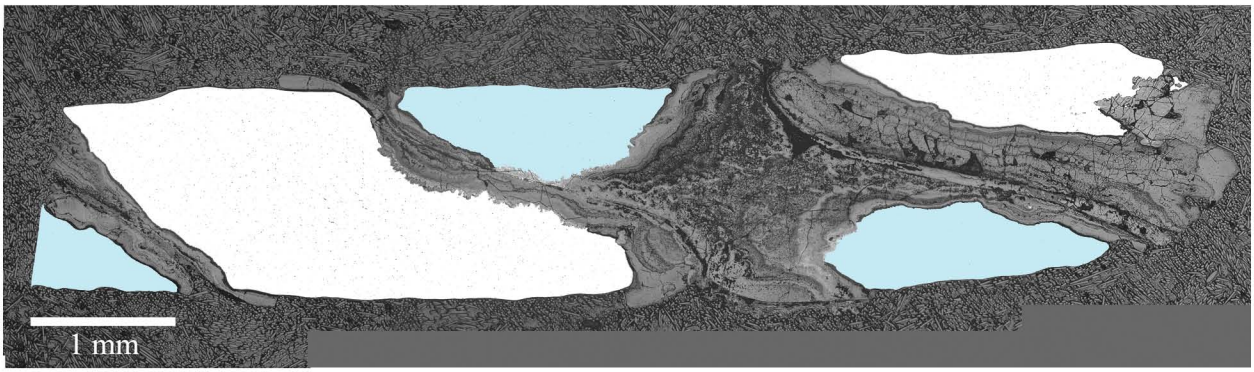

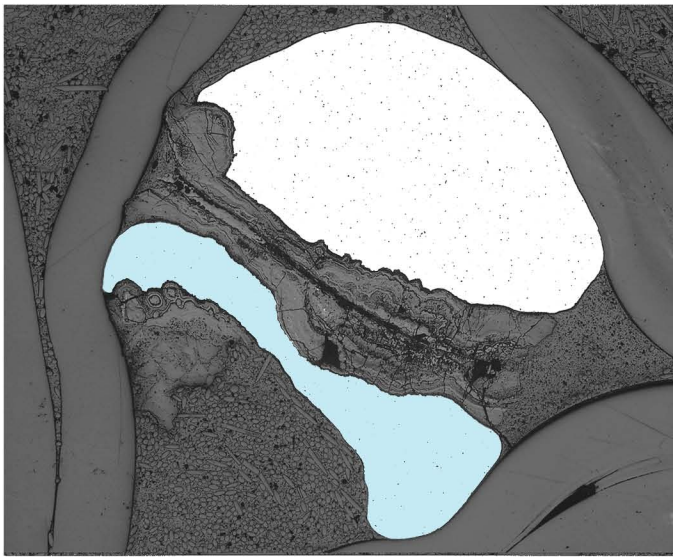

Figure 5.4.4.xi: Earring wire (MIT 5351/Peabody 40-77-40/13451).
Above: Longitudinal cross section (Sample MIT 5351c) as polished. The longitudinal cross section shows two pieces of wire twisted together. The large, cylidrical wire is left white in color, and the thinner, flatter wire has been colored blue. The junctures between the wires can be seen in the corrosion product. (MIT Images 5351c-01-09).
Below: Transverse cross section (Sample MIT 5351b) as polished. The transverse cross section shows the two pieces of wire twisted together. The thinner, flatter wire is colored blue. The thinner, flatter wire is mechanically twisted together with the cylindrical wire to produce the twist portion of the earring wire. The juncture between the two wires can be seen in the corrosion product. (MIT Image 5351b-01).

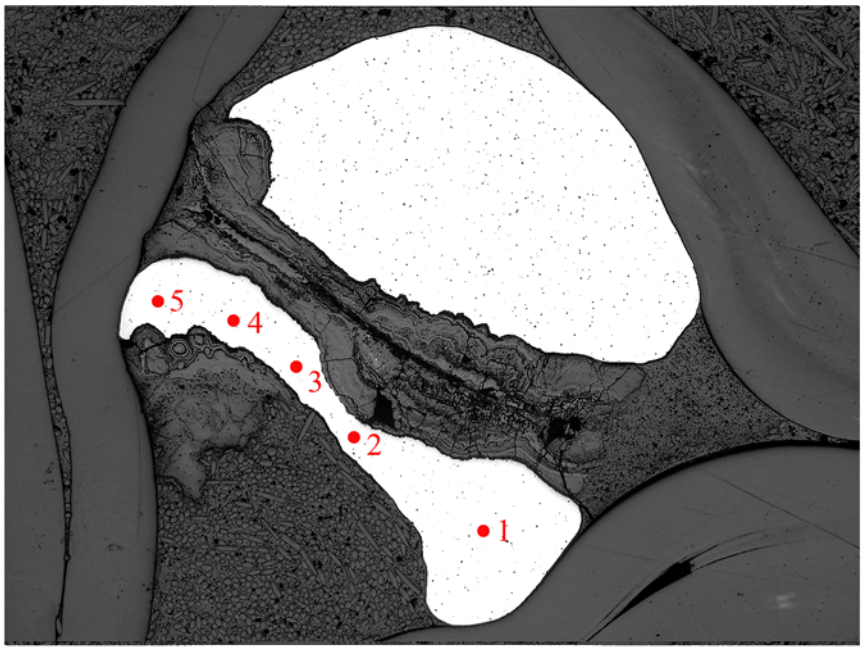

Electron Microbeam Probe Compositional Data

	Cu	Sn	Pb	Sb	As	Ni	Co	Ag	Fe
Pt 1	89.08	12.5	0.1833	n.d.	0.0602	0.1192	0.0429	n.d.	0.1893
Pt 2	88.42	12.69	0.175	n.d.	0.0247	0.1098	0.0522	n.d.	0.2011
Pt 3	89.95	12.95	0.0081	n.d.	0.0901	0.0424	0.0736	0.0029	0.1991
Pt 4	87.91	12.69	0.1119	n.d.	0.0319	0.149	0.0592	n.d.	0.189
Pt 5	87.47	12.73	0.2157	n.d.	0.0579	0.085	0.085	n.d.	0.3429
Average	**88.57**	**12.71**	**0.139**	**n.d.**	**0.053**	**0.101**	**0.063**	**n.d.**	**0.224**

(all values in weight %) n.d.= not determined

Figure 5.4.4.xii: Twisted earring wire (MIT 5351/Peabody 40-77-40/13451).
Above: Points at which compositional data were taken by the electron microbeam probe.
Below: Electron microbeam probe compositional data from each point on the twisted-on portion of the wire.

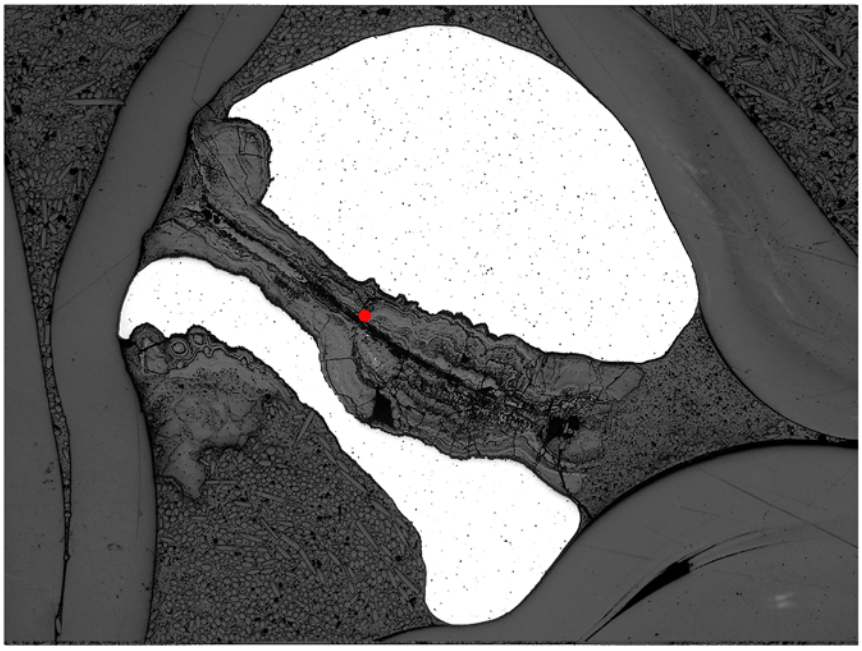

1 mm

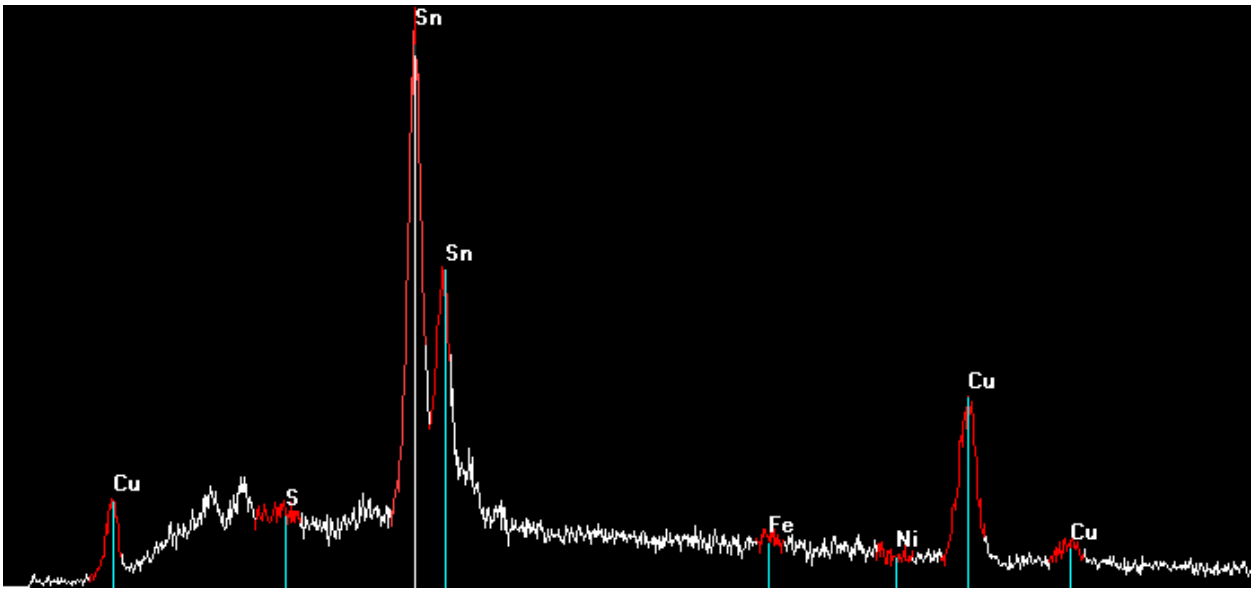

Figure 5.4.4.xiii: Earring wire (MIT 5351)
Above: Point in juncture at which EDS spectrum was taken by the electron microbeam probe.
Below: EDS spectrum of material in juncture.

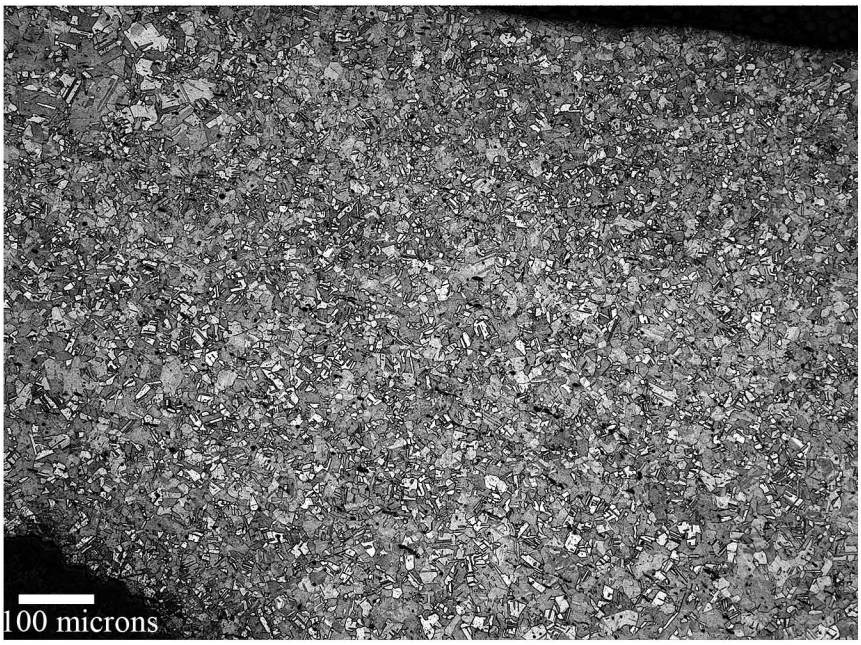

Figure 5.4.4.xiv: Earring wire (MIT 5351/Peabody 40-77-40/13451). Longitudinal cross section (MIT 5351c). Etch: 6 sec potassium dichromate and 2 sec ferric chloride. x100. Microstructural features of interest include small, equiaxed grains with annealing twins. Elongated gray copper sulfide inclusions aligned parallel to the angle of the twist can also be seen. (MIT Image 5351c-12).

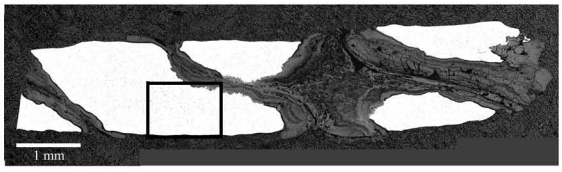

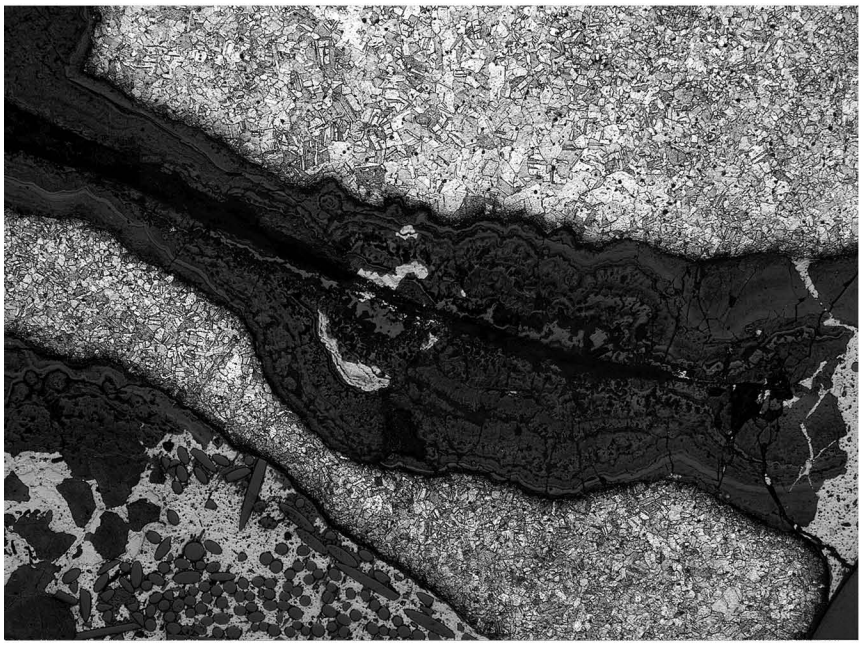

100 microns

Figure 5.4.4.xv: Earring wire (MIT 5351/Peabody 40-77-40/13451). Transverse cross section (MIT 5351b). Etch: 6 sec potassium dichromate and 2 sec ferric chloride. x100. Microstructural features of interest include small, equiaxed grains with annealing twins. A few deformation lines can be seen along the edges of the smaller piece of wire. (MIT Image 5351b-09).

5.4.5: Spirals (MIT 5338/Peabody 40-77-40/13453)

5.4.5a: Provenance and Background

MIT 5338 (Figure 5.4.5.i), a group of fragmented spirals, came from Grave 32 (Wells 1981), which is discussed in detail in Sections 5.3.2 and 5.4.4. The spirals may have been associated with the same earring assemblage as the earring wire discussed in Section 5.4.4. The spirals are unique in Tumulus IV.

5.4.5b: Initial Examination and Observations

The spirals and the spiral chosen for sampling were photographed (Figures 5.4.5.i and 5.4.5.ii), drawn to scale, measured, and observed (Figures 5.4.5.iii and 5.4.5.iv).

There are 10 fragmented spirals that weigh a total of 9.0 g. These spirals are made from thin sheet bent into a loose cylindrical shaped spiral. Only one fragment is diagnostic; it has an intact end, and it has been entirely cleaned of corrosion product. This diagnostic fragment weighs 0.6 g. The remaining fragments are covered with a layer of dark green corrosion product. On each of these fragments there are pseudomorphs that appear to have been made by thin, loose fibers or hair. Most of the fragments appear to be highly mineralized.

The fragment chosen for sampling appears to be slightly more structurally robust than the other fragments. It is made from sheet that is 3.8 mm wide and 0.7 mm thick. The sheet has been bent into a spiral with a roughly circular cross section 9.9 mm in diameter. The fragment is 15.1 mm long, and it weighs 0.9 g.

5.4.5c: Sampling

The spiral fragment was sampled for both bulk composition and metallographic analysis (Figure 5.4.5.v). Sample MIT 5338a was removed with a transverse cut for bulk composition analysis. The remainder of the fragment was taken as sample MIT 5338b, which was mounted longitudinally as noted for metallographic analysis.

5.4.5d: Bulk Composition Analysis

Bulk composition analysis shows that the spirals are made from a leaded tin bronze with tin present at a concentration of 5.5 weight percent and lead present at a concentration of 1.55 weight percent. Other minor and trace elements include As (0.334%), Ni (0.097%), Sb (0.073 %) Ag (0.038 %), Co (0.0579 %) and Fe (0.008%). Bulk composition analysis data are shown below in Table 5.4.5 and in the Appendix.

Table 5.4.5: Bulk Composition Data for MIT 5338 (Spirals)

	Sn	**Pb**	**Sb**	**As**	**Ni**	**Co**	**Ag**	**Fe**
ICP-ES	5.5	1.55	0.073	0.334	0.097	0.043	n.a.	0.008
INAA	4.97	n.a.	0.068	0.284	0.0729	0.0579	0.038	n.d.

(values in weight %) n.a. = not analyzed n.d. = not determined

5.4.5e: Metallographic Analysis

Sample MIT 5338b was mounted as a longitudinal section (Figure 5.4.5.vi). Microstructural features of interest in the as-polished sample include elongated porosities and gray copper sulfide inclusions aligned parallel to the longitudinal axis (Figure 5.4.5.vii). Also apparent in the as-polished sample is internal corrosion product outlining equiaxed grains. The sample was etched for four seconds with potassium dichromate and for one second with aqueous ferric chloride to reveal a structure characterized by small equiaxed grains with annealing twins (Figure 5.4.5.viii). No deformation lines were observed, indicating that the spirals were left in a recrystallized, annealed state.

5.4.5f: Discussion

The spirals are made of a leaded tin bronze with a tin concentration of 5.5 weight percent and a lead concentration of 1.55 weight percent. The spirals are made of a different alloy than the earring wire discussed in Section 5.4.4 (the wire has a tin composition ranging from 10-12 weight percent and a lead composition of 0.5 weight percent). If the spirals were part of the same earring assemblage as the wire, they were mechanically attached to the wire somehow.

The spirals were subject to several cycles of working and annealing to render them into thin sheet. The sheet was left in an annealed state, which would have made it relatively pliable and easy to twist into the final spiral shape. The spirals were not

subject to much use-wear that affected the recrystallized microstructure. The low tin concentration and annealed microstructure suggests that the spirals were for decorative use only as they are relatively malleable.

5.4.5g: Conclusions

- The spirals are made of a leaded tin bronze with a tin concentration of 5.5 weight percent and a lead concentration of 1.55 weight percent.
- The spirals were subject to several cycles of working and annealing to render them into thin sheet, and they were left in an annealed state.
- The spirals were most likely meant for decorative use only, and they did not see much use-wear.

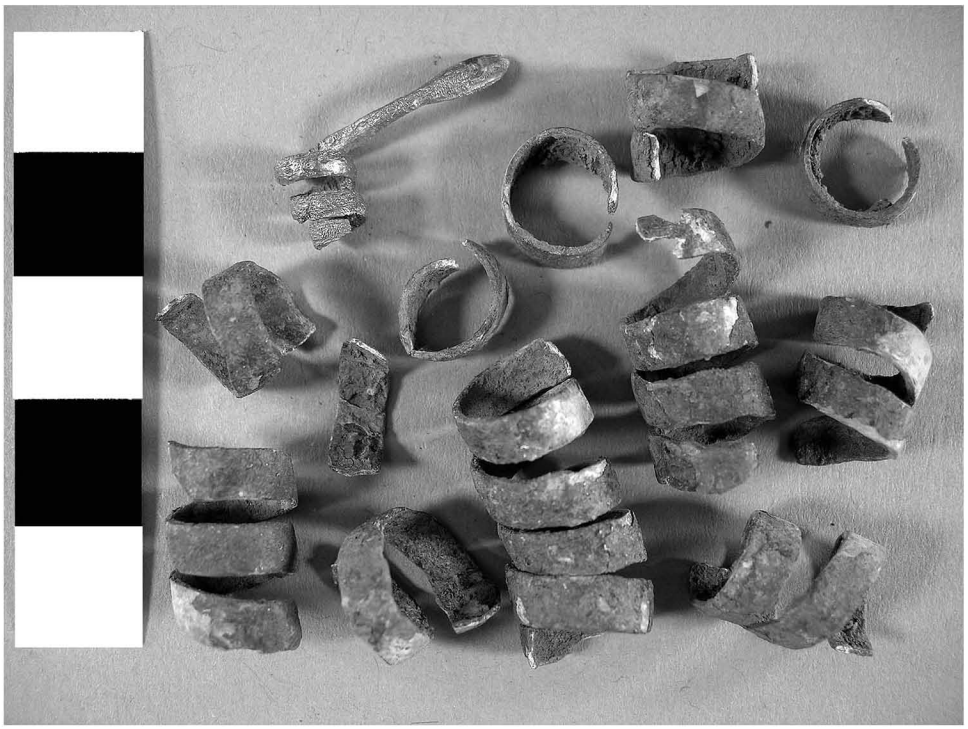

Figure 5.4.5.i: Spirals. (MIT 5338/Peabody 40-77-40/13453). Photograph by E. Cooney. Copyright 2007: President and Fellows of Harvard College.

Figure 5.4.5.ii: Spirals, spiral chosen for sampling. (MIT 5338/Peabody 40-77-40/13453). Photograph by E. Cooney. Copyright 2007: President and Fellows of Harvard College.

Figure 5.4.5.iii: Spirals (MIT 5338). Key object features.

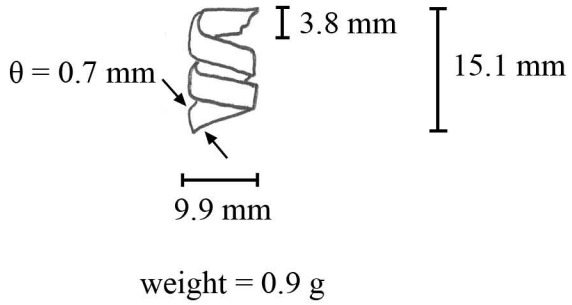

Figure 5.4.5.iv: Spirals (MIT 5338). Drawing and measurements.

Figure 5.4.5.v: Samples removed from spirals. The entire spiral fragment was taken for sampling. MIT 5338a was removed with a transverse cut for bulk composition analysis. MIT 5338b was removed for metallographic analysis was mounted longitudinally as noted.

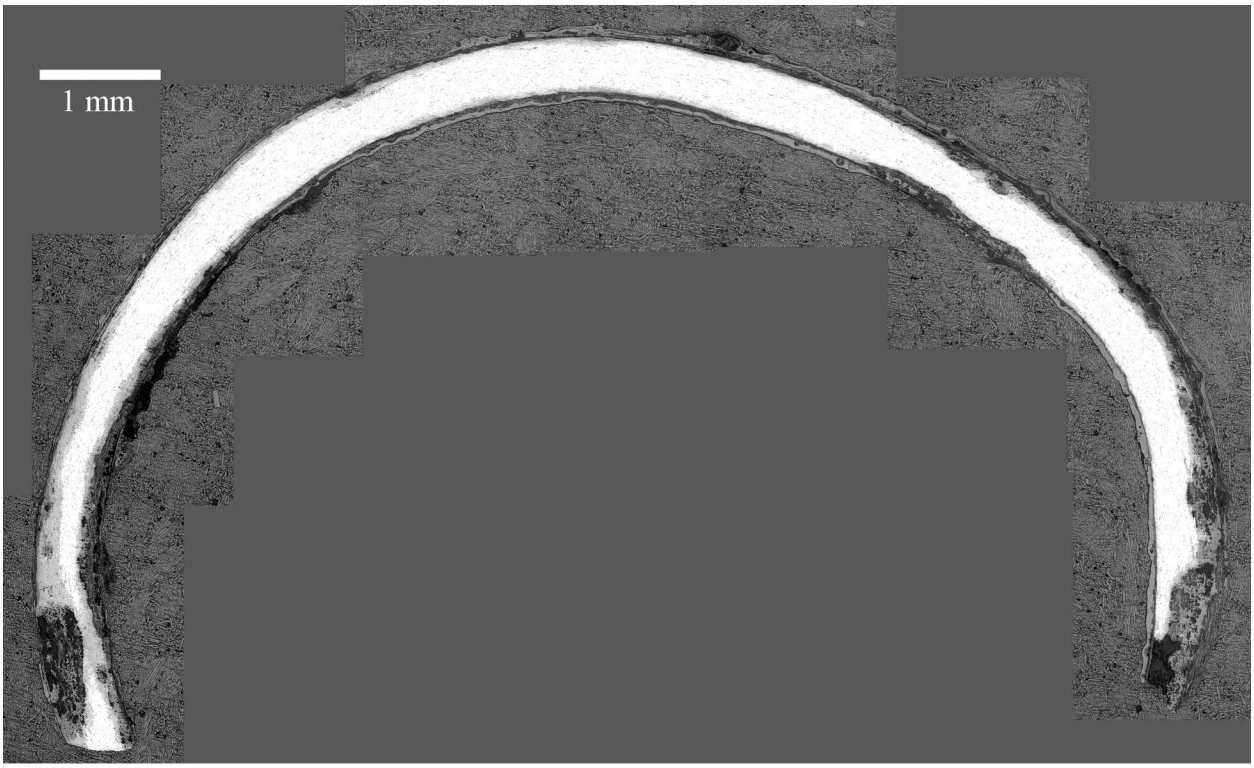

Figure 5.4.5.vi: Spirals (MIT 5338/Peabody 40-77-40/13453). Longitudinal cross section, as polished. Microstructural features of interest include elongated porosities and gray copper sulfide inclusions aligned parallel to the longitudinal axis. Internal corrosion product outlines equiaxed grains. (MIT Images 5338b-01-08.)

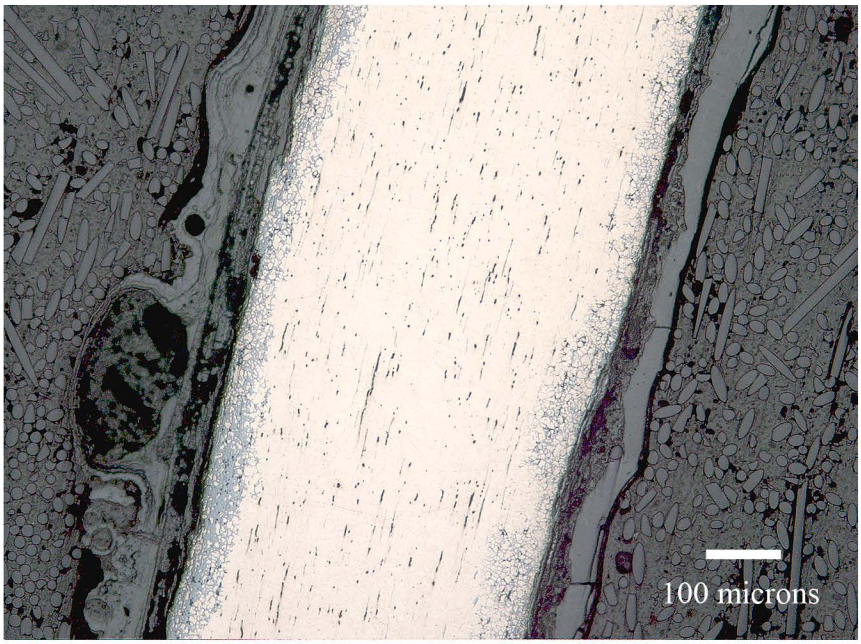

Figure 5.4.5.vii: Spirals (MIT 5338/Peabody 40-77-40/13453). Longitudinal cross section, as polished. x100. Microstructural features of interest include elongated porosities and gray copper sulfide inclusions aligned parallel to the longitudinal axis. Internal corrosion product outlines equiaxed grains. (MIT Images 5338b-10.)

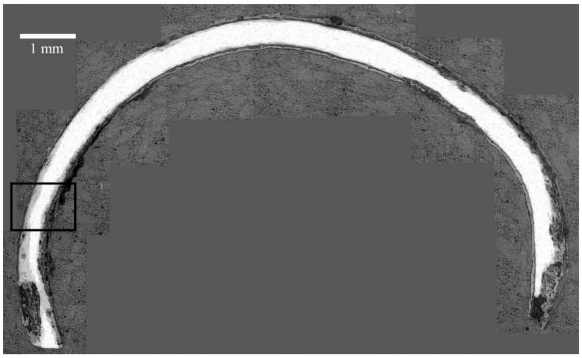

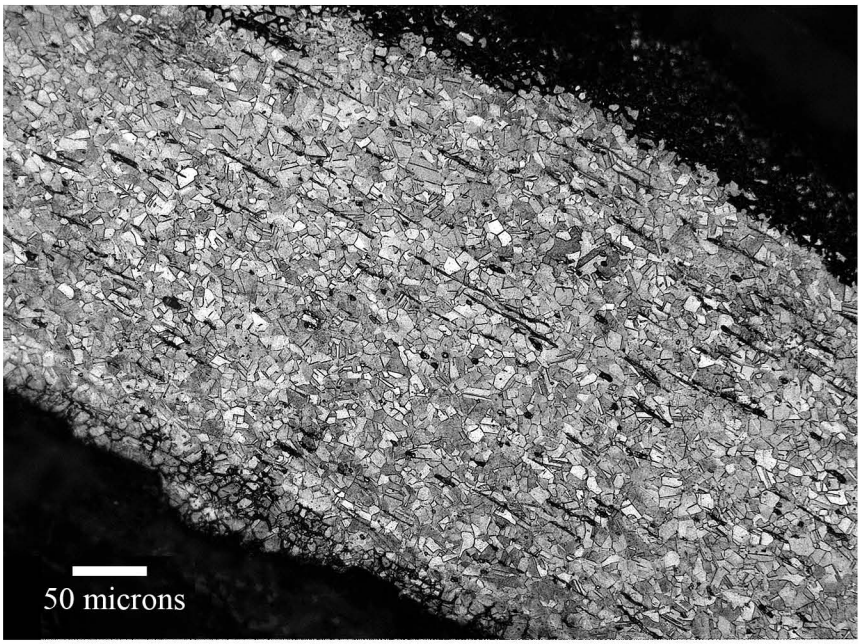

Figure 5.4.5.viii: Spirals (MIT 5338/Peabody 40-77-40/13453). Longitudinal cross section. Etch: 4 sec potassium dichromate and 1 sec ferric chloride. x200. Microstructural features of interest include equiaxed grains with annealing twins, elongated porosities and gray copper sulfide inclusions aligned parallel to the longitudinal axis. (MIT Images 5338b-11.)

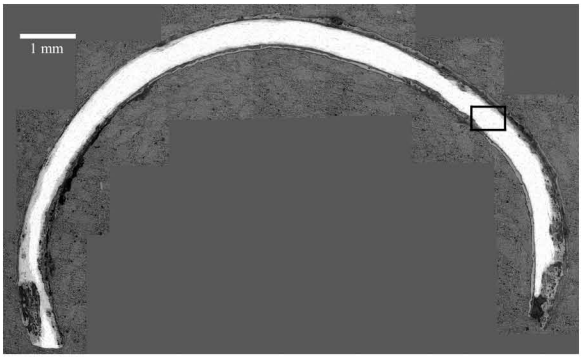

5.4.6: Buttons (MIT 5349/Peabody 40-77-40/13433)

5.4.6a: Provenance and Background

MIT 5349 (Figure 5.4.6.i) came from Grave 30 of Tumulus IV (Wells 1981). MIT 5349 is a group of sixty-seven similar bronze buttons.

Grave 30 was covered with a large packing of stone slabs and was 3.1 m long, 1.1 m wide, and 5.2 m below the surface of the tumulus. Directly beneath the stone slabs was an intact bronze cuirass, discussed in Section 5.4.8. In association with the cuirass were three ceramic vessels, two of which were fine and of an unusual type, two iron spearheads, and sixty-seven round bronze buttons.

There are five other graves from the Mecklenburg excavations at Stična that contain large quantities (50-100) of round buttons like the ones found in Grave 30.

5.4.6b: Initial Examination and Observations

The sixty-seven buttons are all identical. The two buttons chosen for sampling were photographed (Figures 5.4.6.i and ii), drawn to scale, measured, and observed (Figures 5.1.3.iii and 5.1.3.iv).

The buttons are slightly oval and dome-shaped. They have small knobs in the middle of their outside surfaces. On the inside of each button a metal loop stretches across the full length of the button, creating a small buttonhole. This metal loop appears to be a small piece of metal metallurgically attached to the button.

Button A is oval shaped with a cross section measuring 16.0 mm by 16.7 mm. It is 4.7 mm tall, and its knob has a diameter measuring 3.2 mm. Its rim is 0.5 mm thick. Its loop varies in thickness from 1.5 to 0.7 mm, creating a buttonhole that is about 4 mm long and 2 mm high. It weighs 1.5 g.

Button B is oval shaped with a cross section measuring 15.6 mm by 16.4 mm. It is 4.6 mm tall, and its knob has a diameter measuring 3.7 mm. Its rim is 0.7 mm thick. Its loop varies in thickness from 1.0 mm to 1.7 mm, creating a buttonhole that is about 3.5 mm long and 2 mm high. It weighs 1.3 g.

Both buttons appear to be structurally robust. Both are covered with a friable, dark green corrosion product that has worn off in places to reveal dark, oxidized metal.

5.4.6c: Sampling

Button A was sampled twice for bulk composition analysis (Figure 5.4.6.v). Sample MIT 5349a was removed from the body of the button as noted, and sample MIT 5349b was taken from the loop as noted. Button B was sampled for metallographic analysis and was mounted transversely as noted (Figure 5.4.6.v).

5.4.6d: Bulk Composition Analysis

MIT 5349a, the sample taken from the button body, is a ternary copper-tin-lead alloy with a high tin composition of 21 weight percent and a lead composition of 7.13 weight percent. Other major and minor elements include Ag (0.222 %), Sb (0.184%), As (0.178%), Co (0.0987%), and Fe (0.019%). Bulk composition analysis data are shown below in Table 5.4.6.i and in the Appendix.

Table 5.4.6.i: Bulk Composition Analysis Data for MIT 5349a (button body)

	Sn	**Pb**	**Sb**	**As**	**Ni**	**Co**	**Ag**	**Fe**
ICP-ES	21	7.13	0.184	0.178	0.086	0.013	n.a.	0.019
INAA	20.3	n.a.	0.148	0.154	0.0987	0.0146	0.222	n.d.

(values in weight %) n.a. = not analyzed n.d. = not determined

MIT 5349b, representative of the button loop, is a ternary copper-lead-tin alloy with a tin composition of 18.3 weight percent and a lead composition of 7.02 weight percent. Other major and minor elements include Sb (0.159%), As (0.152%), Ni (0.09%), Fe (0.17%), Ag (0.079%), and Co (0.012%). Bulk composition analysis data are shown below in Table 5.4.6.ii and in the Appendix.

Table 5.4.6.ii: Bulk Composition Analysis Data for MIT 5349b (button loop)

	Sn	**Pb**	**Sb**	**As**	**Ni**	**Co**	**Ag**	**Fe**
ICP-ES	18.3	7.02	0.159	0.152	0.09	0.012	n.a.	00.019
INAA	7.16	n.a.	0.054	0.057	0.0519	0.0059	0.079	0.17

(values in weight %) n.a. = not analyzed n.d. = not determined

5.4.6e: Metallographic Analysis

MIT 5349c was mounted transversely. As-polished, the body of the button and the loop can be seen. Both the body and the loop have a high density of porosities

(Figure 5.4.6.vi) and a large volume of Cu-Sn eutectoid (Figure 5.4.6.vii). In both the body and the loop the eutectoid and internal corrosion product outline dendritic structures. There are a few grains of redeposited copper in the button body (Figure 5.4.6.vii).

The sample was etched for 3 seconds with potassium dichromate. Both the button body (Figure 5.4.6.viii) and the loop (Figure 5.4.6.ix) have as-cast structures characterized by primary dendrites surrounded by Cu-Sn eutectoid. The dendrites are not deformed or elongated in any way that would suggest they were hammered or worked after having been formed during the casting operation.

5.4.6f: Discussion

The body of the button and the button loop are made from what appears to be the same alloy, a high tin, leaded bronze with between 18.7-21 weight percent tin and approximately 7 weight percent lead. This high tin composition would have made the buttons hard but also brittle and highly gold in color.

Both the button and the loop have as-cast structures. The as-cast structure and the identical alloy composition indicate that the button and the loop were cast together simultaneously as one object.

5.4.6g: Conclusions

- The body of the button and the button loop are both comprised of the same alloy, a ternary copper-tin-lead alloy with an approximate tin composition of 20 weight percent and an approximate lead composition of 7 weight percent.
- The button body and the loop were simultaneously cast to shape as a single object, and they were left as-cast.
- The buttons were highly golden in color.

Figure 5.4.6.i: Buttons. (MIT 5349/Peabody 40-77-40/13433). Photograph by E. Cooney. Copyright 2007: President and Fellows of Harvard College.

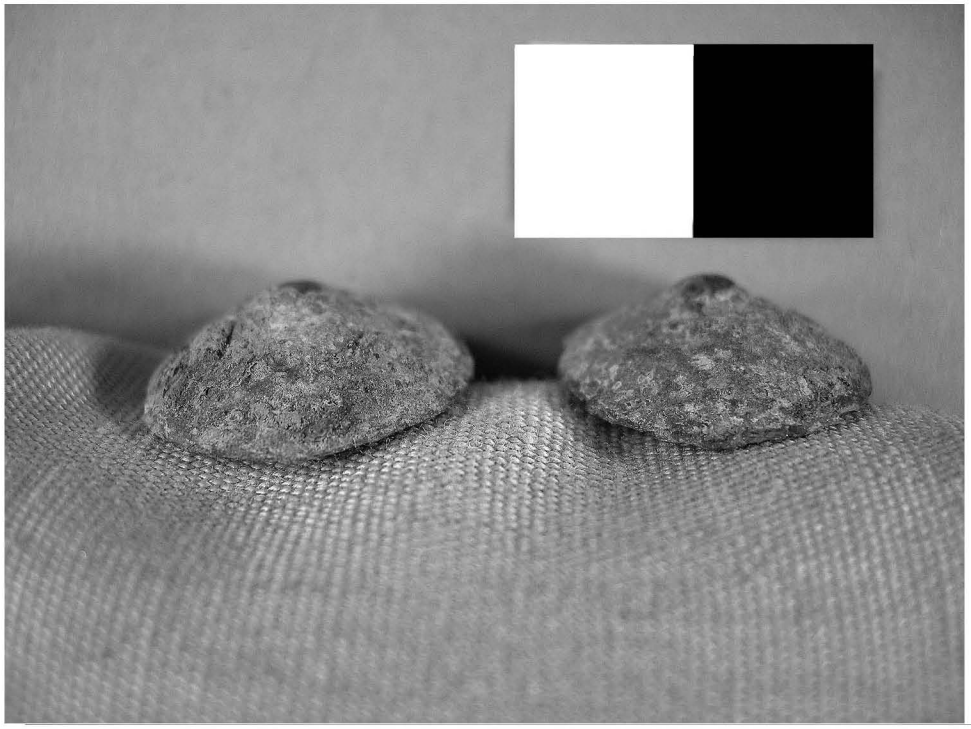

Figure 5.4.6.ii: Buttons. (MIT 5349/Peabody 40-77-40/13433). Photograph by E. Cooney. Copyright 2007: President and Fellows of Harvard College.

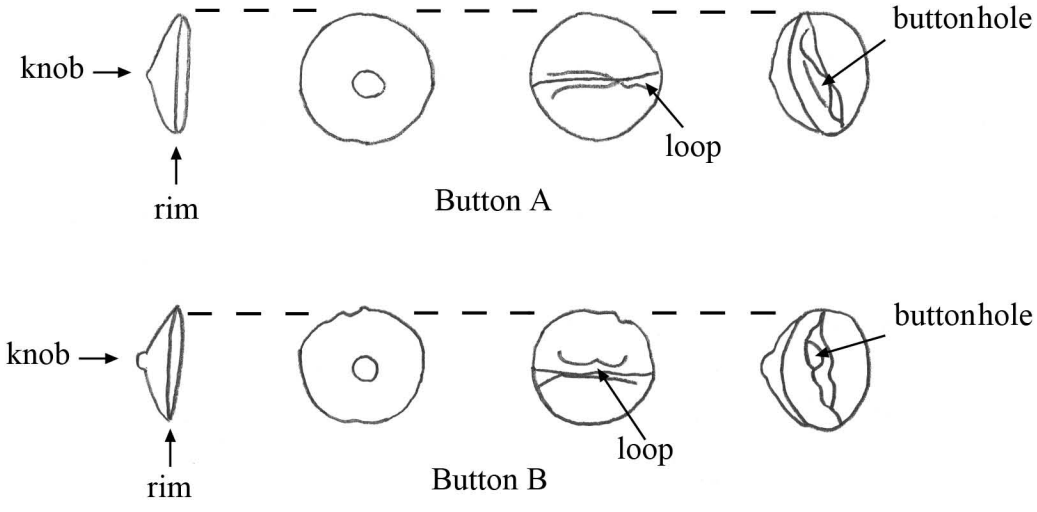

Figure 5.4.6.iii: Buttons (MIT 5349). Key object features.

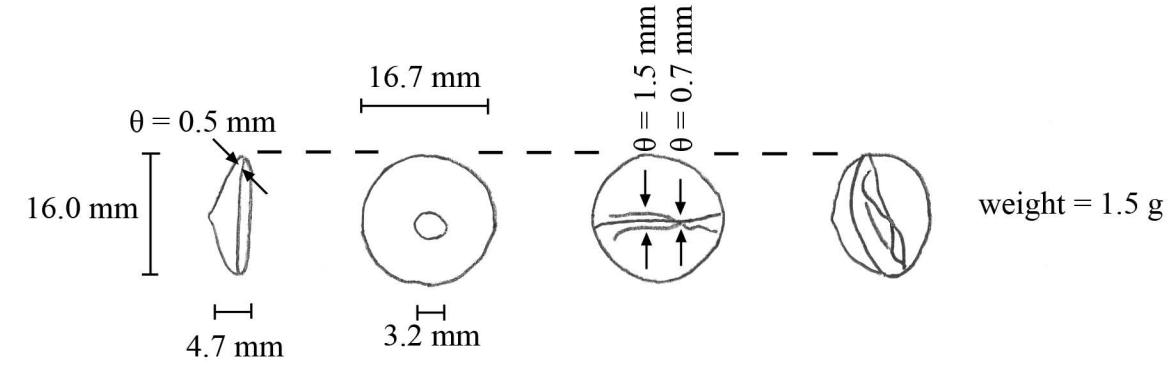

Button A

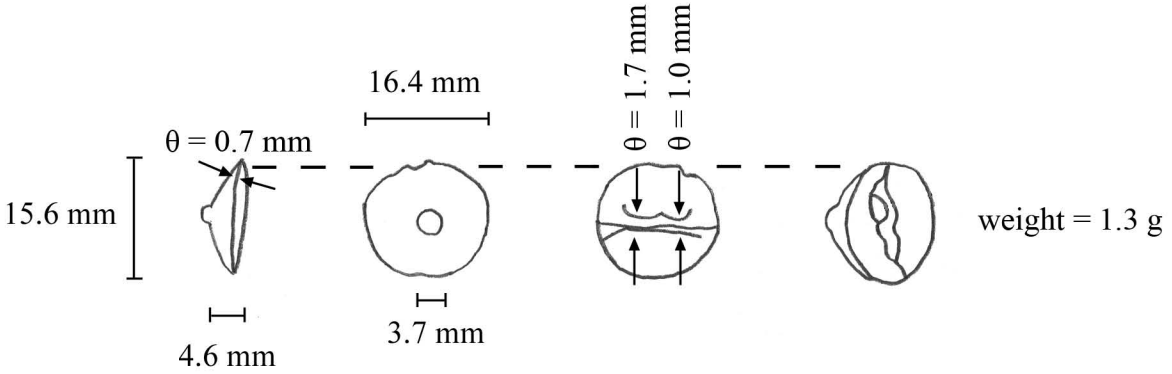

Button B

Figure 5.4.6.iv: Buttons (MIT 5349). Drawing and measurements.

Button A Button B

Figure 5.4.6.v: Samples removed from buttons. Samples MIT 5349a and MIT 5349b were removed from Button A for bulk composition analysis. Sample MIT 5349c was removed for metallographic analysis and was mounted transversely as noted.

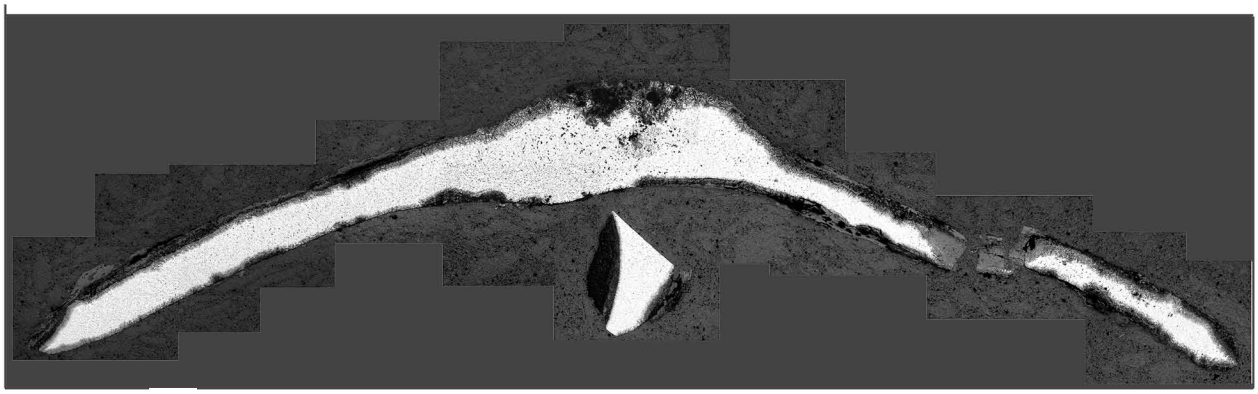

Figure 5.4.6.vi: Buttons (MIT 5349/Peabody 40-77-40/13433). Transverse cross section, as polished. Both the transverse cross section of the button and of the loop can be seen. Other microstructural features of interest include a high density of porosoties. A broken, mineralized portion of the button can be seen on the apparent right of the photomicrogaph. (MIT Images 5349c-01-17.)

Figure 5.4.6.vii: Buttons (MIT 5349a/Peabody 40-77-40/13433). Transverse cross section, as polished. x100. Microstructural features of interest include large amounts of pale blue-green eutectoid outlining dendrites, dark blue-appearing internal corrosion product outlining dendrites, a high density of porosities, and a few grains of redeposited copper. The redeposited copper is pinkish in color. (MIT 5349c-20).

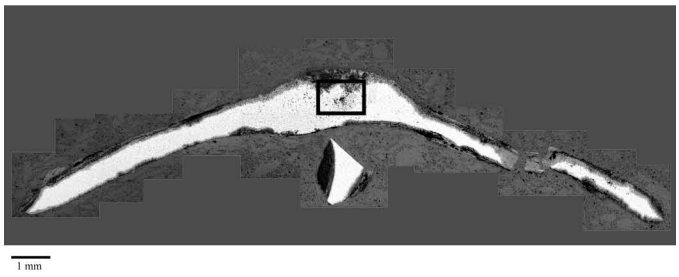

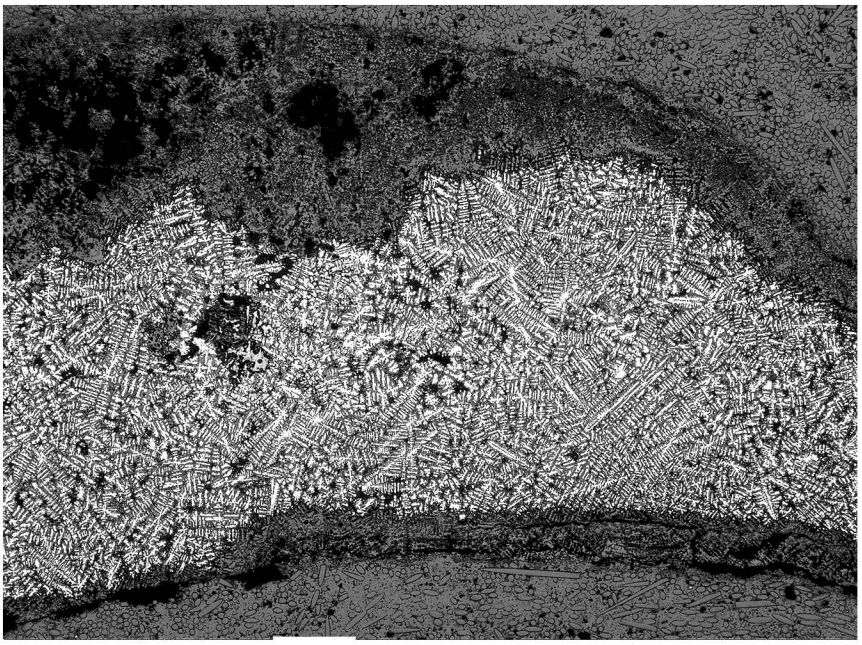

Figure 5.4.6.viii: Buttons (MIT 5349/Peabody 40-77-40/13433). Transverse cross section. Etch: 3 sec potassium dichromate. x 50. The button has an as-cast structure with primary dendrites surrounded by Cu-Sn eutectoid. (MIT Image 5349c-26).

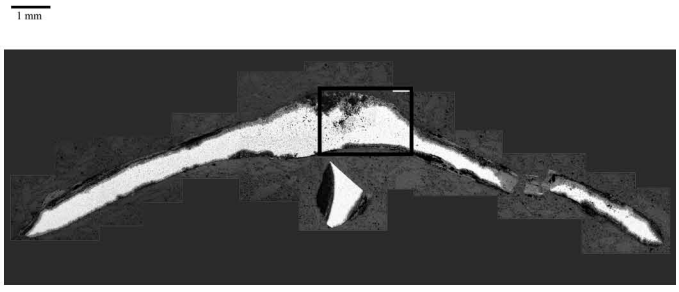

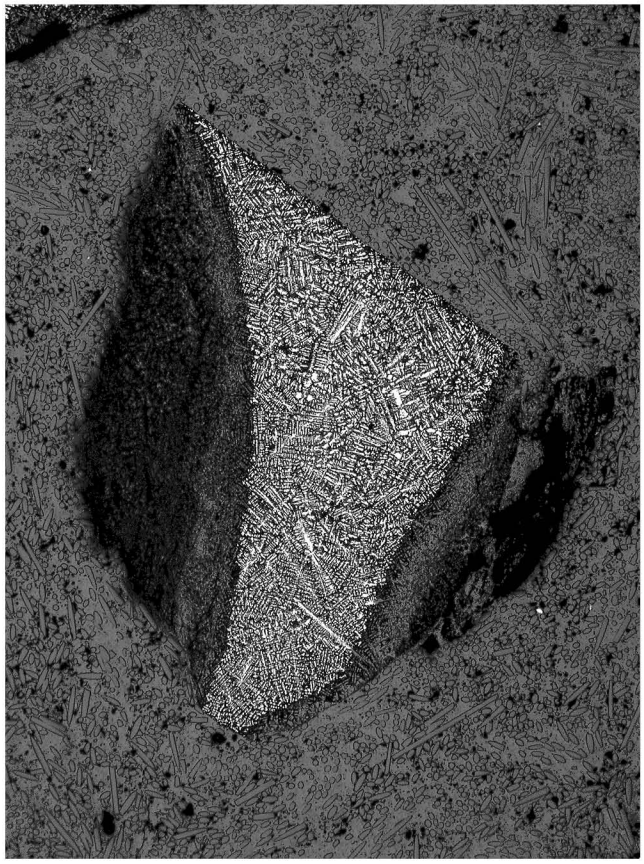

Figure 5.4.6.ix: Buttons (MIT 5349/Peabody 40-77-40/13433). Transverse cross section. Etch: 3 sec potassium dichromate. x 50. The loop has an as-cast structure with primary dendrites surrounded by Cu-Sn eutectoid. (MIT Image 5349c-27).

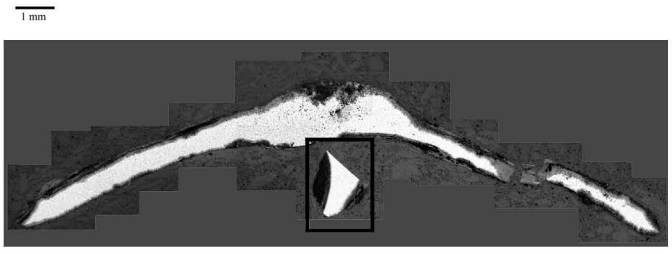

5.4.7: Lump (MIT 5347/Peabody 40-77-40/13410)

5.4.7a: Provenance and Background

MIT 5347 (Figure 5.4.7.i), identified by Wells as a "solid bronze lump" (1981), came from Grave 27. Grave 27 was located directly under a packing of five stones in Grave 23, and it contained fragments of burned bones. Associated grave goods included two iron knives, fibulae fragments, fragments of a flat bronze ring, and a belt plate and attachment assemblage which included the handle-like belt attachment discussed in Section 5.3.5c and the circular "weapon" ring discussed in Section 5.3.5d.

This copper-containing metal lump is unique in reliable graves in Tumulus IV. Two similar copper-containing lumps are associated with Tumulus IV as isolated finds. There are a few similar iron lumps at Stična as well.

5.4.7b: Initial Examination and Observations

The lump was photographed (Figure 5.5.7.i), drawn to scale, measured, and observed (Figure 5.4.7.ii). The lump is covered with a friable light green corrosion product, indicating that it is a copper containing material. The surface of the lump is very rough, almost as if it were cast in a closed sand mold.

The lump is roughly rectangular in shape with one end being slightly larger than the other. It is 20.2 mm long. One end is 13.5 x 14.6 mm and the other end is 12.7 x 11.7 mm. The volume of the lump is roughly 3.5 cm^3. Given the small volume, the lump is very heavy, weighing 19.8 g. The lump's high density indicates that it is highly metallic.

5.4.7c: Sampling

The lump was sampled for bulk composition analysis. Two holes were drilled into the lump using a cleaned steel drill bit (Figure 5.4.7.iii). The initial shavings containing the external corrosion product were discarded. The clean shavings were collected as sample MIT 5347. Sample MIT 5347 was examined under a stereoscopic microscope, and most of the larger bits of corrosion product mixed with the shavings were removed mechanically.

The lump was very metallic. The shavings were a mixture of two different colors and consistencies. Some were light gold in color and appeared metallic, but the majority were dark gray and appeared to have a powdery consistency.

5.4.7d: Bulk Composition Analysis

Bulk composition analysis shows that the lump is a copper-lead alloy with the primary alloying element lead at 34.8 weight percent. There is only a trace amount of tin present in the lump. It is not a tin bronze. Other major and minor elements include As (2.58%), Sb (1.96%), Ag (0.797%), and Ni (0.7640%). Tin, cobalt, and iron are present in trace amounts. Bulk compositional analysis data are shown in Table 5.4.7 and in the Appendix.

Table 5.4.7: Bulk Composition Analysis Data for MIT 5347

	Sn	**Pb**	**Sb**	**As**	**Ni**	**Co**	**Ag**	**Fe**
ICP-ES	0.015	34.8	1.92	2.58	0.755	<0.005	n.a.	0.008
INAA	n.d.	n.a.	1.96	n.a.	0.7640	0.0054	0.797	n.d.

(values in weight %) n.a. = not analyzed n.d. = not determined

5.4.7e: Conclusions

- The lump is not made from a tin bronze alloy as previously reported. The lump is primarily copper with a main alloying element of lead at a composition of 34.8 weight percent. Other major elements include arsenic at a concentration of 2.58 weight percent and antimony at a concentration of 1.92 weight percent.
- The large amount of arsenic and antimony were probably contained within the lead ore before the lead was smelted and are most likely not a deliberate addition to the alloy.
- The lump may have been a copper-lead ingot, or it may have been just a lump of scrap metal. At temperatures higher than 327°C the majority of the lead, over one-third of the metal in the alloy, would have been molten, so it is possible that the current shape of the lump was not its original shape prior to being subject to the temperatures of the crematory fire.

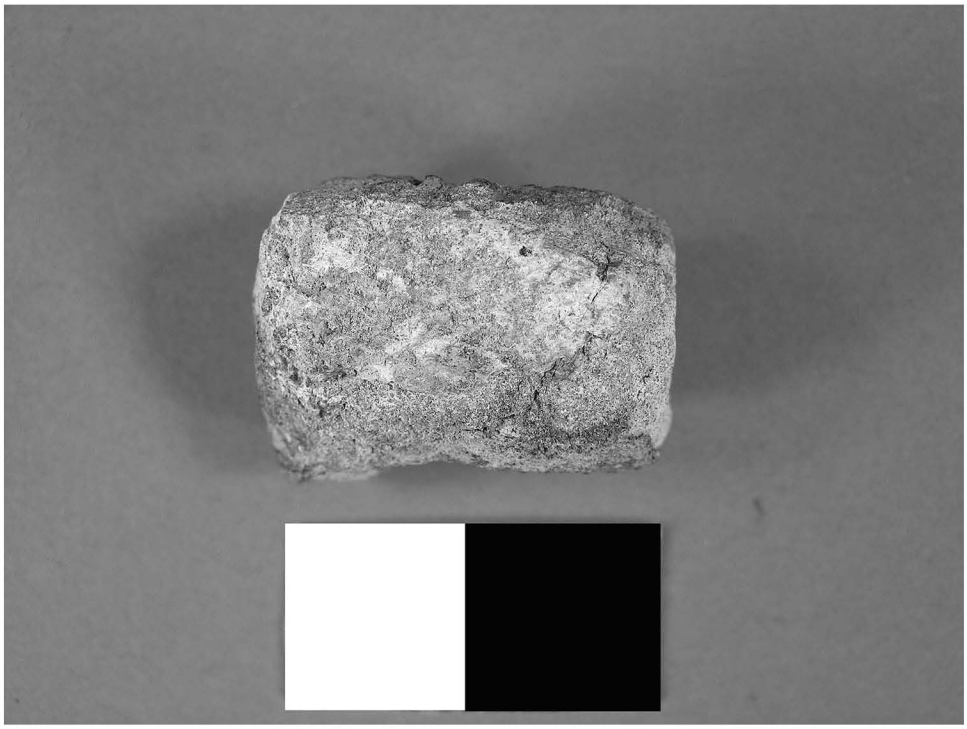

Figure 5.4.7.i: Lump. (MIT 5347/Peabody 40-77-40/13410).
Photograph by E. Cooney.

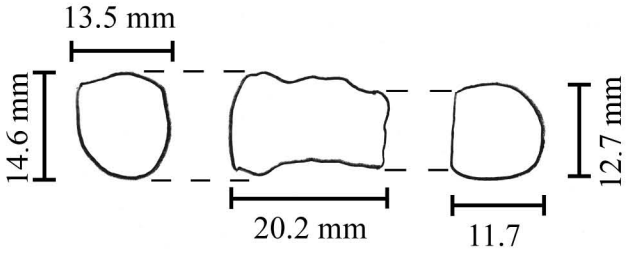

weight = 19.8 g

Figure 5.4.7.ii: Lump (MIT 5347). Drawing and measurements.

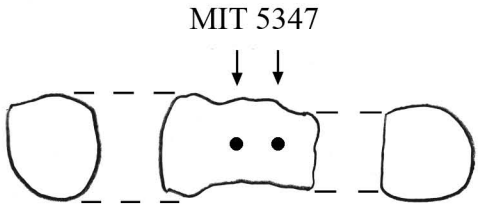

Figure 5.4.7.iii: Lump. (MIT 5347). Sample MIT 5347 was drilled and removed for bulk compositional analysis.

5.4.8: Additional miscellaneous objects not sampled

5.4.8a: Bronze cuirass

The intact bronze cuirass from Grave 30 is unique in the Mecklenburg excavations at Stična. It can be seen in Figure 5.4.8.i, which shows the Duchess of Mecklenburg excavating Grave 30 and the cuirass *in situ.* The cuirass was found in association with the 67 buttons and associated grave goods discussed in Section 5.4.6.

The cuirass is made from sheet bronze in the Greek style and is decorated as a stylized, bare torso. It is made of two separate halves, a front and a back, and would have been worn by lacing the two halves together at the sides. It was once entirely gilded, although just patches of gilding remain. The armor was completely functional, with a flared base permitting the wearer to ride on horseback, large armholes, and a flanged collar to protect the neck. The cuirass is not part of the Peabody's Mecklenburg collection; it is on display in Berlin at the Museum für Vor- und Frühgeschichte (Greis 2006).

5.4.8b: Weapon socket (Peabody 40-77-40/13357)

This weapon socket (Figure 5.4.8.ii) from Grave 19 was originally part of the haft end of an iron dagger or knife (Wells 1981). It is unique in the Mecklenburg collection from Stična. It consists of a single bronze sheet wrapped around on itself to form a hollow cylinder. Two iron rivets pass through the center of the socket perpendicular to each other, piercing the bronze sheet and holding the socket together. Grave 19 was a cremation grave, and associated grave goods included two fragmentary iron spearheads, two shepherd's crook pins (now missing), a sheet bronze helmet (now missing), and sherds from several pottery vessels.

5.4.8c: Bridle knob (Peabody 40-77-40/13496)

This bridle knob from Grave 41a (Figure 5.4.8.iii) is described as being "round with a projecting nipple" (Wells 1981). It consists of a circular piece of bronze connected by four bronze struts to a decorative, nipple shaped top. This particular knob

still has fragments of leather from the two leather bridle straps that were woven through the knob.

There are four such bridle knobs in Grave 41a, which also contains an iron horse bit, ten iron arrowheads, an iron celt, an iron knife, and three small bronze rings. There are three other similar bridle knobs from another grave at Stična in the Mecklenburg collection.

5.4.8d: Sieve (Peabody 40-77-40/13327)

This sieve (Figure 5.4.8.iv) is an example of a vessel made from sheet metal. It was constructed from several pieces of sheet riveted together. The body of the sieve has is decorated with a repoussé pattern of dots. The bottom of the sieve was made from thin sheet covered in punched holes. This sieve came from Grave 15 and was associated with a large burned area and 72 small amber beads (Wells 1981).

There are at least eight other vessels in the Mecklenburg excavations at Stična made from sheet metal riveted together. Handles and other decorations are attached with rivets as well. Vessels made from sheet metal are common at other Eastern Alpine Region Early Iron Age sites (Giumlia-Mair 1995).

Figure 5.4.8.i: Bronze cuirass. This photograph shows the Duchess of Mecklenburg excavating Grave 30. The bronze cuirass *in situ* can be seen in the foreground. The bronze cuirass is now on display at the Museum für Vor- und Frühgeschichte in Berlin.

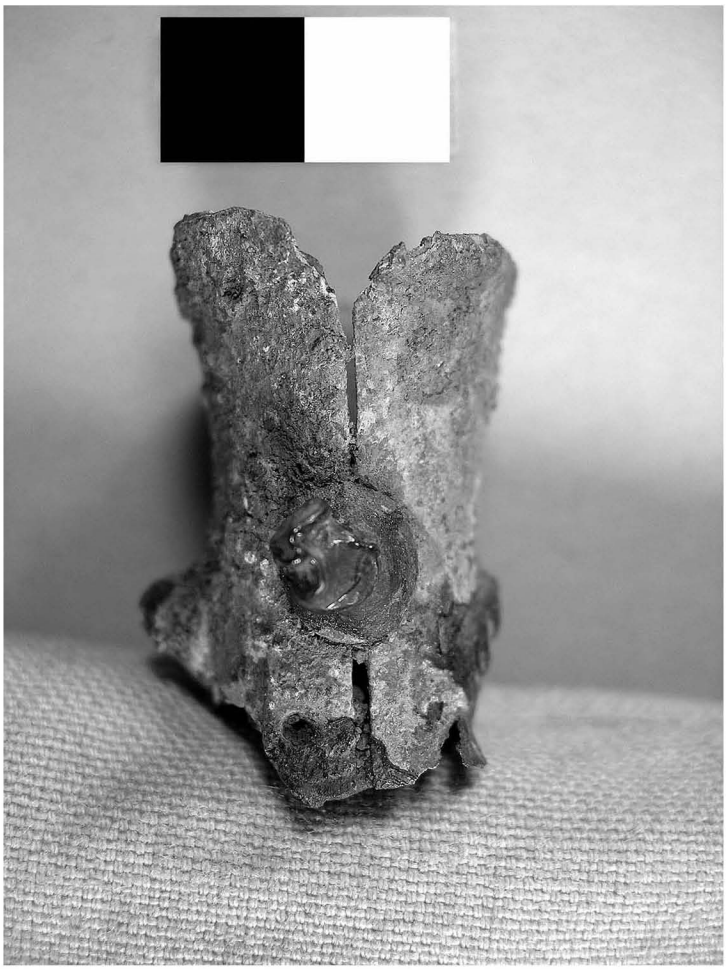

Figure 5.4.8.ii: Weapon socket. (Peabody 40-77-40/13357). This bronze weapon socket is made from a single bronze sheet wrapped around on itself to form a hollow cylinder. It is riveted together with two iron rivets that pass through the interior of the socket perpendicular to one another. The socket is from Grave 19. Photograph by E. Cooney.

Figure 5.4.8.iii: Bridle knob. (Peabody 40-77-40/13496). This bridle knob from Grave 41a still has fragments of two leather bridle bands weaving through its struts. Photographs by E. Cooney.

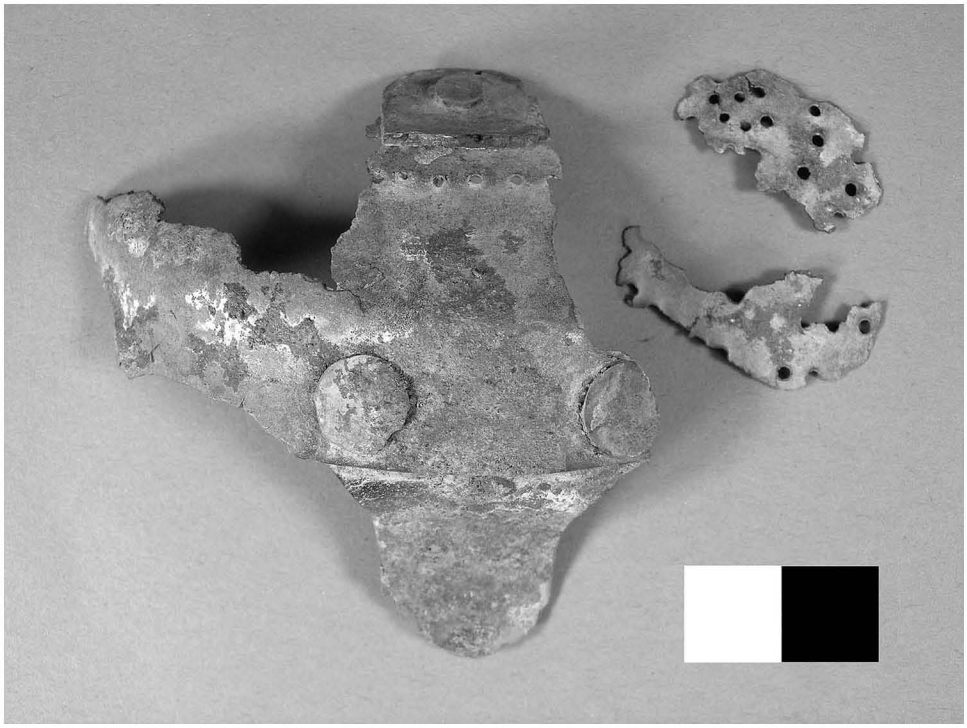

Figure 5.4.8.iv: Sieve. (Peabody 40-77-40/13327). This fragmentary bronze sieve from Grave 15 is constructed from several pieces of sheet metal riveted together. The sieve's body is decorated with repoussé patterns. The sieve's bottom is made from sheet with punched holes. Photograph by E. Cooney.

Chapter 6: Results and Discussion

The purpose of this metallurgical study of bronze objects from Stična was to identify construction techniques, use patterns, and bronze metallurgical technologies from the ancient region of Lower Carniola and to combine composition analyses of various bronze objects with metallographic analyses to serve as a reference metallurgical study for the area.

The results discussed in this chapter combine composition and metallurgical analyses to demonstrate that specific bronze construction techniques and metallurgical technologies were in use at Stična during the Early Iron Age (EIA). This information is then used to compare the bronze metallurgy of Lower Carniola with that of other regions in the Eastern Alpine region during the EIA.

6.1: General tin and lead composition trends

Table 6.1 shows the major, minor, and trace element compositions of the twenty-nine objects analyzed for this study. Figure 6.1 shows the frequency of different ranges of tin and lead compositions.

The twenty-nine objects yield thirty-one sets of composition data because two objects (MIT 5352, the serpentine fibula with disc, and MIT 5368, the belt attachment) had component parts that were analyzed separately from the main object.

Those objects whose compositions were determined with the electron microbeam probe are noted in Table 6.1. These sets of composition data are not as reliable as those determined by bulk composition analysis. Certain minor and trace elements present in these objects, especially lead, which tends to be present inhomogeneously throughout an object, may be underreported.

Thirty of the thirty-one objects and component parts are made from tin bronze. The only non-tin bronze object is MIT 5347, a nondescript lump, which is primarily a copper-lead alloy.

Among the thirty tin bronzes, tin compositions range from 3.34-21 weight percent. The average tin composition of the thirty one objects is 9.39 weight percent. The tin composition of a particular object varies according to its object type and processing;

the ways in which tin composition varies with object type and processing technique are discussed throughout the chapter.

All thirty-one objects from Stična contain lead in at least trace amounts. Lead compositions at Stična range from 0.027-34.8 weight percent, and the average lead composition is 4.50 weight percent. Nine objects, or 29% of those studied, have a lead composition of less than 0.5 weight percent. Fourteen, or 45%, have a lead composition between 0.5 weight percent and 3.5 weight percent. Eight, or 26%, have a lead composition greater than 5 weight percent. As in the cast of tin, the lead composition of a particular object varies according to its object type and processing, and the ways in which lead composition varies with object type and processing technique are discussed throughout the chapter.

Nineteen of the thirty-one objects analyzed in this study, or 61%, are tin bronzes with lead compositions greater than 1%. These 61% can be considered leaded bronzes where lead was purposefully added to the copper and tin to create a ternary copper-tin-lead alloy (Giumlia-Mair 1995).

Giumlia-Mair (1995, 1998) found that the average tin content of the bronze artifacts she analyzed from S. Lucia was 8.93 weight percent with tin present in a range from 0.92-16.7 weight percent; 12.5% of the objects from S. Lucia had less than 0.5 weight percent lead and 25% had greater than 3 weight percent lead. The average tin and lead compositions from Stična and S. Lucia are similar, although the composition ranges differ slightly. This difference in range between Stična and S. Lucia stems from the classes of objects available for study from each site. Giumlia-Mair focused primarily on fibulae and vessels in her study of the S. Lucia bronzes, and this study focuses on a slightly wider range of objects: rings, fibulae, belt attachment parts, and "miscellaneous" objects.

6.2: Rings

Table 6.2 shows the ring type, processing, and major, minor, and trace element compositions of the twelve rings analyzed for this study. Nine of the twelve rings were examined metallographically. Eight of the rings were worked to shape, and one is a

casting. Figure 6.2 shows the frequency of different ranges of tin and lead compositions among the twelve rings.

The tin composition of the rings ranges from 4.68-14.5 weight percent, and the average tin composition is 9.67 weight percent. The lead composition of the rings ranges from 0.027-13.2 weight percent. The distribution of tin and lead in the rings is somewhat bimodal. Seven of the rings, or 58%, have a lead composition of less than 1 weight percent. Four of the rings, or 33%, have a lead composition ranging from 1-3 weight percent. Only the foot ring has a lead composition higher than 3 weight percent; its lead composition is 13.2 weight percent. Forty-two percent of the rings can be considered leaded tin bronzes in which the lead was added purposefully to the alloy.

Three of the rings are made from thin metal sheet. These three rings all have tin compositions between 10.5 and 12 weight percent and lead concentrations equal to or less than 0.5 weight percent. All three were made from cast metal stock which was subsequently heavily worked into thin sheet. The thin sheet was either left heavily worked or was left in an annealed condition. The alloy compositions of these three rings show that metalsmiths at Stična were not using leaded tin bronze or low tin bronze to make thin metal sheet that was formed into rings. The three rings made from sheet metal are further discussed with other items made from sheet in Section 6.6.

Of the remaining nine rings not made from thin sheet, seven are identifiable as open or semi-closed rings. The tin and lead compositions of these seven rings range from 4.68-14.5 and 0.127-3.04 weight percent respectively. Four of these seven were subject to metallographic analysis which showed that the metal was worked to shape. The metal was originally cast into a long ingot which was then worked to the desired thickness, cross-section, and shape. The rings were left either lightly worked or in an annealed condition. The decorations on three of the rings, including segments and grooves or zones of incised lines, were made with engraving tools after the metal had been worked to shape and formed into a ring. The decoration on MIT 5339, a segmented leg ring, was made with a chasing type tool after the metal had been worked to shape and formed into a ring.

The worked, open and semi-closed rings range from low tin and low lead bronzes (MIT 5336, a segmented leg ring) to high tin, non-leaded bronzes (MIT 5334, a

segmented arm ring). As a group, the tin and lead compositions of the worked open and semi-closed rings are similar to the lead and tin compositions of other worked objects from both Stična and S. Lucia. This similarity is discussed further in Section 6.6.

Within the group, however, the tin and lead compositions of the worked open and semi-closed rings do not follow a set pattern. Tin and lead compositions do not appear to be dependent on ring type (leg vs. arm) or on decoration (segmented vs. zoned). They also do not appear to be dependent on grave type. MIT 5335, the child's segmented arm ring, is not noticeably different in composition or processing from the other open and semi-closed rings used by adults, and the composition range of tin and lead in rings associated with cremation graves and inhumations shows no discernable difference.

There may be a correlation between the tin content of a worked, open or semi-closed ring and the wealth of the grave in which the ring is found. MIT 5366 and MIT 5341, a segmented leg and segmented upper arm ring with low tin compositions of 4.68 and 4.97 weight percent respectively, come from Graves 26 and 28. These graves are relatively poor and do not contain any extralocal material such as glass and/or amber beads. The other open and semi-closed rings with higher tin contents all come from graves that contain at least a few glass and/or amber beads.

Only one ring was cast to shape. MIT 5342, the closed foot ring, was cast to shape and very lightly worked. It is made from a copper-tin-lead ternary alloy with a tin composition of 6.57 weight percent and a lead composition of 13.2 weight percent. The lead composition is much higher than in the other rings examined in this study. MIT 5342 is discussed further with the other as-cast objects in Section 6.6.

The rings from Stična cannot be compared with rings from similar sites as no data have been published on rings from other sites.

6.3: Fibulae

Table 6.3 shows the fibulae type, fibulae part, processing, and major, minor, and trace element compositions of the six fibulae parts analyzed for this study. Figure 6.3 shows the frequency of different ranges of tin and lead compositions among the fibulae parts.

The fibulae parts exhibit a range of tin compositions from 7.5-12.7 weight percent and a range of lead compositions from 0.78-5.22 weight percent in a somewhat bimodal distribution. The average tin composition is 10.97 weight percent and the average lead composition is 2.33 weight percent. Five of the six fibula parts have between 10.9-12.7 weight percent tin, and five of the parts have between 0.5-3.14 weight percent lead. It is unclear if the lead in the navicular fibula pin and spring, which has a lead composition of 0.78 weight percent, was added purposefully to the tin bronze; the other five fibula parts, or 83%, are made from tin bronzes to which lead was a purposeful addition.

Four of the six fibula parts were subject to metallographic analysis. Three were worked to shape. They were made from metal originally cast to a blank, were subsequently heavily worked to shape, and were left in a worked condition. MIT 5332, a fibula spring, also appears to have been heavily worked. The worked fibula parts all contain between 10.9-12.7 weight percent tin and between 0.78-1.69 weight percent lead. These ranges are relatively restricted, suggesting that fibulae, at least those parts of fibulae which were worked, had a prescribed alloy composition.

Only one fibula part, MIT 5352, the serpentine fibula disc/fold stopper, was cast to shape and left as-cast. This disc has the lowest tin content, 7.5 weight percent, of the fibulae parts examined, and its lead composition of 3.14 weight percent is slightly higher than the average lead composition of the worked fibula parts.

Giumlia-Mair (1995) found that at S. Lucia the average, overall tin content of fibulae was 9.71 weight percent with a range of 1.87-14.71 weight percent tin. The majority of the objects from S. Lucia analyzed by Giumlia-Mair were fibulae, and they exhibited a wide range of tin compositions. The average fibula tin composition at S. Lucia is consistent with the 10.97 weight percent tin average for fibulae at Stična. Across Early Iron Age sites in northeastern Italy and Slovenia serpentine fibulae have tin compositions ranging from 12-14 weight percent (Giumlia-Mair 2005). Again, the worked fibulae from Stična have a tin content similar to those found at contemporary sites.

6.4: Belt attachments

Table 6.4 shows the belt attachment part, processing, and major, minor, and trace element compositions of the five objects from belt plate and attachment assemblages analyzed for this study. Figure 6.4 shows the frequency of different ranges of tin and lead compositions among the belt attachment parts.

The belt attachment parts exhibit a range of tin compositions from 3.34-13.6 weight percent. The average tin composition is 7.90 weight percent. The range of lead compositions is from 1.86-18.7 weight percent, with an average lead composition of 9.35 weight percent. All six objects are leaded tin bronzes.

Unlike the rings and fibulae, which have somewhat restricted ranges of lead compositions, the lead composition range of the belt attachment parts is wide. This is not unexpected, as a wide variety of different belt attachment parts with different functions was analyzed.

Four of the five objects were subject to metallographic analysis. Three of the objects, the two rivets and the closed segmented ring belt loop attachment, were cast to shape and left as-cast. These three objects have the highest lead contents of the five analyzed belt attachment parts; their lead compositions range from 8.89-18.7 weight percent. The sheet belt attachment is made from cast metal stock which was subsequently heavily worked into sheet and left in a worked condition; it has a lead content of 1.86 weight percent.

Giumlia-Mair (1995, 1998) examined a few belt attachment parts, including sheet, rivets, and belt hooks. She found that the belt fittings at S. Lucia had a wide range of tin and lead compositions like the belt attachment parts from Stična. However, unlike the belt attachment parts at Stična, at S. Lucia tin and lead were only present in the belt attachments in concentrations up to 11% tin and 4% lead respectively. Rivets from S. Lucia, whether from belt fittings or vessels, do not have lead compositions higher than 3.5 weight percent. The amount of lead in the belt attachment rivets is much higher at Stična (8.84-14.4 weight percent) than at S. Lucia, and in general the concentration of tin in the Stična attachments is also higher than in the S. Lucia corpus.

6.5: Miscellaneous Objects

Table 6.5 shows the remaining eight miscellaneous objects, their processing, and their major, minor, and trace element compositions. Figure 6.5 shows the frequency of different ranges of tin and lead compositions among the miscellaneous objects.

The miscellaneous objects exhibit a range of tin compositions from 0.015-21 weight percent with an average tin composition of 8.73 weight percent. They have a range of lead compositions from 0.164-34.8 weight percent with an average lead composition of 6.82 weight percent. Four of the eight objects are leaded tin bronzes with lead present at concentrations between 1.55-7.13 weight percent.

The lump is the only non-tin bronze object analyzed for this study; it has a tin composition of less 0.015 weight percent and an unusually high lead concentration of 34.8 weight percent. The lump has the highest lead composition of all the objects from Stična. The presence of 2.58 weight percent arsenic and 1.96 weight percent antimony in the lump suggests that both the arsenic and the antimony were present in the parent ore from which the copper was smelted. Other objects with high lead contents from Stična also have rather high arsenic and antimony contents.

The extremely high lead concentration of the lump and its rectangular shape indicate that it may have been a copper-lead alloy ingot. Only one object from S. Lucia was not a tin bronze; this object was a fibula made from a copper-lead alloy with 14.5 weight percent lead (Giumlia-Mair 1995). The fibula also had the highest lead composition of all the objects analyzed at S. Lucia. The lump from Stična has the highest lead composition of any published object from an EIA Eastern Alpine site (Giumlia-Mair 1995, 1998, and 2005).

The button also contains a high tin concentration of 21 weight percent. This amount of tin would have made the button highly golden in color. The highest tin composition at S. Lucia is 16.7 weight percent tin (Giumlia-Mair 1995). In Giumlia-Mair's comprehensive review of recent metallurgical investigations into ancient copper alloys in the southeastern Alps (2005), the highest tin concentrations reported are less than seventeen weight percent tin. Giumila-Mair reports that very high tin concentrations, between 14-16 weight percent, are reserved for wheel pendants, certain fibulae, and certain Italian vessels. The button's alloy has one of the highest tin

concentrations from the EIA in the Eastern Alpine region. This high amount of tin was most certainly added to achieve the button's golden color, which makes sense in light of the fact that the button was associated with the gilded cuirass from Tumulus IV, discussed in Section 5.4.8. It is unclear if the button is an import to Stična.

6.6: Alloy composition as a function of processing

Twenty three objects were subject to metallographic analysis to determine their processing for this study. Three different processing techniques were found to have been used at Stična: 1) casting objects to shape, 2) heavily working metal into thin sheet and making objects from the thin sheet, and 3) working objects to shape from cast ingots or blanks.

Six objects, or 26%, were cast to shape and were either left as-cast or were subject to only slight working after having been cast. These objects are shown in Table 6.6. The as-cast objects have an average tin composition of 8.82 weight percent. If the button, which has a very high tin content, is not included, the average tin composition is 6.32 weight percent. The as-cast objects also have a high average lead concentration of 10.91 weight percent.

Six objects, or 26%, were made from metal originally cast to a blank and heavily worked into thin sheet. These objects are shown in Table 6.7. The objects made from sheet have an average tin composition of 9.08 weight percent and a low average lead composition of 0.76 weight percent.

Eleven objects, or 48%, were worked from metal originally cast to a blank and worked to shape. These objects are shown in Table 6.8. The worked objects have an average tin composition of 11.04 weight percent and an average lead composition of 1.63 weight percent.

Figure 6.6 shows the frequency of tin composition ranges for the as-cast objects, the objects made from sheet, and the worked objects. Although the ranges of tin compositions for all three processing techniques overlap, the general trend indicates that as-cast objects have lower tin compositions than objects made from sheet and that objects made from sheet have lower tin compositions than worked objects.

Figure 6.7 shows the frequency of lead composition ranges for the as-cast objects, the objects made from sheet, and the worked objects. Overall, the as-cast objects at Stična have much higher lead compositions than those objects which are worked or made from thin sheet. Among these high compositions, the range of lead compositions in the as-cast objects is wide. By contrast, objects made from sheet and worked objects have restricted ranges of lead compositions. Objects made from sheet contain less than two weight percent lead, and the majority have less than 0.5 weight percent lead. The majority of the worked objects have a lead composition ranging from 0-3 weight percent.

The majority of the worked objects are open and semi-closed rings and fibulae. The tin compositions of these object types are discussed in Sections 6.2 and 6.3. The tin composition of these objects appears to be related to specific object types and to other factors such as grave wealth more than to the processing of the object. The range of tin composition they exhibit is narrow, ranging between 8.7 and 12.9 weight percent (with the exception of one arm ring, MIT 5341, that contains only 4.97% tin). It is striking how uniform the tin content is overall.

Worked objects usually contain between 0-3 weight percent lead, and the lead content in these objects is carefully controlled. The controlled lead content is directly related to the processing of these objects. Worked objects must be able to be worked heavily, and high concentrations of lead in tin bronzes form globules between grain boundaries that may lead to cracking upon hammering (Davis 2001). Considering the two alloying elements, tin and lead, in these worked bronzes, it appears that alloy composition was regulated with respect to both and that a certain measure of uniformity was achieved in leaded bronzes that were to be worked heavily in producing the final product.

Both the tin and lead compositions of objects made from sheet are directly related to the object's processing. The range of tin compositions, 5.5-12.13 weight percent, allows for the thin sheet to be hard and strong without being brittle. Higher amounts of tin would make the sheet fairly brittle, forcing the metalsmith to anneal the metal constantly as it was being reduced to thin sheet. The low amount of lead does not lead to crack formation (Giumlia-Mair 1995).

With the exception of the button, whose tin content is high to affect its color, the tin compositions of the as-cast objects are generally lower than in worked objects and in objects made from sheet. As-cast objects have high or very high concentrations of lead, and the lead composition is not carefully controlled. The tin and lead compositions of the as-cast objects are directly related to the object's processing. Because the objects did not need to be hammered extensively, lead could be used as a cheap "filler" metal in place of copper and/or tin. The lead did not have a large effect on the objects' color; the highly leaded tin bronzes still appeared light gold in color. High concentrations of lead in bronze alloys increase the fluidity of the alloy so that the metal runs more easily into the mold, and the addition of lead also lowers the melting point of the bronze (Gettens 1969). The seemingly random tin and lead compositions indicate that the metal used to make as-cast objects may have been recycled scrap metal.

A comparison of the trace elements present in objects made with different processing techniques suggests that the copper used to make objects from thin sheet may have been subject to purification whereas the copper used to make worked and cast objects was not. While the overall trace element compositions of nickel and cobalt are similar among the three processing techniques, the concentration of antimony, arsenic, silver, and iron in the objects made from sheet is much lower than the concentrations of those elements in the worked and cast objects. This trend may be partly an artifact of the composition analysis method used on different objects; the majority of the objects made from sheet had their compositions determined on the electron microbeam probe. The trend is still noteworthy.

6.7: Copper ore and smelting practices

Trace amounts of iron in ancient copper are a product of both the parent copper ore from which the copper was smelted and of the type of smelting process used to win the metal from the ore. Although iron contents can vary widely among bronze objects, on average the iron content of ancient bronzes indicates the smelting technique used to win the copper from its parent ore (Craddock 1999).

More advanced smelting processes allow for highly reducing conditions and free-flowing slag in a smelting furnace, causing the final iron content of the resulting copper

to be higher than copper smelted using more primitive methods. Less advanced smelting procedures have poor reducing conditions and are often non-slagging. Copper and copper based alloys produced by earlier and/or less technically advanced methods tend to have a much lower iron content than those produced by later or more technically advanced processes. More advanced smelting processes usually produce copper and copper alloy objects with iron present at concentrations of about 0.3 weight percent, while less advanced processes typically produce objects with iron present at concentrations between 0.03-0.05 weight percent (Craddock 1995).

The average iron content of the bronzes at Stična is 0.12 weight percent. Eighteen objects, or 60%, contained less than 0.1 weight percent iron. Three objects, or 10%, contained greater than 0.3 weight percent iron.

The average iron content of the bronzes at Stična suggests that the majority of the copper-alloy objects were made from copper smelted using relatively primitive processes. Bronze objects from related EIA cultures show approximately the same levels of iron as the objects from Stična. Objects from S. Lucia have an average iron content of 0.13 weight percent, with 62% having less than 0.1 weight percent iron and 7.7% having greater than 0.3 weight percent iron (Giumlia-Mair 1995). Northern Italian bronzes from the same period have an average iron content of 0.09 weight percent (Craddock 1987), and some Archaic Greek bronzes have an average iron content of 0.12 weight percent (Craddock 1977).

6.8: Bronzes from Stična compared to bronzes from other EIA Eastern Alpine Region sites

The bronzes at Stična are comparable to those from S. Lucia and other EIA Eastern Alpine region sites with respect to the relationship between an object's tin and lead composition and its processing. Giumlia-Mair (1995) found trends in the composition of cast objects, worked objects, and objects made from sheet at S. Lucia that are similar to those found in this study of objects from Stična.

The majority of objects from S. Lucia made from sheet, such as vessels, contain less than 1.5 weight percent lead and between 9.5-13 weight percent tin. Sheet metal from other Eastern Alpine sites, such as San Zeno, has a wider range of tin, ranging from

3.5-14 weight percent (Giumlia-Mair 2005). These compositions are closely comparable to the compositions of objects made from sheet at Stična.

The majority of worked fibulae from S. Lucia (no rings have been analyzed from S. Lucia) contain between 0-3.5 weight percent lead and between 4.5-14 weight percent tin. These compositions are similar to the compositions of worked rings and fibulae from Stična.

Giumlia-Mair found that cast objects and objects with no mechanical function at S. Lucia contained higher amounts of lead and lower amounts of tin than wrought objects and objects made from sheet. She also found that cast and non-mechanically functioning parts of objects at S. Lucia tended to have random tin and lead compositions. The trend she reports in lead and tin compositions among cast and non-mechanically functioning parts is similar at Stična. However, cast objects at Stična have higher lead contents than those from S. Lucia.

Stična also has an object with a higher tin composition than other sites. The button's high tin content (21 weight percent) has one of the highest reported tin concentrations from the EIA in the Eastern Alpine region (Giumlia-Mair 2005).

There is evidence from trace element compositions that the sheet metal from Stična may have been made from purified copper. Purification of copper was common at many EIA Eastern Alpine sites, including S. Lucia (Giumlia-Mair 1995, Giumlia-Mair 2005).

The iron content in the bronzes from Stična indicates that the copper was smelted with relatively primitive smelting techniques similar to those practiced at other EIA Eastern Alpine sites (Giumlia-Mair 2005).

Decorations at both Stična and S. Lucia are similar. At both sites they consist mainly of engraving, incising, punching, and repoussé techniques (Giumlia-Mair 1995). While no gilding was found on any objects from S. Lucia, the cuirass from Tumulus IV had evidence of gilding. This unique cuirass was probably imported.

Final conclusions on the relationship between bronze metallurgy at Stična and at other contemporary EIA sites can be found in Chapter 7.

Table 6.1: Composition Data for all Objects

	MIT #	Sn	Pb	Sb	As	Ni	Co	Ag	Fe
segmented leg ring	5339	13.7	0.372	0.163	0.101	2.04	0.023	0.071	0.18
segmented leg ring	5336	4.68	1.88	0.791	0.399	0.757	0.0178	0.433	0.008
segmented upper arm ring	5341	4.97	3.04	0.469	0.373	0.293	0.0309	0.254	0.23
segmented arm ring	5334	14.5	0.38	0.158	0.165	0.158	0.019	0.093	0.005
segmented child's arm ring	5335	5.94	0.127	0.265	0.345	1.5	0.179	0.282	0.006
zoned arm ring	5344	11.3	1.87	0.753	0.501	0.2	0.017	0.248	0.028
arm ring	5346	8.72	1.65	1.39	0.793	0.275	0.01	0.719	0.158
arm ring	5340	12.3	0.825	0.58	0.554	0.31	0.0328	0.242	0.23
hollow arm ring*	5366	12.13	0.501	n.d.	0.186	0.104	0.007	n.d.	0.005
flat arm ring*	5365	10.64	0.027	n.d.	0.152	0.398	0.044	0.014	0.042
child's finger ring*	5353	10.54	0.453	0.114	0.216	0.368	n.d.	0.08	0.005
foot ring	5342	6.57	13.2	1.05	1.17	0.492	0.031	0.323	0.054
serpentine fibula	5330	11.4	1.53	0.537	0.485	0.311	0.0591	0.252	0.018
serpentine fibula	5352	10.9	1.69	0.063	0.187	0.061	0.017	0.056	0.007
serpentine fibula disc*	5352	7.5	3.14	0.0118	0.38	0.057	0.0112	0.1138	0.003
navicular fibula	5348	12.7	0.777	0.304	0.375	0.134	0.0099	0.118	n.d.
knobbed fibula	5331	11.2	1.66	0.053	0.157	0.048	0.0192	0.02	0.13
fibula spring	5332	12.1	5.22	0.232	0.219	0.145	0.009	0.485	0.25
rivet	5343	5.12	14.4	0.849	1.06	0.397	0.018	0.282	0.057
rivet*	5368	3.34	8.89	0.5	0.97	0.331	0.013	0.388	0.284
belt sheet*	5368	8.04	1.86	n.d.	0.134	1.147	0.013	0.044	0.021
belt hook	5345	13.6	2.88	0.225	0.359	0.199	0.0456	0.093	0.047
belt ring	5350	9.38	18.7	1.46	1.36	0.763	0.041	0.404	0.073
tweezers	5329	7.55	6.47	0.13	0.204	0.0749	0.0317	0.071	0.16
tweezers	5333	4.79	3.5	0.348	0.253	0.2	0.0219	0.2	0.61
earring (sheet)*	5367	7.61	0.164	n.d.	0.028	0.017	0.007	n.d.	0.028
twisted earring wire	5337	10.5	0.492	0.174	0.222	0.171	0.0401	0.097	0.5
cylindrical earring wire	5351	12.9	0.436	0.115	0.119	0.137	0.0886	0.061	0.47
spirals	5338	5.5	1.55	0.073	0.334	0.097	0.0579	0.038	0.008
button	5349	21	7.13	0.184	0.178	0.0987	0.0146	0.222	0.17
lump	5347	0.015	34.8	1.96	2.58	0.764	0.0054	0.797	0.008
Average		**9.39**	**4.50**	**0.418**	**0.470**	**0.389**	**0.030**	**0.210**	**0.122**

(all values in weight %) n.d. = not detected * = composition determined by electron microbeam probe

Table 6.2: Ring Types, Processing, and Compositions

MIT #	Ring Type	Open/Closed	Decoration/ Description	Processing	Sn	Pb	Sb	As	Ni	Co	Ag	Fe
5339	leg	semi-closed	segmented	worked, left annealed	13.7	0.372	0.163	0.101	2.04	0.023	0.071	0.18
5336	leg	semi-closed	segmented	n.a.	4.68	1.88	0.791	0.399	0.757	0.0178	0.433	0.008
5341	upper arm	open	segmented	worked, unclear how left (cremation)	4.97	3.04	0.469	0.373	0.293	0.0309	0.254	0.23
5334	arm	semi-closed	segmented	n.a.	14.5	0.38	0.158	0.165	0.158	0.019	0.093	0.005
5335	child's arm	semi-closed	segmented	n.a.	5.94	0.127	0.265	0.345	1.5	0.179	0.282	0.006
5344	arm	semi-closed	zoned with segments and incised lines	worked, left lightly worked	11.3	1.87	0.753	0.501	0.2	0.017	0.248	0.028
5346	arm	unknown	zoned with incised lines	worked, left annealed	8.72	1.65	1.39	0.793	0.275	0.01	0.719	0.158
5340	arm	semi-closed	zoned with incised lines	worked, left worked	12.3	0.825	0.58	0.554	0.31	0.0328	0.242	0.23
5366	arm*	closed	hollow ring made from sheet; segmented	worked, left annealed	12.13	0.501	n.d.	0.186	0.104	0.007	n.d.	0.005
5365	arm*	semi closed or open	flat ring with incised lines and chevron pattern	heavily worked, left heavily worked	10.64	0.027	n.d.	0.152	0.398	0.044	0.014	0.042
5353	child's finger*	semi closed or open	flat ring with incised lines and chevron pattern	heavily worked, left lightly worked	10.54	0.453	0.114	0.216	0.368	n.d.	0.08	0.005
5342	foot	closed	segmented	cast to shape, very lightly worked	6.57	13.2	1.05	1.17	0.492	0.031	0.323	0.054
Average					**9.67**	**2.03**	**0.478**	**0.413**	**0.575**	**0.034**	**0.230**	**0.079**

(all values in weight %) n.d. = not detected n.a.= not analyzed * = composition determined by electron microbeam probe

Table 6.3: Fibulae Types, Parts, Processing, and Compositions

MIT #	Fibula Type	Fibula Part	Processing	Sn	Pb	Sb	As	Ni	Co	Ag	Fe
5330	serpentine	pin	heavily worked, left heavily worked	11.4	1.53	0.537	0.485	0.311	0.0591	0.252	0.018
5352	serpentine with disc	bow	heavily worked, left heavily worked	10.9	1.69	0.063	0.187	0.061	0.017	0.056	0.007
5352	serpentine with disc	disc*	cast to shape	7.5	3.14	0.0118	0.38	0.057	0.0112	0.1138	0.0033
5348	navicular	pin and spring	worked, left worked	12.7	0.777	0.304	0.375	0.134	0.0099	0.118	n.d.
5331	"knobbed"	bow	n.a.	11.2	1.66	0.053	0.157	0.048	0.0192	0.02	0.13
5332	unknown	springs	worked, unknown how left	12.1	5.22	0.232	0.219	0.145	0.009	0.485	0.25
Average				**10.97**	**2.34**	**0.200**	**0.300**	**0.126**	**0.021**	**0.174**	**0.068**

(all values in weight %) n.d. = not detected n.a.= not analyzed * = composition determined by electron microbeam probe

Table 6.4: Belt Attachments, Parts, Processing, and Compositions

MIT #	Object	Processing	Sn	Pb	Sb	As	Ni	Co	Ag	Fe
5343	rivet	cast to shape	5.12	14.4	0.849	1.06	0.397	0.018	0.282	0.057
5368	rivet *	cast to shape	3.34	8.89	0.5	0.97	0.331	0.013	0.388	0.284
5368	sheet*	worked, left worked	8.04	1.86	n.d.	0.134	1.147	0.013	0.044	0.021
5345	hook	n.a.	13.6	2.88	0.225	0.359	0.199	0.0456	0.093	0.047
5350	segmented ring	cast to shape	9.38	18.7	1.46	1.36	0.763	0.041	0.404	0.073
Average			**7.90**	**9.35**	**0.607**	**0.777**	**0.567**	**0.026**	**0.242**	**0.096**

(all values in weight %) n.d. = not detected n.a.= not analyzed * = composition determined by electron microbeam probe

Table 6.5: Miscellaneous Objects, Processing, and Compositions

MIT #	Object	Processing	Sn	Pb	Sb	As	Ni	Co	Ag	Fe
5329	tweezers	n.a.	7.55	6.47	0.13	0.204	0.0749	0.0317	0.071	0.16
5333	tweezers	n.a.	4.79	3.5	0.348	0.253	0.2	0.0219	0.2	0.61
5367	earring (hollow wire/sheet)*	heavily worked, left worked	7.61	0.164	n.d.	0.028	0.017	0.007	n.d.	0.028
5337	earring wire/twisted wire	worked, left annealed	10.5	0.492	0.174	0.222	0.171	0.0401	0.097	0.5
5351	earring wire/cylindrical and twisted wire	worked, left annealed	12.9	0.436	0.115	0.119	0.137	0.0886	0.061	0.47
5338	spirals (sheet)	worked, left annealed	5.5	1.55	0.073	0.334	0.097	0.0579	0.038	0.008
5349	button body and loop	cast to shape	21	7.13	0.184	0.178	0.0987	0.0146	0.222	0.17
5347	lump	n.a.	0.015	34.8	1.96	2.58	0.764	0.0054	0.797	0.008
Average			**8.73**	**6.82**	**0.373**	**0.490**	**0.195**	**0.033**	**0.186**	**0.244**

(all values in weight %) n.d. = not detected n.a.= not analyzed * = composition determined by electron microbeam probe

Table 6.6: Compositions of as-cast objects

	MIT #	**Sn**	**Pb**	**Sb**	**As**	**Ni**	**Co**	**Ag**	**Fe**
segmented foot ring	5342	6.57	13.2	1.05	1.17	0.492	0.031	0.323	0.054
rivet	5343	5.12	14.4	0.849	1.06	0.397	0.018	0.282	0.057
rivet*	5368	3.34	8.89	0.5	0.97	0.331	0.013	0.388	0.284
belt ring attachment	5350	9.38	18.7	1.46	1.36	0.763	0.041	0.404	0.073
button	5349	21	7.13	0.184	0.178	0.0987	0.0146	0.222	0.17
fibula disc*	5352	7.5	3.14	0.0118	0.38	0.057	0.0112	0.1138	0.003
Average		**8.82****	**10.91**	**0.676**	**0.853**	**0.356**	**0.022**	**0.289**	**0.107**

(all values in weight %) n.d. = not detected * = composition determined by electron microbeam probe **= Tin average is 6.32 weight percent when the button's tin composition is not considered in the overall average.

Table 6.7: Compositions of objects made from heavily worked sheet

	MIT #	**Sn**	**Pb**	**Sb**	**As**	**Ni**	**Co**	**Ag**	**Fe**
hollow arm ring*	5366	12.13	0.501	n.d	0.186	0.104	0.007	n.d	0.005
flat arm ring*	5365	10.64	0.027	n.d	0.152	0.398	0.044	0.014	0.042
flat finger ring*	5353	10.54	0.453	0.114	0.216	0.368	n.d	0.08	0.005
belt attachment sheet*	5368	8.04	1.86	n.d	0.134	1.147	0.013	0.044	0.021
sheet earring wire*	5367	7.61	0.164	n.d	0.028	0.017	0.007	n.d	0.028
spirals	5338	5.5	1.55	0.073	0.334	0.097	0.0579	0.038	0.008
Average		**9.08**	**0.76**	**0.031**	**0.175**	**0.355**	**0.021**	**0.029**	**0.018**

(all values in weight %) n.d. = not detected * = composition determined by electron microbeam probe

Table 6.8: Compositions of worked objects

MIT #	**Object**	**Sn**	**Pb**	**Sb**	**As**	**Ni**	**Co**	**Ag**	**Fe**
5339	segmented leg ring	13.7	0.372	0.163	0.101	2.04	0.023	0.071	0.18
5341	segmented upper arm	4.97	3.04	0.469	0.373	0.293	0.0309	0.254	0.23
5344	zoned arm ring	11.3	1.87	0.753	0.501	0.2	0.017	0.248	0.028
5346	zoned arm ring	8.72	1.65	1.39	0.793	0.275	0.01	0.719	0.158
5340	zoned arm ring	12.3	0.825	0.58	0.554	0.31	0.0328	0.242	0.23
5330	serpentine fibula pin	11.4	1.53	0.537	0.485	0.311	0.0591	0.252	0.018
5352	serpentine fibula bow	10.9	1.69	0.063	0.187	0.061	0.017	0.056	0.007
5348	navicular fibula pin	12.7	0.777	0.304	0.375	0.134	0.0099	0.118	n.d.
5332	fibula springs	12.1	5.22	0.232	0.219	0.145	0.009	0.485	0.25
5351	cylindrical earring wire	12.9	0.436	0.115	0.119	0.137	0.0886	0.061	0.47
5337	earring wire/twisted wire	10.5	0.492	0.174	0.222	0.171	0.0401	0.097	0.5
Average		**11.04**	**1.63**	**0.434**	**0.357**	**0.371**	**0.031**	**0.237**	**0.188**

(all values in weight %) n.d. = not detected

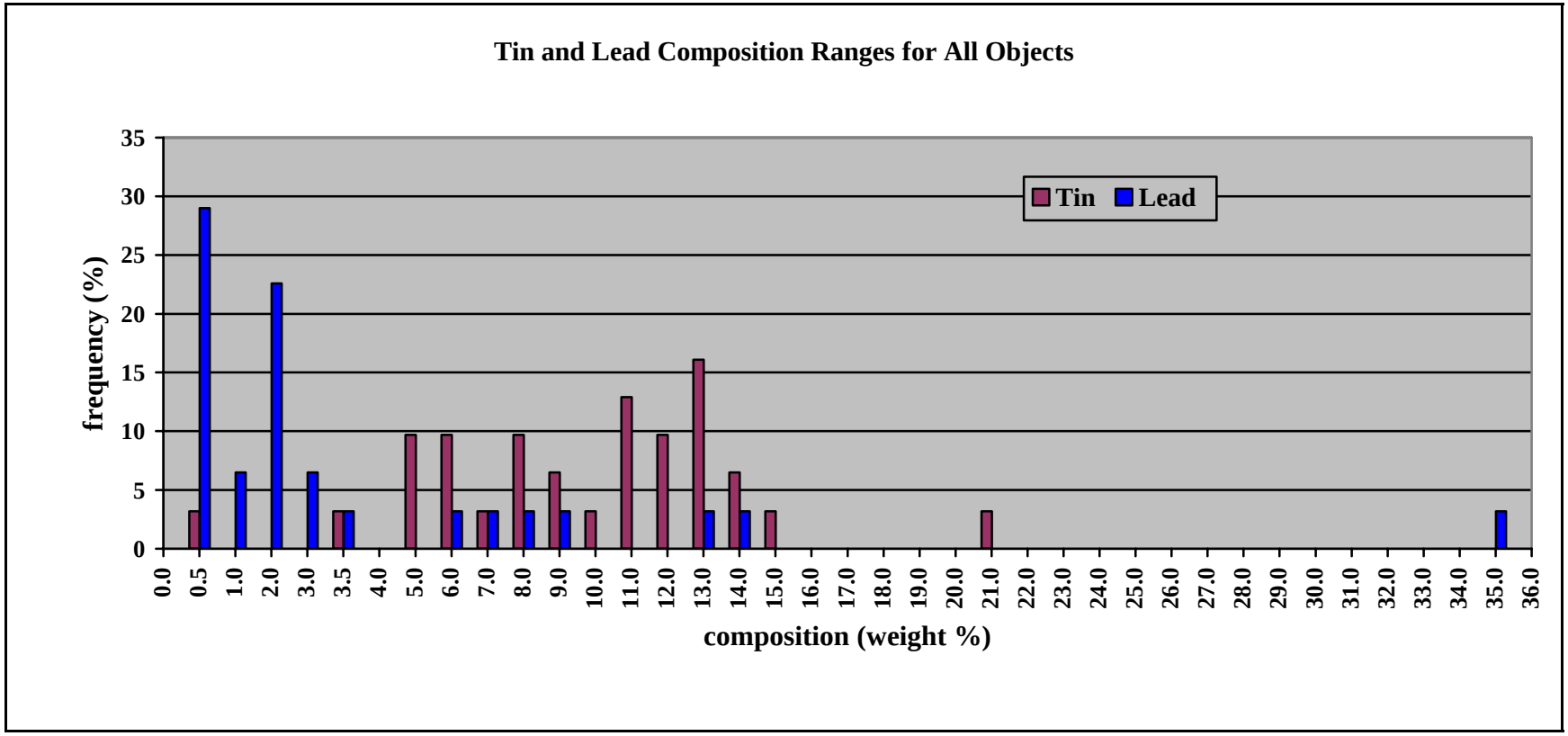

Figure 6.1: Analytical results for all 31 copper alloy objects. The range of tin compositions and the range of lead compositions are independently plotted for all objects. The composition of the 31 objects exhibits a wide spread in tin and lead.

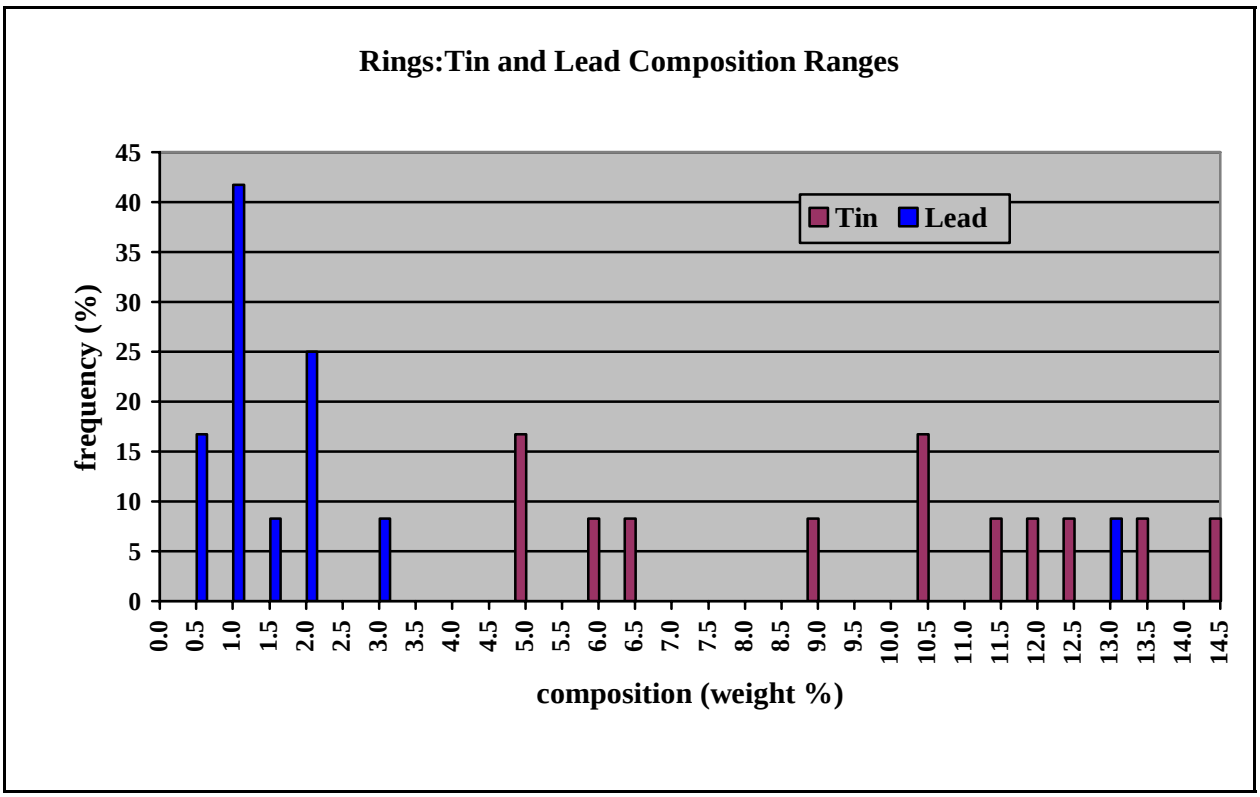

Figure 6.2: Analytical results for the 12 rings. The range of tin compositions and the range of lead compositions are independently plotted for all objects. Forty-two percent of the rings are leaded tin bronzes, and the tin and lead compositions exhibit a bimodal distribution. The majority of the rings have a lead composition of less than 3.5 weight percent

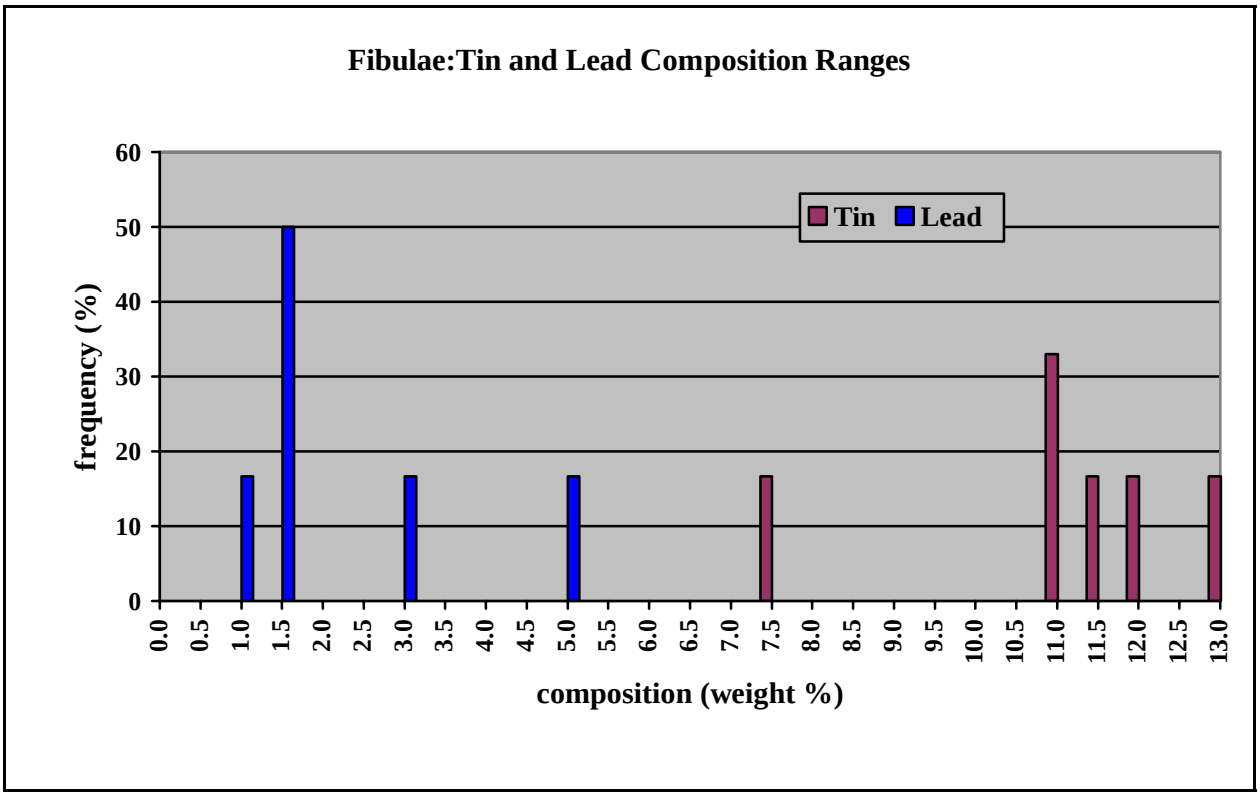

Figure 6.3: Analytical results for the 6 fibulae. The range of tin compositions and the range of lead compositions are independently plotted for all objects. At least 83% of the fibulae are leaded tin bronzes. The majority of the fibulae have a low lead composition ranging from 1-3 weight percent and a high tin composition ranging from 11-13 weight percent; the tin and lead compositions exhibit a bimodal distribution.

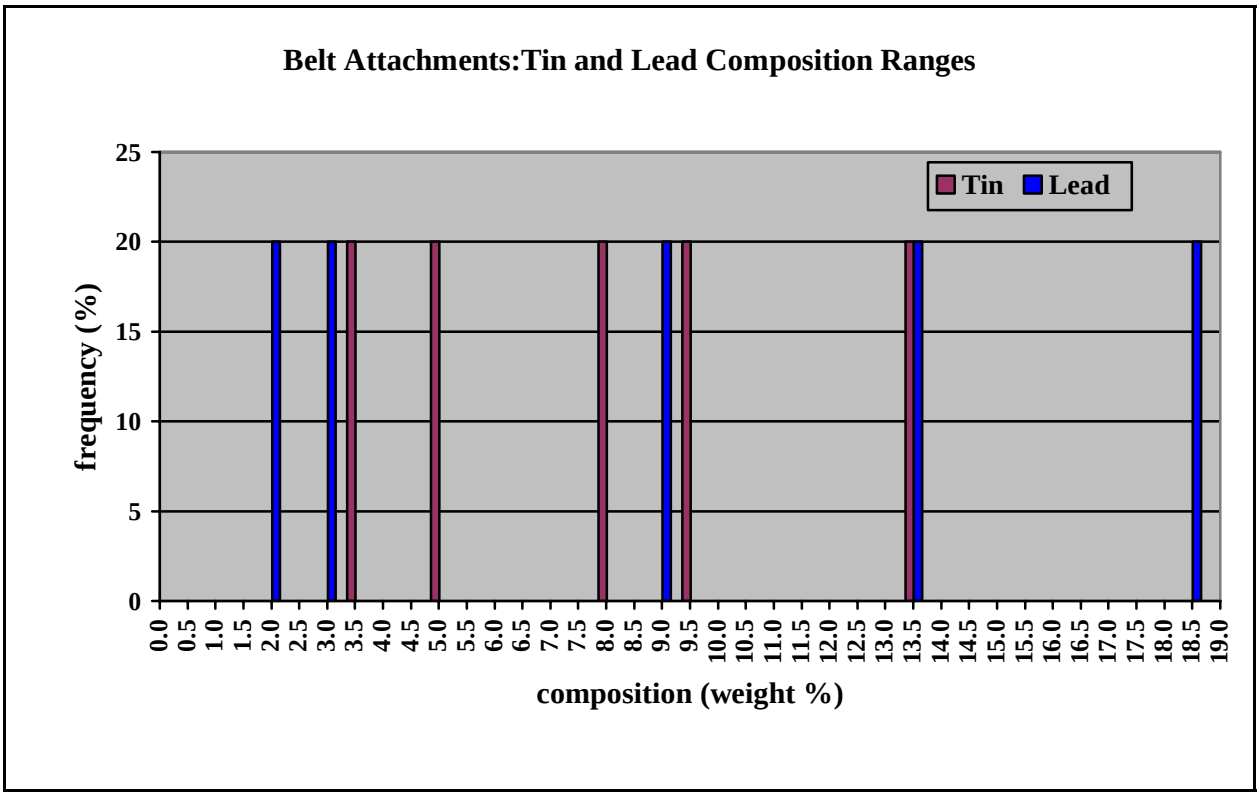

Figure 6.4: Analytical results for the 5 belt attachment parts. The range of tin compositions and the range of lead compositions are independently plotted for all objects. All six belt attachment parts are leaded tin bronzes. The belt attachment parts exhibit a random distribution of tin and lead compositions.

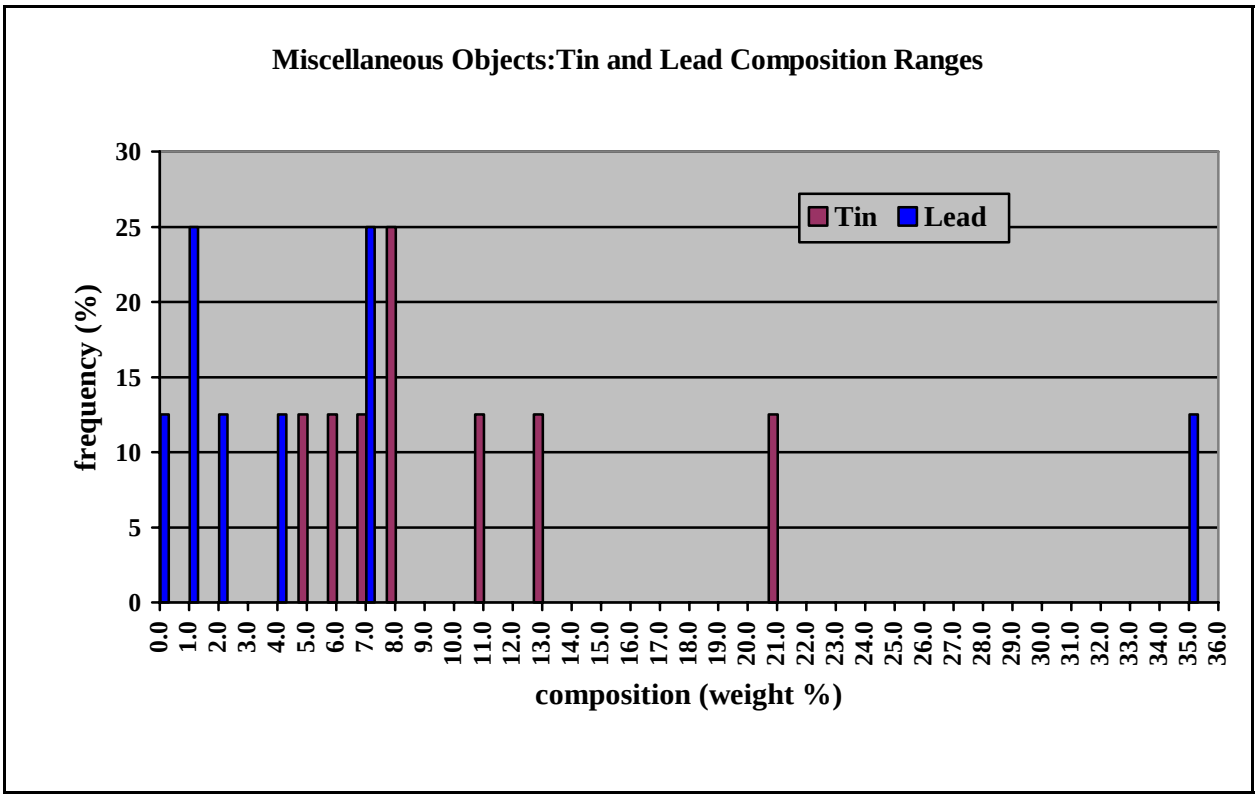

Figure 6.5: Analytical results for the 11 miscellaneous objects. The range of tin compositions and the range of lead compositions are independently plotted for all objects. The remaining, "miscellaneous objects" exhibit a random distribution of tin and lead compositions that reflects the random make-up of this group.

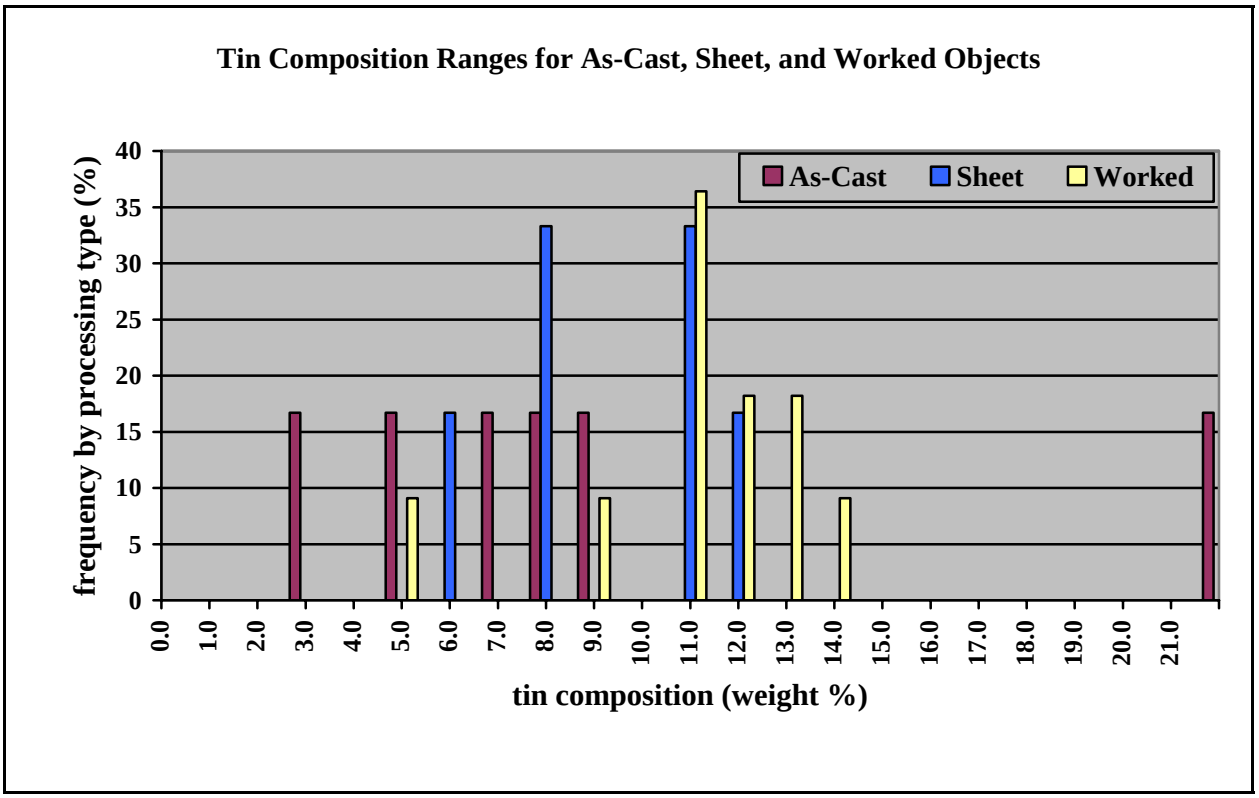

Figure 6.6: Tin composition ranges for as-cast, sheet, and worked objects. Although the ranges of all three processing types overlap, the general trend shows that as-cast objects have lower tin compositions than objects made from sheet and worked objects and that objects made from sheet have lower tin compositions than worked objects.

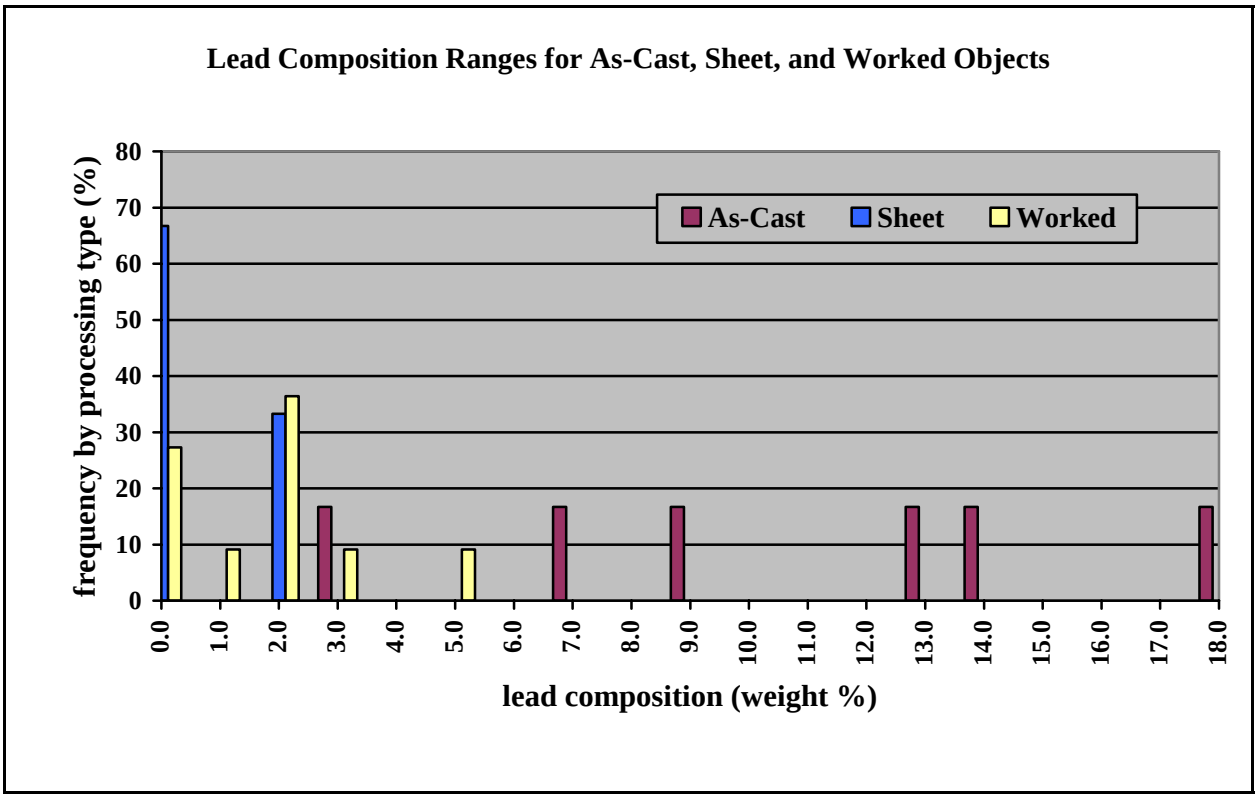

Figure 6.7: Lead composition ranges for as-cast, sheet, and worked objects. The as-cast objects have much higher lead compositions than the worked objects and objects made from sheet; the exact lead composition of each as-cast object appears to be random. The objects made from sheet all have less than two weight percent lead, and the majority have less than 0.5 weight percent lead. The majority of the worked objects have a lead composition ranging from 0-3 weight percent.

Chapter 7: Conclusions and Future Work

7.1: Conclusions

Bronze metallurgy was similar at Stična and at contemporary Eastern Alpine sites. Smiths at Stična and throughout the Eastern Alpine region were using copper produced by relatively primitive smelting techniques, despite their use of more sophisticated alloying techniques (Giumlia-Mair 2005). As no evidence of ancient copper mining or smelting has been found in or around Stična, the exact ore types from which copper was smelted are not clear, although the presence of both arsenic and antimony in many of the alloys suggests that a tetrahedrite-type of ore was a major source of copper. Some of the copper, especially that used to produce metal sheet, was probably refined before being alloyed with tin to make tin-bronze.

The metallographic study of thirty-one bronze objects from Stična, reported here, is the first such study of its kind. The metallographic determinations make clear that at Stična different alloys and processing techniques were combined to produce bronze objects with specific desired physical properties, such as hardness and flexibility. Tin compositions in worked objects and objects made from sheet were controlled to increase hardness and strength while controlling for brittleness. Tin compositions in some cast objects, such as the button (MIT 5349), were also controlled to manipulate an object's color.

Lead was also carefully controlled as an alloying element. It was added when needed to increase the fluidity of a casting, and it was withheld when bronze was used to product thin sheet. Cast objects and non-mechanically functioning parts such as fibula discs were made with high lead concentrations and possibly from recycled bronze, because they did not require a carefully controlled alloy composition.

Metalsmiths at Stična were using slightly more lead in their cast objects than smiths at contemporary EIA sites. These highly leaded tin bronzes still produced bronze that was light gold in color, but they required less tin and copper to make them large and heavy. It is unclear if this use of high amounts of lead was in response to a tin or copper shortage, or if lead was simply used as an additive to recycled bronze scrap to increase

the volume of metal. The variety and number of cast objects in which this high lead content can be found indicates that this use of high lead was a local phenomenon and that these objects were not imported.

As solder was not known or was present only in an incipient form (Guimlia-Mair 1995), even though smiths understood that highly leaded bronze had a lower melting point than tin bronzes containing no or with a low lead content, they were not able to join separate pieces of bronze by metallurgical joining techniques. Thus, many objects with different functional requirements, such as the navicular pin and spring (MIT 5348), were made from only one piece of bronze with one alloy composition.

If an object was made from more than one bronze piece, the pieces were joined mechanically. Several different types of mechanical joins were used. Rivets were most common and were used on a variety of objects from belt attachments (such as MIT 5368) to vessels (such as the sieve shown in Section 5.4.8) to fibulae (such as the dragon fibula shown in Section 5.2.6). Other examples of mechanical attachments include the serpentine fibula and disc (MIT 5352), where the disc was mechanically attached to the fibula by easing the two parts together until they formed a join, and the twisted earring wire (MIT 5351), where two separate pieces of wire were mechanically twisted together.

Decorations such as segments, grooves, and lines were usually added as the last step in the production process by engraving or incising a finished object with an engraving tool. A few instances of repoussé technique, such as that found on the belt attachment (MIT 5368), are also present. Gilding is present only on the cuirass discussed in Section 5.4.8.

The metalsmiths at Stična were clearly part of a common, wide-ranging metallurgical tradition in the Early Iron Age. Within this larger bronze metallurgical framework, however, the artisans at Stična were able to change and adopt bronze technologies to suit the needs of their local community. The bronze technologies present during the EIA at Stična reflect the community's status as an incipient commercial center of increasing importance throughout the EIA and its increasing exposure to extralocal goods and traditions.

7.2: Future Work

Future work on bronze metallurgy from Stična and Lower Carniola should fall into two categories: 1) further work at Stična itself, and 2) a bronze metallurgical study of the other two sites from Lower Carniola in the Mecklenburg collection, Magdalenska Gora and Vinica (Figure 2.1, site numbers 3 and 4).

The largest tumuli and the outlines of the hillfort settlement at Stična were systematically excavated between 1946 and 1964 by Gabrovec (Gabrovec 1964-1965; 1966). Although the chronology of the EIA determined by Gabrovec from his work at Stična is reported by others in English (Hencken 1978; Mason 1996), the majority of his findings and detailed excavation reports are all in Slovenian and thus were not available for this study. Other Slovenian archaeologists, such as Teržan (Teržan 1990; 1995), have examined grave groups from Early Iron Age sites in Slovenia in order to attribute individual characteristics such as age, sex, and social class to particular classes of grave goods. Future work might involve applying the results of this study of bronze technologies at Stična to the other scientifically excavated tumuli at Stična and relating bronze technologies to the age, sex, and social classes of individuals. Most importantly, the hillfort settlement and associated dwellings must be further excavated, and, if bronzes are found in these areas, they should be examined.

The other two sites represented in the Mecklenburg collection, Magdalenska Gora and Vinica, are Late Iron Age (LIA), La Tené sites (Greis 2006). Geselowitz's study (Geslowitz 1987; 1988) of iron objects from Stična, Magdalenska Gora, and Vinica found that iron technologies in Lower Carniola did not change from the EIA to the LIA, even as iron technology was changing fairly rapidly in other areas of Europe such as Italy and Greece. This led him to the conclusion that Lower Carniola, an important region during the EIA, became somewhat of a cultural backwater during the Late Iron Age as Etruscan and archaic Greek cultures expanded. Bronze technologies from Italian and Greek LIA cultures have been studied (Giumlia Mair 2005), and it has been found that LIA bronze technologies were different from EIA bronze technologies in these areas. It would be informative to determine if bronze technology in Lower Carniola changed from the EIA

to the LIA as well, or if, like iron technology in the region, it remained relatively stagnant as neighboring cultures began to overshadow it.

References

Collis, J. (1997). *The European Iron Age*. London: Routledge Press.

Craddock, P. T. (1977). The composition of the copper alloys used by the Greek, Etruscan, and Roman civilizations; 2. The Archaic, Classical, and Hellenistic Greeks. *Journal of Archaeological Science* (3): 93-113.

Craddock, P. T. a. N. M. (1987). Iron in Ancient Copper. *Archaeometry* 29(2): 187-204.

Craddock, P. T. (1995). *Early Metal Mining and Production.* Washington D.C., Smithsonian Institution Press.

Craddock, P. T. (1999). Paradigms of metallurgical innovation in prehistoric Europe. *The Beginnings of Metallurgy: Proceedings of the International Conference The Beginnings of Metallurgy.* A. H. e. *al*. Bochum, Dt. Bergbau-Museum. Beiheft 9**:** 175-192.

Davis, J. R., Ed. (2001). *Copper and Copper Alloys.* ASM Specialty Handbook. Materials Park, OH, ASM International: The Materials Information Society.

Gabrovec, S. (1964-1965). Halstaska kultura Slovenije. *Arheološki vestnik* 15-16: 127-135.

Gabrovec, S. (1966). Zur Hallstattzeit in Slowenien. *Germania* 44: 1-48.

Gabrovec, S. (1974). Die Ausgrabungen in Stična und ihre Bedeutung für die südostalpine Hallstattkultur. *Symposium zu Problemen der jüngeren Hallstattzeit in Metteleuropa*. Vydavatel'stvo Slvenskej Akadémie Vied, Bratislava: 163-187.

Geselowitz, M. N. (1987). *Technological Development and Social Change: Ironworking in Late Prehistoric Central Europe.* Ph.D Thesis. Cambridge, MA: Department of Anthropology, Harvard University.

Geselowitz, M. N. (1988). Technology and Social Change: Ironworking in the Rise of Social Complexity in Iron Age Central Europe. *Tribe and Polity in Late Prehistoric Europe: Demography, Production, and Exchange in the Evolution of Complex Social Systems.* O. B. G. a. M. N. Geselowitz. New York, Plenum Press**:** 137-154.

Gettens, R.J. (1969). *The Freer Chinese Bronzes: Volume II, Technical Studies.* Washington D.C.:Smithsonian Institution Freer Gallery of Art, Oriental Studies, No. 7.

Giumlia-Mair, A. (2003). Iron Age tin in the Oriental Alps. *Le problème de l'étain à l'origine de la métallurgie (The problem of early tin), Acts of the XIVth UISPP Congress, University of Liège, Belgium, 2–8 September 2001, Section 11, Bronze Age in Europe and the Mediterranean, Symposium 11.2.* e. A. G.-M. a. F. L. Schiavo. Oxford, 93–108, BAR International Series 1199, British Archaeological Reports.

Guimlia-Mair, A. (1995). The Copper-Based Finds from a Slovenian Iron Age Site. *Bulletin of the Metals Museum* 23: 59-81.

Guimlia-Mair, A. (1998). The Construction Techniques of the Bronzes from Santa Lucia. *L'Atelier du bronzier en Europe du XX au VIII siécle avant notre ére. Actes du colloque international Bronze '96. Neuchâtel et Dijon. Tome II: Du mineral au métal, du métal â l'object.* C. M. e. *al*. Paris, CTHS**:** 169-182.

Guimlia-Mair, A. (2000). Bronze Technology in the Eastern Subalpine Region Between the Final Bronze Age and Early Iron Age. *Ancient Metallurgy Between Oriental Alps and Pannonian Plain, Workshop-Trieste, 29-30 October 1998.* A. Guimlia-Mair. Aquileia, Italy, Associazione Nazionale per Aquileia**:** 77-91.

Guimlia-Mair, A. (2005). Copper and Copper Alloys in the Southeastern Alps: An Overview. *Archaeometry* 47(2): 275-292.

Greis, G.P. (2006). *A Noble Pursuit: The Duchess of Meckleburg Collection from Iron Age Slovenia*. Cambridge, MA: Peabody Musuem Press, Harvard University.

Hencken, H. (1978). *The Iron Age Cemetery of Magdalenska gora in Slovenia, Mecklenburg Collection, Part II.* Bulletin. A. S. o. P. Research. Cambridge, MA: Peabody Museum of Archaeology and Ethnology, Harvard University.

Mason, P. (1996). *The Early Iron Age of Slovenia*. BAR International Series 643.

Murray, M, Greis, G., and Arnold, B. (1984). Hallstatt Bronzes of the Mecklenburg Collection: Metallurgy through the Microscope. Unpublished.

Phillips, P. (1980). *The Prehistory of Europe.* London: Allen Lane.

Sklenár (1983). *Archaeology in Central Europe: the First 500 Years*. New York, St. Martin's Press.

Teržan, B. (1990). *The Early Iron Age in Slovenian Styria.* Ljublijana: Narodni muzej.

Teržan, B. (1995). Some Thoughts about the Social Status of Craftsmen in the Early Iron Age of South East Europe. *Ancient Mining and Metallurgy in Southeast Europe International Symposium, May 20-25, 1990.* B. Jovanoviæ. Belgrade, Archaeological Institute, Museum of Mining and Metallurgy, Bor. 7: 189.

Trampuž Orel, N. (1999). Archaeometallurgic Investigations in Slovenia: A History of Research on Non-Ferrous Metals. *Arheološki vestnik* 50: 407-429.

Trampuž Orel, N. e. a. (1995). Investigations of Metal Artifacts from Slovenian Late Bronze Age Hoards with ICP-AES Method. *Ancient Mining and Metallurgy in Southeast Europe International Symposium, May 20-25, 1990.* B. Jovanoviæ. Belgrade, Archaeological Institute, Museum of Mining and Metallurgy, Bor. 7: 161-167.

Trampuž-Orel, N. e. a. (1991). Inductively coupled plasma-atomic emission spectroscopy analysis of metals from Late Bronze Age hoards in Slovenia. *Archaeometry* 32(2): 267-277.

Wells, P. S. (1980). *Culture contact and culture change: Early Iron Age central Europe and the Mediterranean World.* Cambridge, Cambridge University Press.

Wells, P. S. (1981). *The Emergence of an Iron Age Economy: The Mecklenburg Grave Groups from Hallstatt and Sticna, Mecklenburg Collection, Part III.* Bulletin. A. S. o. P. Research. Cambridge, MA, Peabody Museum of Archaeology and Ethnology, Harvard University.

Wells, P. S. (1984). *Farms, Villages, and Cities: Commerce and Urban Origins in Late Prehistoric Europe.* Ithaca, NY, Cornell University Press.

Appendix

A.1: ICP-ES Bulk Composition Analysis Data from Activation Laboratories

Element:	Fe	Mn	Ni	Sn	Zn	Pb	Sb	As	P	Co	Mass	Final Volume
Units:	%	%	%	%	%	%	%	%	%	%	g	ml
Detection Limit:	0.005	0.005	0.005	0.005	0.005	0.005	0.005	0.005	0.005	0.005		
Reference Method:	METALS-ICP	METALS-ICP	METALS-ICP	METALS-ICP	METALS-ICP	METALS-ICP	METALS-ICP	METALS-ICP	METALS-ICP	METALS-ICP	METALS-ICP	METALS-ICP
Client I.D.												
MIT 5329	0.008	< 0.005	0.058	7.55	< 0.005	6.47	0.13	0.204	0.018	0.027	0.1863	25
MIT 5330a	0.018	< 0.005	0.184	11.4	0.007	1.53	0.537	0.485	< 0.005	0.054	0.1113	25
MIT 5331	0.007	< 0.005	0.023	11.2	< 0.005	1.66	0.053	0.157	< 0.005	0.015	0.1566	25
MIT 5332	0.01	< 0.005	0.145	12.1	< 0.005	5.22	0.232	0.219	0.021	0.009	0.3045	50
MIT 5333	0.14	< 0.005	0.195	4.79	0.006	3.5	0.341	0.253	0.006	0.016	0.1133	25
MIT 5334	0.005	< 0.005	0.158	14.5	< 0.005	0.38	0.158	0.165	< 0.005	0.013	0.2874	50
MIT 5335	0.006	< 0.005	1.5	5.94	< 0.005	0.127	0.265	0.345	< 0.005	0.179	0.2142	50
MIT 5336	0.008	< 0.005	0.675	4.68	< 0.005	1.88	0.788	0.399	0.017	0.014	0.275	50
MIT 5337a	0.314	< 0.005	0.135	10.5	0.011	0.492	0.174	0.222	0.132	0.037	0.2321	50
MIT 5338a	0.008	< 0.005	0.097	5.5	0.006	1.55	0.073	0.334	< 0.005	0.043	0.2472	50
MIT 5339a	0.038	< 0.005	2.04	13.7	< 0.005	0.372	0.163	0.101	0.086	0.022	0.2038	50
MIT 5340a	0.012	< 0.005	0.283	12.3	< 0.005	0.825	0.58	0.554	0.008	0.029	0.1863	25
MIT 5341a	< 0.005	< 0.005	0.293	4.97	0.01	3.04	0.416	0.35	< 0.005	0.02	0.3863	50
MIT 5342a	0.054	< 0.005	0.015	6.57	0.039	13.2	1.05	1.17	0.043	0.031	0.3837	50
MIT 5343a	0.057	< 0.005	0.267	5.12	0.021	14.4	0.849	1.06	< 0.005	0.018	0.2876	50
MIT 5344a	0.028	< 0.005	< 0.005	11.3	0.008	1.87	0.753	0.501	0.013	0.017	0.2736	50
MIT 5345	0.047	< 0.005	0.139	13.6	0.005	2.88	0.225	0.359	0.016	0.038	0.1619	25
MIT 5346a	0.158	< 0.005	0.275	8.72	0.005	1.65	1.39	0.793	< 0.005	0.01	0.1733	25
MIT 5347	0.008	< 0.005	0.755	0.015	< 0.005	34.8	1.92	2.58	0.028	< 0.005	0.1477	25
MIT 5348a	< 0.005	< 0.005	0.089	12.7	< 0.005	0.777	0.304	0.375	< 0.005	0.008	0.2199	50
MIT 5349a	0.019	< 0.005	0.086	21	0.019	7.13	0.184	0.178	0.207	0.013	0.2231	50
MIT 5349b	0.019	< 0.005	0.09	18.3	0.018	7.02	0.159	0.152	0.094	0.012	0.0848	25
MIT 5350a	0.073	< 0.005	0.505	9.38	0.035	18.7	1.46	1.36	0.008	0.041	0.3028	50
MIT 5351a	0.189	< 0.005	0.094	12.9	< 0.005	0.436	0.115	0.119	< 0.005	0.078	0.1664	25
MIT 5352a	0.007	< 0.005	0.058	10.9	0.006	1.69	0.063	0.187	< 0.005	0.011	0.381	50

A.2: INAA Bulk Composition Analysis Data from Activation Laboratories

Sample Description	Au	Ag	As	BA	BR	CA	CO	CR	CS	FE	HF	HG	IR	MO	NA	NI	RB	Sb	SC	SE
	ppm	%	%	ppm	ppm	%	%	ppm	ppm	%	ppm	ppm	ppm	ppm	%	%	ppm	%	PPM	PPM
MIT 5329	31.9	0.071	0.175	-100	4.0	-1	0.032	-5	-1	0.16	-1	-1	-10	-10	0.04	0.075	-15	0.120	0.2	-3
MIT 5330A	34.9	0.252	0.407	-100	-0.5	-1	0.059	-5	-1	-0.05	-1	-1	-10	-10	-0.02	0.311	-15	0.529	0.3	-3
MIT 5331	24.9	0.020	0.143	-100	5.8	-1	0.019	31	-1	0.13	-1	-1	-10	-10	-0.02	0.048	-15	0.033	0.2	-3
MIT 5332	37.8	0.485	0.155	-100	-0.5	-1	0.010	-5	-1	0.25	-1	-1	-10	-10	-0.02	0.148	-15	0.185	0.2	-3
MIT 5333	25.8	0.200	0.225	-100	4.0	-1	0.022	-5	-1	0.61	-1	-1	-10	-10	-0.02	0.200	-15	0.348	0.4	-3
MIT 5334	38.0	0.093	0.144	-100	-0.5	-1	0.019	21	-1	-0.05	-1	-1	-10	-10	-0.02	0.130	-15	0.140	-0.1	-3
MIT 5335	1.8	0.282	0.249	-100	-0.5	-1	0.173	-5	-1	-0.05	-1	-1	-10	-10	-0.02	1.550	-15	0.224	-0.1	-3
MIT 5336	19.4	0.433	0.376	-100	-0.5	-1	0.018	-5	-1	-0.05	-1	-1	-10	-10	0.01	0.757	-15	0.791	-0.1	-3
MIT 5337A	33.9	0.097	0.175	-100	-0.5	-1	0.040	-5	-1	0.50	-1	-1	-10	-10	-0.02	0.171	-15	0.149	0.2	-3
MIT 5338A	38.4	0.038	0.284	-100	5.2	-1	0.058	-5	-1	-0.05	-1	-1	-10	-10	-0.02	0.073	-15	0.068	0.2	-3
MIT 5339A	14.5	0.071	0.085	-100	-0.5	-1	0.023	-5	-1	0.18	-1	-1	-10	-10	-0.02	2.060	-15	0.126	-0.1	-3
MIT 5340A	20.6	0.242	0.444	-100	-0.5	-1	0.033	-5	-1	0.23	-1	-1	-10	-10	-0.02	0.310	-15	0.565	-0.1	-3
MIT 5341A	19.4	0.254	0.373	-100	-0.5	-1	0.031	-5	-1	0.23	-1	-1	-10	-10	-0.02	0.284	-15	0.469	-0.1	-3
MIT 5342A	15.8	0.323	0.893	-100	-0.5	-1	0.026	-5	-1	-0.05	-1	-1	-10	-10	0.04	0.492	-15	0.920	-0.2	-3
MIT 5343A	18.3	0.282	0.723	-100	-0.5	-1	0.015	-5	-1	-0.05	-1	-1	-10	-10	0.03	0.397	-15	0.695	-0.1	-3
MIT 5344A	21.4	0.248	0.403	-100	-0.5	-1	0.014	-5	-1	-0.05	-1	-1	-10	-10	0.04	0.200	-15	0.678	-0.1	-3
MIT 5345	50.9	0.093	0.322	-100	-0.5	4	0.046	-5	-1	-0.05	-1	-1	-10	-10	-0.02	0.199	-15	0.221	0.2	-3
MIT 5346A	19.6	0.719	0.672	-100	53.1	-1	0.010	-5	-1	-0.05	-1	-1	-10	-10	0.03	0.252	-15	1.37	0.8	-3
MIT 5347	8.9	0.797		-100	-0.5	-1	0.005	-5	-1	-0.05	-1	-1	-10	-10	-0.02	0.764	-15	1.96	0.7	-3
MIT 5348A	17.4	0.118	0.306	-100	-0.5	-1	0.010	-5	-1	-0.05	-1	-1	-10	-10	-0.02	0.134	-15	0.280	0.2	-3
MIT 5349A	30.3	0.222	0.154	-100	-0.5	-1	0.015	-5	-1	-0.05	-1	-1	-10	-10	-0.02	0.099	-15	0.148	0.2	-3
MIT 5349B	11.1	0.079	0.057	-100	-0.5	-1	0.006	-5	-1	0.17	-1	-1	-10	-10	-0.02	0.052	-15	0.054	0.2	-3
MIT 5350A	16.5	0.404		-100	-0.5	-1	0.033	-5	-1	-0.05	-1	-1	-10	-10	0.06	0.763	199	0.210	-0.1	-3
MIT 5351A	22.6	0.061	0.114	-100	-0.5	-1	0.089	-5	-1	0.47	-1	-1	-10	-10	-0.02	0.137	-15	0.104	0.4	53
MIT 5352A	22.1	0.056	0.166	-100	-0.5	-1	0.017	-5	-1	-0.05	-1	-1	-10	-10	-0.02	0.061	-15	0.045	0.2	-3
BLANK	-0.1	-0.001	-0.001	-100	-0.5	-1	0.000	-5	-1	-0.05	-1	-1	-10	-10	-0.02	-0.002	-15	-0.001	-0.1	-3
BCS 207/2	0.4	0.045	0.064	-100	-0.5	-1	0.004	-5	-1	-0.05	-1	-1	-10	-10	-0.02	0.278	-15	0.108	0.2	-3
BSC 183/4	1.1	0.052	0.123	-100	-0.5	-1	0.003	-5	-1	-0.05	-1	-1	-10	-10	-0.02	1.270	-15	0.236	-0.1	-3
NBS 158A	0.2	-0.001	-0.001	-100	-0.5	-1	0.001	-5	-1	1.40	-1	-1	-10	-10	-0.02	-0.002	-15	-0.001	0.2	-3
MA-1B	16.9	-0.001	-0.001	1900	-0.5	5	0.003	198	4	4.87	-1	-1	-10	88	1.41	-0.002	139	-0.001	13.4	-3
BCS 207/2 Cert	0.5	0.044	0.066							0.03						0.280		0.100		
BCS 183/4 Cert	1.2	0.056	0.13							0.06						1.300		0.230		
NBS 158a Cert										1.23						0.001				
MA-1B Cert.	17.0			1800		4.6	0.003	200		4.62				80	1.49		160		13	

Detection limits are elevated due to high concentration of Au, As, Ni and Sb.

Activation Laboratories Ltd.
1336 Sandhill Dr.
Ancaster, Ontario L9G4V5
Canada

A.2: INAA Bulk Composition Analysis Data from Activation Laboratories

Sample Description	SN	SR	TA	TH	U	W	ZN	LA	CE	ND	SM	EU	TB	YB	LU	Mass
	%	%	PPM	PPM	PPM	PPM	PPM	PPM	PPM	PPM	PPM	PPM	PPM	PPM	PPM	g
MIT 5329	7.22	-0.05	-0.5	-0.5	-2.0	-1	-50	-0.5	-3	-5	-0.1	-0.2	-0.5	-0.2	-0.05	0.186
MIT 5330A	10.4	-0.05	-0.5	-0.5	-2.0	-1	-50	-0.5	-3	-5	-0.1	-0.4	-0.5	-0.2	-0.05	0.112
MIT 5331	10.5	-0.05	-0.5	-0.5	-2.0	-1	-50	-0.5	-3	-5	-0.1	-0.2	-0.5	-0.2	-0.05	0.158
MIT 5332	9.27	-0.05	-0.5	-0.5	-2.0	-1	107	-0.5	-3	-5	-0.1	-0.2	-0.5	-0.2	-0.05	0.305
MIT 5333	4.69	-0.05	-0.5	-0.5	-2.0	-1	-50	-0.5	-3	-5	-0.1	-0.3	-0.5	-0.2	-0.05	0.113
MIT 5334	13.1	-0.05	-0.5	-0.5	8.5	-1	-50	-0.5	-3	-5	-0.1	-0.2	-0.5	-0.2	-0.05	0.287
MIT 5335	5.20	-0.05	-0.5	-0.5	-2.0	-1	-50	-0.5	-3	-5	-0.1	-0.2	-0.5	-0.2	-0.05	0.214
MIT 5336	2.65	-0.05	-0.5	-0.5	-2.0	-1	-50	-0.5	-3	-5	-0.1	-0.2	-0.5	-0.2	-0.05	0.226
MIT 5337A	10.1	-0.05	-0.5	-0.5	-2.0	-1	190	-0.5	-3	-5	-0.1	-0.2	-0.5	-0.2	-0.05	0.233
MIT 5338A	4.97	-0.05	-0.5	-0.5	-2.0	-1	129	-0.5	-3	14	-0.1	-0.2	-0.5	-0.2	-0.05	0.260
MIT 5339A	11.2	-0.05	-0.5	-0.5	-2.0	-1	-50	-0.5	22	-5	-0.1	-0.2	-0.5	-0.2	-0.05	0.204
MIT 5340A	10.3	-0.05	-0.5	-0.5	-2.0	-1	-50	-0.5	38	-5	-0.1	-0.3	-0.5	-0.2	-0.05	0.187
MIT 5341A	4.36	-0.05	-0.5	-0.5	-2.0	-1	-50	-0.5	-3	-5	-0.1	-0.3	-0.5	-0.2	-0.05	0.216
MIT 5342A	3.80	-0.05	-0.5	-0.5	-2.0	-1	-50	-0.5	-3	-5	-0.1	-0.2	-0.5	-0.2	-0.05	0.383
MIT 5343A	3.91	-0.05	-0.5	-0.5	-2.0	-1	-50	-0.5	-6	-5	-0.1	-0.2	-0.5	-0.2	-0.05	0.303
MIT 5344A	9.32	-0.05	-0.5	-0.5	-2.0	-1	-50	-0.5	-9	-5	-0.1	-0.2	-0.5	-0.2	-0.05	0.273
MIT 5345	12.8	-0.05	-0.5	-0.5	-2.0	-1	175	-0.5	-3	-5	-0.1	-0.2	-0.5	-0.2	-0.05	0.162
MIT 5346A	6.10	-0.05	-0.5	-0.5	-2.0	-1	-50	-0.5	-3	-5	-0.1	-0.2	-0.5	-0.2	-0.05	0.174
MIT 5347	-0.30	-0.05	-0.5	-0.5	-2.0	-1	-50	4.4	-9	-5	-0.1	-0.2	-0.5	-0.2	-0.05	0.149
MIT 5348A	11.4	-0.05	-0.5	-0.5	-2.0	-1	-50	-0.5	31	-5	-0.1	-0.2	-0.5	-0.2	-0.05	0.220
MIT 5349A	20.3	-0.05	-0.5	-0.5	-2.0	-1	247	2.0	-3	-5	0.3	-0.2	-0.5	-0.2	-0.05	0.220
MIT 5349B	7.16	-0.05	-0.5	-0.5	-2.0	-1	75	-0.5	-3	-5	-0.1	-0.2	-0.5	-0.2	-0.05	0.224
MIT 5350A	6.33	-0.05	-0.5	-0.5	-2.0	-1	392	-0.5	-3	-5	-0.1	-0.2	-0.5	-0.2	-0.05	0.296
MIT 5351A	12.6	-0.05	-0.5	-0.5	-2.0	-1	-50	-0.5	-3	-5	-0.1	-0.2	-0.5	-0.2	-0.05	0.166
MIT 5352A	9.61	-0.05	-0.5	-0.5	-2.0	-1	110	-0.5	14	-5	-0.1	-0.2	-0.5	-0.2	-0.05	0.381
BLANK	-0.01	-0.05	-0.5	-0.5	-2.0	-1	-50	-0.5	-3	-5	-0.1	-0.2	-0.5	-0.2	-0.05	1.00
BCS 207/2	9.86	-0.05	-0.5	-0.5	-1.1	-1	16400	-0.5	-3	-5	-0.1	-0.2	-0.5	-0.2	-0.05	0.306
BSC 183/4	7.09	-0.05	-0.5	-0.5	-1.4	-1	37000	-0.5	-3	-6	-0.1	-0.2	-0.5	-0.3	-0.06	0.295
NBS 158A	1.13	-0.05	-0.5	-0.5	-0.8	-1	20800	-0.5	-3	-5	-0.1	-0.2	-0.5	-0.2	-0.05	0.296
MA-1B	-0.01	-0.05	-0.5	-0.5	-0.5	15	-50	51.7	107	60	10.8	2.8	-0.5	1.6	0.26	0.297
BCS 207/2 Cert	9.74						16000									
BCS 183/4 Cert	7.27						24700									
NBS 158a Cert	0.96						20800									
MA-1B Cert.		0.11				15										